

**School of Civil Engineering
Faculty of Engineering**



UNIVERSITY OF LEEDS

Final Thesis

Submitted in partial fulfilment of the requirements for a degree of
Doctor of Philosophy

**Oil-Based Mud Cuttings as Additional Raw Material
in Clinker and Cement Production**

by

Hilal Saif Rashid Al Dhamri

October 2019

This copy has been supplied on the understanding that it is copyright material and that no quotation from the thesis may be published without proper acknowledgment.

© 2019 *The University of Leeds Hilal Saif Al Dhamri*

The right of Hilal Saif Al Dhamri to be identified as Author of this work has been asserted by his in accordance with Copyright, Designs and Patents Act 1988.

Publication Statements

The candidate confirms that the work submitted is his own, except where work which has formed part of jointly-authored publications has been included. The contribution of the candidate and other authors to this work has been explicitly indicated below. The candidate confirms that appropriate credit has been given within the thesis where reference has been made to the work of others. Part of the work has been published in the following journals and proceedings of conferences:

i. H. Al Dhamri *et al* (2020) **published**

Hilal Al-Dhamri, Sabah A. Abdul-Wahab, Costas Velis, Leon Black
“Oil-Based Mud Cutting as an Additional Raw Material in Clinker Production”,
Journal of Hazardous Materials, Volume 384, 121022, 2020
Doi.org/10.1016/j.jhazmat.2019.121022

ii. S. Abdul-Wahab *et al* (2020) **published**

Sabah A. Abdul-Wahab, Hilal Al-Dhamri, Ganesh Ram, Leon Black
“The use of oil-based mud cuttings as an alternative raw material to produce high sulfate-resistant oil well cement”,
Journal of Cleaner Production, available on line 25 May 2020, 269, 122207.
Doi.org/10.1016/j.jclepro.2020.122207

iii. H. Al Dhamri *et al* (2019) **published**

Hilal Al-Dhamri, Sabah A. Abdul-Wahab, Ganesh Ram, Abdulaziz Al-Moqbali, Leon Black
“Microstructure of Clinker prepared using different ratio of OBM cutting as raw material”
Proceedings of the 15th International Congress of the Chemistry of Cement, Prague
September 2019.

- iv. H. Al-Dhamri *et al* (2015) **published**
Hilal Al-Dhamri, Leon Black, Sabah A. Abdul-Wahab,
“Oil-Based Mud Cutting as an Additional Raw Materials in Clinker Production: The Impact on Phase Composition”,
Proceedings of the 14th International Congress of the Chemistry of Cement, Beijing 2015.
- v. Al-Dhamri and L. Black (2014) **published**
H. Saif Al-Dhamri and Leon Black
“*Use of Oil-Based Mud Cutting Waste in Cement Clinker Manufacturing*”
In: Bernal, SA and Provis, JL, (eds.) 34th Cement and Concrete Science Conference.
34th Cement and Concrete Science Conference, 14-17 Sep 2014, Sheffield, UK. , pp. 427-430, 2014.

Acknowledgements

First of all, I am grateful to Allah, who granted me the ability, patience and strength to accomplish this research, which contributes to completing my PhD degree.

I would like to express my deep appreciation and gratitude to my supervisor, Prof. Leon Black, for his guidance, assistance and supervision. His continuous support, help and valuable suggestions have helped lead to the successful completion of this thesis.

As local supervisor, I would like to express my gratitude to, Prof. Sabah Abdul-Wahab from Sultan Qaboos University, for her guidance and supervision.

Special thanks are extended to Oman Cement Company for providing a fund to further my postgraduate at the University of Leeds. Without the generous supply of raw materials, and use the company laboratory facilities, this research project would have been very difficult to accomplish. I would also like to thank Petroleum Development Oman (PDO) and The Research Council (TRC) for supporting and facilitating aspects of the research and organising site visits.

It gives me great pleasure to thank my family, including my father and mother, my 13 brothers and sisters, and my lovely children (Ayah, Ala'a, Rashid and Talyah). A special thanks go to my lovely wife, Mrs. Nehad Al-Harhi who has believed in me and stood by me throughout my doctoral studies.

Abstract

Oil-based mud (OBM) cuttings are a waste generated during the process of oil well drilling. The drilled rocks are removed from deep within the drilled well and pumped to the surface. These 'cuttings' are a mixture of rocks, mud, water, and oil. Most drilling companies store this waste in open yards without specific treatment. The environmental regulations in Oman specify that cutting storage should involve isolation to prevent contamination of the surface and underground water. This has made OBM cutting waste an environmental problem with an associated cost for oil companies. OBM cuttings, being rich in calcium oxide, silicon oxide, and aluminum oxide, may be a suitable raw material in cement manufacture. Furthermore, the oil content may help to reduce fuel use during the calcination and clinkerisation process. In this research, OBM cutting waste was analysed and used as a constituent of raw meal in cement clinker production. Raw meal mixtures were prepared with increasing OBM content. The impact of adding OBM to the resultant clinker was investigated using analytical techniques such as XRF, XRD, SEM-EDX, and DSC-TGA, and burnability test.

OBM cuttings contain dolomite, which increases the rate of carbonate dissociation and, hence, contributes to lowering the calcination temperature. However, it also leads to a higher free lime content in the resultant clinker, which is a result of the presence of trace elements, such as barium. Clinker can be prepared by simply heating OBM cuttings at 1200 °C without any additives, with the resulting clinker containing belite and a very low free lime content and no alite. Clinker prepared using 12% and 55% OBM cuttings had very similar microstructures, chemical composition and properties to clinker prepared from the limestone normally used in cement production. However, the addition of OBM cutting to the raw meal led to acceptable higher free lime content in the resultant clinker. There are many reasons for this, including the role of trace elements, especially barium, in destabilizing alite, as demonstrated in this study.

The hydration behaviour of the prepared cement was studied by many techniques such as ICC, STA and mechanical properties. XRD plus SEM-EDX analysis of polished cross-sections enabled study of the major hydrate phases. SEM and optical microscopy of the clinker was undertaken to understand if there were any significant changes to the main phases which may influence the cement hydration behaviour. The degree of hydration was obtained and the main hydrated products such as C-S-H and CH were identified. Hydration behaviour was normal with no significant changes observed and no significant differences between the reference sample and industrial cement. Thus, OBM cuttings could be used in the manufacture of Portland cement clinker, providing a cost-effective, environmentally-friendly way to manage OBM cuttings derived from the oil drilling sector.

Table of content

| | |
|--|-----------|
| Publication statements | ii |
| Acknowledgements | iv |
| Abstract | v |
| Table of contents | vi |
| List of figures | xi |
| List of tables | xii |
| List appendices | xiii |
| List of abbreviations | xiv |
| Chapter 1: Introduction..... | 1 |
| Chapter 2: Literature Review | 5 |
| 2.1 Industrial Hazardous waste in Oman | 5 |
| 2.2 OBM waste generated from Oil Drilling Process | 7 |
| 2.3 Shifting from WBM to OBM in Oman | 16 |
| 2.4 Waste as raw materials for clinker production..... | 16 |
| Chapter 3: Description of the problem..... | 22 |
| 3.1 The impact of OBM cutting generated in Oman..... | 22 |
| 3.1.1 Economic impact..... | 22 |
| 3.1.2 Environmental impact..... | 23 |
| 3.2 Possible solutions for disposal of OBM cutting in cement industries..... | 24 |
| 3.3 Use of OBM cuttings as raw materials in clinker manufacturing..... | 25 |
| 3.4 Chemistry of the cement manufacturing process | 30 |
| 3.5 Common cement types used in Oman..... | 34 |
| 3.5.1 Ordinary Portland cement (OPC) and sulfate-resisting cement (SRC)..... | 34 |
| 3.5.2 Oil Well Cement (OWC)..... | 34 |
| Chapter 4: Materials and methods | 36 |
| 4.1 Overview of experimental programme | 36 |
| 4.2 Raw materials..... | 38 |
| 4.2.1 Limestone (Ls) | 38 |
| 4.2.2 Quartzo-phillite (QPh)..... | 39 |
| 4.2.3 Iron ore and kaolin | 39 |
| 4.2.4 Oil-Based Mud cuttings..... | 39 |
| 4.3 Mix design and samples preparation..... | 41 |
| 4.3.1 Mix design | 41 |
| 4.3.2 Raw meal samples (Rm) | 45 |
| 4.3.3 Clinker samples (Ck)..... | 46 |

| | | |
|---|--|------------|
| 4.3.4 | Cement samples (Cm) | 48 |
| 4.3.5 | Hydrated cement samples (HCm) | 49 |
| 4.4 | Characterization and testing techniques | 51 |
| 4.4.1 | XRF and XRD | 51 |
| 4.4.2 | Loss on ignition (LOI) and Free lime test..... | 51 |
| 4.4.3 | Inductively Coupled Plasma (ICP-OES) | 52 |
| 4.4.4 | SEM-EDX..... | 52 |
| 4.4.5 | DSC-TGA | 53 |
| 4.4.6 | Burnability test..... | 53 |
| 4.4.7 | Petrographic analysis | 54 |
| 4.4.8 | Degree of hydration (DoH)..... | 54 |
| 4.4.9 | Physical and mechanical testing | 55 |
| 4.4.10 | Isothermal Conduction Calorimetry..... | 57 |
| Chapter 5: Characterisation of OBM and OBM cuttings | | 59 |
| 5.1 | What is in OBM? | 59 |
| 5.2 | What is in OBM cuttings?..... | 61 |
| Chapter 6: The effect of OBM cuttings on the clinkerisation process..... | | 67 |
| 6.1 | Clinker phase formation..... | 67 |
| 6.2 | CaCO ₃ decomposition | 70 |
| 6.3 | Burnability..... | 75 |
| 6.4 | The XRD and TGA | 84 |
| 6.5 | The Effect of Barium on Clinkerization | 87 |
| 6.6 | Clinker morphology..... | 88 |
| 6.7 | Petrography Study of the Clinker..... | 94 |
| Chapter 7: The effect of OBM cutting on cement properties and hydration..... | | 99 |
| 7.1 | Physical and mechanical properties..... | 99 |
| 7.2 | Hydration and microstructure | 107 |
| 7.3 | Thermal Analysis (STA)..... | 116 |
| 7.4 | Heat of hydration by ICC..... | 119 |
| 7.5 | Degree of hydration (DoH)..... | 123 |
| Chapter 8: Impact of using OBM cutting in cement industry | | 126 |
| 8.1 | Recycling in non-cement industry..... | 126 |
| 8.2 | Oman Cement Company case..... | 131 |
| 8.3 | Impact of introducing OBM cutting to Oman Cement Company as additional raw material 134 | |
| Chapter 9 Summary discussion | | 137 |
| 9.1 | Introduction | 137 |
| 9.2 | OBM cutting..... | 137 |

| | | |
|-------------------------|---|------------|
| 9.3 | The effect of OBM cutting on the clinkerization process | 138 |
| 9.4 | The effect of OBM cutting on the cement properties and hydration..... | 140 |
| 9.5 | Impact of using OBM cutting in cement industries | 143 |
| Chapter 10: | Conclusions and further work | 146 |
| 10.1 | Conclusions | 146 |
| 10.2 | Further work | 147 |
| Appendices | | 160 |

List of Figures

| | |
|--|----|
| Figure 1 Industrial hazardous waste generation in Oman..... | 6 |
| Figure 2 The major functions of OBM during the oil-drilling process ³⁷ | 7 |
| Figure 3 Schematic diagram of an oil well drilling operation. | 8 |
| Figure 4 Crude oil production in Oman from 1980 to 2018 | 16 |
| Figure 5 CO ₂ emission concentrations calculated by atmospheric modelling ⁷ | 20 |
| Figure 6 CO ₂ emissions from energy consumption in Oman ^{55,56} | 23 |
| Figure 7 Gross natural gas production in Oman ^{55,56} | 24 |
| Figure 8 A schematic of the OBM and OBM cutting disposal cycle as raw material in cement manufacturing ⁷⁴ | 27 |
| Figure 9 Storage sites for OBM cuttings..... | 29 |
| Figure 10 Cement manufacturing process..... | 31 |
| Figure 11 Estimated clinker chemical reactions ^{91,92} | 33 |
| Figure 12 A schematic diagram showing the overall stages of sample preparation and the testing methods used at each stage..... | 37 |
| Figure 13 Diagram illustrating the sampling points (black points) for the raw materials obtained from the cement industry | 38 |
| Figure 14 The oil well drilling operation diagram..... | 40 |
| Figure 15 The mix design program in MS Excel sheet..... | 43 |
| Figure 16 Theoretical C ₃ S and C ₂ S contents as a function of OBM cuttings content in raw meal. | 44 |
| Figure 17 The preparation steps of the Portland clinker and Portland cement in the laboratory..... | 47 |
| Figure 18 Hydrated cement samples and isopropanol hydration stopping | 50 |
| Figure 19 SEM Micrograph of hydrated cement. | 55 |
| Figure 20 Overview of the calorimeter setup | 57 |
| Figure 21 Schematic mineral structure of clay | 60 |
| Figure 22 X-ray diffraction pattern of OBM cutting..... | 62 |
| Figure 23 The chemical composition (major oxides) of OBM cuttings..... | 65 |
| Figure 24 The trace and heavy elements content of OBM cutting..... | 65 |
| Figure 25 XRD patterns of the prepared clinkers..... | 67 |
| Figure 26 Clinker phase contents derived from Rietveld analysis and Bogue calculations. | 68 |
| Figure 27 Limestone and OBM cutting petrography analysis..... | 72 |

| | |
|---|-----|
| Figure 28 Particle-size distribution (top) and decomposition temperature (below) of fine-limestone, limestone, and OBM cutting. | 74 |
| Figure 29 Activation energy values of CaCO_3 decomposition reactions in limestone and OBM cutting. | 75 |
| Figure 30 The burnability tests of the raw meal at different burning temperatures. | 77 |
| Figure 31 XRD pattern of the different raw meal samples burned at different temperatures..... | 78 |
| Figure 32 100% OBM cuttings clinker. | 78 |
| Figure 33 The SEM analysis of Rm_{Ref} burned at four different temperatures. | 79 |
| Figure 34 The SEM analysis of Rm-12 burned at four different temperatures..... | 80 |
| Figure 35 The SEM analysis of Rm-55 burned at four different temperatures..... | 81 |
| Figure 36 EDX analysis for Rm_{Ind} showing clinker microstructure development with increasing temperature. | 82 |
| Figure 37 EDX analysis for Rm_{Ref} showing clinker microstructure development with increasing temperature. | 82 |
| Figure 38 EDX analysis for Rm-12 showing clinker microstructure development with increasing temperature. | 83 |
| Figure 39 EDX analysis for Rm-55 showing clinker microstructure development with increasing temperature. | 83 |
| Figure 40 EDX analysis for Rm-100 showing clinker microstructure development with increasing temperature. | 84 |
| Figure 41 Temperatures of calcite decomposition and major phase formation with increasing OBM cuttings content..... | 85 |
| Figure 42 Minor oxide contents in prepared raw meal | 86 |
| Figure 43 The free lime content for each clinker sample | 88 |
| Figure 44 SEM-EDX microstructural analysis of clinker samples burned at 1180 °C. | 90 |
| Figure 45 SEM-EDX microstructural analysis of clinker samples burned from 100% OBM. | 91 |
| Figure 46 XRD of OBM cutting when heated to different temperatures..... | 92 |
| Figure 47 SEM-EDX microstructural analysis of clinker samples prepared by adding 12% and 55% OBM cutting. | 93 |
| Figure 48 Photomicrographs of clinker Ck_{Ref} | 95 |
| Figure 49 Photomicrographs of clinker Ck12..... | 96 |
| Figure 50 Photomicrographs of clinker Ck55..... | 97 |
| Figure 51 SEM images and EDS spectra of clinker samples containing 30% (a, b & d) and 55% (d, e & f) OBM cuttings. | 103 |
| Figure 52 Compressive strength development over time of the prepared cement. | 105 |

| | |
|---|-----|
| Figure 53 Blaine fineness vs compressive strength..... | 106 |
| Figure 54 SEM image of Cmt _{Ind} hydrated for 2, 7 and 28 days | 109 |
| Figure 55 SEM image of Cmt _{Ref} hydrated for 2, 7 and 28 days..... | 110 |
| Figure 56 SEM image of Cmt12% hydrated for 2, 7 and 28 days | 111 |
| Figure 57 SEM image of Cmt55% hydrated for 2, 7 and 28 days | 112 |
| Figure 58 XRD analysis of anhydrous Cm _{Ind} and up to 28 days..... | 113 |
| Figure 59 SEM and XRD analysis of anhydrous Cm _{Ref} . and up to 28 days. | 113 |
| Figure 60 SEM and XRD analysis of anhydrous Cm-12% and up to 28 days. | 114 |
| Figure 61 SEM and XRD analysis of anhydrous Cm-55% and up to 28 days. | 114 |
| Figure 62 XRD Patterns from 8 to14° 2θ showing ettringite formation and the C ₄ AF peak..... | 116 |
| Figure 63 XRD Patterns from 31 to 35° 2θ. | 116 |
| Figure 64 DTA plots from 20 to 950 °C for 2, 7 and 28 day pastes. | 118 |
| Figure 65 An example of different stages of cement hydration based on heat evolution. | 119 |
| Figure 66 Isothermal Calorimetry results showing rate of heat evolution and total cumulative heat to 21 days | 122 |
| Figure 67 Degree of hydration obtained by SEM BSE vs time..... | 124 |
| Figure 68 Aero Thermal Dissolution Unit (ATDU) for thermal treatment of OBM cuttings. | 127 |
| Figure 69 Two types of OBM cuttings collected from storage yard. | 128 |
| Figure 70 Quantities of treated OBM cutting using ATDU and oil recovered ²⁹ | 130 |
| Figure 71 Main source of emissions from the cement kiln system. | 133 |
| Figure 72 Proposed feeding points of OBM cutting..... | 134 |
| Figure 73 Arrangement for feeding OBM cutting at the calciner. | 134 |

List of Tables

| | |
|--|-----|
| Table 1 Pollutant concentration in exhaust gas ⁺ from waste-based clinker ⁶² in mg/Nm ³ | 18 |
| Table 2 Total CO ₂ emissions from plant sources after the addition of OBM ⁷ | 19 |
| Table 3 Calculation of CO ₂ emissions from cement-plant sources before and after the addition of OBM ⁷ | 19 |
| Table 4 The chemical composition of limestone, quartzo-phillite, and OBM cuttings ⁷¹ | 25 |
| Table 5 Major chemical phases in clinker and cement | 32 |
| Table 6 Chemical composition of the raw materials used in this study. | 45 |
| Table 7 Composition of the raw meal mixes for the preparation of Portland clinkers. | 46 |
| Table 8 The cement grinding condition | 48 |
| Table 9 OBM cuttings major and minor chemical composition from different sources (%wt.) | 64 |
| Table 10 OBM cuttings trace & heavy elements analysis (mg/Kg, dry solid) ^{44,52,54} | 64 |
| Table 11 Chemical oxide and clinker phase composition of the prepared clinker | 69 |
| Table 12 The effect of calcite grain size on the dissociation of limestone. | 73 |
| Table 13 BaO content of each phase in each experimental clinker | 87 |
| Table 14 The granulometric composition analysis of the prepared clinker | 94 |
| Table 15 Summary for the OPC standards: Oman Standard ¹⁰⁵ , BS EN ¹⁹¹ and ASTM ¹⁹² ... | 100 |
| Table 16 Physical test results for the prepared cement. | 104 |
| Table 17 The main heat results from ICC test. | 121 |
| Table 18 Cost calculation for OBM cutting recycling options. | 129 |
| Table 19 The estimated OBM cutting production and the rate of growth | 131 |

List of Appendices

| | |
|---|-----|
| Appendix 1 Percentage mixing of the raw materials for the preparation of raw meal..... | 160 |
| Appendix 2 The clinker prepared chemical analysis and calculated mineral composition..... | 161 |
| Appendix 3 Free lime in % (wt./wt.) repeated test of the clinker samples..... | 162 |
| Appendix 4 Burnability test for raw mix prepared with OBM cutting..... | 163 |
| Appendix 5 Calculations of activation energy of decomposition of limestone and OBM cutting | 164 |
| Appendix 6 TGA of OBM cutting and limestone in four different heating rates | 165 |
| Appendix 7 Particle size distribution for the cement samples | 166 |
| Appendix 8 Cement density measurement..... | 167 |
| Appendix 9 Cement Blaine measurement | 168 |
| Appendix 10 Degree of hydration % (DoH) obtained by SEM BSE..... | 168 |
| Appendix 11 Compressive strength measurement for the C_{mInd} | 169 |
| Appendix 12 STA analysis of hydrated cement | 170 |
| Appendix 14 The hydration product obtained from STA analysis..... | 172 |
| Appendix 15 Clinker preparation photos..... | 173 |
| Appendix 16 Raw materials chemical analysis | 176 |
| Appendix 17 Agreement between Oman Cement Company and Petroleum Development Oman Company as a result of this study..... | 181 |
| Appendix 18 Photos for the sit to oil drilling site | 182 |

List of Abbreviations

Cement Nomenclature

| | | |
|-------|---|---|
| C | : | CaO |
| S | : | SiO ₂ |
| H | : | H ₂ O |
| F | : | Fe ₂ O ₃ |
| A | : | Al ₂ O ₃ |
| CH | : | Ca(OH) ₂ (Portlandite) |
| C-S-H | : | Calcium silicate hydrate |
| AFt | : | Alumina Ferric oxide tri-sulfate (Ettringite) |
| AFm | : | Alumina Ferric oxide mono-sulfate |

Clinker Phases and Hydrates

| | | |
|------------------------------------|---|---|
| Alite (Tricalcium silicate) | : | 3CaO.SiO ₂ / Ca ₃ SiO ₅ / C ₃ S |
| Alumina ferric oxide mono-sulfate | : | CaO.Al ₂ O ₃ .CaSO ₄ .12H ₂ O / C ₃ A.CaSO ₄ .12H ₂ O |
| Alumina Ferric Oxide tri-sulfate | : | 3CaO.Al ₂ O ₃ .3CaSO ₄ .32H ₂ O / C ₃ A.3CaSO ₄ .32H ₂ O |
| Aluminate (Tricalcium aluminate) | : | 3CaO.Al ₂ O ₃ / Ca ₃ Al ₂ O ₆ / C ₃ A |
| Belite (Dicalcium silicate) | : | 2CaO.SiO ₂ / Ca ₂ SiO ₄ / C ₂ S |
| Brucite | : | Mg(OH) ₂ |
| Calcium silicate hydrate | : | CaO-SiO ₂ -H ₂ O |
| Ferrite (Tetracalcium aluminate) | : | 4CaO.Al ₂ O ₃ .Fe ₂ O ₃ / C ₄ AF |
| Gypsum (calcium sulfate dihydrate) | : | CaSO ₄ .2H ₂ O / CaH ₄ O ₆ S |
| Periclase | : | MgO |
| Portlandite | : | Ca(OH) ₂ |

Testing Techniques

| | | |
|-----|---|--------------------------------------|
| BSE | : | Back Scattered Electron |
| DoH | : | Degree of hydration |
| DTA | : | Differential Thermal Analysis |
| EDX | : | Energy Dispersive X-Ray Spectroscopy |
| ICC | : | Isothermal Conduction Calorimetry |
| ICP | : | Inductively coupled plasma |
| LOI | : | Loss on ignition |
| SEM | : | Scanning Electron Microscopy |
| STA | : | Simultaneous Thermal Analysis |
| TGA | : | Thermogravimetric analysis |
| XRD | : | X-Ray Diffraction |
| XRF | : | X-Ray Fluorescence |

Elements and compounds

| | | |
|-------------------------|---|-----------------------|
| Al_2O_3 | : | Aluminium oxide |
| As | : | Arsenic |
| CaO | : | Calcium oxide |
| Cd | : | Cadmium |
| Cl | : | Chloride |
| CO | : | Carbon monoxide |
| Co | : | Cobalt |
| CO_2 | : | Carbon dioxide |
| Cr | : | Chromium |
| Cu | : | Copper |
| Fe_2O_3 | : | Iron oxide |
| Hg | : | Mercury |
| K_2O | : | Potassium oxide |
| Na_2O | : | Sodium oxide |
| Ni | : | Nickel |
| NO_x | : | Nitrogen oxide |
| P_2O_5 | : | Phosphorous pentoxide |
| Pb | : | Lead |
| Sb | : | Antimony |
| Se | : | Selenium |
| SiO_2 | : | Silicate |
| Sn | : | Tin |
| SO_2 | : | Sulfur dioxide |
| SO_3 | : | Sulfite |
| TiO_2 | : | Titanium dioxide |
| V | : | Vanadium |

 Other abbreviations

| | |
|------------------|--|
| µm | : micrometre |
| AM | : Alumina module |
| API | : American Petroleum Institute |
| ASTM | : American Society for Testing and Materials |
| BS | : British Standards |
| Ck | : Clinker |
| Cm | : Cement |
| cm | : Centimetre |
| EN | : European Norms (European Standards) |
| g | : Gram (unit for mass) |
| GCC | : Gulf Cooperation Council |
| GHG | : Greenhouse gas |
| GPA | : Gross Domestic Product |
| H/C | : Hydrocarbon |
| HCm | : Hydrated cement |
| hr | : Hour |
| IR | : Insoluble Residue |
| Kg | : Kilogram |
| KL | : Kaolin |
| LC ₅₀ | : Lethal concentration 50 |
| Ls. | : Limestone |
| LSF | : Lime Saturation Factor |
| max | : Maximum |
| min | : Minimum |
| mint | : minute |
| mL | : Millilitre |
| mm | : Millimetre |
| mmBtu | : million British Thermal Units |
| MPa | : Mega Pascal (unit for pressure) |
| N | : Newton |
| OBM | : Oil-Based Mud |
| OS | : Omani Standard |
| QPh | : Quartzo-phillite |
| RM | : Raw meal |
| RPM | : Revolutions per minute |
| SM | : Silica module |
| T | : Tonne (long tonne) |
| TOC | : Total Organic Compounds |
| TSP | : Total Suspended Particulate (in exhaust gas) |
| USD | : United State Dollar (currency) |
| w/c | : Water to cement ratio |
| WEEE | : Waste Electrical and Electronic Equipment |
| Wt./wt. | : Weight / weight as concentration |

Chapter 1

Introduction

Chapter 1: Introduction

Worldwide cement production was 4.1 billion tonnes in 2017 rising from 1.5 billion tonnes 20 years earlier^{1,2}. The vast majority of this cement is produced in Asia, specifically China followed by India, with this region accounting for over 80% of global production. Furthermore, growth is predicted rise by at least 4% in 2019³.

Gulf Cooperation Council (GCC) countries consist of six countries namely: the Kingdom of Saudi Arabia, State of Kuwait, Kingdom of Bahrain, State of Qatar, United Arab Emirates, and Sultanate of Oman. In the GCC region, the cement sector has grown sharply as a reflection of increasing construction activity in the region. The value of current and planned construction projects in the GCC region is approximately 2.41 Trillion USD^{4,5}.

The Sultanate of Oman, which has a population of approximately 4 million people⁶, announced a 116 billion USD construction project in 2013⁴. The sustained economic activities within the GCC, including considerable infrastructure investment are an indication of the size of the cement needed in the GCC region and specifically, in Oman.

Therefore, there is a need to increase cement production capacity, but, it needs to be done within the context of increasing environmental awareness. The cement industry contributes about 7% to global GHG emissions^{7,8,9}. Furthermore, producing one tonne of cement requires the consumption of approximately 1.6 tonnes of raw materials. Thus, there is a need to increase the use of waste materials and industrial by-products. There has been much research into how the cement industry can utilise such materials and much of the research is implemented successfully in the cement industry. However, the recycling concept is still not widely implemented in the GCC region. Most cement plants in the region are operated with virgin raw materials and fuel. Only a few of the region's cement plants use alternative fuels because fuels such as natural gas, diesel, and petcoke are cheap and widely subsidised by the government. However, when the price of crude oil fell in 2013, some governments, such as that of Oman, began raising the price of natural gas. For example, the price of 1 mmBtu of natural gas was fixed at 1.5 USD from 1985 to 2014 and then doubled to 3 USD in 2017^{10,11}, which led to a reappraisal of energy and raw material use in the GCC's cement industry.

Several types of industrial waste are not yet utilised, for example, Oil-Based Mud (OBM) cuttings¹²⁻¹⁹. OBM cuttings are produced during the oil well drilling process and contain oil, heavy metals, organic matter and soils. Drilling a single well can produce thousands of cubic metres of OBM cuttings²⁰. OBM is classified as a hazardous material in Oman²¹, with special storage specifications enforced by the environmental authority⁷.

OBM, also known as drilling fluid mud^{12,13,22}, is defined as the carrier of rock cuttings from the ground during the drilling process and comes in many forms. The fluid mud's main role is lifting the cuttings to the surface during the drilling process, allowing the drilling operation to go deeper into the earth²³⁻²⁵. Once the cuttings are collected at the surface, this mixture of drilling fluid and earth cuttings undergoes a segregation process to remove the cuttings so the fluid can be reused in the drilling process. This segregation step is repeated until the fluid can no longer be treated and is discarded. The discarded fluid is known as fluid-based mud cuttings, the composition of which depends on the type of fluid used. The type of selected fluid depends on the geological formation of the underground rocks. In many cases, water-based Mud²⁶ is used with the addition of oil to enhance the properties of the drilling fluid and optimise the drilling process. This fluid is known as oil-based fluid or oil-based mud. The mud discarded from this process is known as OBM cuttings and is collected in mud waste pits. The OBM cuttings are contaminated with oil, which makes them a potentially hazardous waste that should not be released into the environment.

OBM cuttings have several characteristics that could be utilised in the cement industry²⁷. The cuttings all contain calcium, silica, and alumina, which are essential in cement manufacturing. Also, the oil content gives the cuttings a calorific value and could help reduce fuel demand. From the perspective of the oil industry, using cuttings in cement manufacturing will provide an environmentally friendly waste management solution for this potentially hazardous waste. This is a welcome solution given the estimated 115,000 tonnes of OBM cuttings stored across Oman²⁸. The reported production rate and disposal of OBM cuttings are in the range of 300-500 tonnes per day and are expected to grow in coming years²⁹.

The objective of this study is to establish the effect of using OBM cuttings as raw material in cement manufacture, examining the impact on clinker and subsequent cement performance. The study provides knowledge of the primary factors that may

disturb or enhance the operation and performance of burning during the course of clinker preparation. Moreover, this study provides momentum for the oil drilling and cement manufacturing sectors to seize a recycling opportunity and maximise the utilisation of resources and by-products, such as OBM cuttings.

The scale of a cement plant means that this study has focussed on laboratory-scale production rather than on-site studies at a cement plant scale i.e. typically 60–150 tonnes per hour. A laboratory investigation allowed for clinker preparation using different mix ratios. The obtained clinker was tested via XRD, XRF, SEM-EDX, and free lime determination, as well as ground with gypsum using a tube ball mill to produce cement. The cement was tested according to appropriate standards (i.e., mechanical, physical, and chemical testing).

Chapter 2
Literature Review

Chapter 2: Literature Review

2.1 Industrial Hazardous waste in Oman

The annual rates of hazardous waste generation in the Sultanate of Oman, including industrial waste, healthcare waste, lubricant waste oil, lead acids batteries, Waste Electrical and Electronic Equipment (WEEE), and mineral waste, for 2012–2020 are presented in Figure 1. Different industrial waste materials are generated in Oman, however, although Oman has many environmental regulations, recycling of industrial wastes is not practiced in economic scale³⁰.

The forecast reveals that mineral waste generation is expected to increase sharply to more than 200,000 tonnes per year due to the high expectation of planned oil and gas exploration projects by Oman Government in the coming years³¹. Oman's economy is highly dependent on the oil and gas sector which comprises about 88% of the country GPA. The second large sector is the industrial sector, at 11% of the GPA³². Thus, as a result of the industrial activities, more waste generated.

The pie chart reveals that the four major waste types comprise 86% of Oman's total hazardous industrial waste generation. Each year, 115,000 tonnes of 'mineral waste' (33%), 98,000 tonnes of 'oil-waste–liquid and solid' (28%) 45,000 tonnes of 'waste electrical and electronic equipment' (WEEE) (13%), and 43,000 tonnes of 'fly ash dust from miscellaneous filter sources' (12%) are produced. Industrial mineral waste is the major waste source in Oman, with approximately 117,000 tonnes per year produced by petroleum companies, of which the major content is OBM cutting waste, consisting of drilling cuttings, natural sands, and clay contaminated with oil products. It is produced as a result of oil well drilling. Currently, OBM cuttings are stored at a site with a special storage arrangement without any further treatment or recycling.

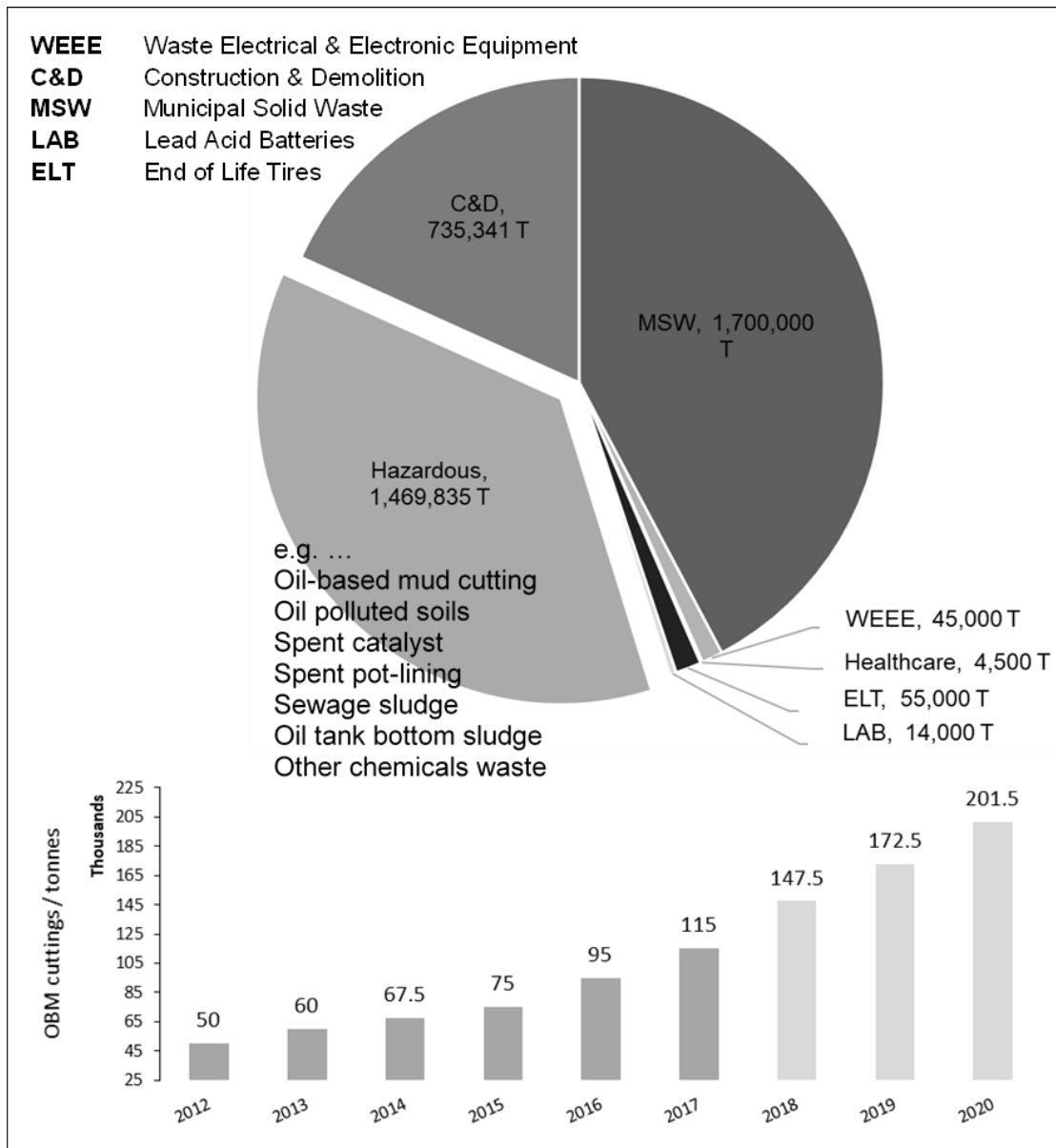


Figure 1 Industrial hazardous waste generation in Oman.

Pie chart (top) showing total annual industrial hazardous waste generation in Oman, in tonnes per year. Graph (bottom) showing OBM cuttings produced from 2012 to 2017 and the estimated amount of OBM cuttings that will be produced from 2018 to 2020 in Oman²⁸.

2.2 OBM waste generated from Oil Drilling Process

Various types of drilling fluid muds are produced by petroleum and oil drilling companies, and they are used as a carrier of rock cuttings from the ground during the drilling process. The main role of this fluid mud, as summarised in Figure 2, is lifting cuttings to the surface for disposal during the drilling process, which allows the drilling operation to go deeper. Once the cuttings are collected at the surface, this mixture of drilling fluid and earth cuttings undergoes a segregation process to remove the cuttings and allow the fluid to be reused in the drilling process. This segregation step is repeated until the fluid can no more be treated and can be discarded. At this stage, the fluid is known as fluid-based mud cuttings, the composition of which depends on the type. Several types of drilling fluid are used, and in some types, the mixture is used along with clay water, seawater or brine. In this case, it is known as water-based mud (WBM) or water-fluid mud (WFM). The type of fluid depends on the geological formation of the underground rocks. In many cases, WBM is used with the addition of oil to enhance the properties of the drilling fluid and optimise the drilling process. This fluid is known as oil-based fluid or oil-based mud. The disposed mud from this process is known as OBM cuttings, which are collected in a mud waste pit as depicted in Figure 3. OBM cuttings are contaminated with oil, making them a hazardous waste that should not be released into the environment without treatment and purification^{33–36}.

- Act as a carrier of cuttings from the hole that permits their separation at the surface.
- Maintain the stability of the well bore.
- Is non-damaging to the producing formation.
- Is cool and cleans the bit.
- Prevents the inflow of fluids from the well bore.
- Be non-hazardous to the environment and personal.
- Reduce friction between the drill pipe and well bore or casing.
- Form a thin, low-permeable filter cake.

Figure 2 The major functions of OBM during the oil-drilling process³⁷.

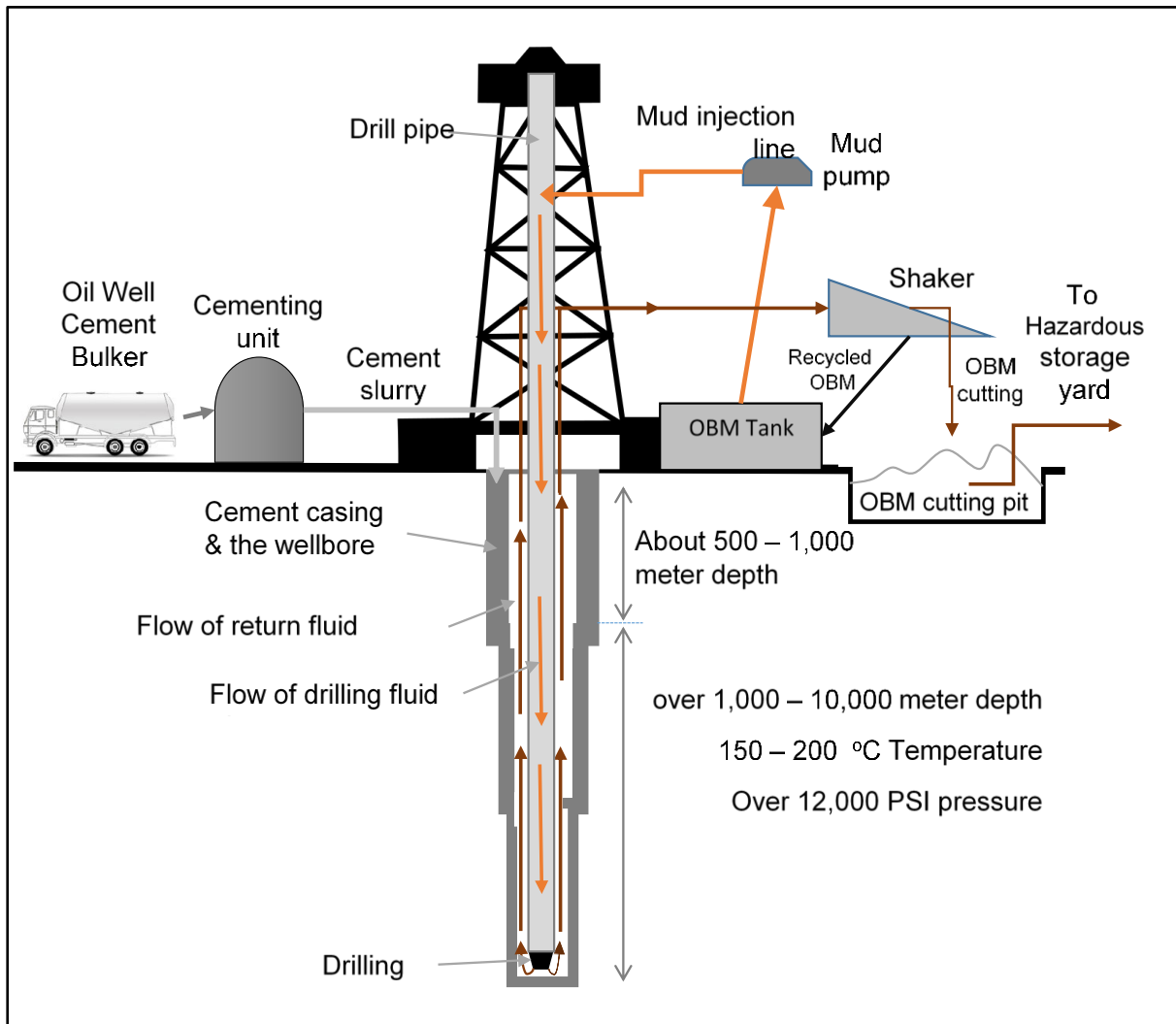


Figure 3 Schematic diagram of an oil well drilling operation.

Breuer et al.³⁸ reviewed the potential accumulation of OBM cuttings produced in the Northern and Central North Sea as a result of drilling operations in this area. The review emphasises that hydrocarbon concentrations in the drilling cuttings remain relatively unchanged over time, and the oil content of the cuttings is about 1%. Caen et. al.¹² describe the replacement of OBM, including synthetic-based fluids and water-based muds. Approximately 5–10% of the wells drilled worldwide use oil muds. However, new drilling fluids have been formulated to replace OBM, including polyalphaolefines, glycols, glycerines, and glucosides. These fluids have the characterisation of oil-based mud, but less handling is required when compared to water-based mud due to their biodegradability. Nevertheless, these fluids have some

limitations depending on the well's conditions and type of formation faced during the drilling process.

Al-Ansary et al.¹² conducted an experiment involving the pre-treatment of drilling cuttings using a stabilisation/solidification method before the discarded cuttings were sent to landfill or re-used in construction projects; the 92/2 and 2000/3 Oslo and Paris Commission Decisions prohibit drill cuttings containing more than 1% oil from being discharged at sea. Samples of drilling cuttings were collected from the North Sea, where an estimated 50,000–80,000 tonnes of drilling cuttings are produced annually. The researchers prepared several samples of drill cuttings mixed with binders, including Portland cement, lime and blast-furnace slag, microsilica, and magnesium oxide cement, to remove the oil content and reduce leachability. The leachability results showed a decrease in release of the synthetic drill cuttings to produce a stable, inert hazardous waste which was found to meet the United Kingdom's specifications for non-hazardous landfills. Furthermore, the 30% blast-furnace slag with Portland cement binder successfully reduced the leached oil concentration.

Khanpour, et al.³⁹ studied an extraction method using supercritical CO₂ to remove the oil from OBM. It was found that the best conditions for removing the oil were at a temperature of 333 K, pressure of 180 bars, flow rate lower than 0.1 cm³/s, and static time of 110 min. SEM and XRD testing confirmed the successful removal of contaminants from the drilling mud without significant crystalline modification.

Eldridge, R.B.³³ conducted pilot-plant experiments and separated oil from OBM using HFC 134a, which is the commercial name for 1,1,1,2-tetrafluoroethane, and propane for supercritical solvent extraction. The objective of the trial was to reuse the contaminated OBM in the drilling operation and provide an economical, environmentally friendly recycling solution. The results reveal that the technique is technically sound and economically viable.

Hou et al.⁴⁰ and Jiang et al.⁴¹ successfully used a separation technique to recover oil from OBM cuttings using an oil recovery agent consisting of a demulsifier compound (15% of the demulsifier AE136 + 15% of the demulsifier AP113) (30%), a coagulant, such as CaCl₂ or AlCl₃ (1.5%), and the flocculant PAM at a concentration of 0.1% (2%). The rate of recovery was found to be greater than 90%, producing recovered oil

that met China's diesel fuel quality standard specifications⁴² (i.e., GB252-2000 and GB/T 19147-2003).

Amani et al.⁴³ conducted a comparative study of OBM and WBM produced by drilling oil wells using high pressure and high-temperature conditions. OBM and WBM both have several characteristics that meet the requirements for high pressure and high temperature well drilling. This establishes engineering guidelines that could be used to decide the most suitable mud for a drilling operation. High temperature and high-pressure conditions arise when the drilling depth is greater than 4,000 metres, where the temperature is about 150 °C and the pressure is 69 MPa. These conditions can impact the rheological properties of the mud. Amani et al. suggest using OBM for HPHT drilling conditions with temperatures up to 205 °C based on the laboratory experiment conducted.

Young et al.³⁶ used the rotary retort distillation technique for the removal of oil from oil-based mud (OBM) to facilitate onsite disposal of the waste in offshore oil rigs after reducing the oil in the cuttings to environmentally acceptable and safe limits. The treatment process was established to process 15 t/h of oil-based cuttings. The resultant products were tested for toxicity and metal leachates. The energy consumption for an offshore rotary retort distillation unit was estimated; moreover, the reliability, minimum environmental impact, wear rate, and safety of the operations were analysed. To determine the required specifications for improved operation, a bed temperature of 427 °C using natural gas fuel was calculated based on the plot of the weight ratio of the solids (in percentage) versus the bed temperature of the cuttings. A two-stage vapour-recovery system was used to recover the evaporated hydrocarbons by means of purging with nitrogen sweep gas to ensure oxygen-free atmosphere. Heavier oil and particulates were collected in the first condenser, while light oils and water were collected during the second stage. The treated solid waste was disposed of directly to the ocean floor after ensuring that it met the environmental requirements. The author concluded that this rotary retort distillation process provided a mature and highly dependable method with lower energy use for the treatment of OBM waste³⁶.

Abbe et al.⁴⁴ used a vitrification and sintering/crystallisation process to convert dried drill cuttings into amorphous glass. A mixture of dried drill cuttings, sodium, and calcium oxide in a weight ratio of 8:1:1 was blended and thermally treated at

approximately 1300 °C for 5 h, and subsequently cooled to obtain an intermediate amorphous solid. This amorphous solids were further treated thermally at approximately 750 to 800°C to produce glass-ceramic. The drill cutting waste used contained 60% to 80% solid rocks, 8% organic matter, 6% minerals, and clay with used drilling liquids. This vitrification process immobilised the waste owing to the melting process favouring the entrainment of potentially hazardous components, thereby preventing these from leaching out. The authors tested the properties of the produced glass-ceramic for its potential use by studying the hardness, fracture strength, fracture toughness, and stability towards leaching. It was concluded that the glass-ceramic had almost zero porosity, with attractive mechanical properties for possible applications as building material⁴⁴.

Oreshkin et al.⁴⁵ investigated the disposal of drilling waste sludge to produce building materials. The mineral composition of the studied drilling sludge mainly consisted of quartz and minor quantities of carbonates including calcite, aragonite, dolomite, and aragonite. The average particle size was in the range of 20 to 30 mm and constituted 50% to 60% of the total weight. The introduction of sorbents and cement along with drilling sludge rendered harmless building material that could be used in the production of brick and small building products. The cement, sorbent, and drilling sludge mixed with water could support the system with a high pH (up to 12). Furthermore, the heavy metal ions from the drilling sludge passed into insoluble compounds, leading to the binding and neutralisation of environmentally toxic heavy metals following subsequent curing. This disposal technique enables ecological improvement and can aid in the restoration of the natural environment⁴⁵.

Hou et al.⁴⁰ used coagulants and flocculants for oil recovery to enable useful recycling and the safe disposal of oil-based drilling fluids containing oil, heavy metals, and organic pollutants. A recovery rate of over 90% was achieved, and the quality of the recycled oil met the requirement of –10# diesel. In the experiment, the authors used compound demulsifier mixtures that were mainly composed of polyoxyethylene polyoxypropylene ethyleredi-amines (AE) and polyoxypropylene polyoxyethylene polyoxypropylene- five ethylenes six amines (AP) demulsifiers, along with industrial coagulants and flocculants. The composition of the oil-recovering agent formula recommended by the author was 30% demulsifier compound, 1.5% coagulant, and 2% flocculant. The residual sludge was used in the construction of a well-site

cofferdam and the roads of the well site. The concentrations of the oil, chemical oxygen demand (COD), and heavy metals were tested in the processed mud and confirmed to be within the accepted range. The water used for the treatment process was tested after the operation and was found to meet the requirements of general emission levels for sewage⁴⁰.

Nahmad et al.⁴⁶ used a combination of chemical, physical, and biological processes to treat non-aqueous fluids such as OBM and synthetic-based muds. Total petroleum hydrocarbons (TPH) of up to 22% were used for the testing, in which the TPH was reduced to less than 1% as per the country regulations for disposal. The team named the process Free-RAD© and demonstrated it as an economically superior process for dealing with wastes. By using highly reactive free radicals, the complex hydrocarbons and organic compounds could be decomposed into lighter molecules such as CO₂ and H₂O. The steps involved in the process comprised hydrocarbon decomposition into CO₂ and H₂O by introducing free radicals, followed by the addition of UV-receptive minerals to promote rapid photodecomposition, and finally, the addition of organic compost to promote bioaugmentation. The authors concluded that the final threshold period for this decontamination process was 22 weeks, and conducted final tests as a remediation process to be used for bearing crops⁴⁶.

Gogan et al.⁴⁷ studied the properties of carbonate OBM cuttings (COBMC) as activated mineral powder when used as an asphaltic concrete mix for road construction following thermal treatment at 340 °C (Gogan et al., 2014). The physicochemical properties such as the water content, hydrocarbons, ash, pH, density, flash point, and COD were determined for the thermally treated COBMC, and based on the results, their suitability for the project was confirmed. According to the specified density and strength of the asphaltic concrete mix, the mineral powder COBMC was mixed with bitumen in varying proportions, and the team confirmed 7 wt.% of COBMC as optimal for use. Using the mix, a motor road was laid with a layer of 5 cm thick and 6 m wide by means of conventional methods. After one month of regular inspection, the team recommend the use of COBMC as a mineral component for road construction, which may provide a solution to critical environmental problems⁴⁷.

A case report by Helmy and Kardena⁴⁸ discussed significant problems faced by Indonesian oil and gas industries regarding environmental management systems

towards effective and responsible waste handling, disposal, and the minimisation of waste generation to reduce potential harm to health and environmental problems. Among the generated wastes, crude oil-contaminated soil, bottom sludge, abandoned sludge pits, burial oil sludge, and produced water were considered as the most abundant by these authors. Bioremediation and co-processing techniques applied for treating oil sludge and produced water included the common practice of gravity-based separation and discharge into water bodies. The oil sludge types were characterised as oil sludge and oil-contaminated soil, with the standard practice for treatment identified as landfarming bioremediation. Laboratory-level data were studied for the oily sludge with oil contents up to 320 g TPH/kg soil using different treatment steps such as soil washing, biodegradation, and biosurfactant treatments. A significant TPH reduction was achieved, with the highest removal efficiency reaching 85%. The authors concluded that the lack of established waste management facilities restricts proper waste disposal, which can be addressed by constructing the necessary facilities. Although this approach is expensive for oil and gas industries in the short term, it can minimise long-term liabilities⁴⁸.

Mostavi et al.⁴⁹ investigated the use of drill cuttings as a partial replacement for cement in concrete structures. The study considered this approach to be not only cost-effective, but also as offering the potential to reduce environmental impacts caused by waste. Laboratory-level studies were carried out by the team based on the compressive strengths of concrete samples and the chemical compositions of the drill cuttings used. The results indicated that the replacement of 5% of cement with drill cuttings reduced the concrete compressive strength by 10%. A further increase in the drill cuttings in the cement concrete by 10%, 15%, and 20% resulted in a strength reduction of 20%. Moreover, the effects of additives such as fly ash and silica fume in this cement mix were studied, and it was concluded that these materials had a significant influence on the compressive strength. The drill cutting particle size distribution was studied, and it was found that the maximum grain size was less than 6 mm, while the coefficients of uniformity and curvature were 8.63 and 1.22, respectively, which classified the particles as fine aggregates in accordance with ASTM C330 for cement concrete mixes. The test specimens used in the study were obtained from five separate batches of concrete, including one control sample and four different combinations containing drill cuttings, fly ash, silica fume, and a mixture of

silica fume and fly ash. Crushed limestone passed at 100% in No. 3/8-inch sieves was used as the coarse aggregate for the study. The authors concluded the optimal mix proportion was 20% drill cuttings with 7.5% silica fume and fly ash, which could increase the compressive strength by 40%⁴⁹.

Shon et al.⁵⁰ used modified drilling waste material (MDWM) with cement in the laboratory as the base-course material in roadway construction. The production of the MDWM from drilling waste mud (DWM) involved various steps. In the first step, water was separated from the drilling mud, following which centrifuges were used for the additional removal of oil contaminants. The second step involved the stabilisation and solidification processes using cement as a binder, which reduced the free movement and minimised the mobility of the pollutants in the waste. The preferred aggregate-to-dried DWM ratio for producing the MDWM was 3:1, with 12% of cement kiln dust added to the mixture. The laboratory-level investigation, in which the MDWM mixture was treated with 3% cement, demonstrated that the material satisfied the requirements for Class M base, with 7-day compressive strength and a minimum of 1225 kPa⁵⁰.

Drilling waste from oil companies that contains toxic polyaromatic hydrocarbons and that was treated using the thermal desorption technique was studied by Piazza et al. (2017)⁵¹. The drill cuttings treatment using this technique was investigated and recommended as the most effective, economical, and environmentally friendly. The indirect thermal desorption treatment was not only found to be safer, minimising the pollution compared to direct heating, but also allowed for recovery without destroying hydrocarbons owing to controlled heating, and the recovered oil was reused for producing fresh OBM. The recovery of hydrocarbons and recycling could reduce the stress on the environment and avoidable economic loss. Approximately 20,000 bbl of oil was recovered using the process, and the endeavour was selected for the Six Sigma Green Belt project⁵¹.

Benlamoudi and Abdul Kadir ⁵² studied the role of petroleum sludge (PS) as a setting retarder in cement, replacing conventional gypsum. The CaO and SO₃ percentages of the PS used in the study were 25.05% and 38.41%, respectively, which aided in delaying the flash setting of the cement. Four different samples were prepared by the team with PS percentages of 0%, 1%, 3.5% and 5%, along with gypsum and cement clinker. Prior to the trial study, the PS collected from the oil drilling field was burned in an industrial kiln to eliminate the organic hydrocarbons and then grinded to pass

through a 1 mm diameter sieve. As per the guidelines for using inductively coupled plasma mass spectroscopy for the leaching behaviour of heavy metals from PS, the results did not exceed the regulatory limits for cement, except for the lead, which exhibited 149.02 ppm for the maximum percentage of cement produced against the statutory limit of 75 ppm. The study concluded that the addition of 5% PS to cement could achieve effective results, and can be used as a replacement for gypsum in cement grinding⁵².

Shon and Estakhri⁵³ used MDWMs and seashells as a base material for road construction, and compared the performance with conventional gravel base-course material. Experiments were carried out on field-cored samples using non-destructive tests including ground penetration radar, falling weight deflectometry, dynamic cone penetration, and rusting tests to evaluate the performance. For the cored samples, further properties such as the moisture content, dry and wet density, stiffness and seismic modulus, unconfined compressive strength, and modulus of rupture were evaluated. Using the MDWM waste materials, 91.44 m of roadway was paved for the study, and based on the field performance, the author recommended the materials for use as embankments, subbase materials, patching materials, base materials for low-volume roadways, shoulders, and bases for maintenance activities⁵³.

In their research, Ayati et al.⁵⁴ investigated the technical feasibility of waste drilling oil cuttings into lightweight aggregate (LWA) for construction work. Pre-treated drill cuttings were pelletised with the addition of 25 ± 2 wt.% water and formed into spherical pellets of 7 and 14 mm in size. Owing to the high concentration of chloride, the author recommended washing the pre-treated oil drillings prior to the heat treatment process to reduce the leaching effects. The green pellets were then subjected to thermal treatment at temperatures between 1160 and 1190 °C in a muffle furnace at a rate of 10 °C/min. The produced LWAs were tested for physical properties including their water absorption capacity and compressive strength, and a mineralogical study was conducted using optical microscopy and X-ray diffractometry. The results were compared with the properties of existing commercial products, demonstrating a particle density of 1.29 g/cm³, water absorption of 3.6%, and compressive strength of 4.4 MPa. The mineralogical study of the LWA confirmed that the main composition following thermal treatment was CaMgSi₂O₆. The authors

concluded that an industrial-scale study would be required for commercial production⁵⁴.

2.3 Shifting from WBM to OBM in Oman

In Oman, oil production declined gradually from 970,000 barrels per day in 2000 to 710,000 barrels per day in 2007^{55,56} due to many technical issues encountered during the well drilling process. The vertical depth of the well was about 4,500–4,800 metres, where tight sandstone and dolomitic limestone with thick mudstone were encountered, which caused the bore hole to become unstable^{57–60}. Furthermore, drilling these complex formations takes longer, slowing the production rate. After intensive studies, the drilling companies implemented several measures to improve the situation, including switching from WBM to OBM because this type of geological formation and drilling conditions require a higher mud weight to maintain the overbalanced drilling^{59–61}. As a result, the drilling time was reduced by 25 days, which saved about 1.25 million USD per well⁵⁷.

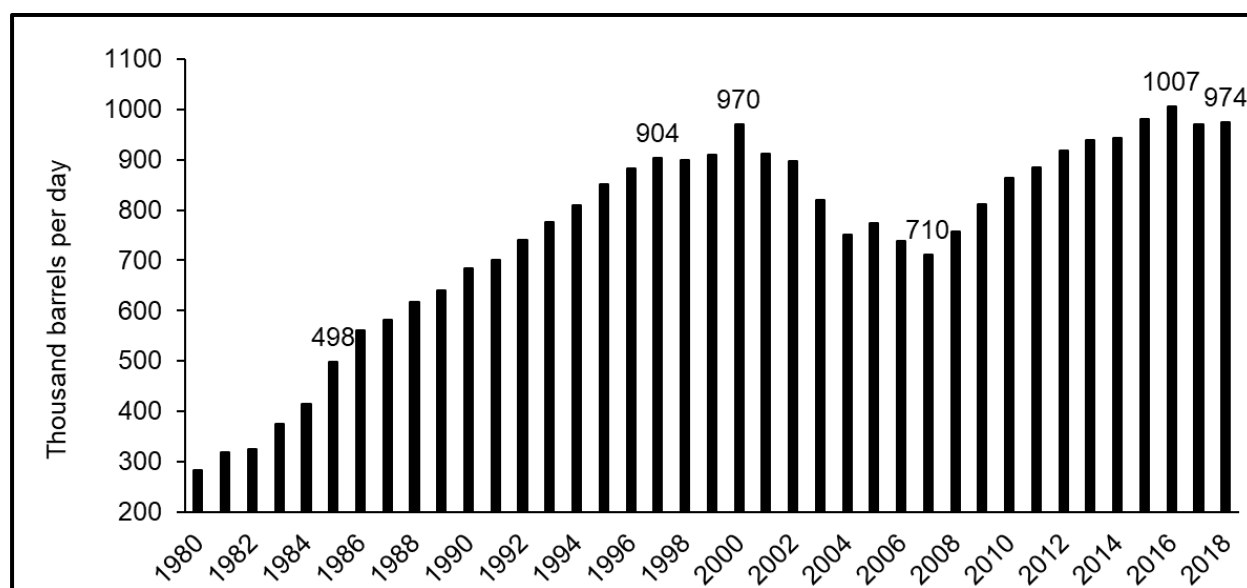


Figure 4 Crude oil production in Oman from 1980 to 2018

(USEIA and BP^{55,56})

2.4 Waste as raw materials for clinker production

Bernardo et al.⁶² tested the burnability of kiln feed using OBM cuttings as additives, partially replacing limestone and clay in the kiln feed. The test was conducted at the

plant scale by preparing two types of kiln feed mixtures and making comparisons to clinker produced without OBM cuttings. The kiln was run for 10 days for each mixture. The researchers successfully achieved a replacement of 30% of limestone (mixture 1) and 44% of clay (mixture 2). The burnability indices (BI*) were 10.7 (mixture 1), 44.2 (mixture 2), and 19.8 (the reference mixture). According to Bernardo and et al.⁶², BI values lower than 60 indicate very satisfactory burning behaviour. The phase composition of the prepared clinker, calculated according to the Bogue formulae, was found to be within the range expected for conventional clinker phase composition. In addition, the mechanical, physical, and chemical parameters of Portland cement were also found within the specified range in the European standard for cement: EN197-1:2011. The Bogue formulae calculate approximate clinker contents based on chemical analysis. Other methods, such as X-ray diffraction, provide more precise results. Nevertheless, Bogue formulae afford fast, easy estimates which may be used in the preparation of the mix in clinker preparation. Most cement plants depend highly on this calculation.

The testing of cement properties (mechanical, physical and chemical) are necessary to ascertain cement quality, with testing in accordance with standards such as ASTM and BS/EN, as presented in Chapter 7 Table 15. During the trial test, the pollutant concentration in the exhaust gas for waste-based clinkers was measured and compared to the calculated limiting value according to the formula stated in Table 1.

Table 1 Pollutant concentration in exhaust gas⁺ from waste-based clinker⁶² in mg/Nm³.

| Pollutant | Mixture 1 | | Mixture 2 | |
|------------------|------------------|----------------|------------------|----------------|
| | Measured value | Limiting value | Measured value | Limiting value |
| TSP | 22.00 | 27.46 | 21.40 | 24.00 |
| SO ₂ | 0.98 | 87.07 | 0.65 | 79.75 |
| CO | 92.00 | 98.06 | 88.00 | 98.44 |
| HCl | 2.00 | 4.25 | 2.50 | 5.39 |
| HF | 0.70 | 1.17 | 0.60 | 1.34 |
| Cd+Ti | 0.03 | 0.08 | 0.04 | 0.07 |
| Hg | 0.04 | 0.08 | 0.03 | 0.07 |
| Sb+As+Pb+Cr+Co+ | 0.19 | 0.43 | 0.29 | 0.43 |
| Cu+Mn+Ni+V+Sn | | | | |
| TOC | 8.90 | 9.80 | 8.20 | 9.84 |

Pollutant Concentration
According to ⁶²

$$C = \frac{A_{waste}C_{waste} + A_{process}C_{process}}{A_{waste} + A_{process}}$$

A_{waste} : % mass flow rate of the waste
 C_{waste} : Pollutant maximum allowable concentration in the exhaust gas when waste alone is used ($A_{waste} = 100\%$; $A_{process} = 0\%$)

$A_{process}$: % mass flow rate of the reference
 $C_{process}$: Pollutant concentration in the exhaust gas measured when no waste is used ($A_{waste} = 0\%$; $A_{process} = 100\%$)

*BI : the burnability Index, $BI = \frac{A+B+2C+3D}{\sqrt[4]{A-D}}$, where A,B,C, & D are the free lime content in % wt/wt. in raw meal burnt at 1350, 1400, 1450 & 1500 °C respectively. A low BI value indicate good burnability⁶²
+The fuel used in the cement plant of the study is natural gas only.

Abdul-Waha et al.⁷ studied the impact of adding OBM on CO₂ emissions in a cement plant using only natural gas as fuel. The main objective of the study was to determine the impact of replacing limestone used in cement manufacturing on carbon dioxide gases emissions. The study was completed in three parts. First, the amount of CO₂ emitted from the operation of a known cement plant in Oman was calculated using data collected from the plant in 2013, including calcination, fossil fuel combustion, power generation, and emissions from activities related to limestone transportation by heavy vehicles. Next, limestone was replaced with OBM at different percentages (0–5%), and the resultant CO₂ was calculated for each OBM percentage. Finally, the CO₂ emissions were forecast for each kiln in the plant and CO₂ dispersion to the surroundings were projected using an advanced integrated modeling system comprised of the California PUFF-Weather Research and Forecasting model (WRF/CALPUFF*)^{63–65}.

*WRF/CALPUFF is a type of simulator software designed and produced by Exponent® and has the ability to predict and forecast the air concentrations of various pollutants emitted during the operation of an industry based on specific input parameters.

Table 2 Total CO₂ emissions from plant sources after the addition of OBM⁷.

| OBM % | 0% | 1% | 2% | 3% | 4% | 5% |
|-----------------|--|--------|--------|--------|--------|--------|
| | CO ₂ emissions per tonne cement (Kg/ tonne) | | | | | |
| Calcination | 442.84 | 437.47 | 432.11 | 426.74 | 421.38 | 416.01 |
| Fuel combustion | 181.62 | 181.62 | 181.62 | 181.62 | 181.62 | 181.62 |
| Power plant | 47.29 | 47.29 | 47.29 | 47.29 | 47.29 | 47.29 |
| Vehicular | 1.92 | 1.92 | 1.92 | 1.92 | 1.92 | 1.92 |
| Total* | 673.67 | 668.30 | 662.94 | 657.57 | 652.21 | 646.84 |

*The CO₂ emissions are lower than in many reported studies because the cement plant uses only natural gas as fuel.

CO₂ emissions before and after the OBM cutting addition are shown in Table 2 and Table 3. The total amount of CO₂ emitted was 673.67 Kg CO₂/tonne of produced cement. The major source of CO₂ emissions (442.84 Kg CO₂ /tonne cement, 65.74% of other sources) was the calcination step of the raw meal which consists of approximately 82.54% limestone. The CO₂ emitted due to calcination decreased as the OBM percentage increased (Table 2).

The lowest CO₂ emissions were at 5% OBM with 416.01 Kg CO₂ per tonne cement. The result obtained from the modelled CO₂ concentrations in the calcination step using the WRF/CALPUFF simulator showed a decrease in CO₂ emissions as a result of adding OBM cuttings (Figure 5). They concluded that due to high CO₂ emissions from the cement manufacturing process, mainly from the calcination reaction, adding OBM to raw materials in the cement plant could be a viable way to safely dispose of OBM cuttings without reducing cement quality⁷.

Table 3 Calculation of CO₂ emissions from cement-plant sources before and after the addition of OBM⁷.

| OBM cutting | Limestone consumption (T per year) | Clinker production (T per year) | CO ₂ from raw meal (T per year) | CO ₂ per tonne of clinker (Kg per T) | CO ₂ per tonne of cement (Kg per T) |
|-------------|---------------------------------------|------------------------------------|---|--|---|
| 0% | 2,542,301 ⁱⁱ | 1,875,901 | 889,805 | 474.33 | 442.84 |
| 1% | 2,511,502 | 1,875,901 | 879,026 | 468.59 | 437.47 |
| 2% | 2,480,702 | 1,875,901 | 868,246 | 462.84 | 432.11 |
| 3% | 2,449,903 | 1,875,901 | 857,466 | 457.10 | 426.74 |
| 4% | 2,419,103 | 1,875,901 | 846,686 | 451.35 | 421.38 |
| 5% | 2,388,304 | 1,875,901 | 835,906 | 445.60 | 416.01 |

ⁱ Loss on ignition at 950 °C is 35%.

ⁱⁱ This figure is the actual limestone consumption during 2013 collected from Oman Cement Company.

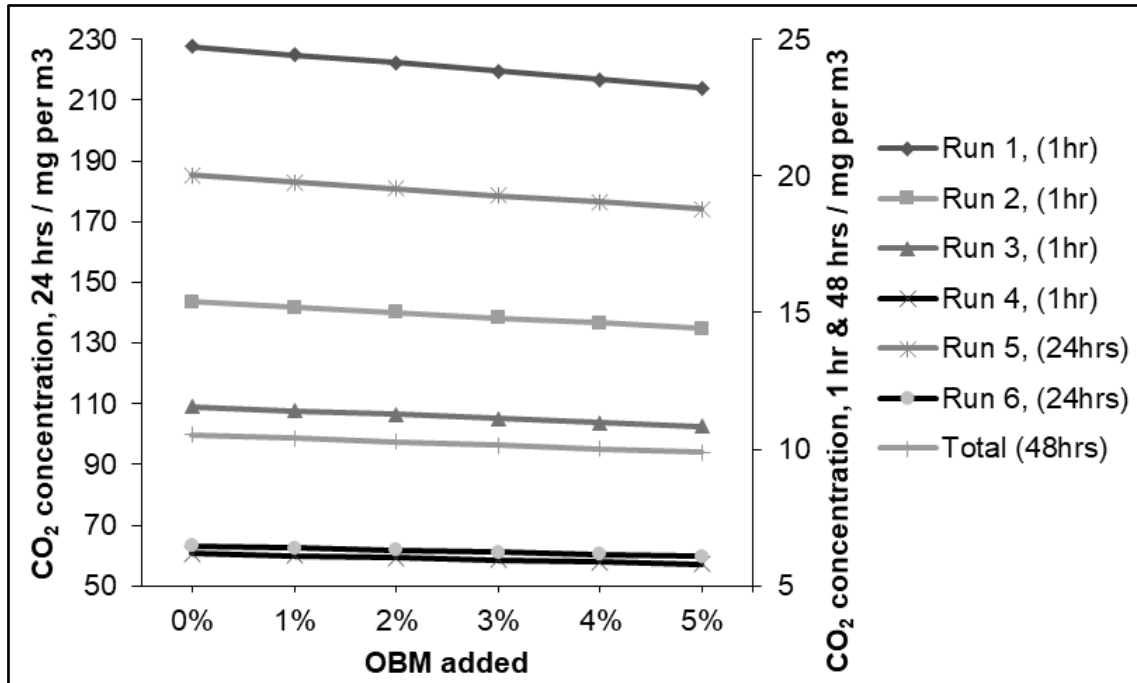


Figure 5 CO₂ emission concentrations calculated by atmospheric modelling⁷.
(Using the WRF/CALPUFF modelling system)

Chapter 3

Description of the problem

Chapter 3: Description of the problem

3.1 The impact of OBM cutting generated in Oman

Currently, the options for treating OBM cutting waste are very limited, and it is often simply stored in a lined pit, awaiting further treatment. Because OBM cuttings are classified as a hazardous waste, the Government of Oman is keen to find a suitable waste management solution. Fortunately, the mineralogical composition of OBM cutting waste and the presence of organic residues from the crude oil make it potentially useful in cement clinker production. In fact, the challenges of cement manufacturing in Oman is the raw materials' chemistry, specifically, the availability of raw materials rich in silica. The limestone is high-grade, which means its silica content is very low. However, raw meal must be approximately 14% silica, and effective raw meal preparation in the cement factory requires silica additives. The most common silica-containing raw material used in most cement plants is sand. Quartz is another option, widely used in many countries, including Oman. However, the quartz (quartzo-phillite rock) reserves in Oman are very limited and have very high free silica content, and making it reactive requires increased energy consumption. It may also lead to operational problems during pyroprocessing due to the higher concentrations of alkalis and chloride compared to other raw materials.

When OBM cuttings, are analysed, they are found to contain significant quantities of calcium oxide (CaO) and silicon dioxide (SiO₂). They are also saturated with oil and residual crude oil. The presence of these inorganic constituents makes drilling waste a suitable material for cement manufacturing as they are also the basic oxides required in the cement industry, where the cement clinker is made from raw materials of limestone (CaCO₃) that is rich in calcium oxide (CaO). Hence, theoretically, OBM cutting waste can be used as an alternative to lime-based materials for clinker production.

3.1.1 Economic impact

As predicted by Be`ah Oman ⁶⁶, it is projected that oil and gas exploration in Oman will increase sharply in the coming years, at least until 2030^{67,68}. This will cause more OBM to be produced, which will lead to more OBM cutting generation. Handling OBM cutting is very expensive, requiring special isolated pits. The cost of one pit is about

260,000 USD for the storage of about 10,000 tonnes of OBM cuttings²⁹. Treating of OBM cutting to remove the contaminated oil is also very expensive. The cost of this treatment is in the range of 150–200 USD per tonne, which is too expensive compared to disposal in cement manufacture, which only costs 8 USD per tonne¹⁰. To date, there are no disposal facilities or treatment plants for hazardous materials in Oman.

3.1.2 Environmental impact

The emission of greenhouse gases (GHG) is one of the major serious environmental pressures on industry to improve operational processes. In Oman, the major source of GHG is from the oil and natural gases activities, mainly the result of energy extraction, oil drilling, and electricity generation^{69,70}.

The fast growth of oil and gas activities, rapid industrial growth, and construction development in Oman have contributed significantly to increased GHG emissions as shown in Figures 6 and 7. Estimated GHG emissions due to natural gas consumption or related activities are in the range of 50–400 million m³. However, because of a rapid increase in activity involving natural gas, emissions have also increased, beginning in 1989 and increasing progressively until 2018. Correspondingly, GHG emissions associated with oil production and consumption have increased annually as can be seen in Figure 6. Consequently, the increase in GHG emissions has impacted daily life in Oman. Furthermore, climate change, which is causing more severe heat waves, and poorer air quality due to population density are hazardous to the population's general health⁷⁰.

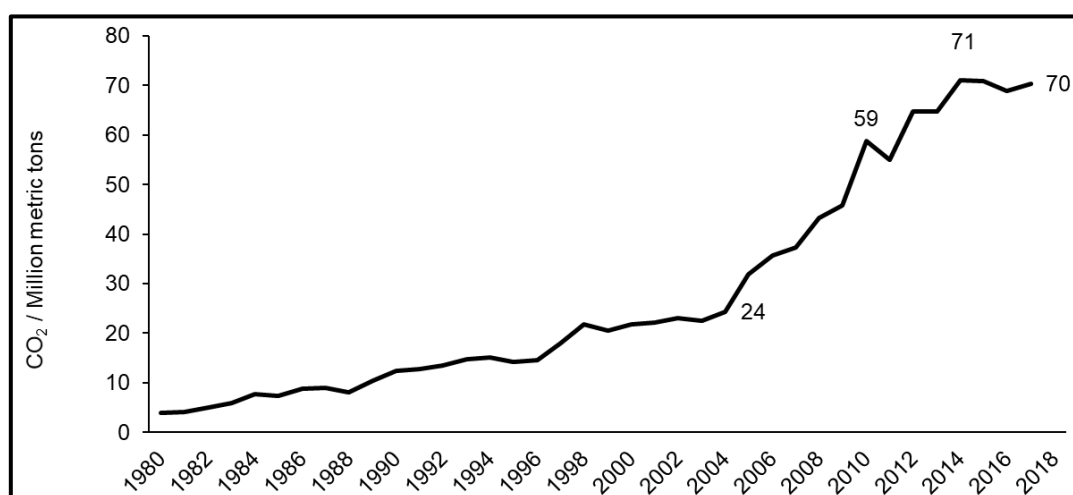


Figure 6 CO₂ emissions from energy consumption in Oman^{55,56}

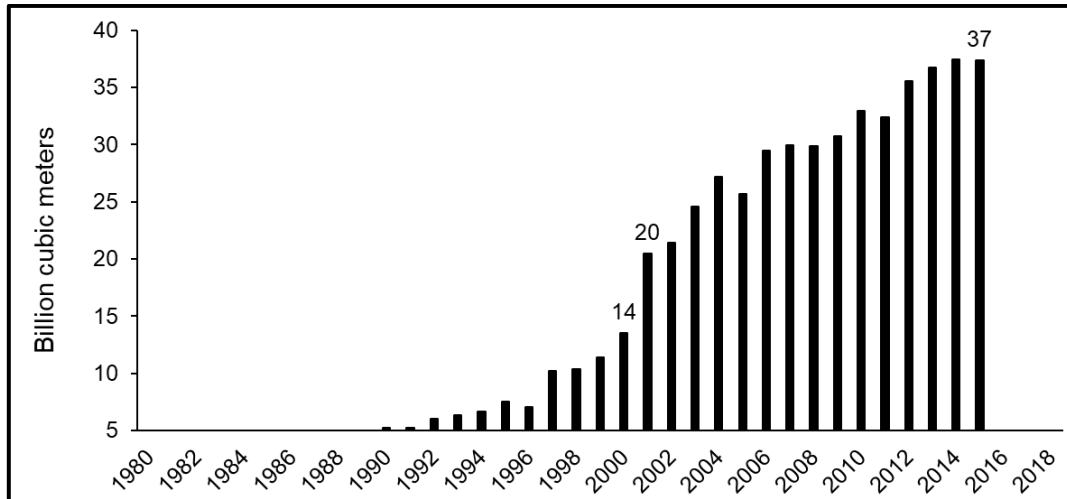


Figure 7 Gross natural gas production in Oman^{55,56}

3.2 Possible solutions for disposal of OBM cutting in cement industries

The disposal of such a large quantity of this solid drilling waste is expensive as it requires a lot of land and causes a number of serious environmental problems. The waste can easily contaminate soil and groundwater when the hydrocarbons and other chemicals leach into the earth. One promising strategy to reduce the threat of hazardous waste and diminish its accumulation in disposal sites is utilising it in other industries. From the viewpoint of recycling, this can be considered a sustainable approach to waste management and may reduce the amount sent to final disposal.

The experimental findings of this project are anticipated to play a primary role in recycling drilling waste and eliminate the cost of its disposal and, thus, avoid the contamination of soil and groundwater in Oman. Therefore, specific attention is paid to the use of OBM cutting waste in cement manufacturing as additional raw materials. Furthermore, this will result in reducing the consumption of a considerable amount of natural resources, such as limestone and natural mineral additives, in Oman. It will be a change towards diverting drilling waste from landfills and nil waste disposals, as well as a chance to develop cement manufacturing processes that are more sustainable and less damaging to the environment.

Different types of waste materials can replace primary raw materials in the cement industry. This will contribute to economic goals in reducing cost, reducing environmental impact and saving natural resources. The economic aspect is reflected in reducing the need for additional construction of costly new engineering storage areas that have high environmental regulation standards. Other costs are also reduced, such as handling, transportation and environmental monitoring. The accumulation of OBM cuttings with increasing oil exploration and production will lead to increased requirements for constructing new storage facilities. In general, industrial waste may be accepted as fuel; additional raw materials must add value to the cement manufacturing by generating caloric value as fuel to replace expensive energy or as feedstock to replace the raw materials in the cement industry.

3.3 Use of OBM cuttings as raw materials in clinker manufacturing

Utilising this drilling waste as a partial substitution for limestone in cement manufacturing will reduce the consumption of limestone considerably, thus reducing abiotic depletion. Due to the chemical composition of OBM cutting waste, it could, theoretically, be used to replace limestone (Table 4) and supplement some of the principal elements in the process of clinker phase formation, such as calcium, silicon, and aluminum. The calorific value of OBM cutting waste also makes it a valuable component in reducing the thermal energy requirement of clinkerisation, which reduces the amount of fuel used during clinker manufacturing.

Table 4 The chemical composition of limestone, quartzo-phillite, and OBM cuttings⁷¹

| Oxide | Limestone* | | Quartzo-phillite [#] | | OBM Cutting ⁺ | |
|--------------------------------|------------|-------|-------------------------------|-------|--------------------------|--------|
| | Wt./Wt. % | | Wt./Wt. % | | Wt./Wt. % | |
| SiO ₂ | 5.94 | ±1.69 | 74.25 | ±4.84 | 19.00 | ±15.11 |
| Al ₂ O ₃ | 0.62 | ±0.19 | 5.49 | ±0.97 | 3.66 | ±1.96 |
| Fe ₂ O ₃ | 0.51 | ±0.18 | 5.53 | ±1.15 | 1.67 | ±0.54 |
| CaO | 50.86 | ±0.95 | 4.01 | ±0.95 | 34.06 | ±10.47 |
| MgO | 0.48 | ±0.14 | 4.09 | ±1.67 | 2.94 | ±1.07 |
| SO ₃ | 0.13 | ±0.10 | 0.03 | ±0.01 | 1.92 | ±0.83 |
| Na ₂ O | 0.05 | ±0.01 | 1.22 | ±0.22 | 0.89 | ±0.36 |
| K ₂ O | 0.07 | ±0.04 | 0.68 | ±0.16 | 0.61 | ±0.19 |
| LOI @950 | 39.51 | ±0.93 | 3.99 | ±1.96 | 34.07 | ± 1.10 |

* Average 10 samples, Mn₂O₃ 0.02%, TiO₂ 0.04±0.01%

Average 13 samples, Mn₂O₃ 0.19 ±0.08%, TiO₂ 0.51±0.11%

+ Average 20 samples, 5.96±3.23 % moisture.

The formation of the major clinker phases, such as alite and belite, are controlled by the heat conditions, as well as the raw meal chemicals and their physical properties. In this study, the raw meal is prepared with different percentages of OBM to investigate the effect on clinker quality after replacing raw meal with OBM. Using drilling waste to replace a major raw material in cement production is an ideal solution, especially since the consumption of limestone is high. For example, the cement plant in Oman has been designed for the consumption of approximately 13,000 tonnes of raw materials per day. If 1% of the raw material is replaced by drilling waste, then the rate of consumption of this waste is approximately 130 tonnes per day, or about 39,000 tonnes per year, assuming 300 operational days per year.

The main objective of the proposed research is to study the effect of using drilling waste as partial replacements of natural raw materials in a cement plant. The study focuses on the use of drilling waste (OBM cuttings) to replace a portion of the raw materials used in cement manufacturing. Figure 8 shows the steps involved in producing OBM and demonstrates the proposed recycling process in the manufacture of different types of cement. In this work, OBM cuttings will be mixed, at different proportions, with the raw materials used to produce cement. The effects of this addition can be studied by designing and conducting laboratory experiments that will help detect how cement performance is impacted by adding this type of waste during the manufacturing process.

This research is based on manufacturing cement in the lab. Drilling waste will be added, at varying proportions, that are proportional with the operations and conditions of the cement plant in Oman. The influence of this waste addition will be investigated to examine its effects on cement products and determine how much OBM cutting waste can be added to the raw materials used in the cement industry without affecting the product's quality. Figure 8 shows different process activities involved in operating an oil drilling rig, as well as the generation and handling of OBM cutting⁷² and the cement and concrete manufacturing process⁷³. Three different areas have been identified after OBM cutting generation to recycle the waste and facilitate a proper environment for processing OBM cuttings and, subsequently, convert it to a product as presented in Figure 8.

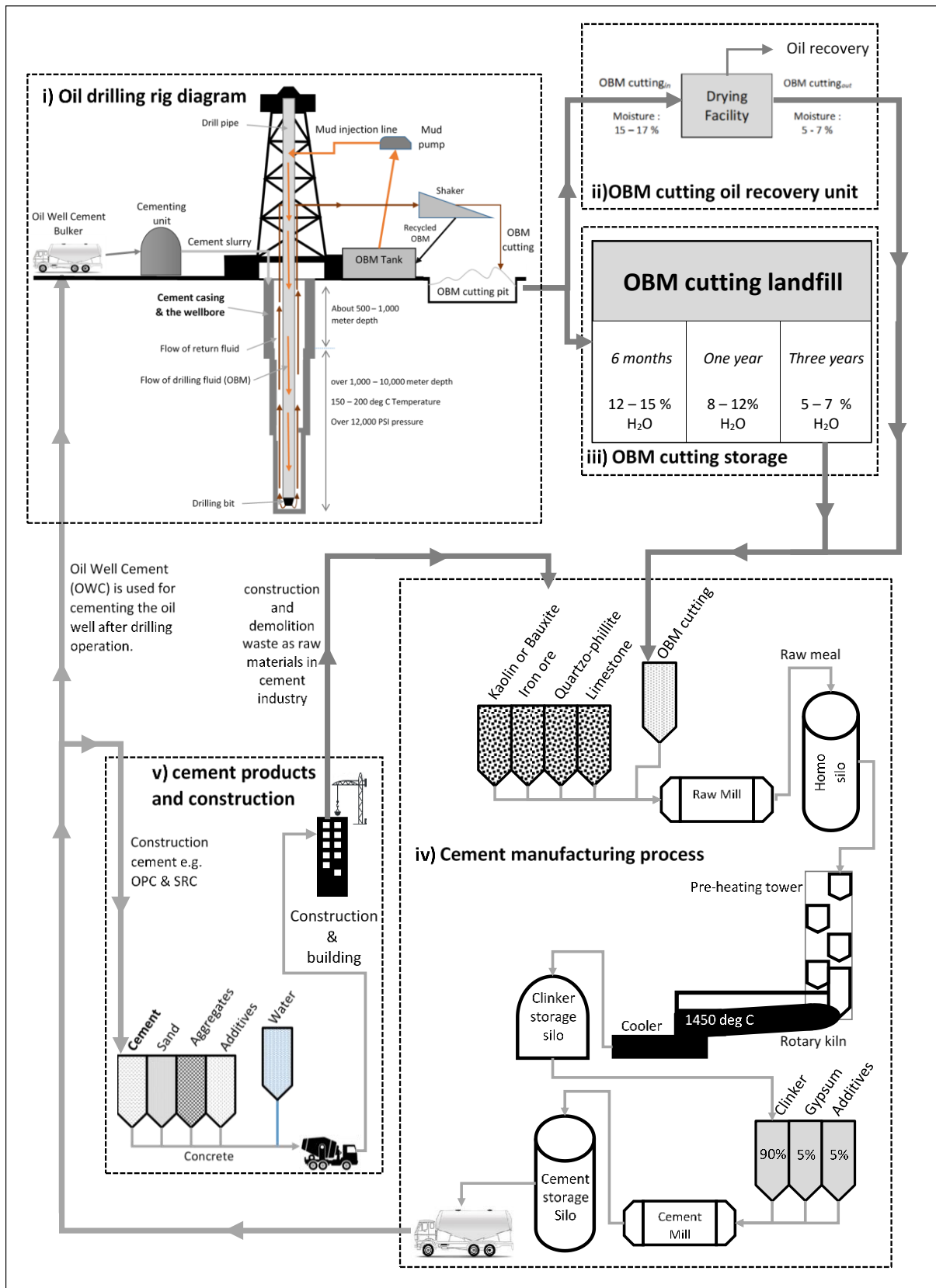


Figure 8 A schematic of the OBM and OBM cuttings disposal cycle as raw material in cement manufacturing⁷⁴

After OBM cuttings are generated by an oil well rig, they are transferred to an engineered landfill^{20,16}. The landfill is open, exposed to direct sunlight, and is typically located in the desert. OBM cuttings are wet because they contain a significant amount of oil and water, as shown in Figure 9. At this stage, storage is used to dry OBM cuttings and remove the water content by means of the sun and high temperatures in the desert. Another option, to accelerate the drying process, is using a drying unit where heat is applied to the wet OBM cuttings. This process produces vapor and could recover the oil content from OBM cuttings.

Dry OBM cuttings could be shipped to a cement factory to produce cement clinker. In the cement factory, OBM cuttings are added to limestone, as a replacement, at a level that produces raw meal within an acceptable range of quality. The first step, after mixing them with the raw materials, is grinding. Two common types of raw mill grinding are used in cement technology: ball mill grinding and vertical roller mill grinding^{75,76}. Ball mill grinding employs dry raw materials. If the raw materials contain moisture above 3%, hot dry gas is applied during the grinding step. The maximum water content of the raw materials in ball mill grinding is 3–8%⁷⁷. However, in the vertical roller mill, grinding can occur even when the moisture level is high (up to 20%^{78,79}). If OBM cuttings are shipped to a cement plant that has a vertical mill, the drying process is eliminated or reduced to conserve time and energy. After the grinding step, the produced powder, known as raw meal, is homogenised in a homo silo and then preheated and calcined in a preheater tower. Next, the calcined raw meal is burned in a rotary kiln at 1450 °C and then cooled to yield the clinker. In the final step, the clinker is ground with 5% gypsum to produce the final product, Portland cement.

There are many types of cement with different applications in construction^{80,79}. For example, ordinary Portland cement (OPC) and sulfate-resistant cement (SRC) are used in the construction industry by mixing cement with different aggregates, additives, and water as shown in Figure 8 (v). Buildings are also recycled in cement manufacturing; many studies have demonstrated the successful use of raw materials derived from demolished buildings in the cement industry^{81,82,83,84}.

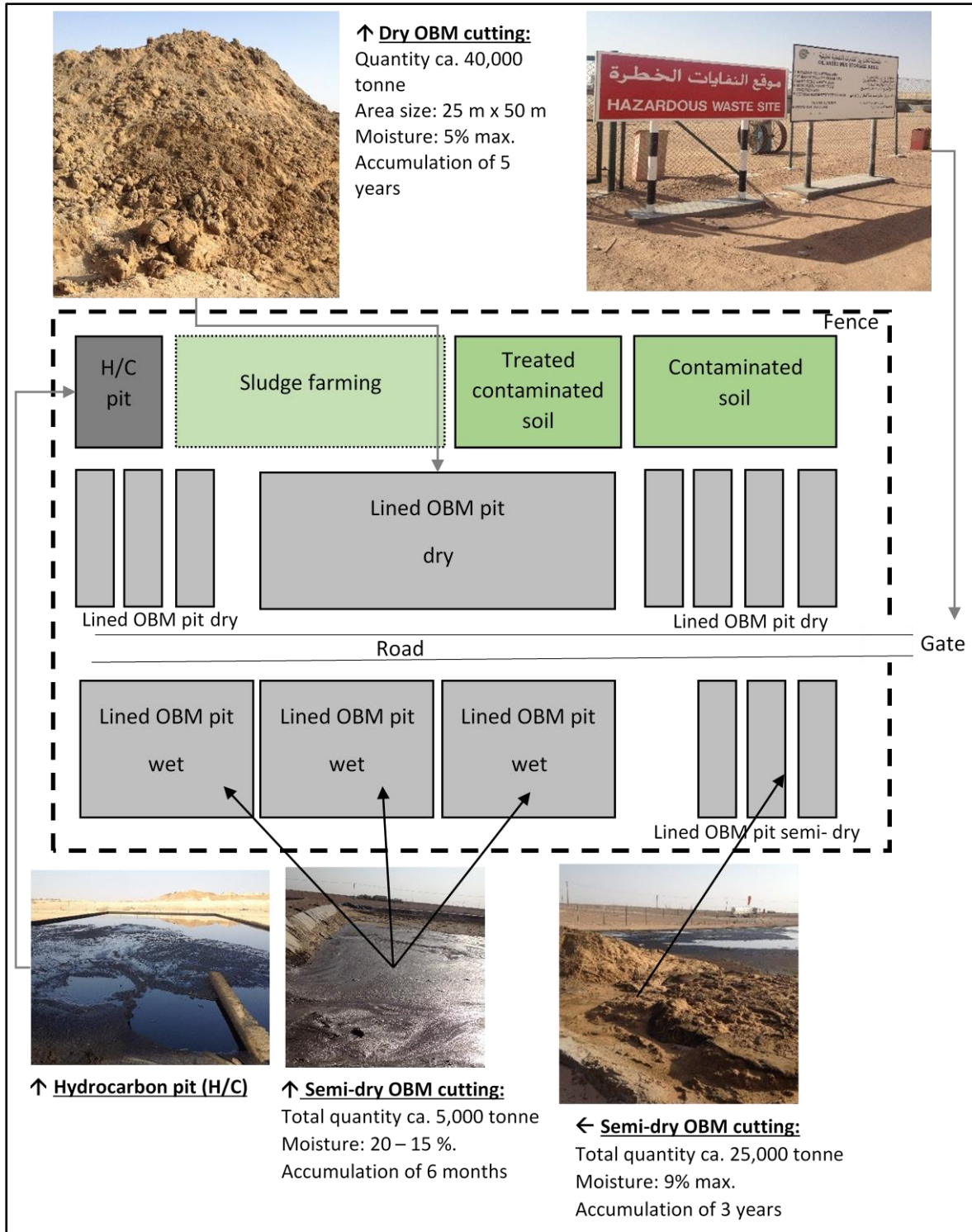


Figure 9 Storage sites for OBM cuttings.

Another type of cement, known as Oil Well Cement (OWC)^{85,86–88}, is a special cement⁸⁹ used for oil well construction. It has different physical properties and chemical content compared to construction cement. It also has greater compressive

strength and a longer setting time to meet specific requirements, such as being pumped deep in an oil well while drilling and finalising the oil rig. OWC quality plays a major role in the oil rig process. The American Petroleum Institute (API) has established international specifications and standards for producing OWC suitable for the construction of durable casing that supports oil and gas extraction⁸⁹.

Linking all the steps—beginning with the process of generating OBM cuttings in the oil and gas sector and ending where OBM cuttings are generated—helps provide a full, closed-cycle process for recycling the hazardous waste and eliminating the generation of by-products. Additionally, the closed cycle provides effective environmental and economic solutions where the three different sectors (oil and gas, the cement industry, and the concrete sector) are integrated so that an output from one sector becomes an input for another sector.

3.4 Chemistry of the cement manufacturing process

The Portland cement clinker may be defined as follows, "at least two-thirds of it consist of the two calcium silicates, namely tri- and di-calcium silicate, which are richest in CaO and can react when mixed with water and harden reasonably rapidly. It is, therefore, a hydraulic substance"⁹⁰.

Cement is made by mixing four raw materials, specifically, limestone (80%), quartzophyllite (12%), iron ore (5%), and bauxite or kaolin (3%). The raw materials are crushed and homogenised using a mixed-bed method, transferred to a raw mill, and ground to a fine powder to produce raw meal. The raw meal is stored in a homogenising silo in which it is homogenised using air blowers. Figure 10 shows the process schematically.

Next, the raw meal is introduced to a heating tower known as preheater tower, which consists of multistage cyclones. The meal is introduced to the top preheater and flows into the bottom by gravity against a hot gas flow from the bottom, coming from the rotary kiln. The meal is heated gradually through the heat exchange process. In the preheater, the calcination of CaCO_3 occurs, and CO_2 gas is released at about 650 °C by the exothermic reaction producing CaO. The calcined meal is taken to the rotary kiln and classified into different zones according to the temperature profile of the rotary kiln. The first zone is in the range of 900–1100 °C, where the liquid phase is formed,

followed by the transition and burning zones, where some other clinker phases, such as belite (dicalcium silicate, C_2S) and alite (tricalcium silicate, C_3S), are formed at about 1400 °C. The output from the rotary kiln falls into the cooler, where the material is cooled using air blowers to reduce the temperature of the burned raw meal from 1400 °C to about 200 °C within one h. The product is called Portland cement clinker, and it is stored in large silos. In the next step, the clinker is mixed with 5% gypsum ($CaSO_4 \cdot 2H_2O$) and ground in a cement ball mill. The particle size of the resultant cement is classified according to the Blaine results. The coarser material is returned to the mill for further grinding, and the finer material is transferred to the cement storage silos.

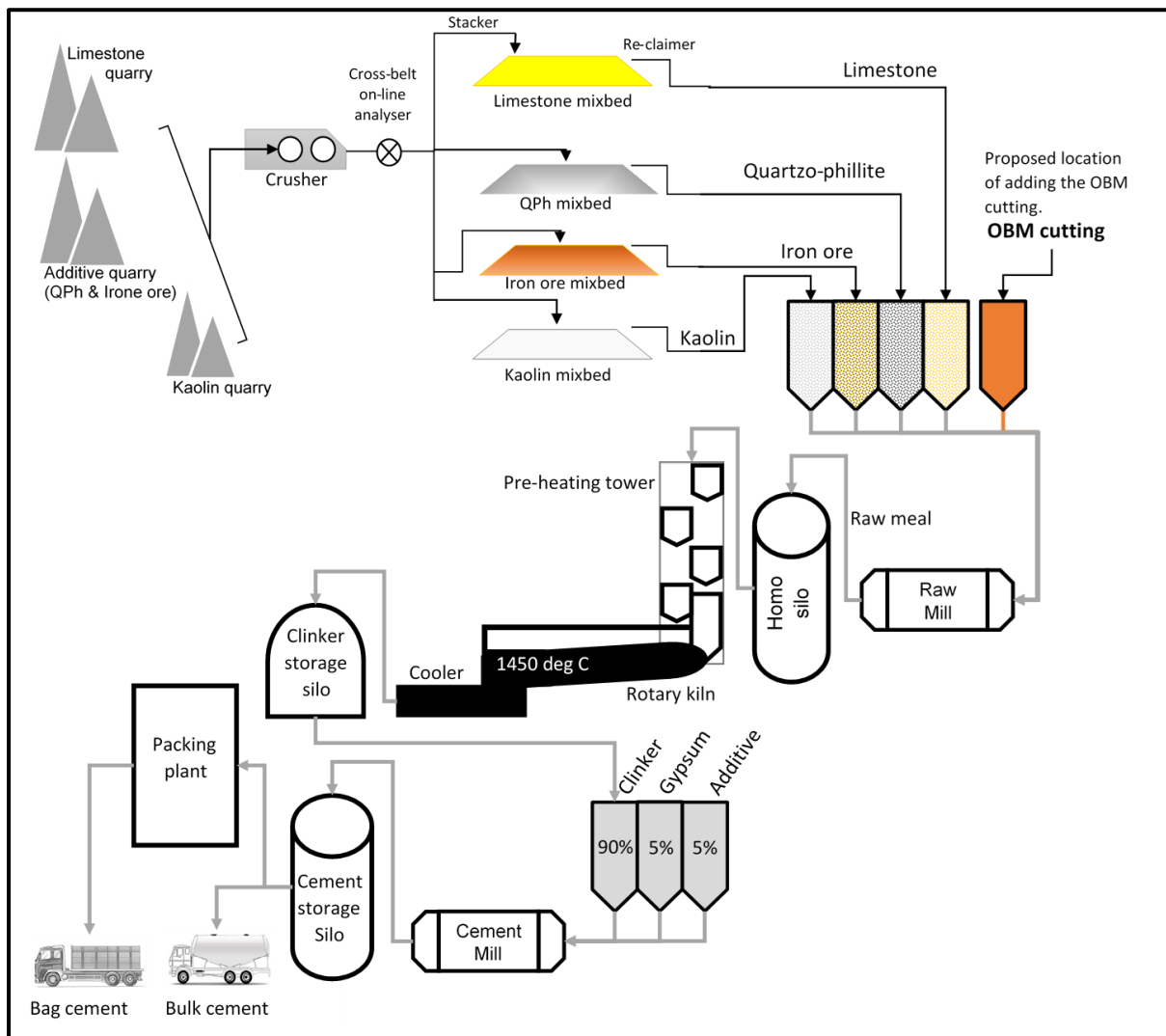


Figure 10 Cement manufacturing process

Table 5 Major chemical phases in clinker and cement

| Clinker Phase | | Approximate Chemical Formula | Cement Industry Abbreviation |
|---------------|---|---|------------------------------------|
| Alite | Tricalcium silicate | $3\text{CaO} \cdot \text{SiO}_2$ | C_3S |
| Belite | Dicalcium silicate | $2\text{CaO} \cdot \text{SiO}_2$ | C_2S |
| Aluminate | Tricalcium aluminate (Aluminate) | $3\text{CaO} \cdot \text{Al}_2\text{O}_3$ | C_3A |
| Ferrite | Tetracalcium aluminoferrite (Aluminoferrite) | $4\text{CaO} \cdot \text{Al}_2\text{O}_3 \cdot \text{Fe}_2\text{O}_3$ | C_4AF |
| Free Lime | CaO | CaO | CaO_f |

Figure 11 describes the chain of reactions in the pyro-process and illustrates the stages of clinker phase formation, beginning with the raw materials. The first four steps mainly concern calcination of the raw meal associated with the release of CO_2 and the production of reactive lime CaO . At about $1000\text{ }^\circ\text{C}$, which is normally at the first rotary kiln portion, C_3A is produced, along with a small amount of C_2S . As the material proceeds along the kiln, the temperature rises, and at about $1280\text{ }^\circ\text{C}$, the iron and alumina form the liquid phase, which facilitates the conditions for further C_2S formation and helps the material flow smoothly inside the kiln. The liquid phase is also important because it establishes a stable coating inside the kiln, which protects the kiln shell in the higher temperature zone. Finally, the C_2S combines with unreacted lime CaO at a high temperature of $1450\text{ }^\circ\text{C}$ to form the major clinker phase C_3S .

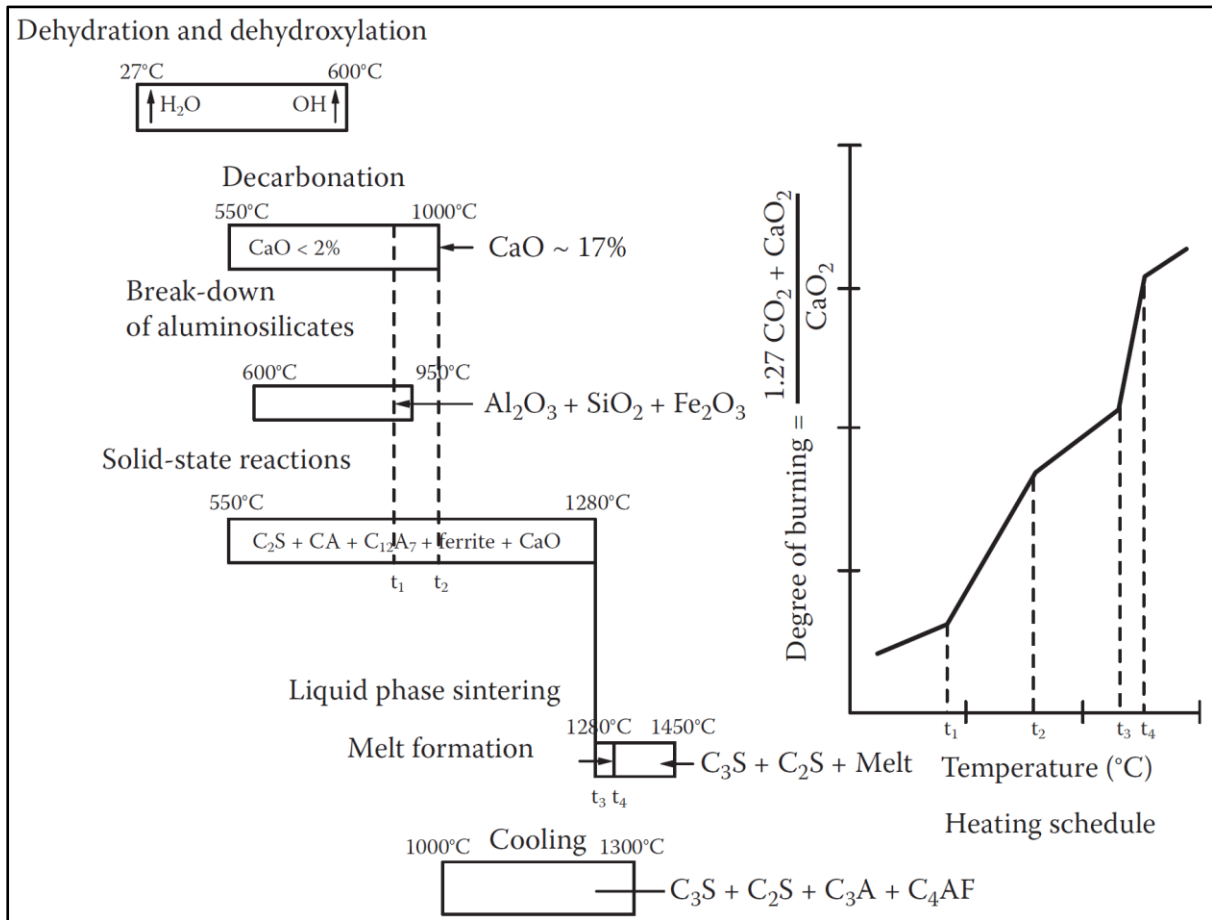


Figure 11 Estimated clinker chemical reactions^{91,92}

3.5 Common cement types used in Oman

3.5.1 Ordinary Portland cement (OPC) and sulfate-resisting cement (SRC)

OPC and SRC are two types of construction cement commonly used in Oman. Although both cement types undergo the same manufacturing steps, SRC clinker is prepared using raw materials with a lower alumina content to maintain a C_3A level below 5% and meet the ASTM standard for this type of cement. This can be achieved by reducing the alumina modulus (AM) while the raw meal is mixed.

3.5.2 Oil Well Cement (OWC)

OWC is defined as being based on coarsely ground sulfate-resisting Portland cement clinker with one or more retarders (gypsum or lignosulfonates) to give it a long enough thickening time to pump cement out at high temperatures and pressures. The amount and type of retarder used are dependent on the oil well's depth⁹³.

This type of cement is used to construct a hard layer between the oil well casing and the surrounding geological formation to prevent the well bore from collapsing. The well bore is deep, possibly reaching 6,000 metres, with very high pressure (200 MPa) and temperatures (up to 205 °C)⁹⁴. There are a number of significant roles for OWC in the process of oil well production. It protects oil-producing zones from salt water flow coming from underground water, prevents collapses, and provides stability to the bore hole. Moreover, it protects the well by, for example, preventing corrosion, reducing groundwater contamination, having a strong bond, and acting as a secondary casing^{86,87}.

Cement slurry designed for well cementing is a function of various factors that should be optimised for successful well operation. These factors include the well bore geometry, casing type, formation geography, and specification of the drilling mud used⁸⁶.

OWC is manufactured the same as conventional types of cement, OPC and SRC. However, the quality of the raw materials, in term of chemical composition, is controlled to produce the raw meal and specific clinker design.

Chapter 4

Experimental Section: Materials and Methods

Chapter 4: Materials and methods

4.1 Overview of experimental programme

This investigation, which was planned as described in Figure 12, can be divided into five major steps:

- (1) collecting the raw materials,
- (2) preparing the raw meal (Rm),
- (3) preparing and characterising the clinker (Ck),
- (4) preparing the cement (Cm), and
- (5) characterising the hydrated cement (HCm).

These steps were defined as such because they follow the same material life cycle experienced in the cement industry and cement applications. Appropriate analyses and characterisations were performed at each step. Some of the techniques used, for example, XRF, XRD, and SEM, were repeated in more than one stage, but the operating conditions and sample preparation procedures remained the same. All of the samples were not investigated at each stage; instead, the focus gradually progressed through each stage (see Figure 12).

Because this project has a strong industrial focus, the focus was on practical samples that could be made by the cement industry, from an economic standpoint and with a chemical composition that meets cement quality specifications. Samples with different amounts of OBM cuttings were chosen to observe the changes that occurred with increasing OBM content.

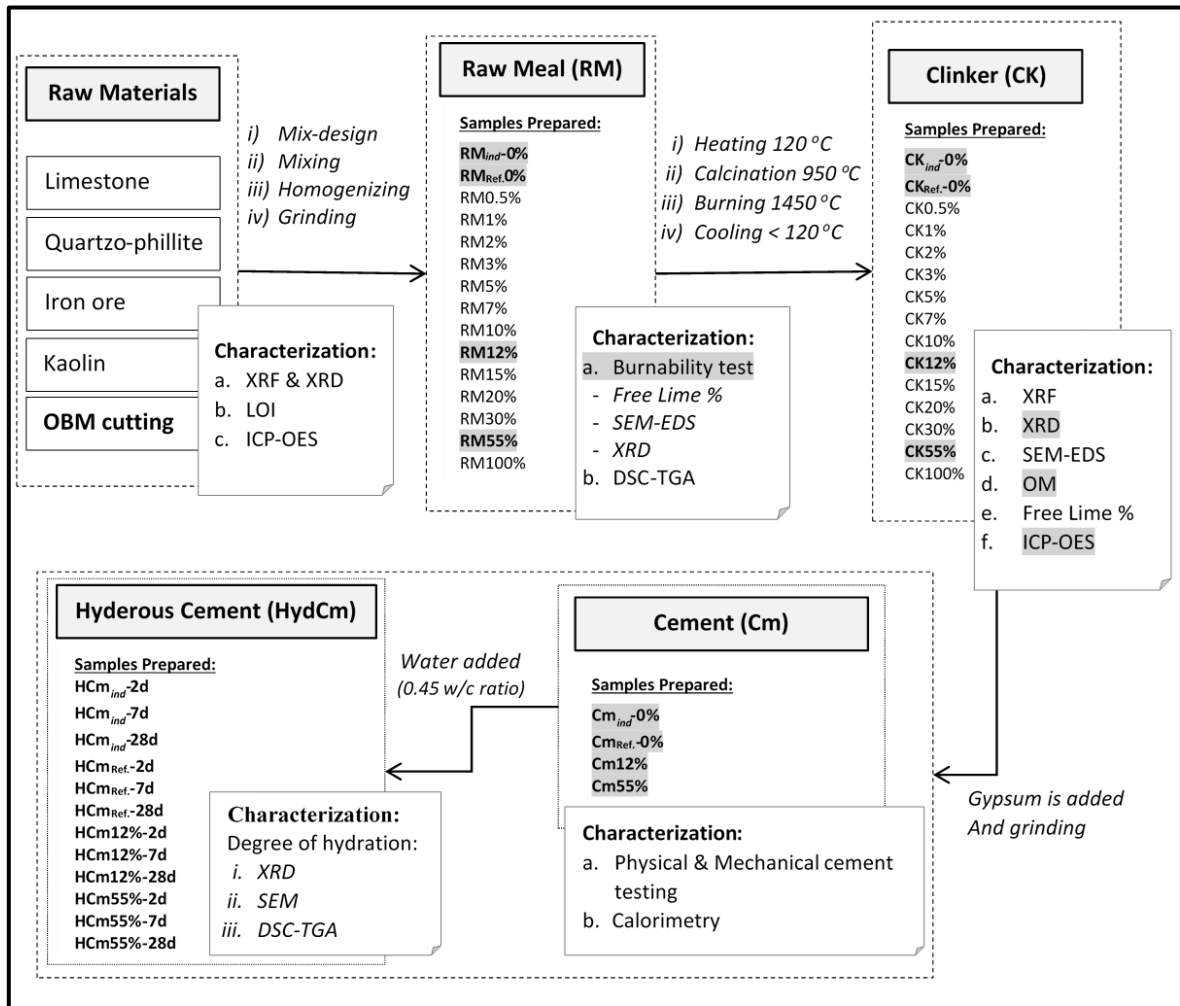


Figure 12 A schematic diagram showing the overall stages of sample preparation and the testing methods used at each stage.

4.2 Raw materials

The raw materials used in the investigation were limestone, quartz-phyllite, iron ore, kaolin and oil-based mud cutting (OBM cutting). All raw materials used in this investigation apart from kaolin were sampled from Oman Cement whose source is the quarry next to the factory. Kaolin was sourced from a quarry located 400 km away from cement plant⁹⁵. All raw materials were sampled after the initial homogenization stage (blending beds) where the raw materials went through all the steps of quarrying, crushing and stacking (see Figure 13).

The stacking underwent the usual industrial quality control procedures to ensure consistent homogenization of the raw materials before the grinding stage. As a result, the particle size of the collected samples was below 25 mm. All raw materials were characterized by XRF and XRD when they were received. The OBM cutting was also characterized by ICO-OES for the heavy and trace metals, plus moisture and organic content determination. For further investigation of OBM cutting, thermogravimetric analysis and XRD were performed.

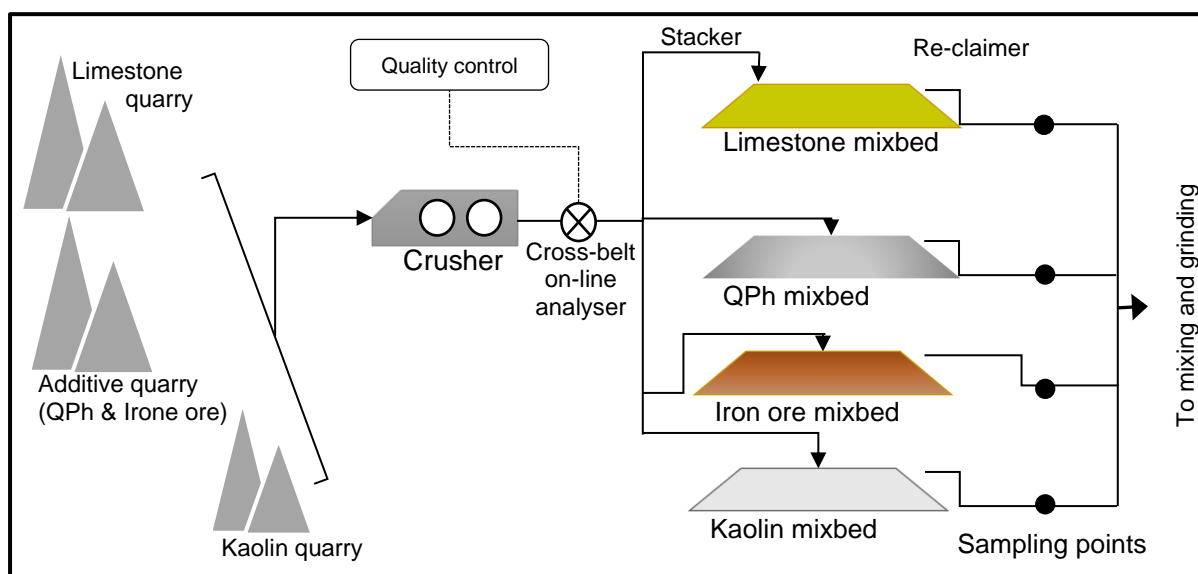


Figure 13 Diagram illustrating the sampling points (black points) for the raw materials obtained from the cement industry

4.2.1 Limestone (Ls)

Limestone is a major component in cement production due to its CaCO_3 content which is essential for the formation of the principal clinker component, alite. Oman is rich in high-grade limestone, with a CaCO_3 content above 95%. This is significant for the cement industry since the higher the CaCO_3 content, the more flexible can be the mix-

design to meet the targeted specifications of cement e.g. chemical and physical properties.

4.2.2 Quartzo-phillite (QPh)

An additional raw material essential for cement making is one with a high silica (SiO_2) content - quartz is one such material. The silica is important for the kiln reactions since it will be combined with CaO to form different clinker phases. The Quartzo-phillite (QPh) materials located near the factory in Oman has a silica content which varies from 75% to 85% SiO_2 .

4.2.3 Iron ore and kaolin

Iron ore and kaolin are additive materials used to correct the chemistry of raw mix. Furthermore, a certain amount of Al_2O_3 and Fe_2O_3 are needed to enhance the reaction in the kiln, by forming the flux (melting phase) during clinkerization and phase formation in the kiln. Iron ore is available in commercial quantities next to the factory with medium grade (Fe_2O_3 content range 40 – 45% wt/wt.).

Kaolin is transported by trucks to the factory and crushed in the same way as the other raw materials. It is an essential source of Al_2O_3 , ranging from 32% to 36% wt/wt⁹⁵. This low content of Al_2O_3 compared with bauxite would normally not be favored. However, because bauxite is not available in Oman, and is therefore more expensive, kaolin is used as a replacement^{96,97}.

In fact, the shift from imported bauxite to kaolin has been shown to be advantageous in this application economically and also chemically because of its high silica content (40 – 47% wt./wt.)⁹⁸.

4.2.4 Oil-Based Mud cutting

The OBM cutting was obtained from a drilling company in Oman (Petroleum Development of Oman, PDO²⁹). The cuttings were sampled from the PDO storage yard of OBM cutting storage facility in Qaran Al-Alam (Qran Al-Alam oil field, oil field no. 52, operated by Halliburton[®] Oman) as shown in Figure 9 and Figure 14.



Figure 14 The oil well drilling operation diagram
(Qran Al-Alam oil field, oil field no. 52, operated by Halliburton© Oman)

4.3 Mix design and samples preparation

Samples were prepared from dried OBM cutting blended with a number of raw materials used in the preparation of raw meal, namely; limestone, quartzo-phillite, iron ore and kaolin. The chemical composition of these materials is given in Table 6. These compositions of the blends were calculated to give the same phase composition as a real Portland cement clinker. Using the Bogue's calculation, the amount of C_3S , C_2S , C_3A and C_4AF in raw meal after the heating process were calculated^{99,100}.

4.3.1 Mix design

The aim of the study was to investigate the effect of adding OBM cutting on clinker composition and cement performance. The aim was to maximize the OBM content e.g. 10% and above. The mix design was cautiously made considering the following points:

- Maximum OBM cutting that could be added to produce clinker meeting standard cement specification chemistry and physical properties.
- Preparing raw meal with lower burnability, or at least the same as the industrial raw meal, and so does not required extra fuel to burn considering the overall heavy metal content.
- Use minimum additives in the raw mix design such as iron ore and kaolin. This is will contribute on reducing the cost of production as those materials are 30 to 50% more expensive than limestone.
- Use minimum quartzo-phillite (QPh) which is the source of free silica (quartz). Quartz is hard to burn¹⁰¹ and needs a higher temperature compared with silica coming from other raw materials such as kaolin (clay).
- Maintain the heavy metal content in the prepared cement.

For raw material selection for preparation of the right chemistry of the raw mix for the clinker production process, a mix calculation was required to get the optimal portion of OBM cutting used together with the raw materials. For this, an Excel sheet was used, as shown in Figure 15. The composition of the clinker was calculated to provide the same phases as the main phases of a real Portland clinker. Using the Bogue's calculation, see below, the theoretical amount of C_3S , C_2S , C_3A and C_4AF in raw meal after the heating process was calculated^{102,90}.

The theoretical calculation shows OBM cutting could be added to a maximum 55% to produce clinker with the correct OPC specification. The advantage of this mix (RM55%

as stated in Table 7) is that it was prepared using only 4 raw materials namely; limestone, kaolin, iron ore and OBM cutting. There was zero quartzo-phillite in the mix and silica supply could be provided by other raw materials.

Bogue's equations:

$$C_3S (\%) = 4.071 \cdot (CaO) - 7.602 \cdot (SiO_2) - 6.718 \cdot (Al_2O_3) - 1.43 \cdot (Fe_2O_3) \quad \text{Equation 1}$$

$$C_2S (\%) = 2.87 \cdot (SiO_2) - 0.754 \cdot (C_3S) \quad \text{Equation 2}$$

$$C_3A (\%) = 2.65 \cdot (Al_2O_3) - 1.692 \cdot (Fe_2O_3) \quad \text{Equation 3}$$

$$C_4AF (\%) = 3.043 \cdot (Fe_2O_3) \quad \text{Equation 4}$$

To ensure the clinker quality, the following composition parameters were controlled. Typically, the lime saturation factor (LSF) was defined as 0.92 to 0.96, the silica ratio was set to 2.35 to 2.6 and the alumina modului (AM) was set to 0.69 – 1.25 depending on the type of clinker to be produced (OPC has AM greater than 1.00, SRC has AM 0.85 and OWC has AM less than 0.69)¹⁰³.

| RAWMIX DESIGN WITH OBM - LSF : 92, SM : 2.5, AM : 1.15 | | | | | | | | | | | | | | | |
|--|--------------------|----------------------------------|----------------------------------|-------|-------|-------------------|--------------------|---------------------|------|-------|-------|---------|------|------|------|
| Raw Material | % SiO ₂ | % Al ₂ O ₃ | % Fe ₂ O ₃ | % CaO | % MgO | % SO ₃ | % K ₂ O | % Na ₂ O | % Cl | %LOI | TOTAL | % Usage | | | |
| Limestone | 6.21 | 0.52 | 0.60 | 49.20 | 1.02 | 0.01 | 0.05 | 0.24 | 0.01 | 41.9 | 99.76 | 80.00 | | | |
| QPH | 73.20 | 7.93 | 2.98 | 5.54 | 1.19 | 0.06 | 1.19 | 0.64 | 0.01 | 6.6 | 99.34 | 6.10 | | | |
| Kaolin | 41.68 | 32.22 | 5.38 | 2.26 | 0.30 | 0.27 | 0.21 | 0.37 | 0.15 | 12.9 | 99.3 | 4.90 | | | |
| Iron Ore | 24.76 | 5.95 | 43.11 | 0.68 | 1.82 | 0.31 | 0.14 | 0.18 | 0.01 | 22.5 | 99.46 | 3.80 | | | |
| OBM | 28.78 | 6.82 | 2.73 | 21.45 | 2.14 | 3.42 | 0.42 | 0.74 | 0.26 | 33 | 99.76 | 5.20 | | | |
| Raw meal | 13.91 | 3.06 | 2.71 | 40.95 | 1.08 | 0.21 | 0.15 | 0.29 | 0.03 | 35.50 | 97.90 | | | | |
| | | | | | | | | | | | | | LSF | SM | AM |
| | | | | | | | | | | | | | 92.3 | 2.41 | 1.13 |

Target raw meal setting points

Chemical analysis of each raw materials used in the raw meal preparation

Calculated raw meal analysis as a result of mixing of the raw materials

Ratio of mixing to prepare the targeted raw meal set points

Figure 15 The mix design program in MS Excel sheet

$$LSF = \frac{CaO}{2.8 \cdot SiO_2 + 1.18 \cdot Al_2O_3 + 0.65 \cdot Fe_2O_3} \quad \text{Equation 5}$$

$$SM = \frac{SiO_2}{Al_2O_3 + Fe_2O_3} \quad \text{Equation 6}$$

$$AM = \frac{Al_2O_3}{Fe_2O_3} \quad \text{Equation 7}$$

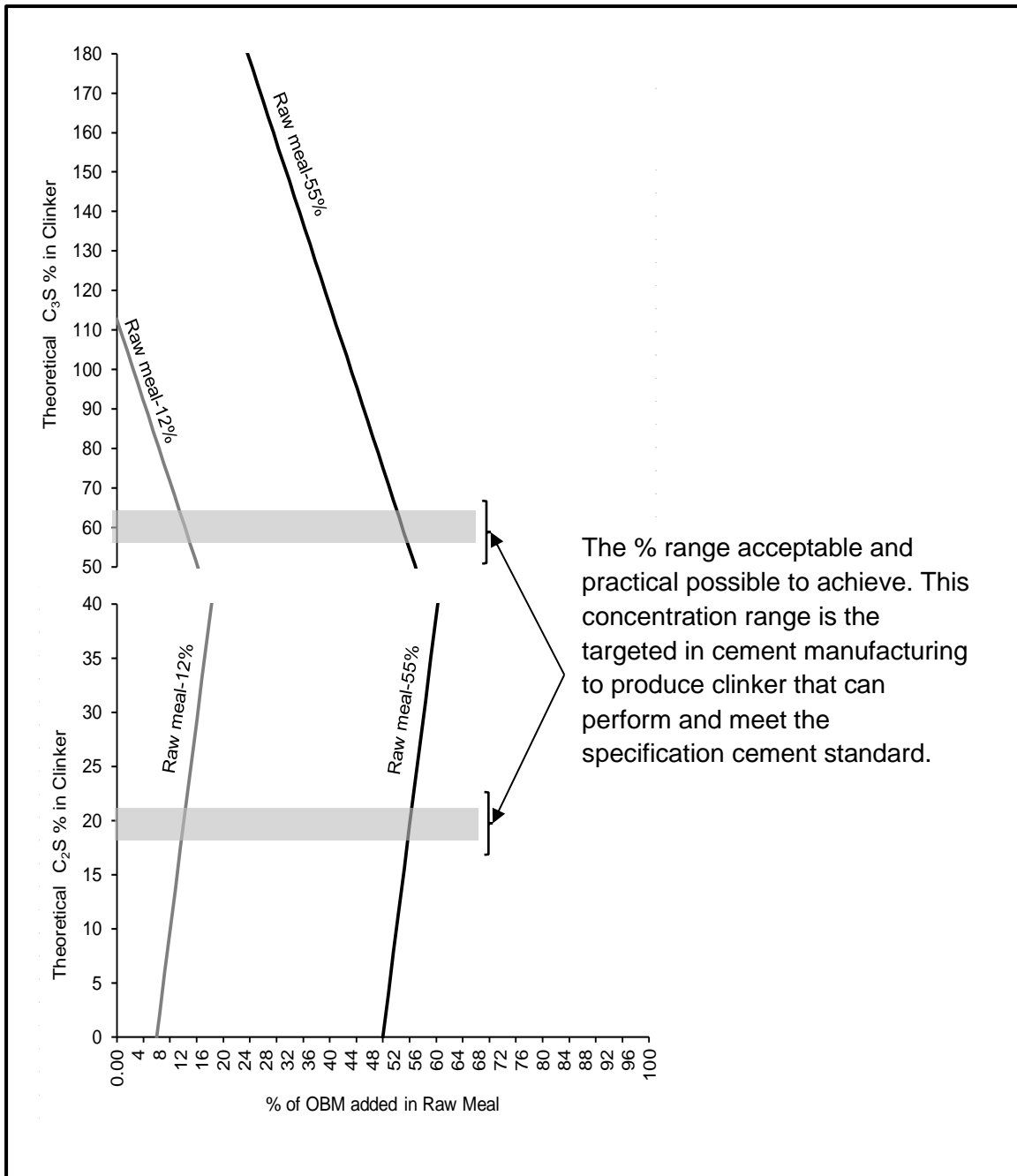


Figure 16 Theoretical C_3S and C_2S contents as a function of OBM cuttings content in raw meal.

Note:

The two figures show theoretical predicted C_3S and C_2S contents derived from Bogue's equations. The two graphs were established by changing the % OBM cutting in the raw mix. The two grey shadows highlight the % range acceptable and practically possible to achieve. This range is the target in cement manufacture known to produce clinker meeting the necessary standard specifications and in accordance with Oman Cement Company's operating quality control setpoints.

Table 6 Chemical composition of the raw materials used in this study.

| | Limestone | QPH | Kaolin | Iron Ore | OBM cutting |
|--|-----------|-------|--------|----------|-------------|
| Main & minor oxides (% wt./wt.) | | | | | |
| SiO ₂ | 3.60 | 76.30 | 41.28 | 18.28 | 20.90 |
| Al ₂ O ₃ | 0.55 | 9.20 | 33.27 | 10.32 | 4.74 |
| Fe ₂ O ₃ | 0.40 | 6.69 | 6.69 | 54.00 | 2.35 |
| CaO | 52.25 | 5.90 | 2.18 | 0.48 | 31.85 |
| MgO | 0.19 | 1.46 | 1.46 | 1.98 | 2.22 |
| SO ₃ | 0.04 | 0.26 | 0.18 | 0.12 | 1.81 |
| K ₂ O | 0.92 | 0.32 | 0.28 | 0.14 | 0.41 |
| Na ₂ O | 0.06 | 0.12 | 0.21 | 0.18 | 0.89 |
| LOI @ 950 °C | 41.59 | 2.42 | 14.15 | 9.98 | 32.70 |
| Trace oxides (mg/kg) | | | | | |
| BaO | - | - | - | - | 5500 |
| Cr ₂ O ₃ | 100 | 200 | 37000 | 100 | 100 |
| MnO | 100 | 1500 | 7600 | 100 | 300 |
| Mn ₂ O ₃ | 100 | - | - | 100 | 300 |
| P ₂ O ₅ | 600 | 900 | 200 | 200 | 1100 |
| TiO ₂ | 100 | 5400 | 4300 | 500 | 100 |

Table 6 shows the chemical composition of the raw materials used in this study. The trace BaO content in OBM cutting is high compared to that in other raw materials. This could be because of the oil content. Also it is noticed that the P₂O₅ content is high in OBM cutting. In addition, kaolin shows high concentrations of Cr₂O₃ and MnO.

4.3.2 Raw meal samples (Rm)

Five raw meal mixtures were prepared by mixing different ratios of raw materials according to theoretical mix-design calculations. Raw meal samples were prepared with OBM cutting contents from zero (as a control sample) to 55%. A final sample was prepared from 100% OBM, with no raw materials added. The samples prepared are referred to as Rm_{Ref.}, Rm12, Rm55 and Rm100% respectively. In addition, one sample of raw meal was obtained direct from a cement plant. This sample contained no OBM cutting and was identified as Rm_{ind} and later Ck_{ind}. Selected raw meal mixtures are given in Table 7.

The raw meals were prepared and homogenized by grinding the mixture in laboratory drum mill (model TNS-50, Siebtechnik). The material fed into the drum mill was

pulverized by the freely moving grinding media (steel balls ranging in size from 5–50 mm). As well as size reduction, the grinding process also aided material homogenization. The machine has a volume of 55 dm³, runs at 50 rpm, and has a grinding media weight capacity of 92 kg.

In addition to the aforementioned prepared raw meal, and to study the thermal behaviour and understand the formation of clinker phases with temperature as a function of OBM cutting content, fourteen additional raw meal mixtures (Table 7) were prepared by mixing different ratios of raw materials according to the theoretical mix-design calculation, increasing OBM cutting contents, from zero percent (as control sample) up to 55%. A final sample was used comprising 100% OBM, with no raw materials added.

Table 7 Composition of the raw meal mixes for the preparation of Portland clinkers

| Raw meal | Limestone | Quartzo-phillite | Kaolin | Iron | OBM cutting | Total |
|------------------------|-----------|------------------|--------|------|-------------|--------|
| Rm _{Ref.} -0% | 80.90 | 11.35 | 5.65 | 2.10 | 0.00 | 100.00 |
| Rm0.5% | 80.00 | 12.70 | 4.70 | 2.10 | 0.50 | 100.00 |
| Rm1% | 80.00 | 12.70 | 4.20 | 2.10 | 1.00 | 100.00 |
| Rm2% | 80.00 | 12.10 | 3.80 | 2.10 | 2.00 | 100.00 |
| Rm3% | 79.10 | 10.15 | 5.65 | 2.10 | 3.00 | 100.00 |
| Rm5% | 77.25 | 10.00 | 5.65 | 2.10 | 5.00 | 100.00 |
| Rm7% | 76.60 | 10.00 | 4.00 | 2.40 | 7.00 | 100.00 |
| Rm10% | 74.40 | 9.80 | 3.70 | 2.10 | 10.00 | 100.00 |
| Rm12% | 72.60 | 8.60 | 4.70 | 2.10 | 12.00 | 100.00 |
| Rm15% | 70.40 | 8.50 | 4.00 | 2.10 | 15.00 | 100.00 |
| Rm20% | 67.00 | 6.25 | 4.65 | 2.10 | 20.00 | 100.00 |
| Rm30% | 60.00 | 4.50 | 3.40 | 2.10 | 30.00 | 100.00 |
| Rm55% | 43.00 | 0.00 | 0.50 | 1.50 | 55.00 | 100.00 |
| Rm100% | - | - | - | - | 100.00 | 100.00 |

4.3.3 Clinker samples (Ck)

Nodules 5-8 mm in diameter were prepared from the raw meal by adding water. After drying overnight at 120 °C, the dried raw meals specimens were fired using a platinum

dish¹⁰⁴ in a static air high-temperature furnace (Carbolite, model RHF 16/3). The clinker was prepared according to Al-Dhamri and Melghit⁹⁷ (Figure 17). The heating rate was set at 10 °C/min. The sintering temperature was kept at 1450 °C for 45 minutes. Immediately after, the samples were cooled to below 100 °C using an air blower.

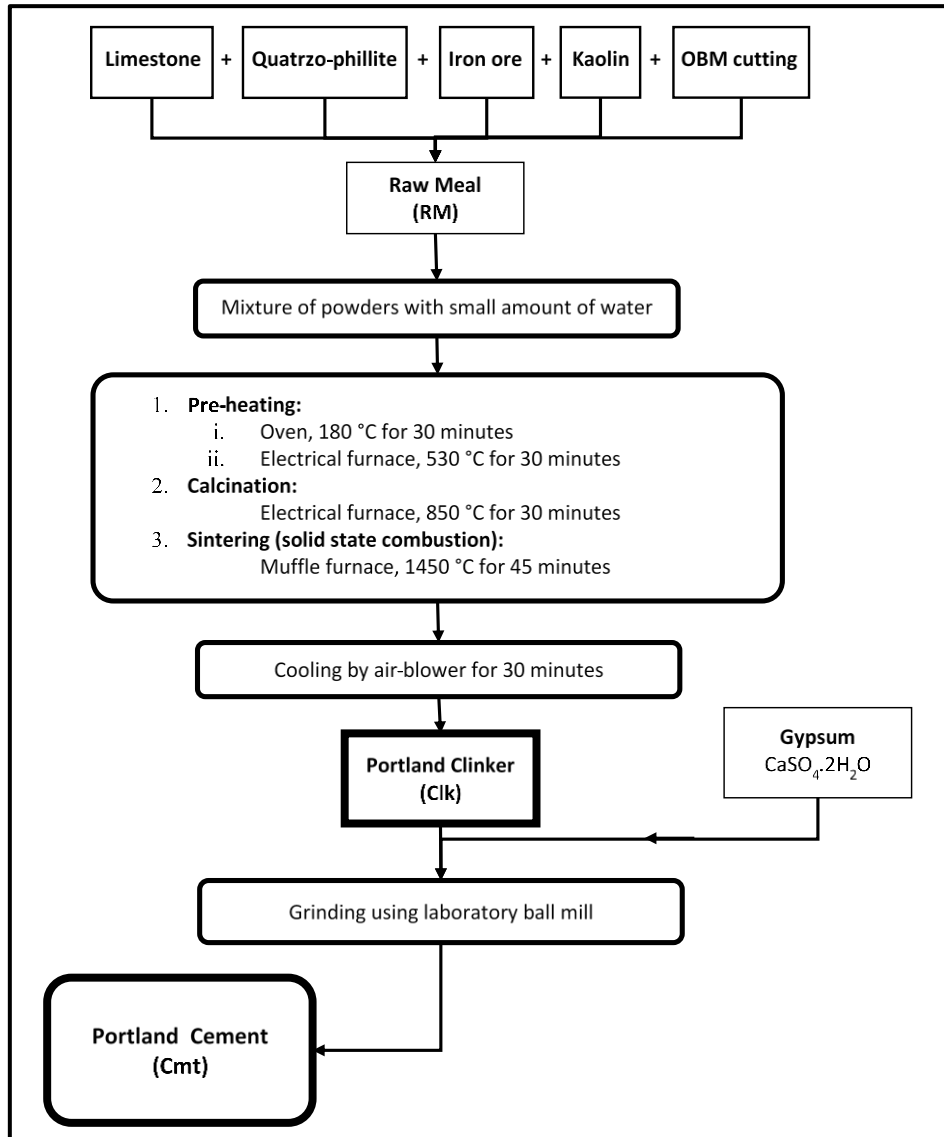


Figure 17 The preparation steps of the Portland clinker and Portland cement in the laboratory

(after Al-Dhamri and Melghit⁹⁷)

The heating time of lab clinker preparation was based on the procedure followed for clinker preparation in the Oman Cement Company¹⁰ laboratory, which is established with accordance with the best optimum heating temperature for obtaining complete clinker formation.

4.3.4 Cement samples (Cm)

Cement was prepared by grinding the clinker with gypsum. The grinding time varied according to the clinker composition. The known cement standards such as Cement Omani Standard¹⁰⁵ (OS 7/2001), as well as British and European standards do not specify fineness. However, the ASTM (ASTM C 150-99a Type I) does specify the minimum requirement¹⁰⁶. However, the cement was ground so that the Blaine fineness fell within a specified range of $320 \pm 50 \text{ cm}^2/\text{g}$, as followed by the cement industry in Oman. All samples were ground to fit the Blaine fineness close to this value.

The ratio of clinker to gypsum was rounded 6%, as shown in Table 8. The 6% added gypsum was calculated using Equation 8, which is the difference between the desired % SO_3 content of the cement and the % SO_3 in the clinker used divided by the % SO_3 content in the gypsum added. The grinding was carried out using laboratory tube ball mill (NETZSCH, D-8672, 3Kg grinding capacity). The milling of different clinker samples was performed batch wise under identical conditions, which are shown in Table 8.

Table 8 The cement grinding condition

| Sample ID | Cumulative grinding time | | | Particle size | | Gypsum added % |
|-------------------------|--------------------------|----------------------------------|---|------------------|------------------|-------------------|
| | Time Minutes | Blaine cm^2/g | Final Blaine cm^2/g | 45 μm | 90 μm | |
| Cm _{Ind.} -0%* | - | - | 318 | 14.9% | 1.5% | 5.57 \cong 6.00 |
| Cm _{Ref.} -0% | 21 | 280 | 335 | 13.3% | 1.4% | 6.02 \cong 6.00 |
| | 29 | 303 | | | | |
| Cm-12% | 34 | 335 | 329 | 14.6% | 1.3% | 5.97 \cong 6.00 |
| | 15 | 216 | | | | |
| | 25 | 296 | | | | |
| Cm-55% | 30 | 329 | 324 | 14.1% | 1.6% | 6.07 \cong 6.00 |
| | 15 | 227 | | | | |
| | 20 | 256 | | | | |
| | 30 | 324 | | | | |

*This sample was sampled from the cement plant.

The percentage gypsum required for desired SO_3 in cement was calculated according to the following formula¹⁰⁷:

$$x = \frac{a - c}{b} \times 100 \quad \text{Equation 8}$$

Where:

x = % gypsum to be added to clinker

a = desired % SO₃ in cement (2.60%)

b = % SO₃ in gypsum (41.86%)

c = % SO₃ in clinker

(0.08%, 0.10% & 0.06%, Ck_{Ref.}, Ck-12% & Ck-55% respectively)

4.3.5 Hydrated cement samples (HCm)

The reactivity of the cement powders was investigated by preparing pastes with water/cement ratios of 0.45 to 0.55. The samples were cast in polyethylene vials where they underwent curing for 2, 7 and 28 days in a water bath at a temperature of 20° C. After the desired hydration time, the hydrated cement samples were cut into ½ mm discs using a rotary saw. Hydration was stopped by immersion in isopropanol¹⁰⁸ for 24 hours. The powdered samples were then collected and stored under vacuum until they were taken for analysis.

The ½ mm disks were used for SEM analysis (Figure 18), as described in section 4.3.4. The powdered portion of the sample was ground further for XRD and DSC-TGA analysis.

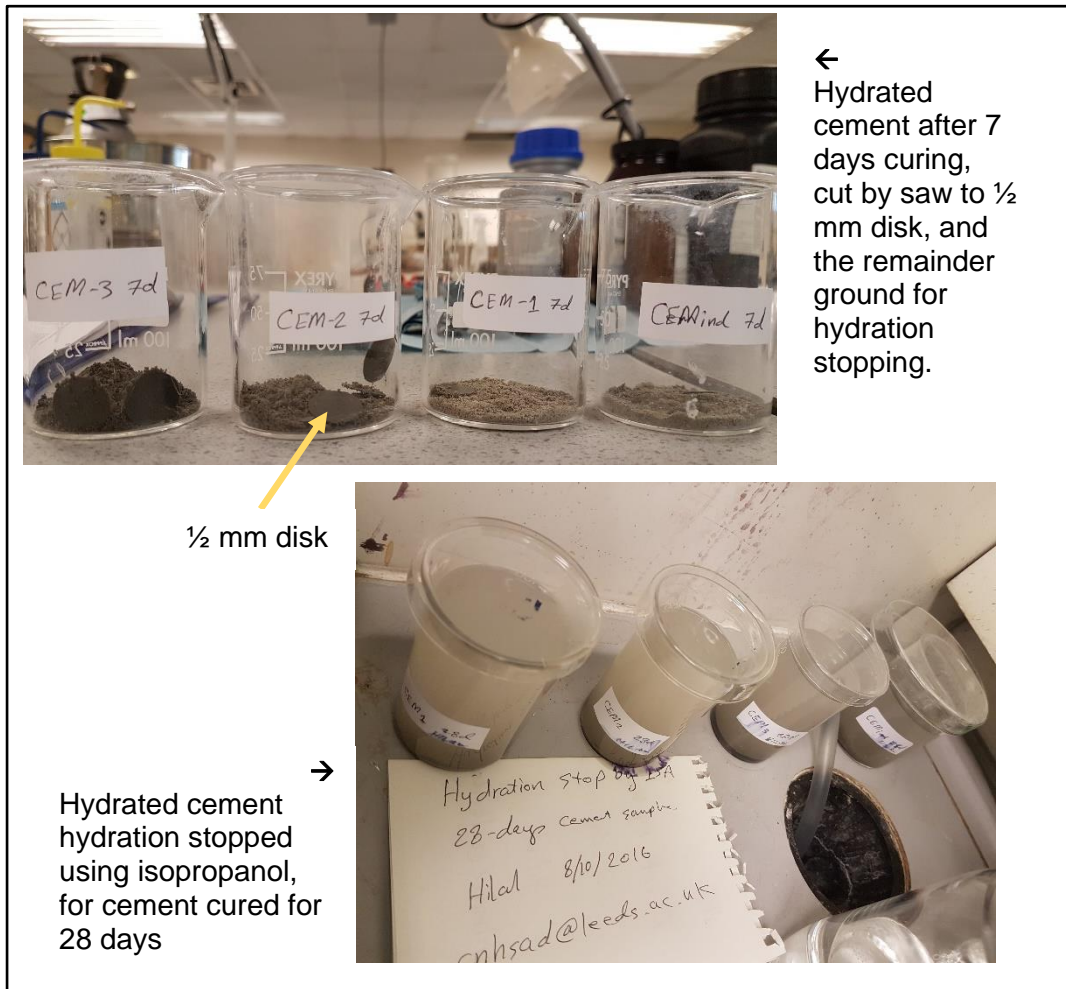


Figure 18 Hydrated cement samples and isopropanol hydration stopping

4.4 Characterization and testing techniques

4.4.1 XRF and XRD

A small portion of this sample was weighed into a platinum crucible and lithium metaborate / tetraborate flux added and mixed. The mixture was melted on a fusion machine to get a solution which automatically poured to a platinum moulded where it was cooled slowly to form a glass bead. The resultant glass bead was used for analysis by X-Ray fluorescence (XRF).

XRF analysis was carried out using a PANalytical Axios Fast spectrometer to determine the composition of the main oxides. XRF was performed with fixed detector channels working at Argon and Methane gases with 9:1 ratio consecutively. The radiation tube is Rhodium (SST-mAX) having power of 50 kV and 40 mA. The samples were analysed at vacuum pressure of less than 10 Pascals.

For powder X-ray diffraction (XRD), the samples were analyzed at room temperature using a CubiX3 PANalytical diffractometer, with Cu K α radiation operating at 45kV and 40 mA. The measurements were carried out by step wise scanning method (2θ range from 10° to 65°) with scanning rate of 0.021° per second and a step time of 14 seconds with full run lasting for 50 minutes. The crystalline phases were identified and refined using Rietveld refinement available with the HighScore $\text{\textcircled{C}}$ program from PANalytical.

4.4.2 Loss on ignition (LOI) and Free lime test

LOI was determined in an oxidizing atmosphere by igniting a known mass of the sample at 950°C in a platinum crucible in an electrical muffle furnace¹⁰⁹.

The free lime test measures the quantity of residual CaO after heating the raw meal to the clinkerisation temperature (1450°C). However, it is also an indication of the burnability of the raw meal when measured at different temperatures - between 1100°C and 1550°C . For example, hard burning raw meal has higher free lime content when compared with another raw meal sample of different composition¹¹⁰. The free lime content in any sample, either clinker or heated raw meal above 1100°C , could be measured by XRD. Another method is by titration using the ethylene glycol testing method, which is used in cement industries¹¹¹. In this method, the percentage of free lime is obtained by refluxing a known quantity of ground clinker (about 1 g) in an

alcoholic solution of ammonium acetate under slow heating to boiling temperature. The mixture is filtered and titrated with 0.04 M EDTA to the endpoint^{112,113}.

4.4.3 Inductively Coupled Plasma (ICP-OES)

The raw materials (limestone, quartzo-phillite, iron ore, kaolin and OBM cutting) and the prepared clinker samples were tested for determination of the trace and heavy elements. A small portion of the sample was weighed into a digestion vessel, to which concentrated nitric acid, followed by concentrated hydrochloric acid was then carefully added. The mixture was heated at 110 °C for 90 minutes to digest the sample and, after cooling, diluted with deionized water. The mixture was filtered to separate any remaining solid material, and the supernatant liquid decanted off for analysis. The digested sample was analysed for metals using an inductively coupled plasma optical emission spectrophotometer (ICP-OES) analytical instrument (Agilent 5110 SVDV) with nebulizer flow of 0.70 L/min, plasma flow 12.0 L/min, Stabilization time 6 seconds and RF power 1.20 kW.

The sample was sprayed into an argon plasma at approximately 10000 °C, at which temperature of the sample atoms and ions emit light at particular wavelengths dependent on the element and the intensity of which is proportional to the concentration. Quantification was achieved by comparison of the emission signal for each element with prepared metal standards. The concentration of the metals was reported in mg/kg.

4.4.4 SEM-EDX

The prepared samples such as heated RMs (section 4.3.2), Clinker (CK section 4.3.3), and hydrated cement (HCM section 4.3.5) were analysed by SEM-EDX. The aim of the SEM analysis was different in each case. The SEM for RMs and clinker samples was to identify the formation temperature of various clinker phases by scanning the samples that had been burned at different temperatures from 1180 °C up to 1500 °C. Also, the method was used to detect the presence of any trace elements.

SEM of the hydrated cement however was performed to observe the hydration of the cement at different time periods (2, 7 and 28 days).

Polished section specimens were prepared by impregnating samples in epoxy resin (mixing ratio 25:3) which was hardened at 40° C for 48 hours. The specimens were ground on a rotating wheel with 10 Newton load and 90 RPM using silicon carbide

paper (SiC) 600, 1200 and 2500 μm . Next, the specimens were polished using diamond paste to 0.25 μm roughness. As a final point before investigation by SEM, the specimens were exposed to carbon coating to prevent charging of the sample¹¹⁴.

The polished sections of the samples were studied in backscattered scanning electron (BSE) mode using Carl Zeiss EVO MA15 SEM. The back scattered images of the area of interest were obtained at a beam voltage of 15 kV with a working distance of 8 mm, while 20 kV was used for the elemental maps.

4.4.5 DSC-TGA

The differential scanning calorimetry & thermogravimetric analysis (DSC-TGA) of the raw meals (RM_{ind} , $\text{RM}_{Ref.}$, $\text{RM}_{100\%}$) was performed using DSC-TGA Universal V4.5A TA Instrument (Simultaneous DSC-TGA). The samples were manually ground to fine particles and 35 – 36 mg were analyzed using an alumina crucible. The heating rate was 10 $^{\circ}\text{C}/\text{min}$, under normal atmospheric condition from 20 $^{\circ}\text{C}$ to 1450 $^{\circ}\text{C}$ ¹¹⁵.

4.4.6 Burnability test

The term burnability describes the nature of the raw meal and the ease with which the principal clinker phases are formed at temperatures of 1450 or 1500 $^{\circ}\text{C}$ ¹¹⁰. It is an indication of the mass transfer properties of the constituents of the raw meal. Burnability is a function of time and temperature and it is measured by determining the free lime content after heating the raw meal for time (t) at temperature (T)^{116,117}.

$$\text{CaO}_f \% = f(t, T)$$

Burnability can be determined in a number of ways. Firstly, the free lime content can be determined with a constant burning time and variable temperatures. Here, rising free lime contents equate to low burnability. Alternatively, it can be defined by the time taken at constant temperature to achieve a free lime content below 1.5 - 2.0%. Increasing times correspond to low burnability. The former method was used in this study. The burnability test was conducted for the samples Rm_{ind} , $\text{Rm}_{Ref.}$, $\text{Rm}_{12\%}$, $\text{Rm}_{55\%}$ and $\text{Rm}_{100\%}$ by sintering them in laboratory furnace for 45 minutes at five different temperatures (1300, 1350, 1400, 1450 and 1500 $^{\circ}\text{C}$). After sintering, the samples were cooled, ground and analyzed by the standard ethylene glycol testing method to determine the free lime content ^{111,118}.

4.4.7 Petrographic analysis

Clinker samples were also investigated by optical microscopy. There are various approaches to sampling clinker for examination by optical microscopy, and these vary according to the purpose of the examination, such as studying kiln operation, identifying problems, improving fuel consumption etc. One well known method of sampling is that of Hofmänner (1973)¹¹⁹ who recommends sampling in intervals of five minutes or less, taking three 2-kg samples, mixing, and quartering down to 500 g. However, this step was skipped, as there was insufficient clinker produced in this study, and it was judged sufficient to apply the following steps. The clinker sample was crushed to 5-mm particles and quartered until an adequate amount remained for resin encapsulation in a 25-mm-diameter. Particles were then randomly select from the clinker subsequently exposed upon polishing. Each clinker nodule surfaces was first flattened by coarse grinding, before the flattened nodule was placed in a plastic vial, resting on its flattened surface. The vial was filled with 1:5 araldite mix (one part hardener – HY951 and five parts resin CY-230). Next, the vial was placed in a desiccator and evacuated, by means of a vacuum pump, for 30-40 minutes. Finally, it was put in an oven at 50 °C for 10 minutes and allowed to cool at room temperature. The sample was ready for coarse grinding after breaking the plastic vial¹²⁰.

An Ecomat III polisher and grinder, along with automat lapping oil and 120 to 200 mesh carborundum powder were used for coarse grinding on a diamond grinding disc – 70 µm. The final grinding was done by using 600 to 1500 mesh carborundum powder on a glass disc. The polishing was done on Metadi II polisher using 9, 6 and 3 micron diamond polishing compound on a diamond grinding disc. Polished clinker samples were etched to distinguish alite from belite using HF-vapour by cooling the sample to 10 °C below etching temperature prior to etching¹²¹. For viewing the aluminate phase, samples were etched using 10% NaOH solution^{119,122}. Polished clinker sections were examined using a reflected light microscope (Olympus BX 60).

4.4.8 Degree of hydration (DoH)

The ½ mm disks prepared in section 4.3.5 were used to study the degree of hydration by SEM-EDS analysis. The polished specimens were prepared using resin impregnation method as described in section 4.4.4. The degree of hydration was measured by acquiring 30 images at 400x magnification with a working distance of 8 mm and an acceleration voltage of 15 KeV using SEM Carl Zeiss EVO MA15. The

maps were collected using Oxford Xmax SDD detector with 80 mm² detector. The grey-level histogram analysis was done using ImageJ software.

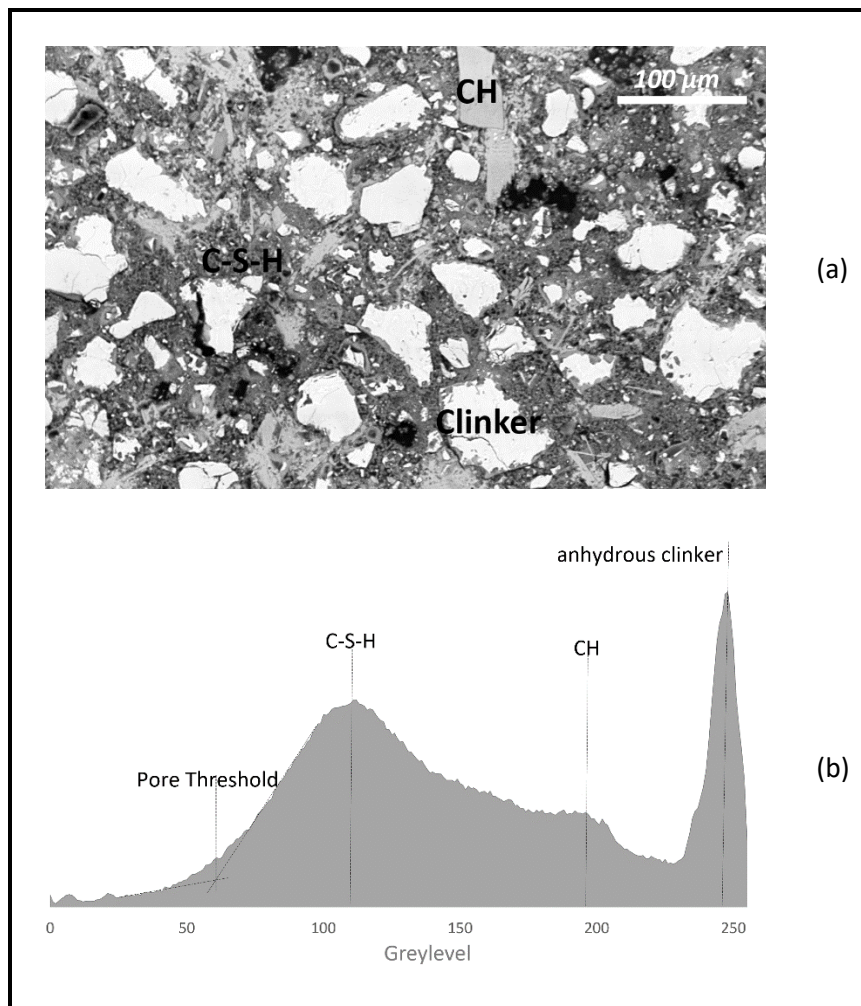


Figure 19 SEM Micrograph of hydrated cement.

(a) Cured for 7 days, and its (b) associated grey level histogram

4.4.9 Physical and mechanical testing

The specific gravity of cement was measured according to the Standard test method for density of cement: ASTM C188-16¹²³. The empty dry Le Chatelier flask was filled to the mark between 0 and 1 mL with kerosene (recorded as V_i). Then, about 64 g of dry cement sample was placed into the flask. The flask was half-filled with kerosene and the mixture was stirred with a glass rod. The mixture was being continually stirred, adding more kerosene until the flask was filled (recorded as V_f). For each sample, the

measurement was repeated four times. The density of cement was calculated according to the following equation:

$$P = M/V_d \quad \text{Equation 9}$$

where:

- P = Density of cement, g/cm³
 M = Mass of cement, g
 V_d = Displaced volume of liquid, cm³
 V_d = V_f - V_i where V_f is final volume and V_i is initial volume

The surface area of prepared cement samples was measured, as fineness by air permeability (Blaine method), by obtaining the time taken for a known amount of air to flow through a compressed cement sample bed of specified dimensions and porosity. The test was carried under standard conditions at 20° C and humidity not exceeding 65%, the specific surface of the sample was correlated to t^{1/2} where 't' was the time taken for a known air volume to flow through the pressed cement bed¹²⁴.

The setting time and the soundness of the cement pastes (cement-water ratio being 500 g: 125 ml) were determined according to the European Standard EN 196-3. Vicat apparatus was used to determine the setting time by noting the penetration of a needle into cement paste until it reached the specified depth. The soundness is determined using Le Chatelier apparatus by noting the volume expansion of cement paste as indicated by the relative movement of two needles¹²⁵.

The compressive strength development of the various cement samples (Cm_{ind}, Cm_{Ref.}, Cm-12% and Cm-55%) was conducted using mortar samples according to the European Standard for Portland cement testing. The cement mortars were prepared by mixing cement, standard sand and distilled water with the ratio of 1:3:0.5 respectively. The standard sand used was supplied by Normensand, conforming to ISO 679, EN 196-1 Germany. The cement mortars were prepared by mechanical mixing and then compacted in a standard steel mold (dimensions 40 mm x 40 mm x 160 mm). The specimens in the mold were stored in a moist atmosphere overnight. Demolded specimens were stored in a water bath for periods of 2, 7 and 28 days at 98% relative humidity and 20° C ± 2. After each period, the specimens were tested for compressive strength using the compressive machine (made ELE, model ADR-1500) with a lab temperature of 22° C ± 2° C and lab humidity of 55% ± 3%. Each strength result was an average of three measured data¹²⁶.

4.4.10 Isothermal Conduction Calorimetry

Isothermal conduction calorimetry (50), ICC, was used to study the hydration process of cement by measuring the heat given off by the hydrating cement as a function of time. The heat given off by a sample is compared to a reference sample. The reference used had the same thermal properties of the sample. Quartz has close specific heat capacity to cement (quartz = $0.8 \text{ J.g}^{-1}.\text{K}^{-1}$, cement = $0.75 \text{ J.g}^{-1}.\text{K}^{-1}$). Six grams of dry cement sample were mixed with three ml of distilled water, keeping the water to cement ratio of 0.5. The mixing was performed outside the calorimeter. The mix was placed in a 20 mL disposable polyethylene ampoule and the measurement was performed using TAM Air with eight channel isothermal heat flow calorimeter. The container was placed in a chamber which was then placed in water bath at constant temperature of 20°C . All samples were prepared after each other and then loaded into ATM Air at the same time. The determination testing was set for measuring heat of hydration over 28 days. The data obtained was used to establish two type of graphs, first heat of flow rate evolved from the cement hydration against the time. And second, graph that showing total heat resulted from the hydration against the time¹²⁷.

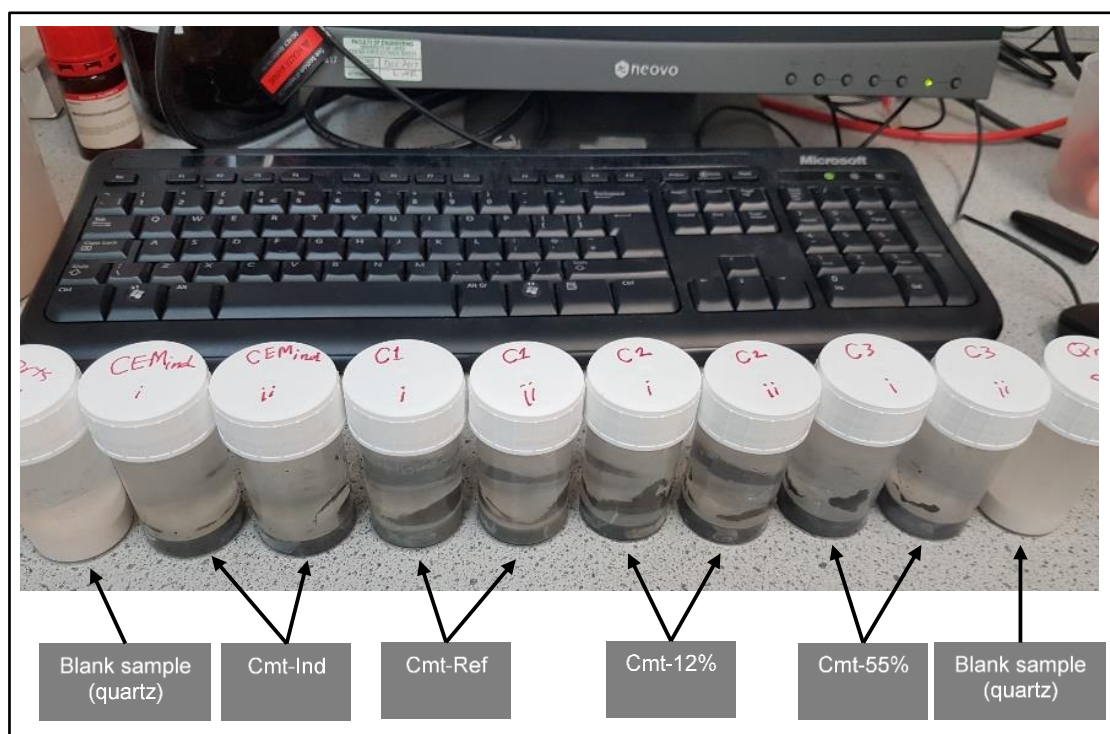


Figure 20 Overview of the calorimeter setup

showing two sets of samples: one containing 9g of sample paste and the reference sample containing 9g of a quartz analogue.

Chapter 5

Characterisation of OBM and OBM cuttings

Chapter 5: Characterisation of OBM and OBM cuttings

5.1 What is in OBM?

OBM is a fluid prepared to be used in the oil drilling process. There are several types of OBM, and the specific type used depends on different factors, such as the well's depth, geological formation, and ground composition. The ground and geological conditions are the basic principles for decision-making regarding the specific type of fluid to be used. Some areas, where the shell is an active type that reacts with water and unlike condition are formed, which cause the damage to the well during the drilling process. In critical conditions, oil is used to replace the water in the fluid. The major components of OBM are oil, water, mud, and an additive. It is used because it facilitates drilling underground where the temperature and pressure are excessively high.

The basic components of OBM:

- 1- Basic fluids, such as oil or diesel.
- 2- Mud, a solid part of the fluid, which consists of water, clay, and sand.
- 3- Additives, which control the properties of OBM, such as weight (specific gravity or density), viscosity, fluid loss, and chemical reactivities.

Diesel is banned from use in Oman by law ⁴⁶ to meet the environmental rules and regulations agreed to in the 1980s regarding the use of oil containing aromatic compounds, such as oil-based drilling fluids ^{128,129}. Diesel is 5–10% polyaromatic hydrocarbons (PAH)¹³⁰ so falls under the hazardous waste category and has a highly toxic impact. Low-toxicity oil synthetics are formulated and known as nonaqueous drilling fluids. The reported lethal concentration (LC₅₀) for the aquatic toxicity of nonaqueous-based fluids is 1560 – 7131¹³¹ mg/L, tested on an amphipod species called *Corophium volutator*. Diesel-based OBM's LC₅₀ is 840¹³² mg/L when tested on the same species and, according to the United States' Environmental Protection Agency (EPA), its drops to 639¹³³ mg/L when tested on *Leptocheirus plumulosus*, another amphipod species.

A few examples of base oils used in Oman in the preparation of OBM and their toxicity are as follows:

- Mineral oil of alkanes (paraffin) is oil that has carbon-hydrogen single bonds with a carbon chain link of C10 to C22. This type of oil has lower toxicity and higher viscosity, but it is costly.
- Mineral oil of Alkenes (olefins) is oil that has a double bond between carbon and hydrogen and a carbon chain length of C15 to C18 (linear, iso or blends). This type of oil is moderately viscous and moderately cost¹³⁴. It is also less toxic than diesel-based OBM.

The mud in OBM is comprised of inorganic colloids, which are active clay ingredients, and has different particles sizes depending on its design. In Oman, the particle size used is fine, in the range of 44–74 μm in sieve size 325¹³⁵ with a large surface area. The mud's properties are important when selecting the type of OBM. It plays a major role in stabilising the well during the drilling process, which depends largely on the interaction between OBM and the exposed shale formation. The colloids in the mud can be classified into two categories: (1) clay minerals and (2) organic colloids. Clays consist of a heterogeneous blend of very fine minerals, such as quartz, feldspars, calcite, and pyrites¹³⁶, and have a mica-type structure in which the flakes are composed of small crystal platelets stacked together and facing each other to form a unit layer. Each unit layer consists of an octahedral sheet and one or two sheets of silica tetrahedra¹³⁷ as shown in Figure 21.

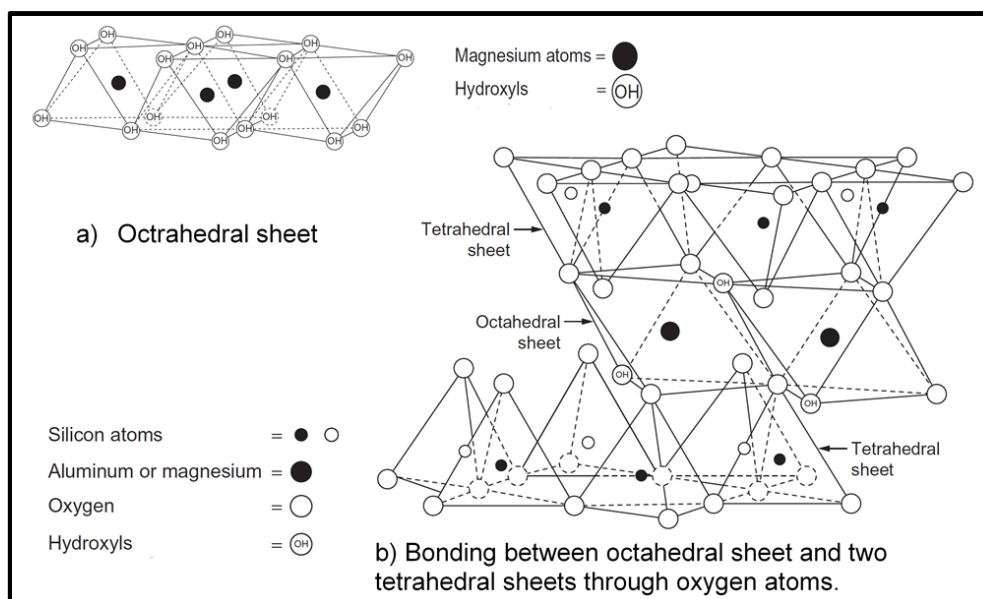


Figure 21 Schematic mineral structure of clay

(Grim¹³⁷ and Darley et al.¹³⁶)

Most drilling companies in Oman use Barite as an additive to control the properties of OBM, such as its weight (specific gravity or density), viscosity, fluid loss, and chemical reactivities. Barite (BaSO_4) is chemically inert and insoluble. Adding Barite gives OBM a specific gravity of 4.2–4.5 g/cm^3 , meeting the API's specifications¹³⁸, so its role is a weighting agent used to increase the density of OBM as desired based on the well conditions. OBM's density is important because well bore fluid must have an adequate density to convey the cuttings to the surface, and it contributes to the stability of the bore hole¹³⁹ by increasing the pressure exercised by the well bore fluid against the surface of the hole¹⁴⁰. In addition, higher density results in a higher penetration rate during the drilling process¹⁴¹. Other additives are used very infrequently, such as calcium carbonate, hematite, ilmenite, and manganese tetroxide. However, barite is widely used because it is the most effective and economically feasible.

5.2 What is in OBM cuttings?

OBM cuttings are a mixture of OBM and the drilling cuttings produced during the oil well drilling process. The variation in chemical analysis of OBM cuttings is very high compared to regular raw material obtained from a specific quarry. This is due to the nature of the oil drilling location. OBM cutting analyses obtained from different literature are summarised in Tables 9 and 10.

The chemical analysis of the major and minor oxides show some consistency on oxides important to the cement industry. The concentrations of SiO_2 and calcium carbonate (as CaO) fall within the cement raw materials specification as additional additives rather than major constituents.

The XRD analysis of the OBM cuttings obtained and shown in Figure 22 concludes that the OBM contains mainly calcite (CaCO_3), dolomite ($\text{CaMg}(\text{CO}_3)_2$), quartz (SiO_2), iron oxide (Fe_2O_3) and Barite (BaSO_3).

In the XRD and chemical composition, most analyses show that the OBM cuttings are a heterogeneous mixed material composed of a few major types: gravel, limestone, clay and shale. The gravel and limestone are cuttings from the oil drilling process that contaminate the circulated material and become part of the OBM cutting. Limestone (calcite) and clay are added during the preparation of the OBM. Shale is of low CaO content (below 40%) and high SiO_2 content (above 20%)⁷⁶. The alumina content in

OBM cuttings is probably coming from the clay that used in OBM preparation. The major mineral in clay is alumina in the form of aluminium silicates. In some cases, as shown in Table 9, this content is above 10%. Alumina is present in many forms, such as bauxite, gibbsite and kaolinite¹⁴². However, the OBM cutting used in this study has a lower alumina content (4.47% wt.).

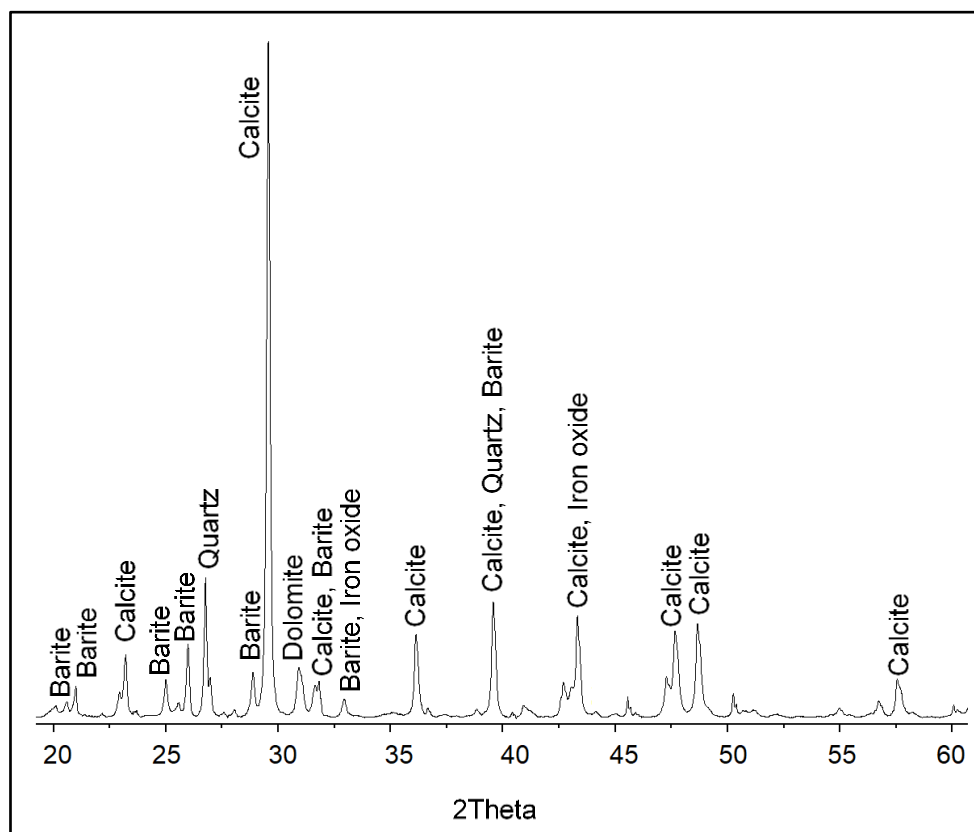


Figure 22 X-ray diffraction pattern of OBM cutting

The XRD (Figure 22) and chemical analysis also showed the presence of Barium in the OBM cuttings in a form of barite (barium sulphate, BaSO_4). The major source of barite is the preparation of the OBM used during the oil well drilling process. It is used as an additive (known in drilling engineering as weight material or a weighting agent) and has a major role in the drilling process. The weight material is added in the preparation of OBM to develop a mud system that yields good well stability. Density, or mass per unit volume, is one factor controlled by this material during the well engineer's mix design. The wellbore OBM must have adequate density to transfer the cuttings to the surface during the drilling process¹⁴⁰. Besides increasing density, the weight material

also creates sufficient hydrostatic pressure in the hole and minimizes OBM slurry loss by forming a thick filter cake on the walls of the well.

Example of economic weight material are powdered minerals of barite, calcite or hematite. Barite is an inert and insoluble chemical compound with a specific gravity of 4.2–4.4 and hardness 2.3–3.5. It is the most economic material widely used as weighting material in the well drilling process^{140,143}.

OBM cuttings also contain heavy and trace metals from several sources in very low concentrations. These are mainly from the additives used or from the cutting and the crude oil. PDO specifies the maximum permissible metal concentration in by-products (drilling waste) generated as a result of oil drilling operations. These include contaminated sludge, soil, WBM cuttings and OBM cuttings^{144,145}. The metal concentration must be within the specified limits in order for the material to be disposed of in engineered landfills or other facilities subject to approval from the environmental authority in Oman. When comparing the limits of the PDO and API guidelines, few metals are not specified by PDO, such as As and Ba; only the metal Se is not specified in API. The limits given in the PDO specifications and API guidelines are similar. The OBM cuttings obtained in this study have metal contents that fall below the limits specified by PDO.

The trace element content (also known as potentially toxic elements, PTE¹⁴⁶) in OBM cuttings is reported in Table 10 and presented in Figure 24. Because barite is a common minerals in the OBM used, BaO levels were high in the OBM cuttings. These were much higher than when compared with other results reported for OBM cuttings in the literature^{44,52,54} as could be seen in Table 10. Other trace elements could result from contamination by the oil used to replace the water base in the preparation of the OBM slurry before pumping the mud in the drilling hole.

API has developed criteria for drilling waste based on well-developed scientific information¹⁴⁷, stated in Table 10. trace metals in the studied OBM cuttings were much lower than the limits specified by the API guidelines¹⁴⁷. The concentrations of As, Cd, Cu and Ni are 9.8, 1, 18 and 3.3 mg/Kg respectively, which indicates that the OBM used meets the environmental requirement for use of oil-based fluid, and thus reflects lower trace elements that threaten the environment. In addition, the highest concentrated trace element is barium, which still shows a lower concentration than the

stated limits of API at only 5,500 mg/Kg, against the 180,000 mg/Kg maximum limit from API. Other elements of environmental concern, zinc and lead, are 107.6 and 32.8 mg/Kg, respectively. This was similar to the conclusion of many studies of OBM cutting, which reported 102.4 mg/Kg (Ayati et al. ⁵⁴) and 125 mg/Kg (Abbe et al. ⁴⁴) for zinc and 38.5 mg/Kg (Ayati et al. ⁵⁴) for lead. In addition, P₂O₅ is known to retard cement and potentially, in combination with SO₃, to stabilize belite¹⁴⁸.

Table 9 OBM cuttings major and minor chemical composition from different sources (%wt.)

| Reference | 45 | 54 | 52 | 27 | 71 | 44 | This study |
|--------------------------------|-------|-------|-------|------|-------|-------|------------|
| SiO ₂ | 44.85 | 41.18 | 5.47 | 38.5 | 17.64 | 47.60 | 20.90 |
| Al ₂ O ₃ | 14.19 | 12.75 | 1.29 | 9.9 | 2.36 | 13.54 | 4.74 |
| Fe ₂ O ₃ | 7.49 | 3.29 | 0.56 | 4.1 | 1.23 | 6.34 | 2.35 |
| CaO | 17.51 | 14.95 | 25.05 | 13.0 | 28.17 | 2.78 | 31.85 |
| MgO | 1.76 | 7.34 | 3.47 | 3.6 | 3.64 | 2.31 | 2.22 |
| SO ₃ | 3.11 | - | 38.41 | 5.0 | 3.96 | - | 1.81 |
| K ₂ O | 2.69 | 2.53 | 0.27 | 1.7 | 0.56 | 2.33 | 0.41 |
| Na ₂ O | 1.05 | 17.32 | 3.29 | 1.1 | 1.48 | 1.17 | 0.89 |
| Cl | 1.29 | | | 0.31 | 1.23 | | 0.01 |
| LOI | | 8.2 | | 22.9 | 19.35 | 11.63 | 32.70 |
| Moisture | | | | 14.5 | 2.30 | 17 | |
| NCV* | | | | 633 | | 633 | - |
| BaO | 4.98 | | | | | 11.39 | |
| TiO ₂ | 1.08 | | | | | 0.65 | 0.10 |

*Net caloric value in kcal/kg OBM cutting

Table 10 OBM cuttings trace & heavy elements analysis (mg/Kg, dry solid) ^{44,52,54}

| Reference | 54 | 52 | 44 | This study | PDO specification ¹⁴⁵ | API guideline ¹⁴⁷ |
|-----------|-------|--------|------|------------|-----------------------------------|------------------------------|
| | | | | | Maximum permissible concentration | |
| As | 11.8 | - | 11.8 | 9.8 | NS* | 41 |
| Ba | 32.02 | - | - | 5500 | NS | 180,000 |
| Cd | - | 0.44 | 0.3 | 1 | 20 | 26 |
| Cr | 74.3 | 0.48 | 116 | 100 | 1000 | 1,500 |
| Cu | 23.9 | 3.43 | 32.9 | 18 | 1000 | 750 |
| Hg | - | - | - | 0.2 | 10 | 17 |
| Ni | 36.0 | 0.34 | 65 | 3.3 | 300 | 210 |
| Pb | 38.5 | 149.02 | 11.2 | 32.8 | 1000 | 300 |
| Se | - | - | - | 3.4 | 50 | NS |
| Zn | 102.4 | 0.20 | 125 | 107.6 | 3000 | 1,400 |

*NS: not specified

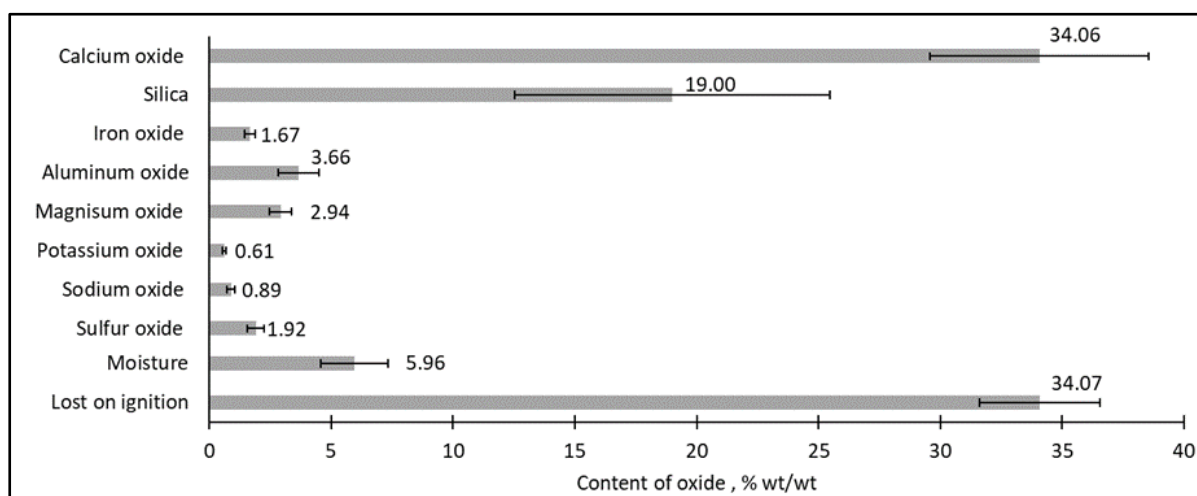


Figure 23 The chemical composition (major oxides) of OBM cuttings (average of 20 samples)

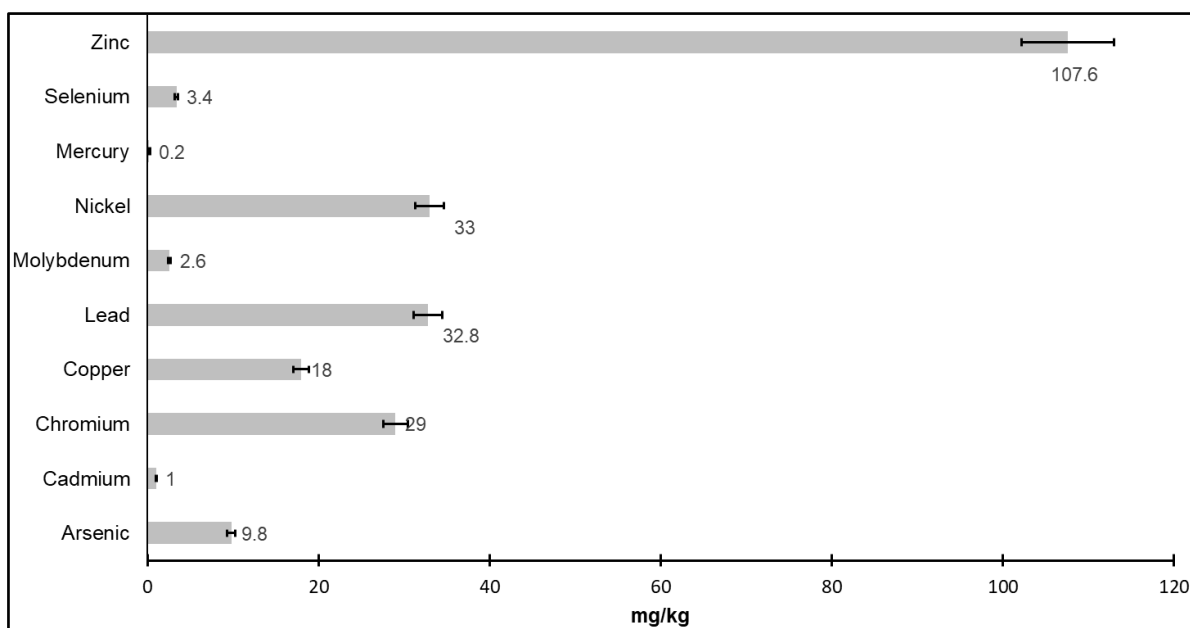


Figure 24 The trace and heavy elements content of OBM cuttings (average of 20 samples)

Chapter 6

The effect of OBM cuttings on the clinkerisation process

Chapter 6: The effect of OBM cuttings on the clinkerisation process

6.1 Clinker phase formation

XRD patterns reveal changes in clinker phase composition as a function of the OBM cutting content. The main phases in all the investigated clinkers are reported in Figure 25, namely alite (C_3S), belite (C_2S), tricalcium aluminate (C_3A) and ferrite (C_4AF). The concentrations of alite and belite versus OBM cutting content are reported in Figure 26. This figure shows the results from both the Rietveld refinement of the XRD patterns and theoretical calculations based on Bogue equations Table 11.

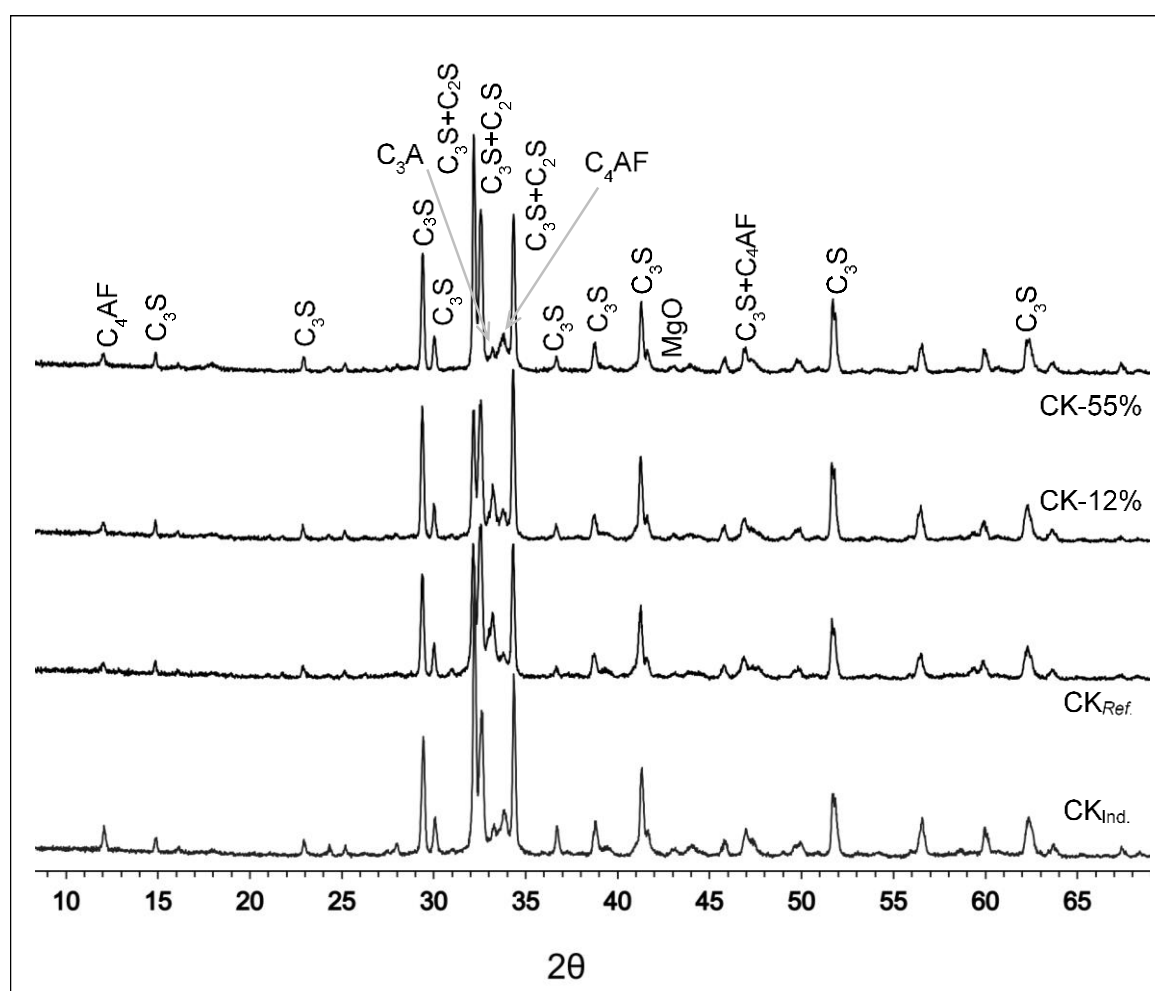


Figure 25 XRD patterns of the prepared clinkers.

There were no discernible changes in the alite or belite polymorph with OBM cutting content (Figure 25). However, the levels of alite and belite formed were dependent on the OBM cutting content (Figure 26). This result was not predicted by the Bogue

calculations, but the Rietveld refinement data showed a gradually decreasing alite content (and corresponding increasing belite content) with increasing OBM cutting content. Indeed, it is noteworthy that the Bogue calculations underestimated the alite content and overestimated the belite content at OBM cutting content up to 5%.

While the industrial clinker showed the highest levels of alite, adding OBM cuttings to the reference raw meal led to increased alite content. It was not until the OBM cutting level was over 15% that the alite content dropped below that observed for Ck_{ref} . These differences could be explained while exploring the other parameters, such as the influence of trace element content, raw material characterisations, and OBM cuttings' behaviour. However, the reference clinker sintering conditions were likely different to those of the industrial clinker produced in a real cement kiln, for example the absence of mixing under lab conditions.

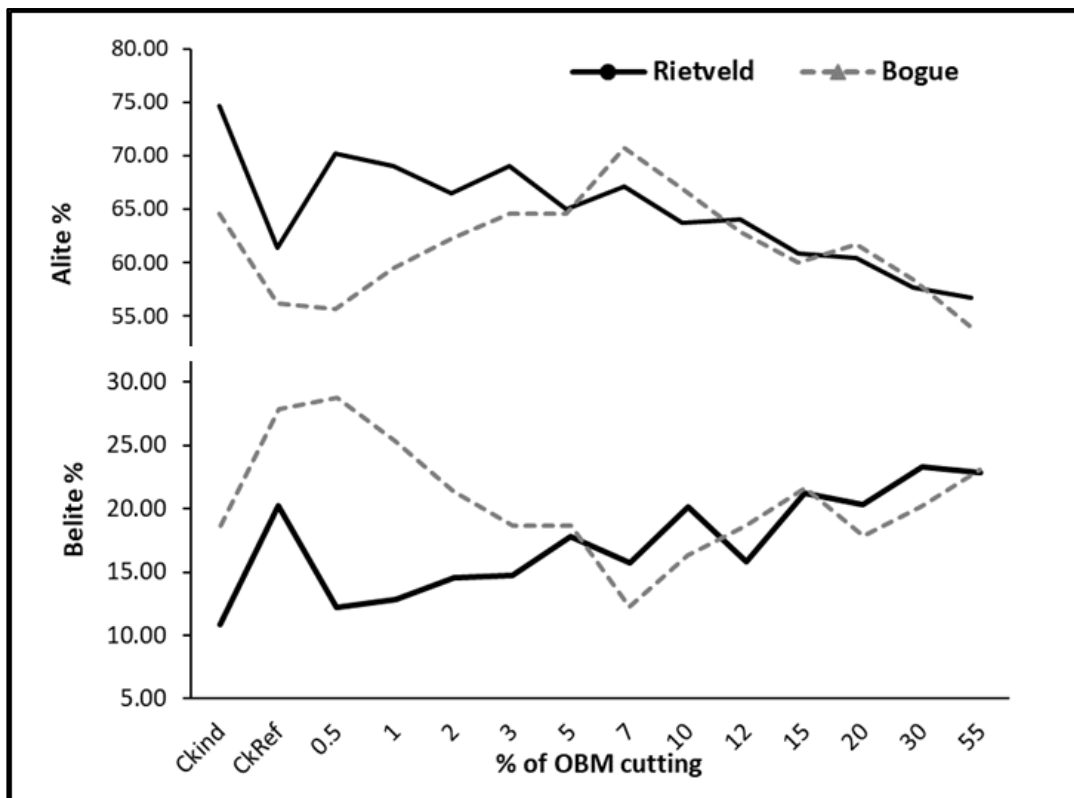


Figure 26 Clinker phase contents derived from Rietveld analysis and Bogue calculations.

Rietveld analysis (thick, black line)

Bogue calculations (grey, dotted line)

Table 11 Chemical oxide and clinker phase composition of the prepared clinker

| | $CK_{Ind.}$ | $CK_{Ref.}$ | Ck-12% | Ck-55% | Ck-100% |
|--|-------------|-------------|--------|--------|---------|
| Major oxides (% wt./wt.) | | | | | |
| SiO ₂ | 22.19 | 22.58 | 21.79 | 21.88 | 32.49 |
| CaO | 65.45 | 65.32 | 65.87 | 65.68 | 51.55 |
| Al ₂ O ₃ | 4.06 | 5.46 | 5.37 | 5.02 | 7.82 |
| Fe ₂ O ₃ | 4.07 | 3.86 | 3.82 | 3.88 | 3.88 |
| LOI @950 °C | 0.25 | 0.12 | 0.07 | 0.06 | 0.04 |
| Minor oxides (% wt./wt.) | | | | | |
| MgO | 0.78 | 0.81 | 1.24 | 1.43 | 1.66 |
| SO ₃ | 1.40 | 0.30 | 0.83 | 1.57 | 0.33 |
| Na ₂ O | 0.25 | 0.32 | 0.35 | 0.34 | 0.20 |
| K ₂ O | 0.39 | 0.25 | 0.07 | 0.02 | 0.11 |
| Trace oxides (×100 mg/kg) | | | | | |
| BaO | - | - | 23 | 85 | 115 |
| Cr ₂ O ₃ | 12 | 11 | 7 | 6 | 5 |
| MnO | 4 | 5 | 4 | 4 | 4 |
| P ₂ O ₅ | 9 | 12 | 11 | 12 | 12 |
| TiO ₂ | 24 | 32 | 28 | 20 | 20 |
| Clinker Module factors | | | | | |
| LSF | 92.53 | 90.5 | 94.33 | 94.22 | 48.45 |
| SM | 2.46 | 2.42 | 2.37 | 2.46 | 2.95 |
| AM | 1.22 | 1.41 | 1.41 | 1.29 | 2.02 |
| Clinker main phases (%) by Bogue^{149,93} | | | | | |
| C ₃ S | 64.66 | 52.06 | 60.97 | 61.78 | - |
| C ₂ S | 14.93 | 25.55 | 16.57 | 16.21 | <36.63 |
| C ₃ A | 3.87 | 7.94 | 7.77 | 6.74 | 14.16 |
| C ₄ AF | 12.39 | 11.75 | 11.62 | 11.81 | 11.80 |

6.2 CaCO₃ decomposition

Thermal analyses of various raw meal samples showed that the calcination temperature decreased with OBM cutting content increases. Calcite decomposition occurred at 817 °C when no OBM was in the sample, falling consistently with increasing OBM cutting content until the OBM cutting alone (Rm100%) showed decomposition at 763 °C. The greater than 50 °C decomposition temperature difference between limestone and OBM cuttings is of interest. To understand why the addition of OBM cutting reduces the calcination temperature, it is important to study the nature of the calcite in OBM cuttings and compare it with that in the limestone.

Many studies^{150–154} have reported limestone reactivity and linked it to the calcite structure. Different grain sizes¹⁵⁵ and impurities within the limestone can cause variations in the limestone's textural and mineralogical properties and, subsequently, influence the calcination temperature¹⁵⁶. This may also influence both the crystallisation temperature in different phases of the clinker formation and free lime content in the produced clinker^{117,157}. It has also been reported that the presence of dolomite in limestone helps speed up the calcite decomposition rate¹⁵⁷.

In 1962, Dunham¹⁵⁸ established a systematic classification scheme for carbonate sedimentary rocks. Initially known as the 'Dunham Classification', it was later modified by Embry and Kloven^{159–161} to include coarse-grained limestone and became known as the 'modified Dunham Classification'. It has become the most commonly used classification in petrographic thin sections for identifying and distinguishing different types of limestone based on the grain-size, ratio, shape and microstructure.

The Dunham classification divides limestone into six sub-classes based on the presence or absence of mud supporting the carbonate grains, the grain content, and nature of the matrix during deposition. Limestone may be further defined by two sub-groups: (1) grain-supported limestone and (2) mud-supported limestone. This division depends on the percentage of the grains (known as allochems) or mud matrix (known as orthochems). Grain-supported limestone is characterised by a texture with little or no lime mud but an abundant framework of grains that support each other, while the mud-supported limestone consists of grains floating in a muddy, mainly calcitic matrix¹⁶².

Analyses of petrographic thin sections of the limestone used here shows calcite crystals of a depositional texture, with no regular shape and unevenly distributed without common direction, (Figure 27). The grains are coarse (>3mm) and compact with no void space between calcite crystals, appearing flat and with some fractures. This limestone can be classified as crystalline limestone according to the Dunham classification¹⁵⁸.

The OBM cuttings, meanwhile, show different petrography, with the calcite being mud-supported with loosely packed grains and high porosity. The clay grains are mostly present as developed clusters and immersed in oil. Lath-shaped plagioclase grains with sharp grain margins are also present as shown in Figure 27 (c) & (d). The calcite show round sub-millimetre grains, which are highly brittle and fragile in nature. Later XRD analyses of OBM cuttings show the presence of dolomite. Therefore, the OBM cuttings' classification can be considered be a mix between two or three types of limestone, falling between mudstone and Wake stone. However, the classification is certainly different from the limestone used in this research.

These differences help explain the lower decomposition temperature of OBM cuttings compared to limestone. First, OBM cuttings contain dolomite, while none is present in the limestone. Dolomite in limestone lowers the decomposition temperature of the calcination process. Marinoni¹⁶³ showed that limestone decomposition starts with the rapid dissociation of dolomite in the first few min, followed by calcite decomposition. Dolomite dissociation occurs in a single step without a calcite intermediate phase. This suggests that the presence of dolomite reduces the calcination activation energy^{117,157,163}. Marinoni¹⁵⁷ proposed that limestone dissociation starts with dolomite decomposition, resulting in the formation of grain cracks due to the $\text{CaMg}(\text{CO}_3)_2$ structure, increasing the surface area, allowing CO_2 diffusion^{157,153,164}.

The lower decomposition temperature in OBM cuttings may also be related to the calcite texture therein, which differs from the calcite in limestone as explained above. Finally, OBM cuttings are more porous than limestone, allowing more surface area for heat transfer. As seen petrographically, the calcite grains float in the mud, with larger spaces between grains than in the limestone (Figures 28 [c] & [d]).

Similar results were obtained by Marinoni et al¹⁵⁷ and Galimberti et al¹¹⁷ when studying the thermal decomposition and burnability of limestone used to manufacture industrial

cement clinker. Using different limestone sources revealed that the texture of mud-supported limestone had a strong impact on the calcite decomposition temperature and its decomposition rate. According to the Dunham calcite classification^{160,161}, raw meal where the limestone is of grain-supported origin is more reactive.

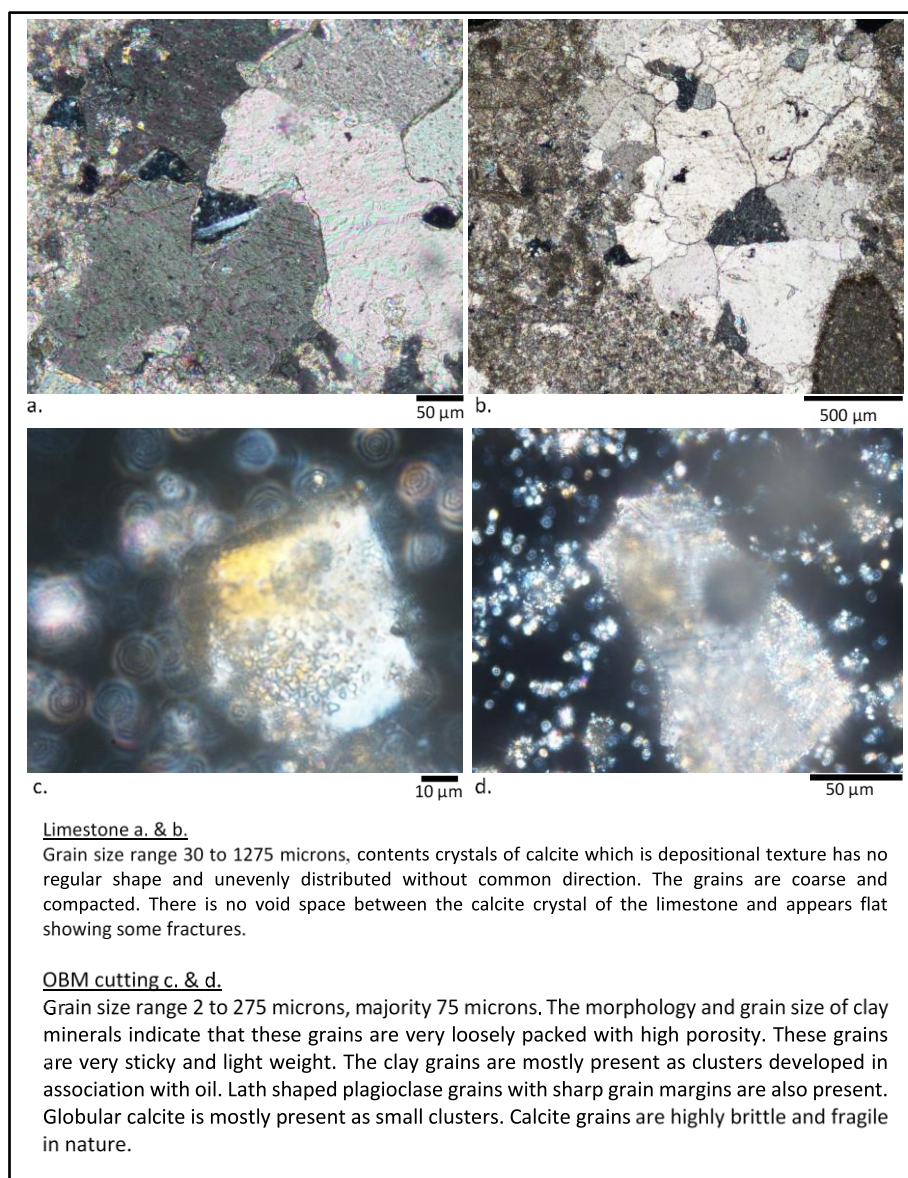


Figure 27 Limestone and OBM cutting petrography analysis

The calcite grain size also has an effect on both the rate of decomposition and the temperature at which decomposition occurs. Coarser grains show higher decomposition temperatures and lower rates of decomposition⁹¹, as illustrated in Table 12.

Table 12 The effect of calcite grain size on the dissociation of limestone (according to Chatterjee⁹¹)

| Crystallinity | Grain size, mm | Relative rate of dissociation | Relative dissociation temperature |
|---------------------|----------------|-------------------------------|-----------------------------------|
| Very coarse grained | > 1.00 | Lowest | Highest |
| Coarse grained | 1.00 – 0.50 | ↓ | ↑ |
| Medium grained | 0.5 – 0.25 | | |
| Fine grained | 0.25 – 0.10 | | |
| Very fine grained | 0.10 – 0.01 | | |
| Microcrystalline | < 0.01 | | |

The effect of particle size was confirmed by grinding the limestone for 5 min and then obtaining two fractions: one passing a 212-micron sieve and one passing a 63-micron sieve. These two fractions were compared against ground OBM cuttings passing through a 212-micron sieve. The particle size distributions of the three resultant materials are comparable to materials used in a cement plant and are shown in Figure 28, along with thermogravimetric analysis (TGA) of the three samples. The finer limestone decomposed at a lower temperature than the standard limestone, with OBM cuttings decomposing at an even lower temperature. Thus, the lower decomposition temperature of OBM cuttings may be explained by the finer calcite grains (Figures 28 [c] & [d]) and the presence of dolomite. The calculated activation energies (E_a) of CaCO_3 decomposition for limestone and OBM cutting are $154.43 \text{ J.mol}^{-1}$ and $181.46 \text{ J.mol}^{-1}$ respectively (Figure 29), confirming the observations made by Chatterjee et al.⁹¹.

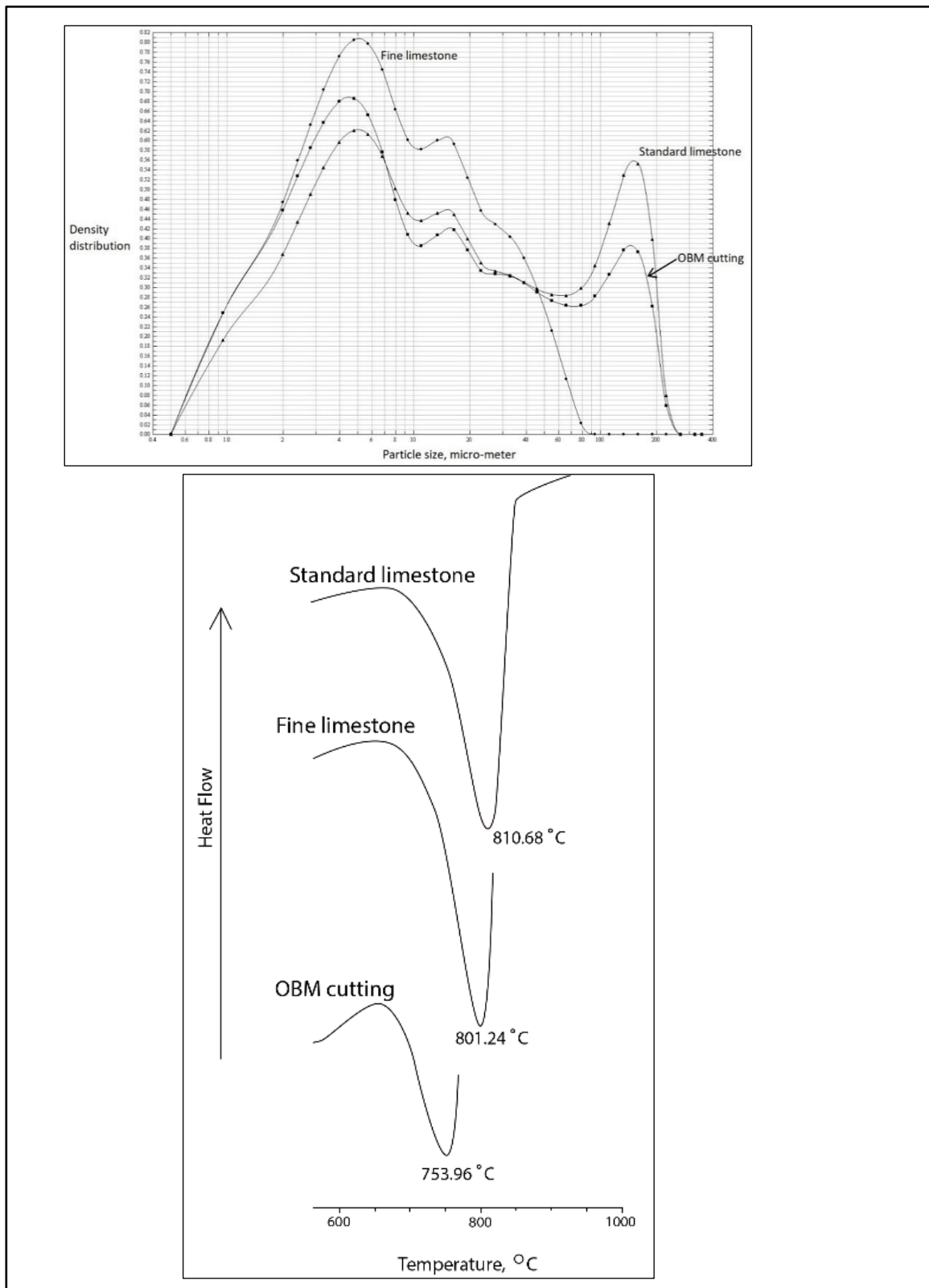


Figure 28 Particle-size distribution (top) and decomposition temperature (below) of fine-limestone, limestone, and OBM cutting.

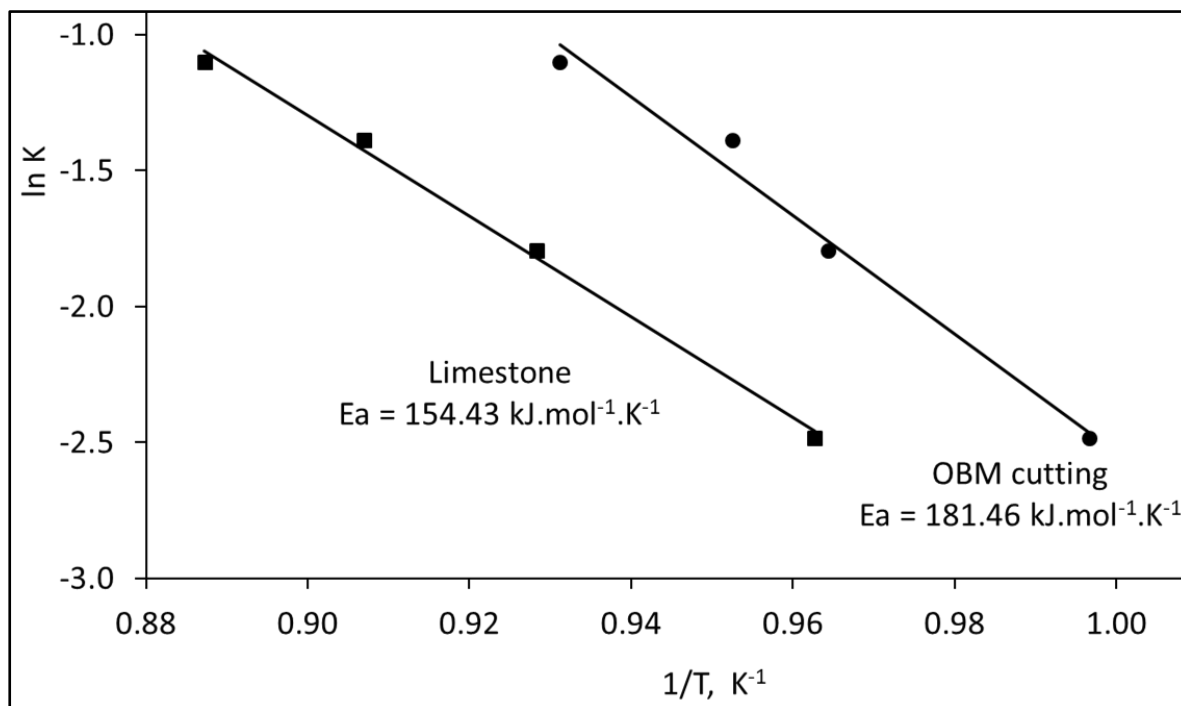


Figure 29 Activation energy values of CaCO_3 decomposition reactions in limestone and OBM cutting.

6.3 Burnability

Figure 30 shows the burnability data obtained in this study. Figure 30 (a) shows the data obtained from cement industry raw meal (Rm_{Ind}) and the reference raw meal prepared in the laboratory (Rm_{Ref}). The free lime content for both mixes fell with increasing temperature. However, the free lime content of Rm_{Ind} was always greater than that of Rm_{Ref} , with the difference between the two decreasing with increasing temperature, until the difference was minimal at 1400 °C and above. The higher free lime content for Rm_{Ind} could be due to its higher LSF, i.e. 92.53 compared to 90.50 for Rm_{Ref} . Thus, there is more CaO to be consumed during clinkering. This is supported by the convergence of the two data sets with increasing temperature. Both mixes showing similar burnability behavior validates the use of the reference raw meal in comparisons with raw meal prepared using OBM cutting.

Figure 30 (b) shows the burnability results for Rm_{Ref} plus raw meal prepared using 12%, 55% and 100% OBM cuttings. Despite the falling free lime contents with increasing temperature, there was an increase in free lime with increasing OBM cutting content, suggesting harder burnability. However, this did not apply to the sample

prepared from 100% OBM cutting. This sample showed very easy burning behaviour (Figure 30 c). The free lime dropped significantly, even at 1300 °C (0.2% free lime), then showing only 0.02% free lime content when heating at 1500 °C. However, as shown by XRD analysis (Figure 31), when burned at 1200 °C, the 100% OBM cutting showed belite formation and a very low free lime content. Higher temperatures still led to no alite formation due to there being no CaO remaining, as shown in Figure 31. This was confirmed by SEM-EDX analysis (Figure 32), where no alite was observed. The absence of alite can easily be understood in terms of the LSF, which at 48.45 was considerably lower than for all of the other samples.

The consumption of calcium oxide to form C_2S at temperatures below 1300 °C explains the low free lime concentrations in the Ck-100. While Clk-55 contains more calcium oxide (e.g. higher LSF factor), part of it reacts to form C_2S while some remains to react with C_2S to form C_3S at higher temperatures (above 1450 °C). This thermodynamic chemical reaction is reversible, meaning that when the temperature drops, the C_3S decomposes to free lime and C_2S , especially if the cooling process is slow, resulting in increased the free lime content in the clinker burned at a higher temperature if the clinker is not quenched (rapid cooling).

Figures 34 to 36 show the SEM analysis of raw meal burned at different temperatures to study clinker phase formation at each temperature (e.g. 1200 to 1500 °C). The observation of each SEM images are presented within the figure. Also the EDX images of corresponding SEM images are shown in Figures 37 to 41.

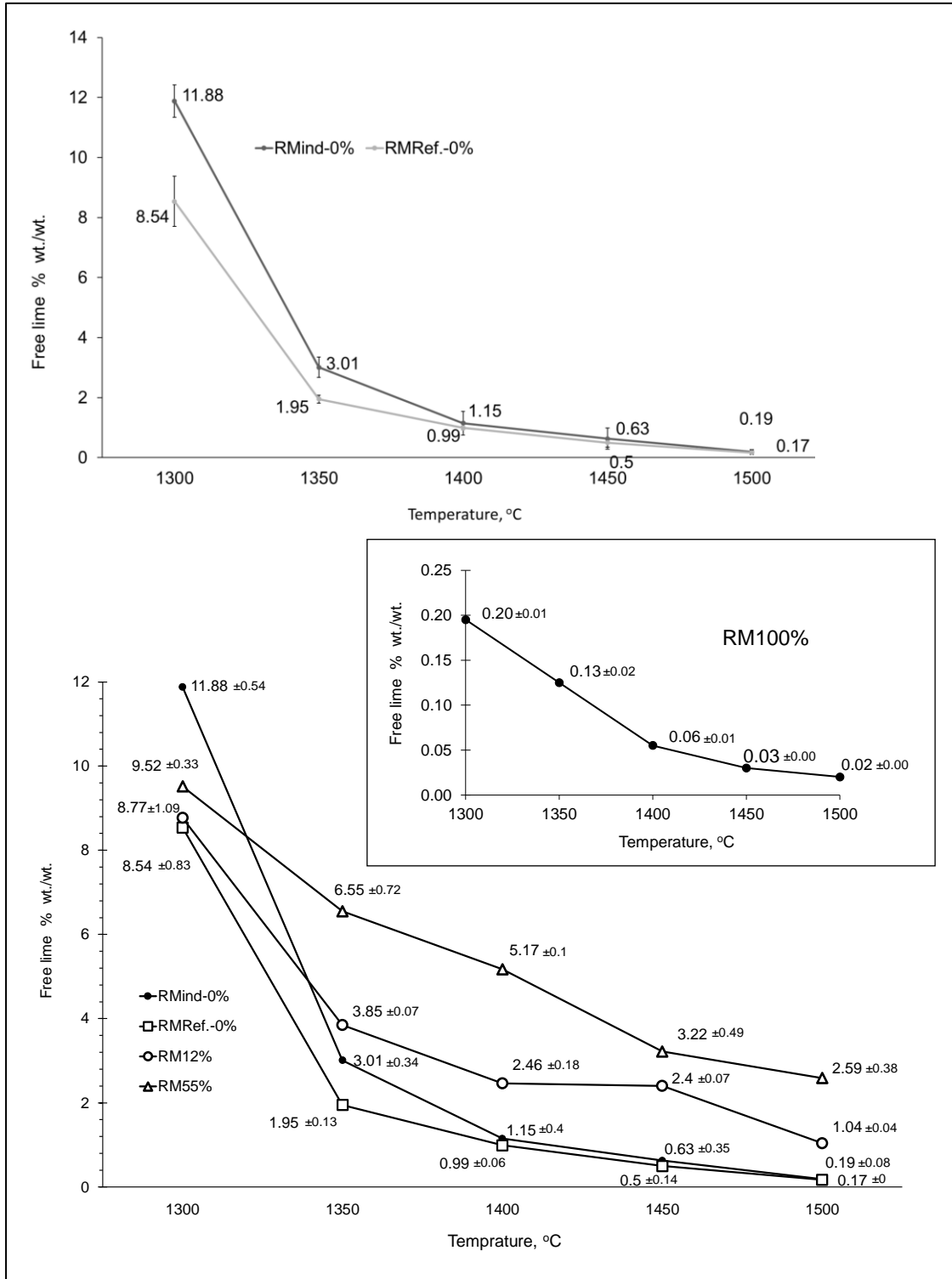


Figure 30 The burnability tests of the raw meal at different burning temperatures.

Top: reference sample vs. industrial raw meal

Bottom: reference sample vs. raw meals with 12%, 55% and 100% OBM cuttings

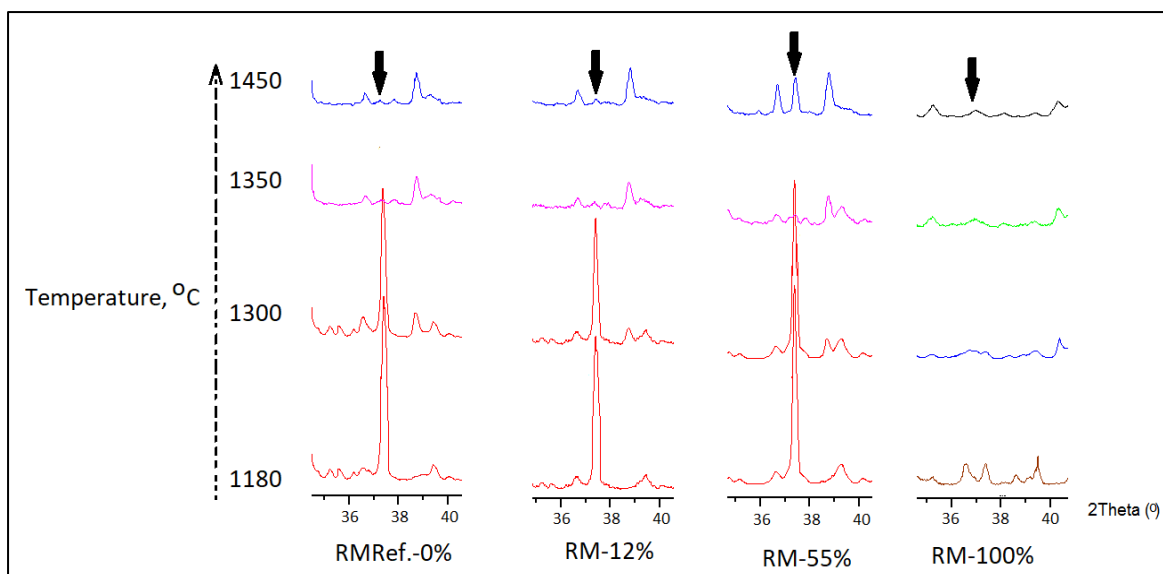


Figure 31 XRD pattern of the different raw meal samples burned at different temperatures.

The arrows show the free lime peak at $2\theta = 37.36^\circ$, the highest intensity when calcined at 1450°C is for the raw meal prepared with 55% OBM cutting.

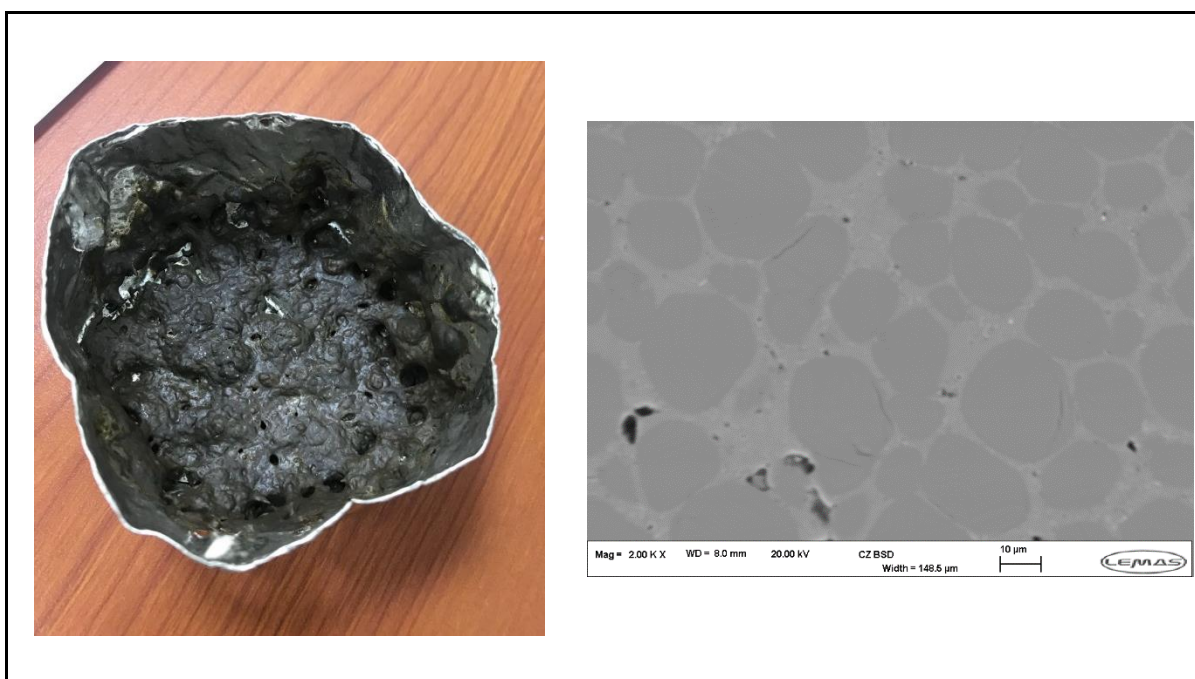


Figure 32 100% OBM cuttings clinker.

Left: Clinker sample (100% OBM cutting) after burning at 1450°C in platinum crucible for 30 minutes.

Right: SEM image analysis of the same clinker sample.

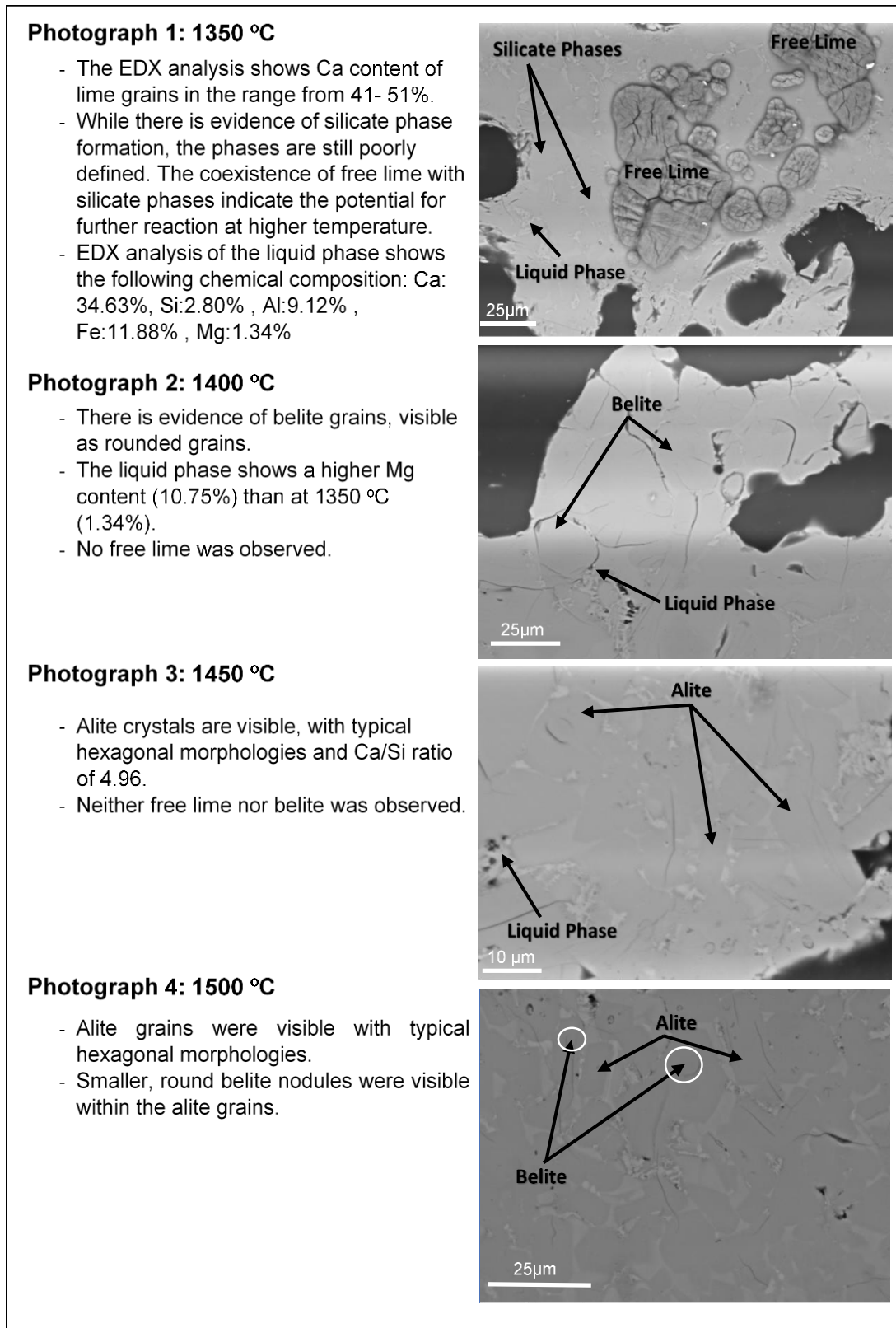
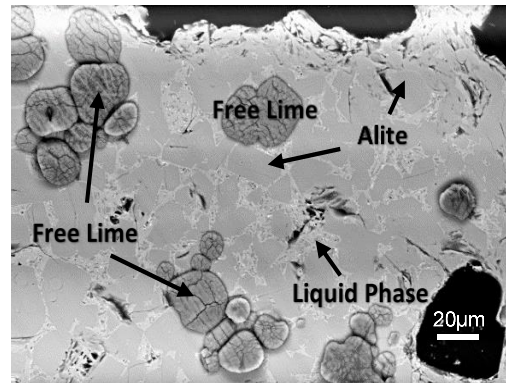


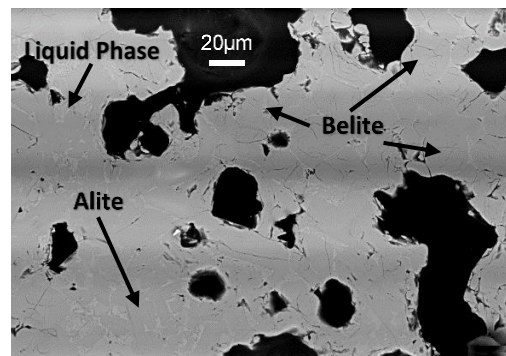
Figure 33 The SEM analysis of Rm_{Ref} burned at four different temperatures.

Photograph 1: 1350 °C

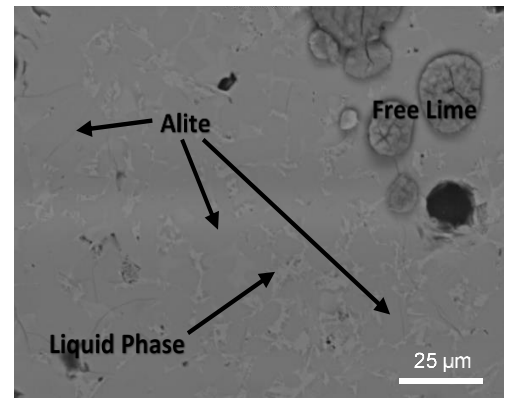
- Early formation of alite phases at lower temperature 1350 °C.
- Free lime grains, the EDX analysis shows Ca content in the range 44-47%.
- Present of alite grain and free Lime grain without present of belite indicate that at higher temperature no further alite formation expected.

**Photograph 2: 1400 °C**

- Belite formation at 1400 °C, which are shown rounded grains. The Ca/Si ratio is 3.51.
- Alite formed are smaller grains compared to belite.
- No free lime observed.
- Trace elements observed in the LP are: Mo, Zr, Ni, Co, Mn, Cr, and Ti

**Photograph 3: 1450 °C**

- Formation of alite crystals, associated with free lime. This is indicating hard burning clinker. The free lime will remain unreacted due to no belite grains are present near the free lime.
- Alite crystals shows hexagonal-shaped grains.

**Photograph 4: 1500 °C**

- Formation of alite crystals.
- Alite crystals shows hexagonal-shaped grains.
- No belite grains observed however, still free lime is appearing with alite.

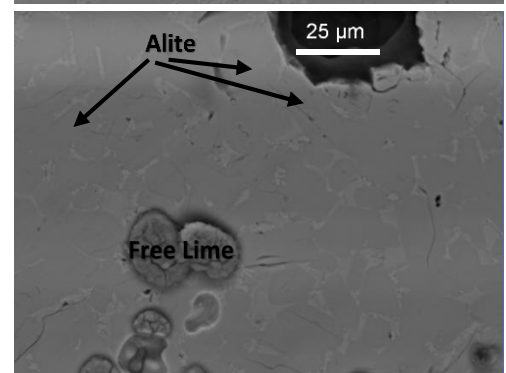


Figure 34 The SEM analysis of Rm-12 burned at four different temperatures.

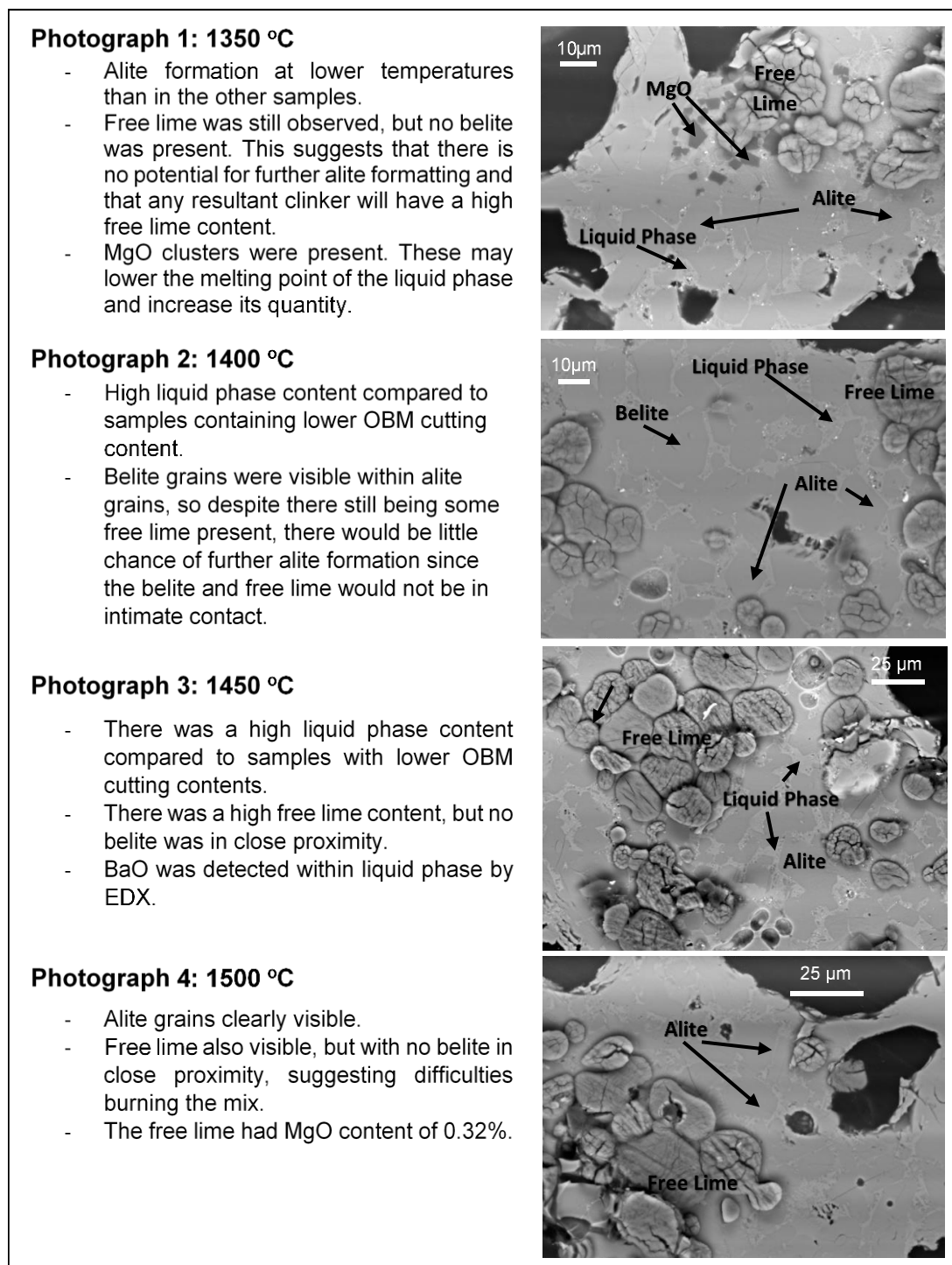


Figure 35 The SEM analysis of Rm-55 burned at four different temperatures.

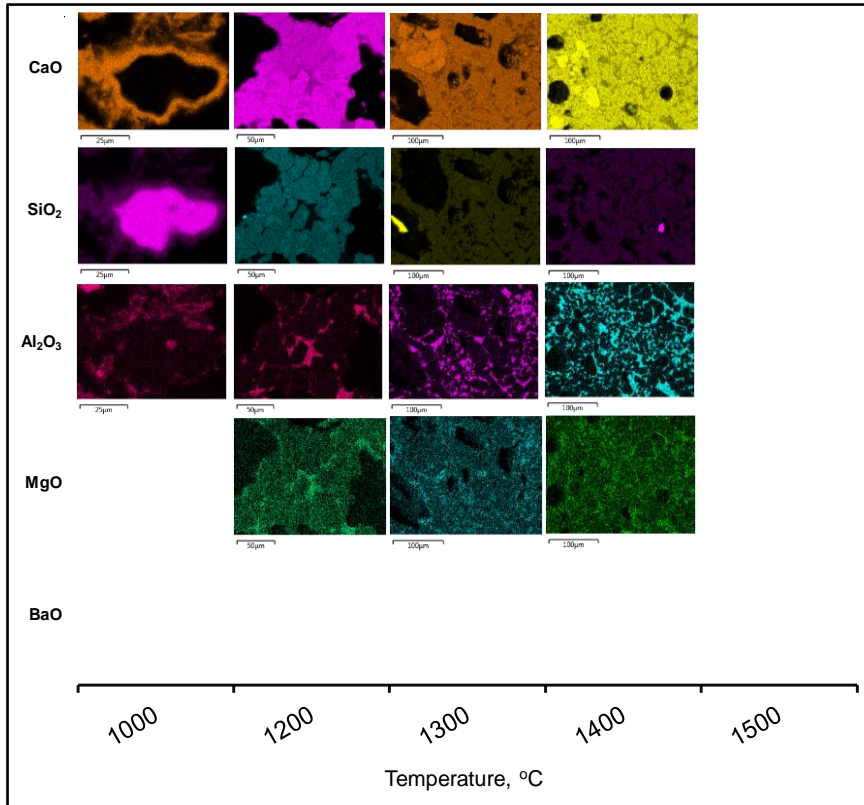


Figure 36 EDX analysis for $R_{m_{Ind}}$ showing clinker microstructure development with increasing temperature.

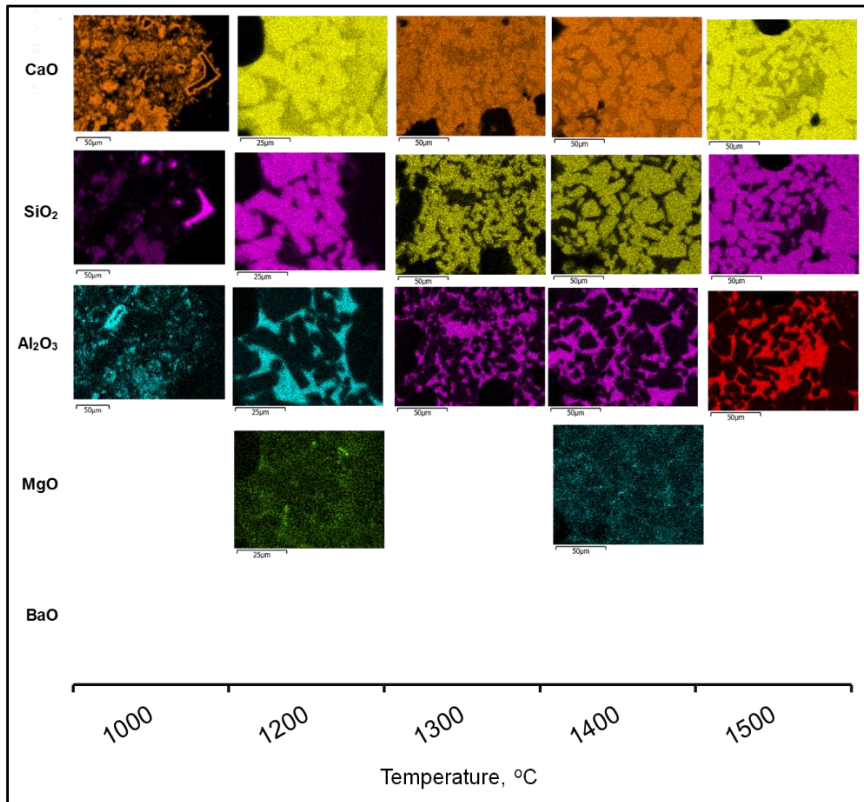


Figure 37 EDX analysis for $R_{m_{Ref}}$ showing clinker microstructure development with increasing temperature.

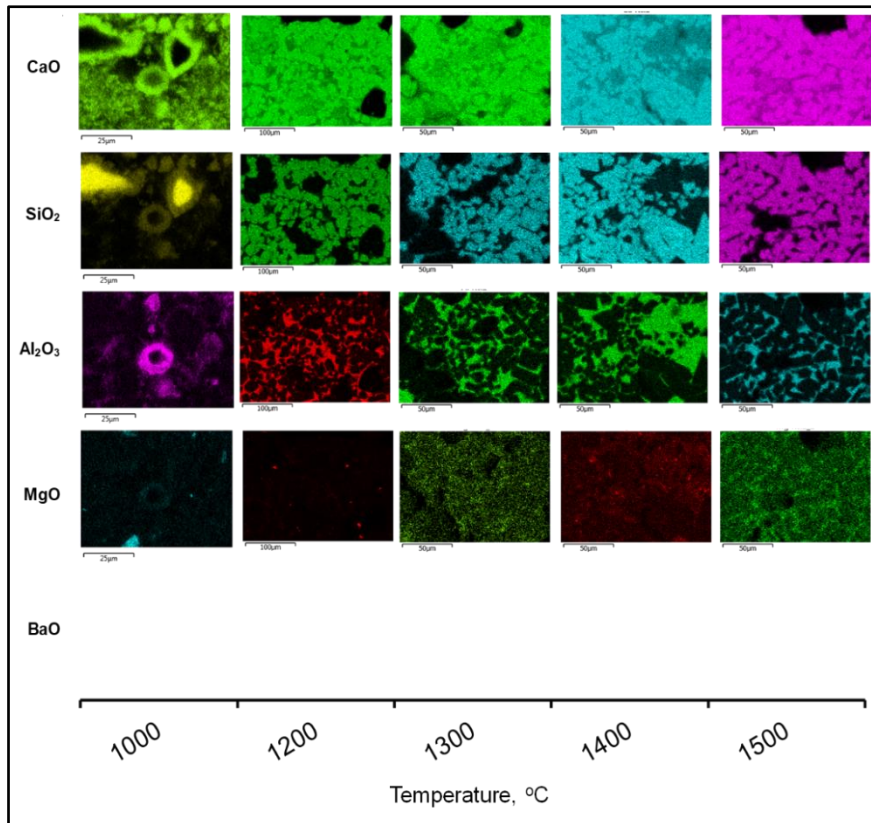


Figure 38 EDX analysis for Rm-12 showing clinker microstructure development with increasing temperature.

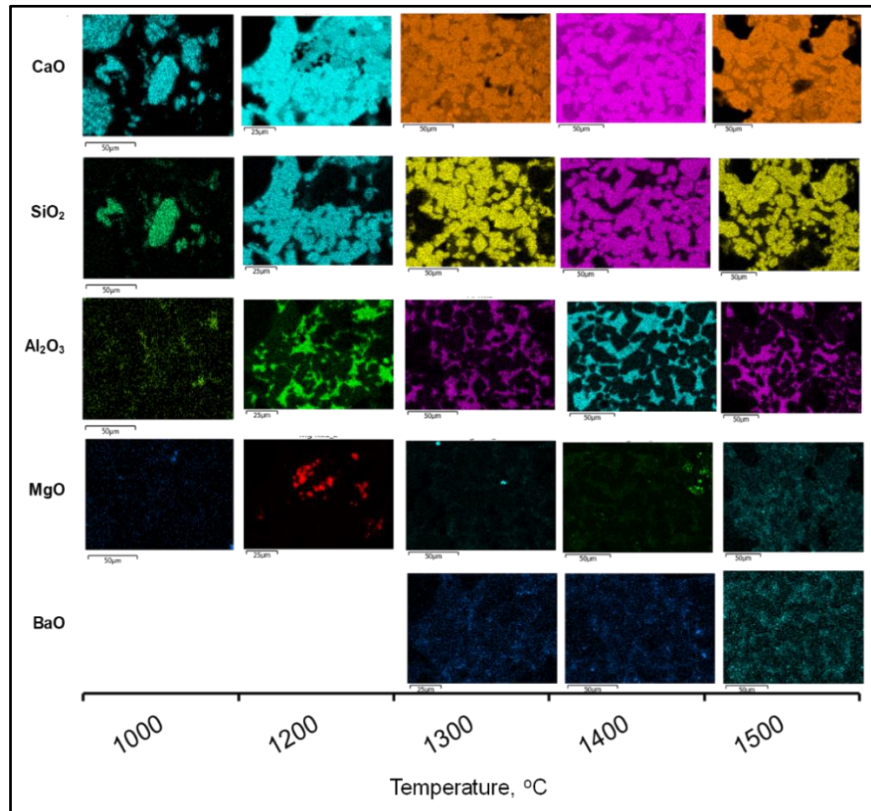


Figure 39 EDX analysis for Rm-55 showing clinker microstructure development with increasing temperature.

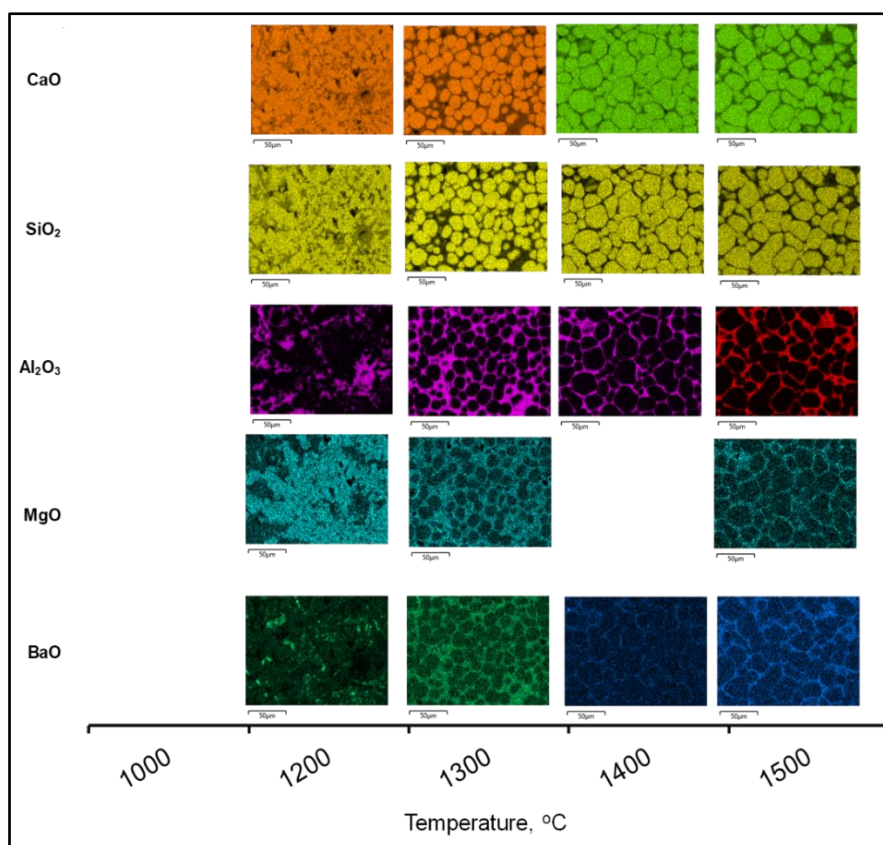


Figure 40 EDX analysis for Rm-100 showing clinker microstructure development with increasing temperature.

6.4 The XRD and TGA

XRD and TGA were used to measure clinker phase composition and obtain information on the changes in clinkerization during the heating process. Thermal analysis (Figure 41) showed that all of the changes occurring during the heating process, including CaCO_3 decomposition, belite formation, liquid phase and alite formation (liquid phase sintering) shifted to lower temperatures as the OBM cutting content of the raw meal increased.

The effect of OBM cutting on CaCO_3 decomposition temperature was described earlier, but the effect on other phases is described below. At higher temperature (above $1338\text{ }^\circ\text{C}$)¹⁶⁵ the liquid phase develops. This comprises mainly Al_2O_3 and Fe_2O_3 bearing phases. These are essential fluxes, lowering the energy required for completing the clinkerization process. When melting commences, the liquid content can increase significantly, up to 15 – 25%¹⁶⁵. The presence of other minor oxides such as SO_3 , MgO and alkalis can have an influence by lowering the energy required to form the flux. In this study RM_{Ind} showed the presence of a liquid phase from 1334

°C, very close to temperature of liquid phase reported in the literature ¹⁶⁵. However, RM_{Ref} showed temperature of formation of the liquid phase from 1331 °C which also close to industrial sample. However, with increasing OBM cutting content, the liquid phase formed at ever lower temperatures, decreasing to 1320 °C with 55% OBM cutting and 1263 °C when 100% OBM cutting was clinkerised. This could be attributed to the present of minor oxides from the OBM cutting, as shown in Figure 42. Additionally, periclase was found in the liquid phase when 100% OBM was used, with 10.75% MgO determined in the liquid phase (Figure 33).

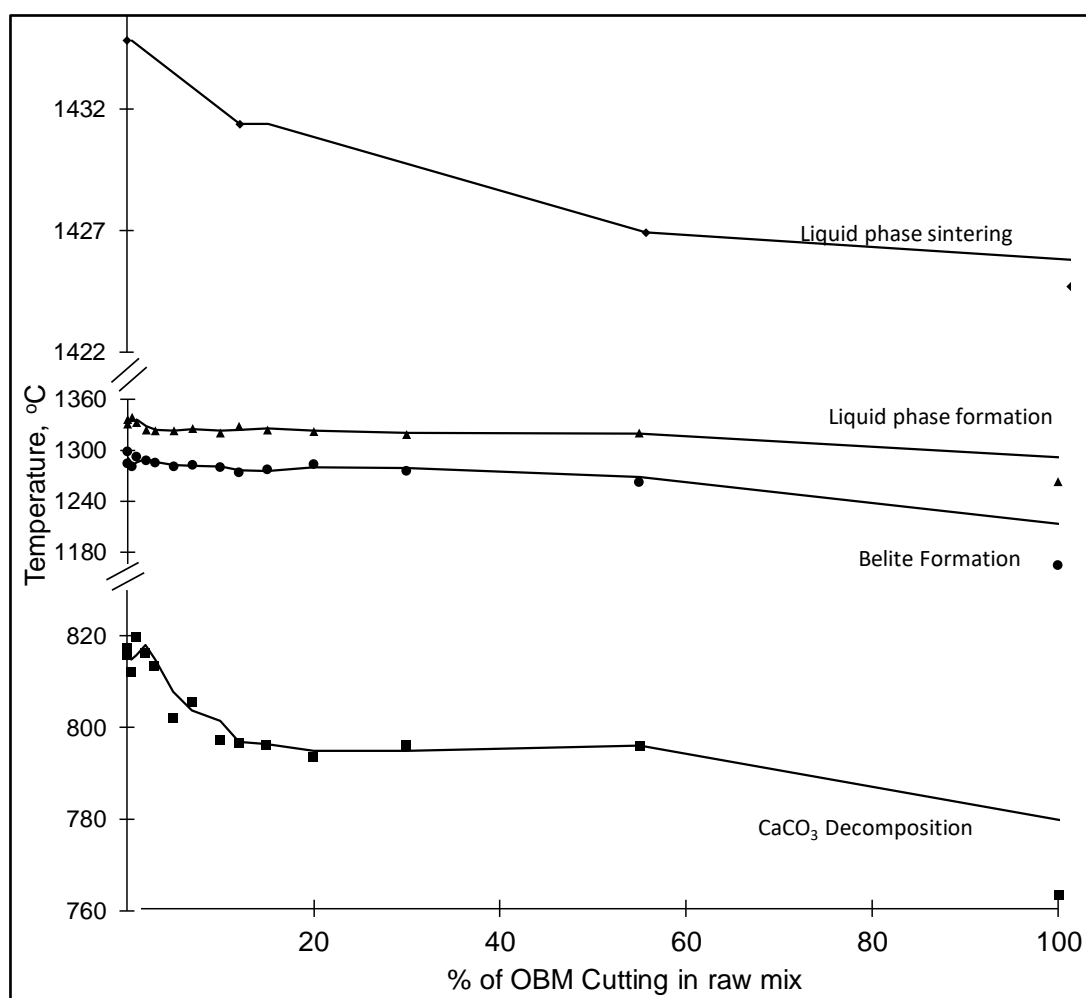


Figure 41 Temperatures of calcite decomposition and major phase formation with increasing OBM cuttings content.

The temperatures were determined by DTA. The trend lines are moving averages.

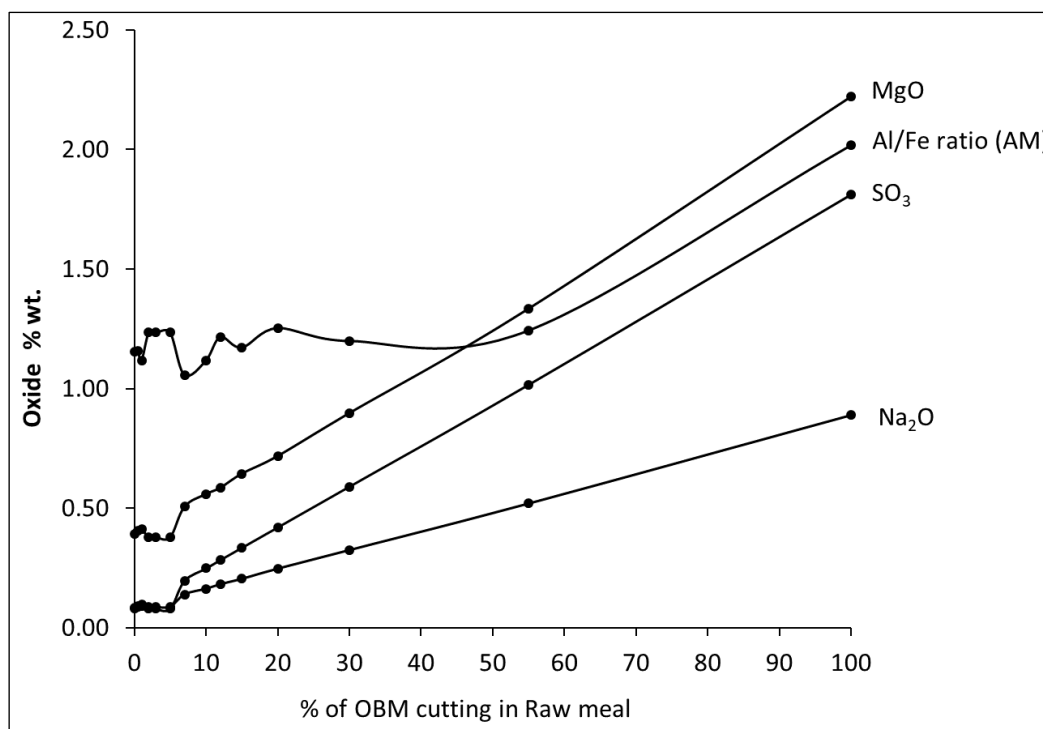


Figure 42 Minor oxide contents in prepared raw meal

The decreasing temperature for the onset of liquid phase formation with increasing OBM cutting content also influenced the sintering temperature. The role of the liquid phase at this stage is very important and critical to the clinkerization mechanism. The liquid wets the solid grains, forming an interpenetrating film¹⁶⁵. This has two main functions: 1) its surface tension pulls the solid grains together, serving to form clinker nodules. 2) It also eases transport of the main oxides in the liquid phase during the sintering stage and aids formation of alite and belite. The lower temperature for the onset of liquid phase formation, due to the presence of the minor oxides, impacts also on the sintering temperature, which were too close for Rm_{Ref} and Rm12 at 1434 °C and 1431 °C respectively. However, the sintering temperature falling to 1424 °C for Rm55. The liquid phase (flux) plays a major role in facilitating the chemical reactions to form the major clinker phases such as C₂S and C₃S. Sufficient liquid phase is required to wet reactants and thereafter the rate of formation of desired clinker phases is limited largely by liquid phase diffusion¹⁶⁵.

The clinker sample made with 100% OBM cutting, CK100%, showed formation of belite at 1200 °C, as indicated by XRD and SEM-EDX analysis. At higher temperatures, no further new phases were formed. The CK-100% at 1450 °C showed

belite grains swimming in a high melt content (Figure 32), a result of the high concentration of Al_2O_3 and Fe_2O_3 % in the mix.

6.5 The Effect of Barium on Clinkerization

As shown above, the incorporation of OBM cutting had a slight, yet noticeable effect on clinker composition. Initial elemental analysis of the raw materials showed that a number of trace elements were present in the OBM cuttings (Table 6), while the presence of some trace elements plays a major role on clinker phase formation^{166–173}. This was thus investigated further, with particular focus on the barium content which was present in high quantities in the OBM cuttings and subsequently in clinkers prepared with higher levels of OBM cuttings.

In R_{mRef} , the belite and liquid phase formation temperature was 1284 and 1331 °C respectively, but these fell upon incorporation of OBM cutting. SEM-EDX and ICP analysis (Table 13) both showed an increase in barium content with increasing OBM cutting content. Furthermore, SEM-EDX analysis revealed the distribution of barium through the clinker phases. The highest barium concentration was found in the liquid phase.

Table 13 BaO content of each phase in each experimental clinker

| Sample | Ck _{Ind} | Ck _{Ref.} | Ck12 | Ck55 | Ck100 |
|---------------|-------------------|--------------------|------|------|-------|
| Alite | - | - | 0.35 | 0.42 | -* |
| Belite | - | - | 0.25 | 1.98 | 6.40 |
| Liquid phases | - | - | 2.57 | 2.46 | 14.32 |

*no alite observed in Ck100.

The effect of barium on phase composition is related to the free lime content. An increased free lime content indicates reduced burnability and incomplete formation of the main clinker phases. This is due either to alite formation being discouraged or decomposition to CaO and belite being promoted. As stated earlier, the addition of OBM cuttings decreased burnability and the free lime contents increased (Figure 43). With the OBM cuttings containing 0.85 wt% BaO, the barium content of the clinker

increases with increasing OBM cutting content. It has repeatedly been shown that BaO has a negative influence on alite formation, thus increasing the free lime content. Kolovos et al.^{168,174} studied the effect of raw meal BaO content on the reactivity of the CaO-SiO₂-Al₂O₃-Fe₂O₃ system. They noticed that the addition of 1% BaO to the raw meal then sintering at 1200 °C and 1450 °C led to an increase in free lime compared with the reference sample. This BaO was then shown, by SEM analysis, to concentrate in the melting phase of the clinker.

Other studies^{175,176,177,168,148} have also reported on the impact of barium on clinkerisation reactions. These mostly confirm that the free lime content increases with barium content, and that barium is mainly concentrated in the melting phase. Furthermore, Zezulova et al.¹⁷⁵, in addition to showing high BaO contents in the melting phase, also reported higher concentrations of BaO in belite than alite. This is possibly caused by the crystal lattices of alite and belite, with the belite structure being more accommodating of foreign ions^{175,178}.

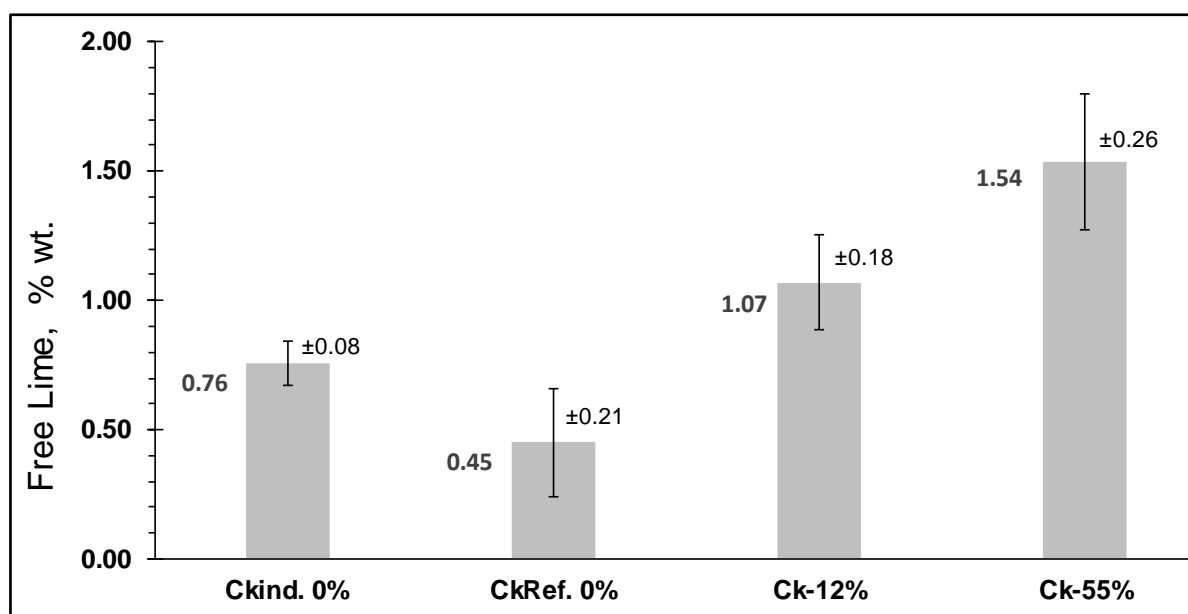


Figure 43 The free lime content for each clinker sample

6.6 Clinker morphology

Clinker morphology and chemical composition was then studied by SEM/BSE imaging and EDX analysis. Below 1250 °C, clinkerization proceeded through solid-solid reactions, in the absence of the liquid phases. These reactions occurred at the original phase boundary between the solids¹⁷⁹, leading to the formation of belite, see Figure 44 A1. This happens through diffusion of the CaO on the SiO₂ surface as could be

seen in the SEM-EDX in the reference clinker sample $Ck_{Ref.}$ and the industrial sample Ck_{Ind} which are shown in Figure 44 A1 and B1. EDX analysis revealed a cluster of SiO_2 surrounded by the CaO . This led to belite formation, which is known to form between $900\text{ }^\circ\text{C}$ and $1250\text{ }^\circ\text{C}$ ^{180,181} with the precise formation temperature defined by a number of factors, such as minor compounds ^{166,168,170,173,182,183}, particle sizes ¹⁸⁴ and retention time ¹⁰⁴.

The raw meal containing 12% OBM cutting showed some formation of alite at $1350\text{ }^\circ\text{C}$ (Figure 44 A1). Free lime was present in clusters, but belite was not observed. The co-existence of alite and free lime without belite suggest that no further alite could be formed, irrespective of temperature, because no belite is available to react with any free lime. Figure 45 shows the SEM images with EDX mapping for $Ck_{100\%}$ heated at three different temperatures; 1300 , 1350 and $1400\text{ }^\circ\text{C}$. At all temperatures, belite was the dominant phase, showing rounded to regular edges. XRD patterns from $Ck_{100\%}$ heated to $1000\text{ }^\circ\text{C}$ showed formation predominantly of belite, plus free lime (Figure 46). However, upon heating to $1300\text{ }^\circ\text{C}$ there was no evidence of free lime in either the XRD patterns nor the SEM images. The same was observed when the temperature was raised further, to $1350\text{ }^\circ\text{C}$. While temperatures above $1400\text{ }^\circ\text{C}$ would normally be expected to yield alite, the lack of free lime in the $Ck_{100\%}$ sample meant that alite formation was not expected. XRD analysis confirmed the absence of alite. Finally, EDX mapping revealed the concentration of magnesium and barium in the liquid phase, at all temperatures (Figure 47 B1 & B2), with the formation of C_3A and ferrite.

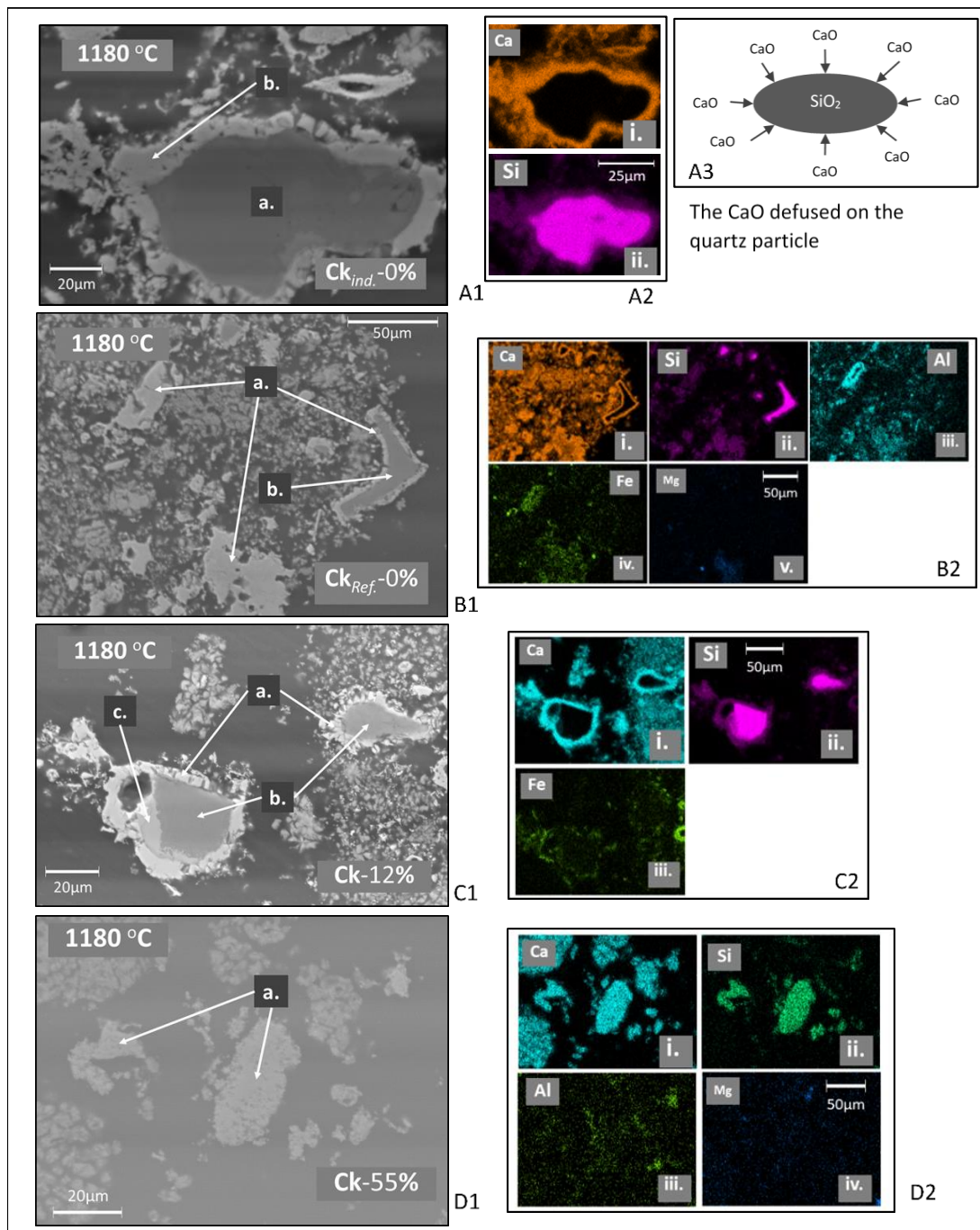


Figure 44 SEM-EDX microstructural analysis of clinker samples burned at 1180 °C.
a) CaO, b) SiO₂ c) Fe₂O₃, Formation of belite by solid-solid reactions.

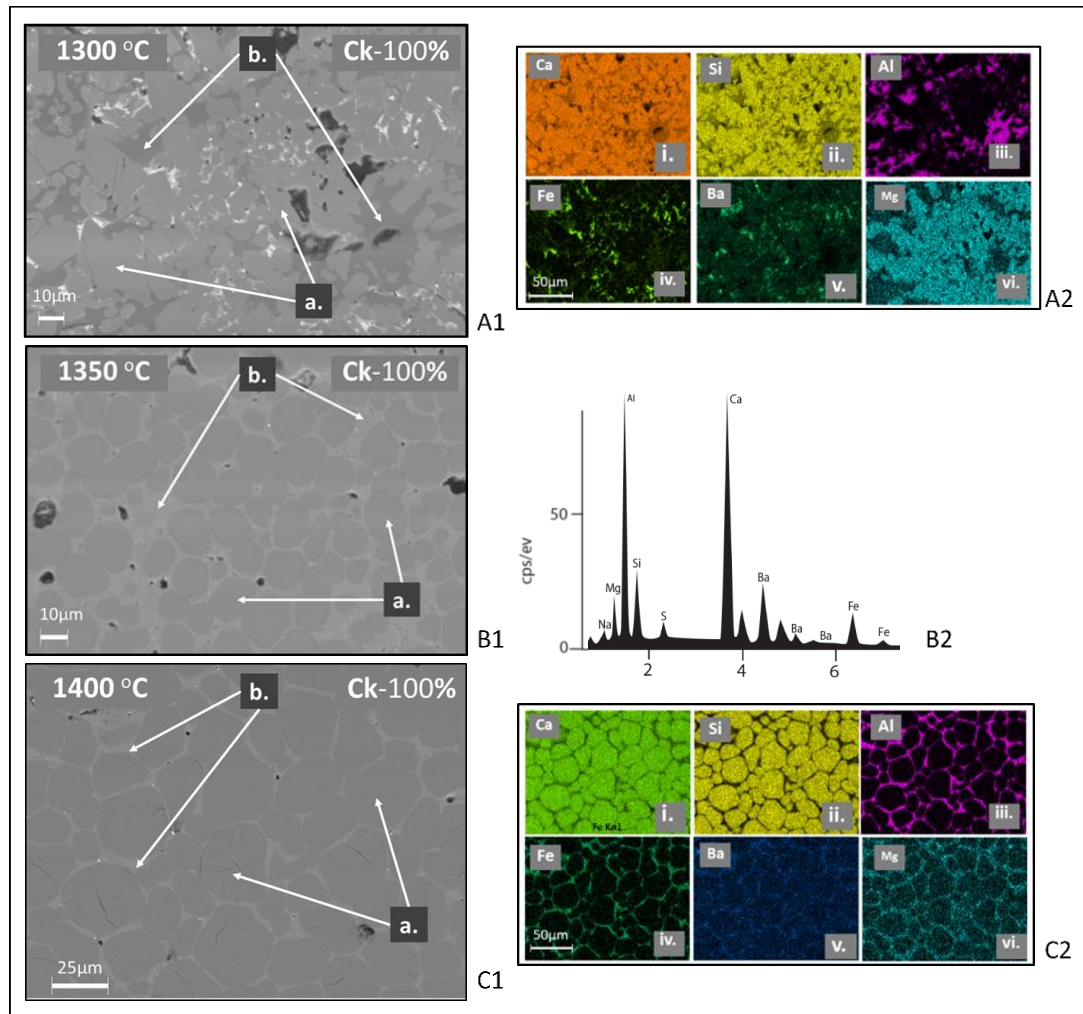


Figure 45 SEM-EDX microstructural analysis of clinker samples burned from 100% OBM.

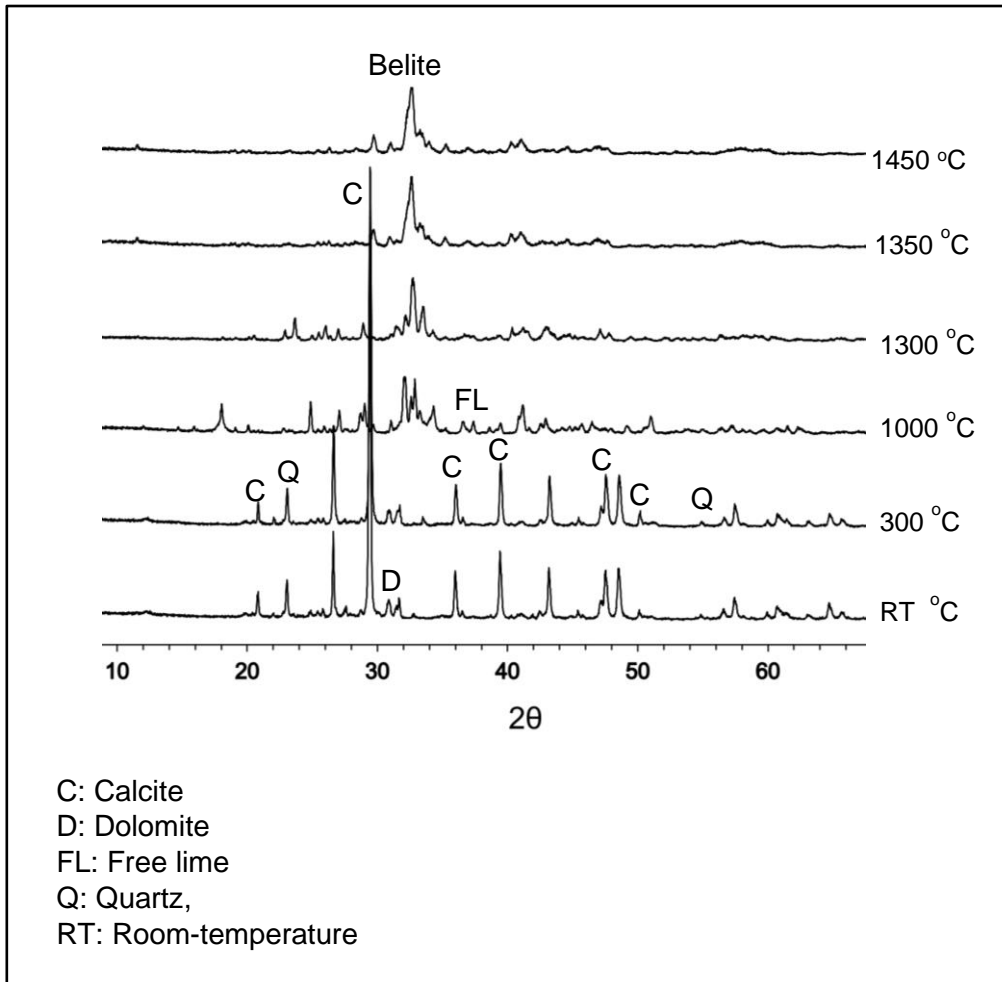


Figure 46 XRD of OBM cutting when heated to different temperatures.

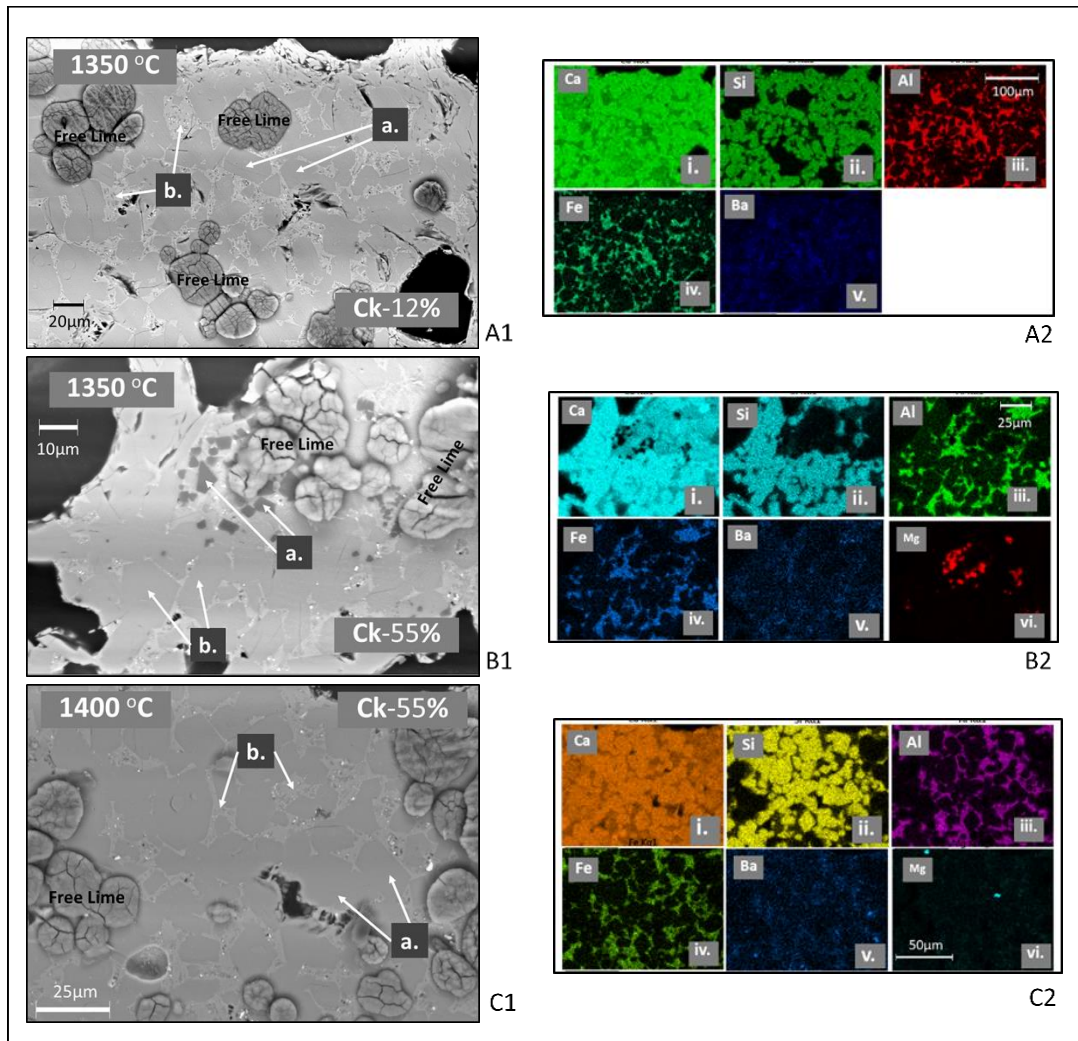


Figure 47 SEM-EDX microstructural analysis of clinker samples prepared by adding 12% and 55% OBM cutting.

6.7 Petrography Study of the Clinker

The clinker samples were also analysed by optical microscopy. Table 14 summarises the data obtained from the petrographic thin sections. As observed by optical microscopy, increased OBM cutting content led to an increased liquid phase content and a slight reduction in alite content. Changes were also seen in both maximum and average grain sizes. With increasing OBM cutting content there was a clear decrease in belite grain size, while conversely free lime grains increased in size. There was also a slight reduction in the size of the C_4AF grains with increasing OBM cutting content.

The granulometric composition analysis is clearly indicate that the raw mix of all the samples is rich in Al and Fe component. These two components mainly participate in the early stages of phase formation consuming the calcium Aluminate component. Hence, in C_3S phase amount, very slight variation could develop in all the three samples.

Table 14 The granulometric composition analysis of the prepared clinker

| Phase | % | | | Granulometry Max (in μm) | | | Granulometry Average (in μm) | | |
|--------------------|-------------|------|------|--|------|------|--|------|------|
| | $Ck_{Ref.}$ | Ck12 | Ck55 | $Ck_{Ref.}$ | Ck12 | Ck55 | $Ck_{Ref.}$ | Ck12 | Ck55 |
| C_3S | 58 | 56 | 54 | 72 | 73 | 70 | 34 | 35 | 33 |
| C_2S | 23 | 21 | 22 | 76 | 68 | 64 | 38 | 32 | 29 |
| $CaO_{free\ lime}$ | 1 | 1 | 2 | 36 | 38 | 40 | 17 | 19 | 22 |
| C_3A | 12 | 16 | 17 | 26 | 29 | 28 | 14 | 15 | 13 |
| C_4AF | 6 | 6 | 5 | 20 | 18 | 16 | 9 | 8 | 7 |

The clinker phases in $Ck_{Ref.}$ were moderately developed and homogeneously distributed. Porosity was high and the majority of alite grains were hexagonal to pseudo hexagonal in shape, with sharp grain boundaries. Many polygonal alite grains were also present, with numerous inclusions present in larger alite grains. Most of these inclusions were globular belite grains.

Sub-micron alite grains were often present on the edges of alite phenocrysts in the reference clinker sample $Ck_{Ref.}$ (Figure 48 [a]) with quite large variations in alite grain size (Figures 49 [b], [c] and [d]). Fused alite grains were also observed (Figure 48 [b]) while the formation of sub-micron belite grains and C_3A grains of various shapes and sizes was seen (Figure 48 [b]).

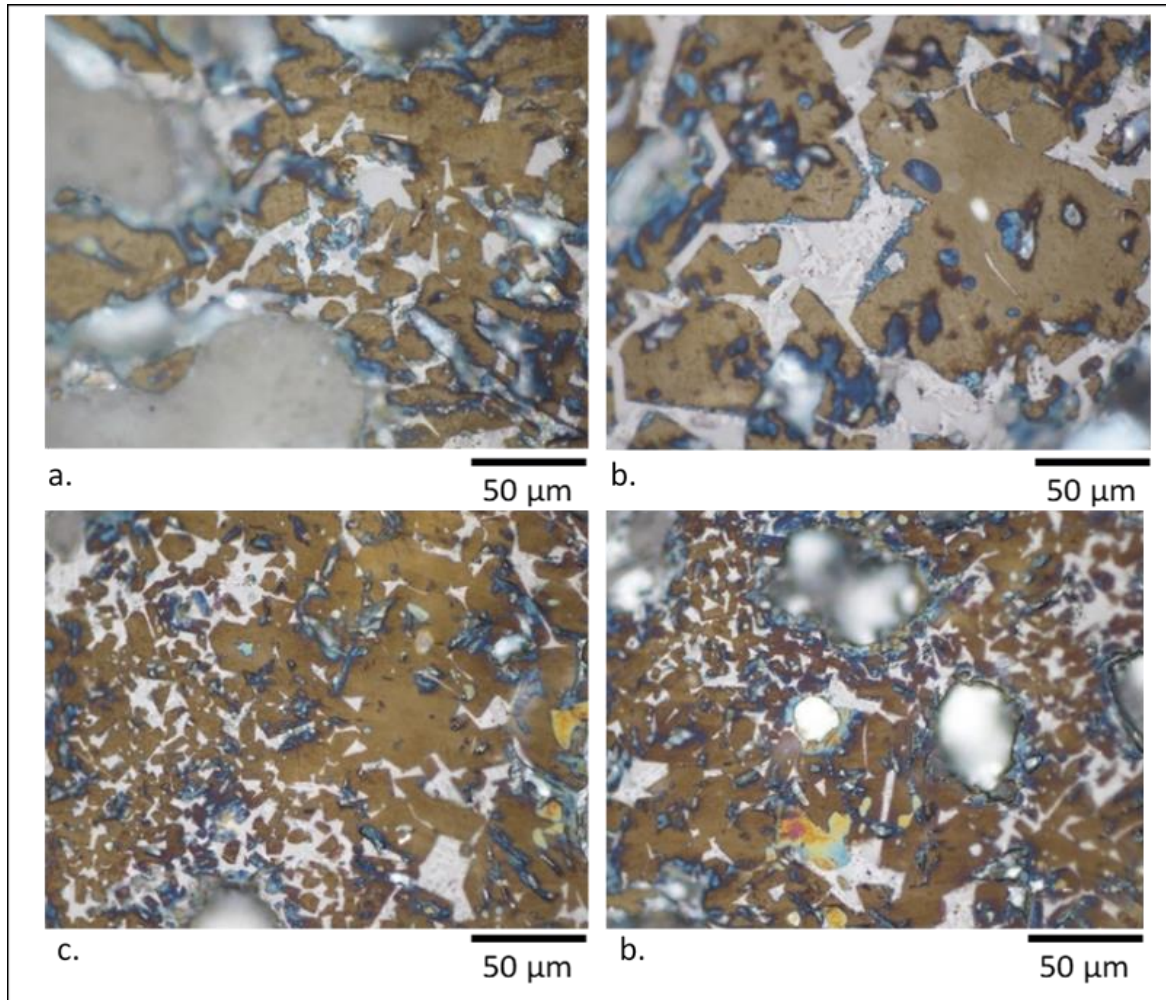


Figure 48 Photomicrographs of clinker Ck_{Ref} .

Ck12 showed moderate development of the various clinker phases, with an inhomogeneous distribution and a high porosity. There was also a marked increase in the amount of liquid phase present compared to Ck_{Ref} . The majority of the alite grains were pseudo hexagonal with rough profiles (Figure 49 [a]). Fine grained polygonal belite grains were commonly observed on the edges of alite grains (Figure 49 [b]) present in various polymorphic forms as small clusters and surrounded by liquid phase. Many polygonal alite grains¹⁸⁵ also developed in the clinker (Figure 49 [e]) with no change in alite grain size.

Sub-micro sized grains of both alite and belite developed on the edges of alite phenocrysts (Figure 49 [c]). Most of the belite grains were well-developed (Figure 49 [e]) with smooth grain edges. In several instances, liquid phase (Figure 49 [d] and [e]) remained on the edges of rounded belite grains. There was considerable variation in belite grain size.

The phases in Ck55 were moderately developed and inhomogeneously distributed, with the majority of the alite grains being hexagonal to pseudo hexagonal^{180,186–188}, with sharp grain boundaries (Figures 51 [a], [b] and [c]). Numerous polygonal alite grains¹⁸⁹ had also developed . In addition, numerous globular¹⁹⁰ belite inclusions (Figure 50 [d]) were present in alite phenocrysts.

It could also be seen that the transformation of belite into alite did not reach equilibrium (Figures 51 [e] and [f]). There were also many fused alite grains in all the nodules. This indicates a large variation in carbonate composition in the raw mix¹¹⁹. Significantly, the percentage of fused alite grains increased with increasing OBM cutting content. This supports the observations made earlier regarding the nature of the carbonate in the limestone and OBM cutting.

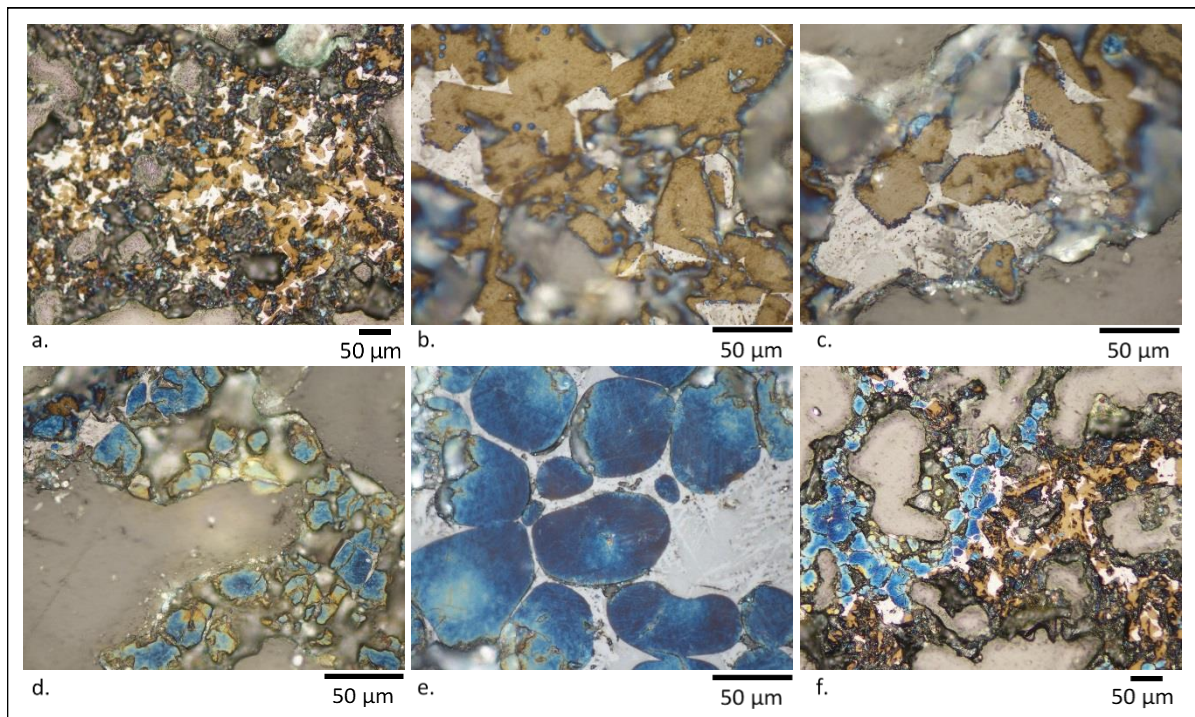


Figure 49 Photomicrographs of clinker Ck12

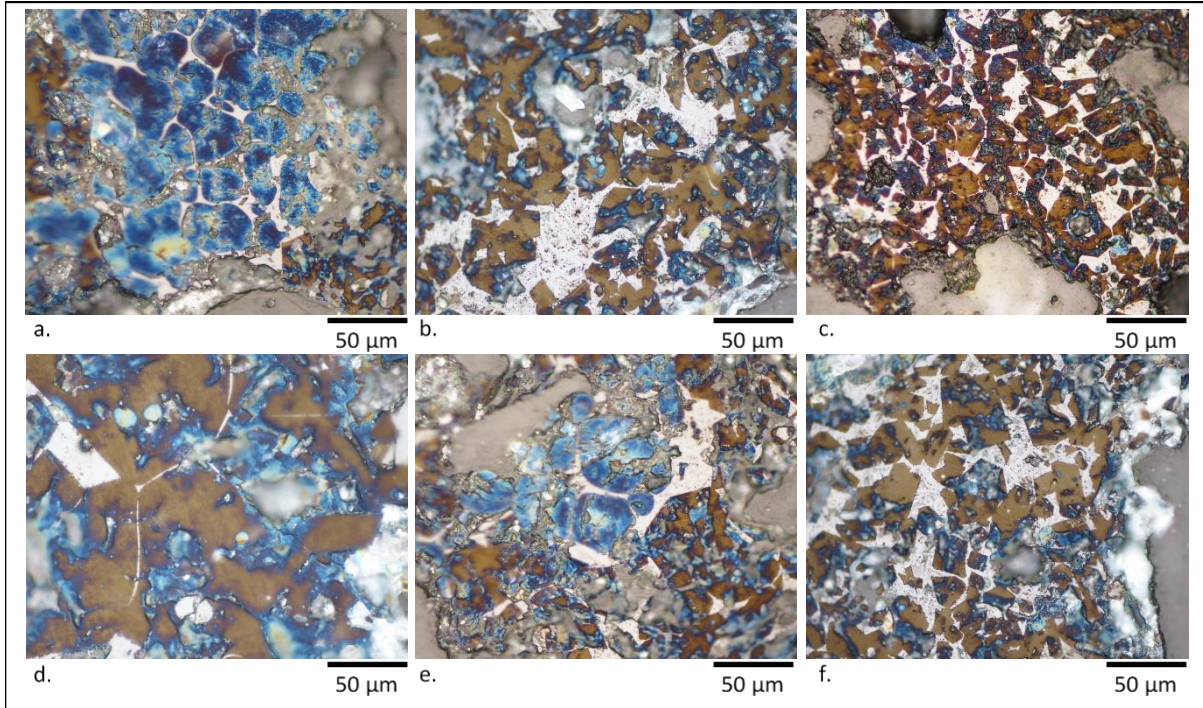


Figure 50 Photomicrographs of clinker Ck55

Chapter 7

The effect of OBM cuttings on cement properties and
hydration

Chapter 7: The effect of OBM cutting on cement properties and hydration

The previous chapter showed that Portland cement clinker could be produced with OBM cutting included within the raw meal. However, it is also important to understand the cement hydration behaviour of the resultant clinker.

To obtain comparable results, the cement clinker was ground to a similar fineness and blended with the same quality and quantity of gypsum. This allowed an understanding as to whether OBM cutting ratio had an impact on cement hydration.

Cement hydration was studied by many techniques such as isothermal conduction calorimetry (ICC) and simultaneous thermal analysis (STA). The mechanical strength was determined and compared with the standard specification implemented in Oman (OS7/2001). Also, the physical testing such as setting time, Blaine, soundness and density were measured. Using XRD complemented with SEM-EDX analyses of polished cross-sections, the major hydrate phases were studied. The SEM of the clinker was also observed to understand if there were any significant changes to the microstructure of the main phases, which may influence the cement hydration behaviour. The degree of hydration (DoH) was obtained by applying grey level segmentation based on the histogram of BSE images to quantify elements in polished section of cement samples using SEM-BSE analytical technique. Finally, the main hydrated products such as C-S-H and CH were identified and correlated to other findings, if any.

7.1 Physical and mechanical properties

Oman has its own cement standard¹⁰⁵ (OS 7/2001) which specify only one type of cement, namely that used for general construction purposes and specified in many other standards such as BS/EN ¹⁹¹ (197-1 for type I) and ASTM ^{106,192} (C 150 type I). The cement types are defined by their chemical composition and physical/mechanical performance which are presented in

Table 15.

Table 15 Summary for the OPC standards: Oman Standard¹⁰⁵, BS EN¹⁹¹ and ASTM¹⁹²

| Standard Test | | OS 7/2001 | | BS EN 197-1-2011 CEM I 42.5N | | ASTM C150/150m-18 Type I | | |
|-------------------|---------------------------------------|-----------|-------------------|---------------------------------|-------------------|--------------------------------|-------------------------------|-----------------|
| | | Max | Min | Max | Min | Max | Min | |
| Chemical Analysis | SiO ₂ % | -- | -- | -- | -- | -- | -- | |
| | Al ₂ O ₃ % | -- | -- | -- | -- | -- | -- | |
| | Fe ₂ O ₃ % | -- | -- | -- | -- | -- | -- | |
| | CaO % | -- | -- | -- | -- | -- | -- | |
| | MgO % | 6.00 | -- | 5.00* | -- | 6.00 | -- | |
| | Na ₂ O % | -- | -- | -- | -- | -- | -- | |
| | K ₂ O % | -- | -- | -- | -- | -- | -- | |
| | IR % | 1.50 | -- | 5.00 | -- | 0.75 | -- | |
| | LOI % | 3.00 | -- | 5.00 | -- | 3.00 ⁺ | 3.50 [§] | |
| | SO ₃ % | 3.50 | -- | 3.50 | -- | 3.00 C ₃ A <= 8% | 3.50 C ₃ A > 8% | |
| | Cl % | 0.10 | -- | 0.10 | -- | -- | -- | |
| | Alkalies % | 0.60 | -- | 0.60 | -- | 0.6 | -- | |
| | C ₃ S % | -- | -- | -- | -- | -- | -- | |
| | C ₂ S % | -- | -- | -- | -- | -- | -- | |
| | C ₃ A % | 9.00 | -- | -- | -- | -- | -- | |
| | C ₄ AF % | -- | -- | -- | -- | -- | -- | |
| | 2C ₃ A+C ₄ AF % | -- | -- | -- | -- | -- | -- | |
| | LSF | -- | -- | -- | -- | -- | -- | |
| | SM | -- | -- | -- | -- | -- | -- | |
| AM | -- | -- | -- | -- | -- | -- | | |
| Physical Tests | Blaine M ² /Kg | -- | -- | -- | -- | -- | 280 | |
| | Air content volume % | -- | -- | -- | -- | -- | -- | |
| | Soundness | 10 mm | -- | 10 mm | -- | 0.80 % | -- | |
| | Setting time in Minutes | Initial | -- | 60 | -- | 60 | 45.00 | |
| | | Final | 600 | -- | -- | -- | 375 | |
| | Heat of Hydration in KJ/Kg (7days) | -- | -- | -- | -- | -- | -- | |
| | Compressive Strength | | N/mm ² | | N/mm ² | | MPa | |
| | | 2/3 days* | -- | 10.00 2 days | -- | 10.00 2 days | -- | 12.00 3 days |
| 7 days | | -- | -- | -- | -- | -- | 19.00 | |
| 28 days | | -- | 42.50 | 62.50 | 42.50 | -- | -- | |

*MgO% content in Portland clinker used for manufacturing cement

+ grinded without limestone addition

§ grinded with limestone addition

The chemical composition limits in OS are similar to those in BS/EN standard except regarding MgO, insoluble residue (IR), and C₃A content. In addition, OS specifies the range of cement LSF and AM factors. The OS has more restrictions when compared to BS/EN. For example, the highest allowed IR and C₃A in the cement are 1.5% and 9.00% respectively. Prescription of low IR value in OS compared to BS/EN limits the ratio of additives such as limestone during cement grinding process to below 3%. In contrast, 5% of additives (such as limestone) could be added during clinker grinding in BS/EN standard. In addition, IR is essential parameter to control the quality of gypsum. The lower quality (purity) of gypsum the higher % of IR which impacts the strength of cement and setting time. Also, it may require high quality of clinker in term of C₃S content and low free lime content to keep the IR result within allowable values and maintain 28 day strength above 42.5 N/mm². Since the OBM cutting is added as part of the raw materials, it has no effect on the ratio of clinker and additives used during the grinding and production of cement. The cement obtained using the OBM cutting is meeting the standard requirement and fulfilling the chemical and physical/mechanical limits used in all samples obtained (e.g. 12 and 55%) as shown in Table 16.

The soundness (expansion test) of the prepared cement increased as OBM cutting content increased (Table 16). Higher expansion could be due to several reasons, such as i) high free lime content in clinker (above 2%) or ii) high MgO content in cement (above 3%)¹⁴⁹. The free lime contents in all samples were kept below 2% (Figure 43), thus this is probably not a reason for higher expansion results. Therefore, the significant contribution for the expansion may be attributed to the presence of a high concentration of MgO (periclase) in cement prepared with higher OBM cutting contents in the raw meal. The prepared cement showed MgO levels below the maximum limits in standards (OS 7/2001, BS EN 197-1 and ASTM C 150-99a Type I)

The MgO that is not combined in clinker phases appears as periclase^{193–195}. Most specifications limits MgO in cement in the range 3-6 %¹⁶². In some standards, including European ones, periclase (MgO) is limited to 5% maximum because of its potential expansive reactions with aggregates¹⁶³. Higher contents in cement lead to long-term expansion. This is because of the slow hydration accompanied with expansion in concrete at late ages according to the following chemical reaction^{149, 197}.



The source of MgO in the cement is likely the clinker as a result of its high concentration in the raw materials. Limestone can contain magnesium in many forms, such as dolomite ($\text{CaMg}(\text{CO}_3)_2$). Alternatively, it may be found as magnesite (MgCO_3)¹⁹³. In addition, other sources could be from the grinding media during the grinding process in a ball mill, or MgO contamination from added additives during cement grinding such as limestone and gypsum. Since all parameters were similar during testing and sample preparation, the only difference is the OBM cutting % in each sample. The MgO % in the as-received OBM cutting is 2.22%, which is the highest of all the raw materials, as shown in Table 6. The magnesium was present as dolomite in the OBM cutting found, as seen from the XRD analysis presented in Figure 22. The MgO content in the clinker samples increased, as shown in the previous chapter in Figure 42.

Hence, higher soundness in the cement sample of 55 % OBM cutting is more likely due to the higher content of MgO coming from OBM cutting. The SEM-EDX analysis also confirms the presence of MgO in cements prepared with 30% and above OBM cutting (Figure 51). The energy-dispersive X-ray spectroscopy (EDS) confirmed the presence of periclase, as shown in the spectra c & f in Figure 51. Seen in the figure as black and grey polygonal and circular clusters shape with clear borders.

According to the literature, this could be explained because Mg^{2+} can replace Ca^{2+} in major clinker phases such as C_3S and C_2S when MgO concentration in the raw meal is up to 1.5%¹⁹⁸. Also, it has been reported that C_2S , C_3A , and C_4AF can incorporate in its crystal lattice up to 0.5, 2 and 4.4% MgO respectively^{149,199}. At equilibrium, the solubilities of MgO in the liquid phase is much higher than the concentrations of MgO replacement, which is reported in the range of 5 - 5.5%. The highest quantity of MgO that can be incorporated within clinker phases is dependent on the quantity of liquid phase formed, and the clinkerization temperature. The higher the clinkerization temperature, the more MgO is dissolved in the liquid phase and hence the higher amount of MgO crystallising as periclase at the cooling stage¹¹⁴. Therefore, periclase is formed during the clinker burning process in the thermal decomposition reaction of magnesium-containing carbonates such as dolomite (CaMgCO_3) and magnesite (MgCO_3). This partly dissolves in the liquid phase as temperature increases and some remains within clinker phases such as C_3S and C_2S . In fact, the SEM EDX shows MgO largely within the liquid phase as shown in Figure 51 d. Particles of MgO grains are

within the liquid phase, in agreement with the literature^{198,149,199}. The fineness of the raw meal influences the distribution of MgO between the liquid phases and clinker phases of the raw meal^{166–169}.

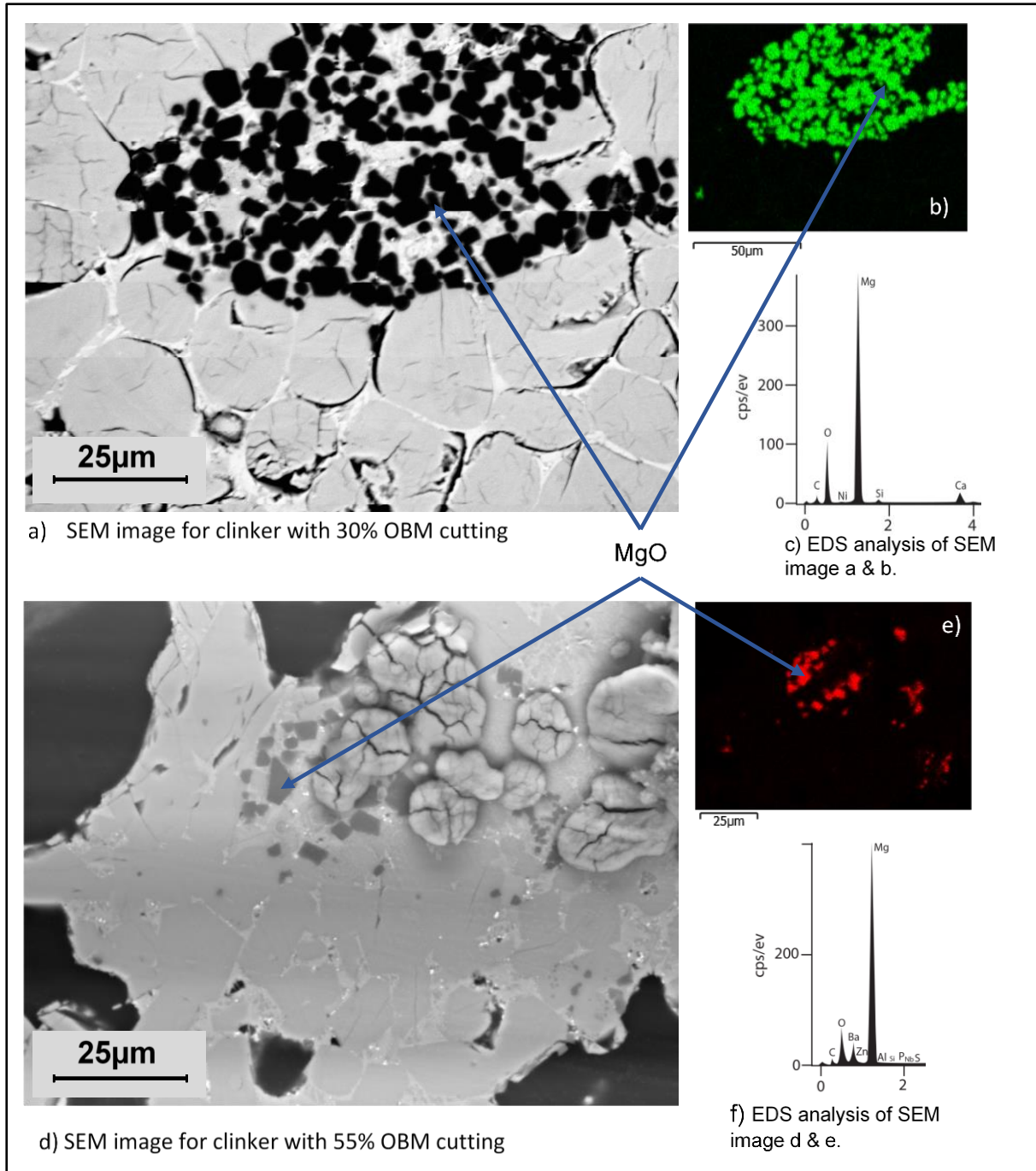


Figure 51 SEM images and EDS spectra of clinker samples containing 30% (a, b & d) and 55% (d, e & f) OBM cuttings.

The black and dark grey particles represent MgO.

Blaine (or fineness) and particle size was purposely kept consistent during clinker lab grinding to remain within the industry standard and meet the OS, i.e. falling in the range 319 – 329 m²/Kg. This helped to ensure that any differences were due to changes in hydration chemistry.

Setting time results are presented in Table 16 and show no significant change between the samples with OBM cutting and the reference sample. The initial setting time is 137 minutes for the reference sample and 126 minutes and 131 minutes for the 12% and 55% OBM cutting, respectively. The results therefore meet the OS specification.

Density is obtained for the purpose to be used in the calculation of the hydration degree. It is in fact, not a strictly a quality parameter in cement manufacturing. The density of Portland cement is ranging between 3.10 – 3.25 g/mL¹⁹⁷. The cement prepared has the density as shown in Table 16.

Table 16 Physical test results for the prepared cement

| Physical Test | | <u>Cm_{ind.}</u> | <u>Cm_{Ref}</u> | <u>Cm-12%</u> | <u>Cm-55%</u> | <u>OS*</u> |
|--|--------------------|--------------------------|-------------------------|---------------|---------------|------------|
| Setting Time (±0.02) | Initial, mint. | 183 | 137 | 126 | 131 | 45 min. |
| | Final, mint. | 245 | 198 | 182 | 181 | 600 max. |
| Soundness Lechat (±0.01) | mm | 1.02 | 1.03 | 2.00 | 3.00 | 10 max. |
| Blaine Fineness (Blaine Air Permeability) | m ² /Kg | 319 ±1.03 | 325 ±1.87 | 329 ±0.84 | 324 ±0.75 | 225 min. |
| Particle size | < 45 <u>micron</u> | 14.6 | 13.30 | 16.00 | 16.60 | -- |
| | < 90 <u>micron</u> | 1.50 | 1.40 | 1.30 | 1.60 | -- |
| Density by Le <u>Chatelier</u> (±0.008) | g / mL | 3.13 | 3.13 | 3.12 | 3.11 | -- |

*OS: Omani Standard for Portland cement production¹⁰⁵

An indirect measure of cement hydration is the development of compressive strength, where standards stipulate mortar test specimens arranged, cured and tested according to the testing standard. There are three factors responsible for developing the strength. Namely formation of hydrated phases, non-hydrated residual and porosity. Compressive strengths were measured on mortars cured at 20 °C in a distilled water chamber.

Compressive strength increased with hydration for 2, 7 and 28 days, as shown in Figure 52. At two days, the two reference samples (C_{mInd} and C_{mRef}) showed slightly lower strengths than the OBM cutting cement ones (12% and 55%). By 7 days, the strengths of all samples increased and the OBM-containing remained slightly stronger than the reference samples. At 28 days, $C_{m12\%}$ was the strongest, with no significant difference between others. With alite being the principal phase responsible for later-age strength, given the minimal difference in alite contents Table 11 between the samples, the similarity in performance is not surprising.

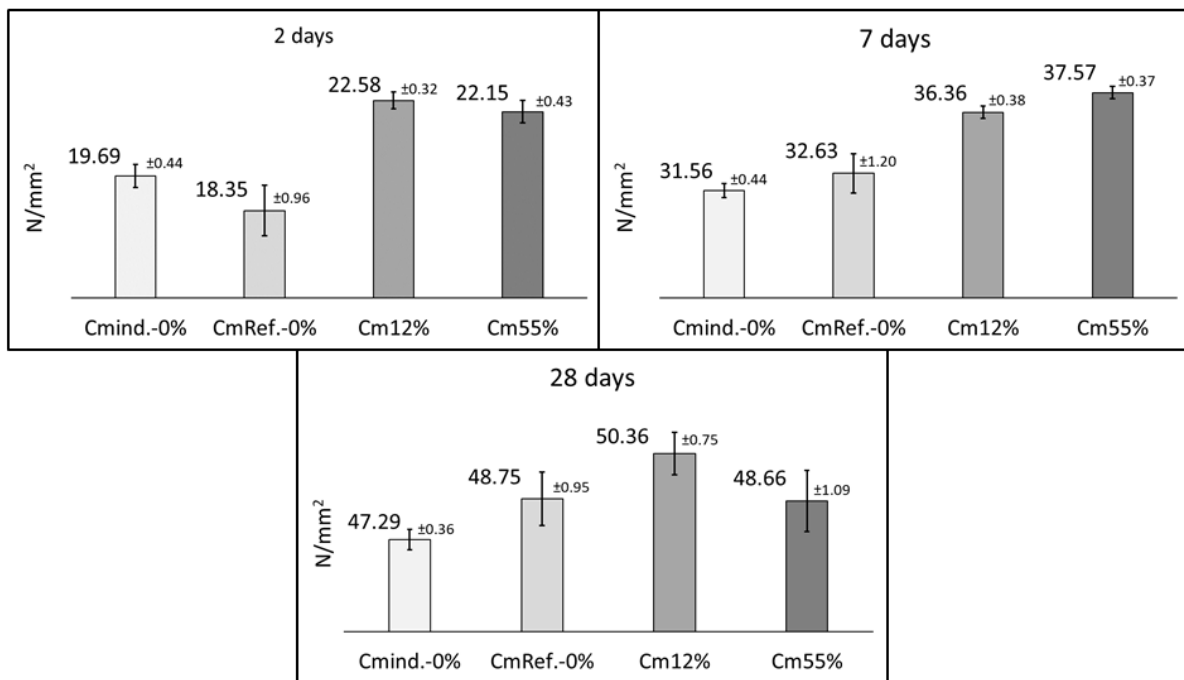


Figure 52 Compressive strength development over time of the prepared cement.

It is possible that the slight variations in Blaine fineness could explain the slight differences in strength. Fineness plays a dominant role in compressive strength development, with higher fineness leading to higher strength due to cement grains having more surface area exposed during hydration²⁰³.

There was a linear correlation between 28 day compressive strength and Blaine fineness, with an R^2 of 0.9795 as shown in Figure 53. Thus, the slight difference in strength may be explained by variations in cement fineness only and the incorporation of OBM cutting within the clinker does not appear to affect strength development. The cement sample with 12% and 55% OBM cutting shows 28 day compressive strength that conforming to the Omani standard and other international cement standard such as EN/BS.

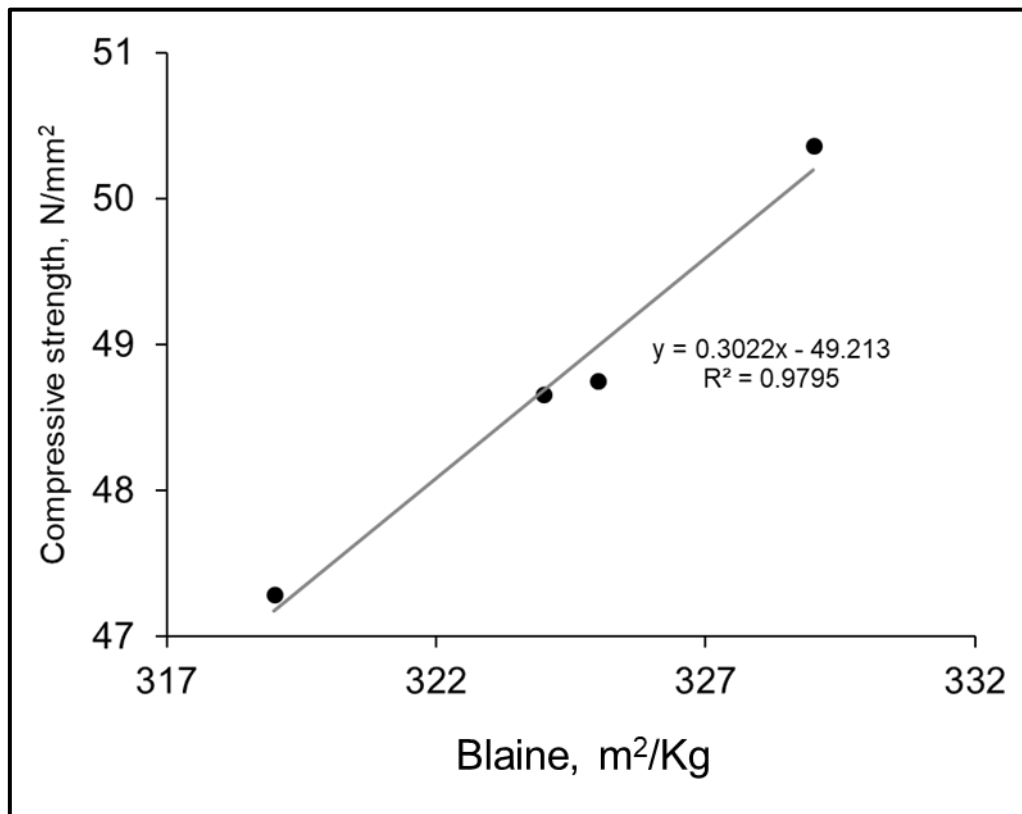


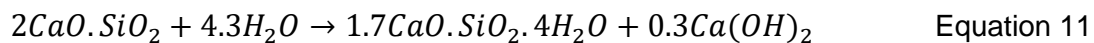
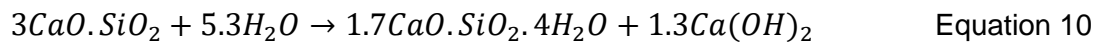
Figure 53 Blaine fineness vs compressive strength.

There is a wide range of factors that affect the compressive strength of cement, especially in the early period, including the fineness of cement, the ratio of gypsum (calcium sulfate), the chemical composition, and the water-to-cement ratio. It is noted that the reference sample C_{mRef} is the least in compressive strength compared to other samples, with the exception of the industrial sample C_{mInd} . There is no apparent reason for this difference in strength results. Still, it is noted that the results of the examination are very close, and this difference in results may be the result of laboratory errors.

7.2 Hydration and microstructure

The major microstructure of hardened cement paste could be summarised as comprising five main features¹⁹⁷ as mentioned below and explained chemically by the subsequent equations.

- Calcium silicate hydrate (C-S-H) comprising about 50% of the paste.
- Calcium hydroxide, Ca(OH)₂ (known also as portlandite) is the second product formed during hydration, comprising about 12% of the paste.
- Monosulfate hydrates and its derivatives, comprising about 13%.
- Pores contributing about 20% of the paste volume.
- Anhydrous clinker phases which constitute about 5%.



The composition calcium-silicate-hydrate (C-S-H) is assumed to be 1.7CaO.SiO₂.4H₂O in Equation 10 and Equation 11, however, the ratio of Ca/Si varies between 0.83 – 2.00 depend on many factors such as water ratio²⁰⁴.

Ettringite is a calcium sulphoaluminate hydrate complex compound, 3CaO.Al₂O₃.3CaSO₄.32H₂O, which has composition of hexagonal prismatic shape. The octahedral column is consist of [Al(OH)₆]³⁻ linked to [Ca₆.Al₂(OH)₁₂]⁶⁺. [3SO₄²⁻.26H₂O]⁶⁻ while in between the columns are linked by water and sulphate. The water between the column is lost at above 100 °C while the water from the dihydroxylation of aluminium hydroxide is lost at temperature range from 200 – 400 °C²⁰⁵.

Figures 54 to 57 show the SEM images of Portland cement samples hydrated for 2, 7 and 28 days. Respective XRD plots are shown in Figures 58 to 61. The micrographs show a combination of the features described above. Anhydrous material appears white while pores are black. The hydrate phases appear grey. After two days the pastes are dominated by anhydrous material and pores, although hydrates could be seen. The most commonly observed hydrates are portlandite (CH), with a light grey colour, and outer product C-S-H, with a dark grey colour. At later ages, namely seven days hydration, the inner product C-S-H further increased in presence and encircled the hydrated larger grains. With increasing hydration, the total pore is reduced. Eventually, after 28 days hydration, all investigated cement samples showed similar

microstructures, as illustrated by the SEM images and XRD plots. The major clinker phases are consumed, with corresponding increases in different hydration products. XRD showed that ettringite reduced over time, with no observation of monocarbonate nor monosulfate formation. It is expected to observe no formation of monocarbonate (AFm) in all hydrated cement samples including reference and industrial sample because the monocarbonate results from the hydration of C₃A with CaCO₃ from limestone that added in the cement during the grinding²⁰⁶. However, in this research, the cement prepared has no limestone added. Therefore, the hydration process will not expose to CaCO₃, hence no monocarbonate formed expected during the hydration process.

The amount of ettringite in hydrated cement is depend on the ratio of gypsum to C₃A content. At low ratio (3/2)²⁰⁷, AFt is formed at early hydration and then convert to monosulfate phase (AFm). When gypsum to C₃A ratio is high, the monosulfate is unlikely to be formed²⁰⁸.

There was no significant effect on the crystal phases formed upon hydration at 2, 7 and 28 days, despite the greater potential of magnesite (MgCO₃) formation which is observed in samples Cm-12% and Cm-55% as shown in Figure 60 and Figure 61. In all investigated samples the AFm (Ettringite) is formed which is visible at 2 days hydration, while no formation observed in all investigated cement sample for Aft (monocarboaluminate nor monosulfate) at all hydration ages. The formation of AFt is highly depend on the C₃A content in cement. With high C₃A content in cement, the monocarboaluminate appears at early age of hydration, probably is visible on 7 days of hydration²⁰⁹.

The analysis by optical microscopy for the clinker phases analysis (Table 14) shows an increase in C₃A content as the OBM cutting increase. The C₃A content in Ck_{Ref.}, Ck12 and Ck55 are 12, 16 and 17% respectively.

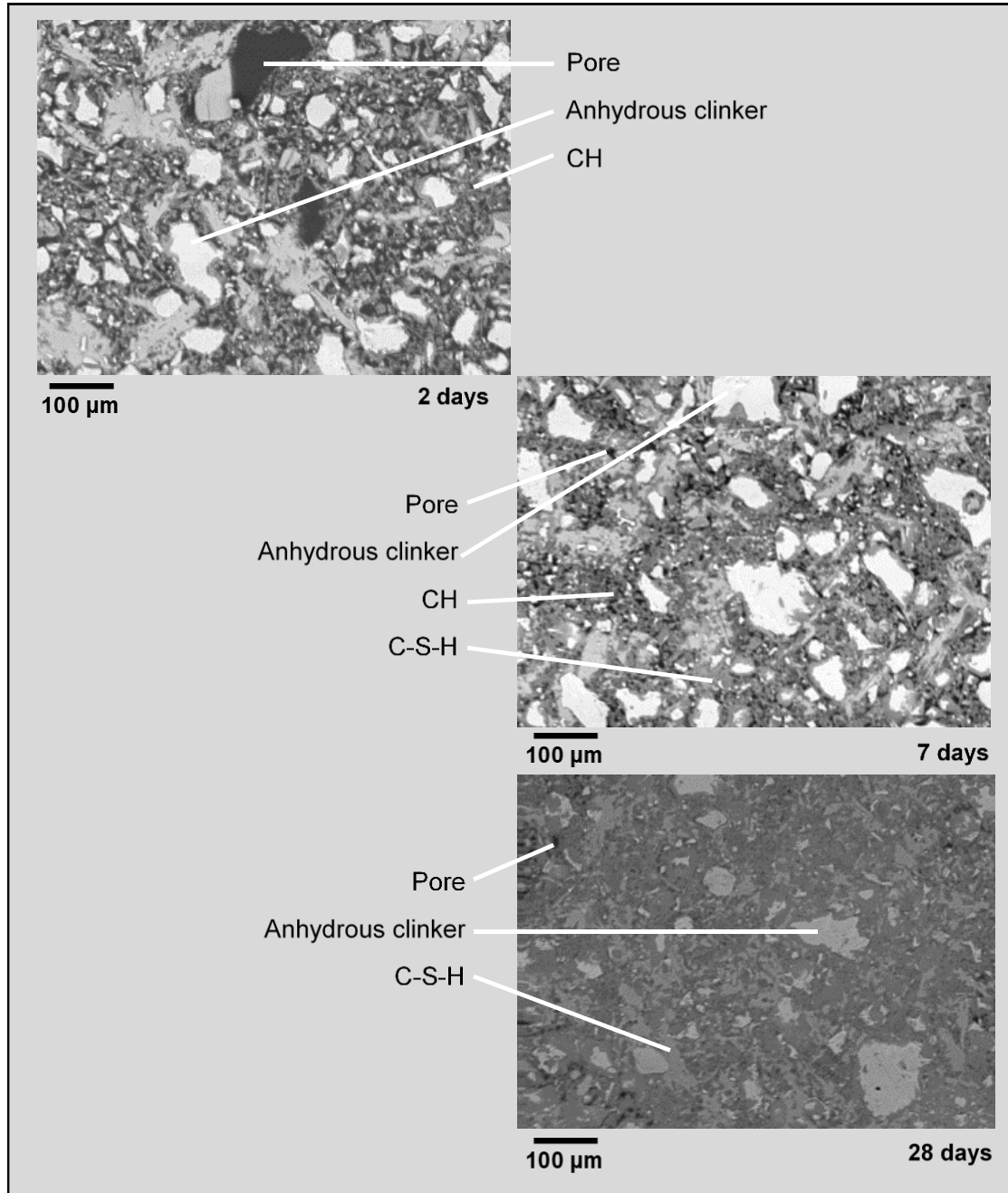


Figure 54 SEM image of Cmt_{Ind} hydrated for 2, 7 and 28 days

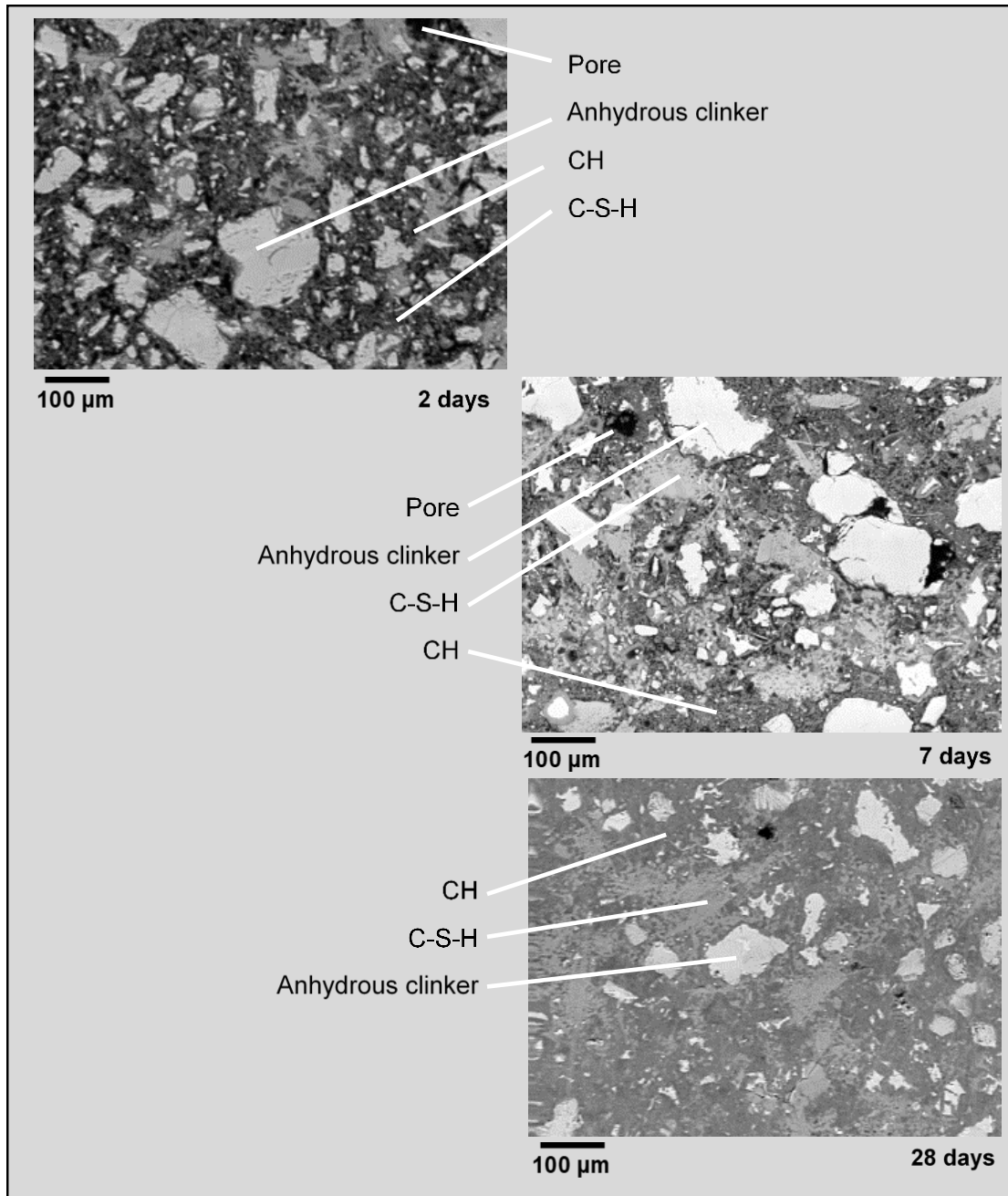


Figure 55 SEM image of Cmt_{Ref} hydrated for 2, 7 and 28 days

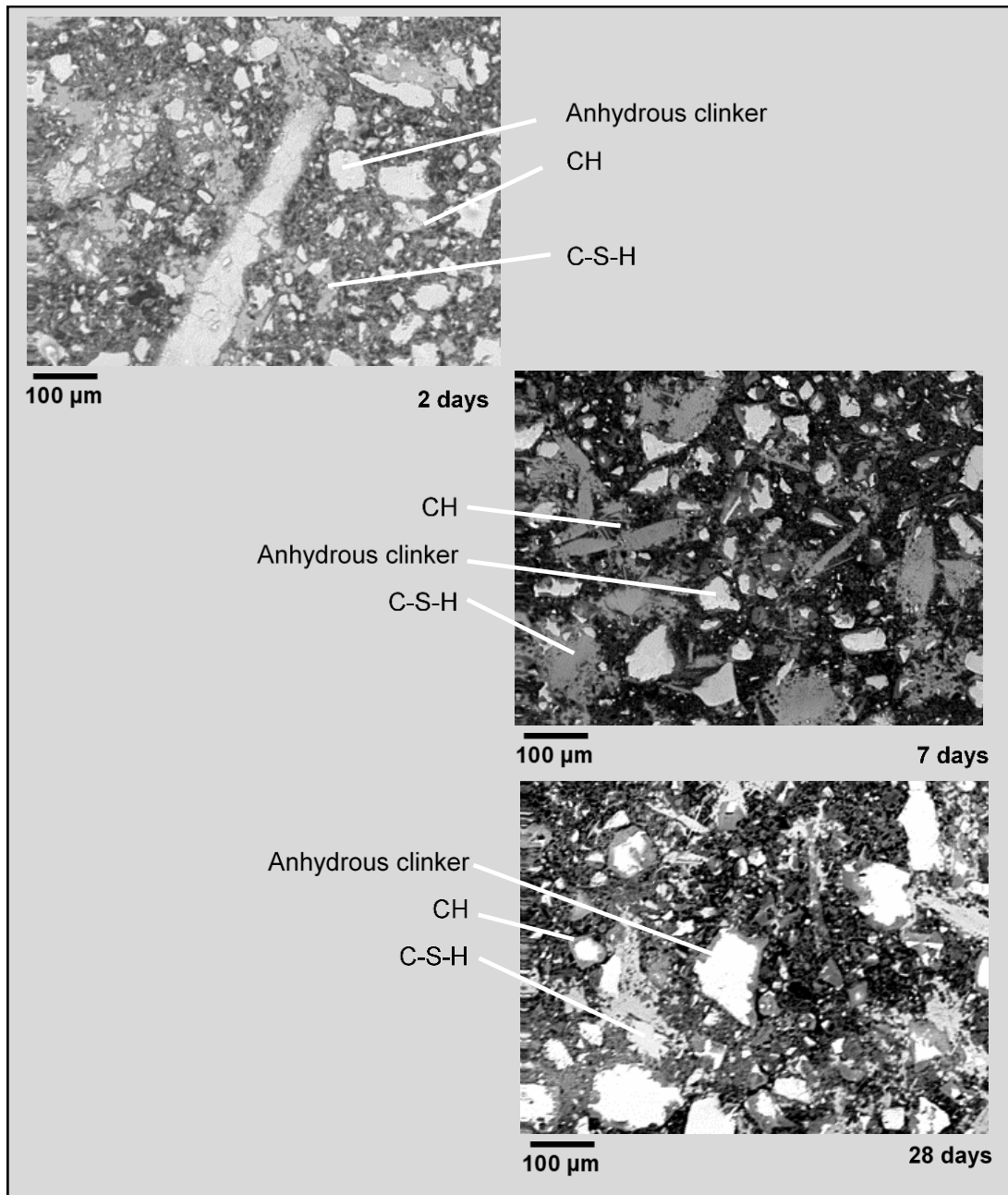


Figure 56 SEM image of Cmt12% hydrated for 2, 7 and 28 days

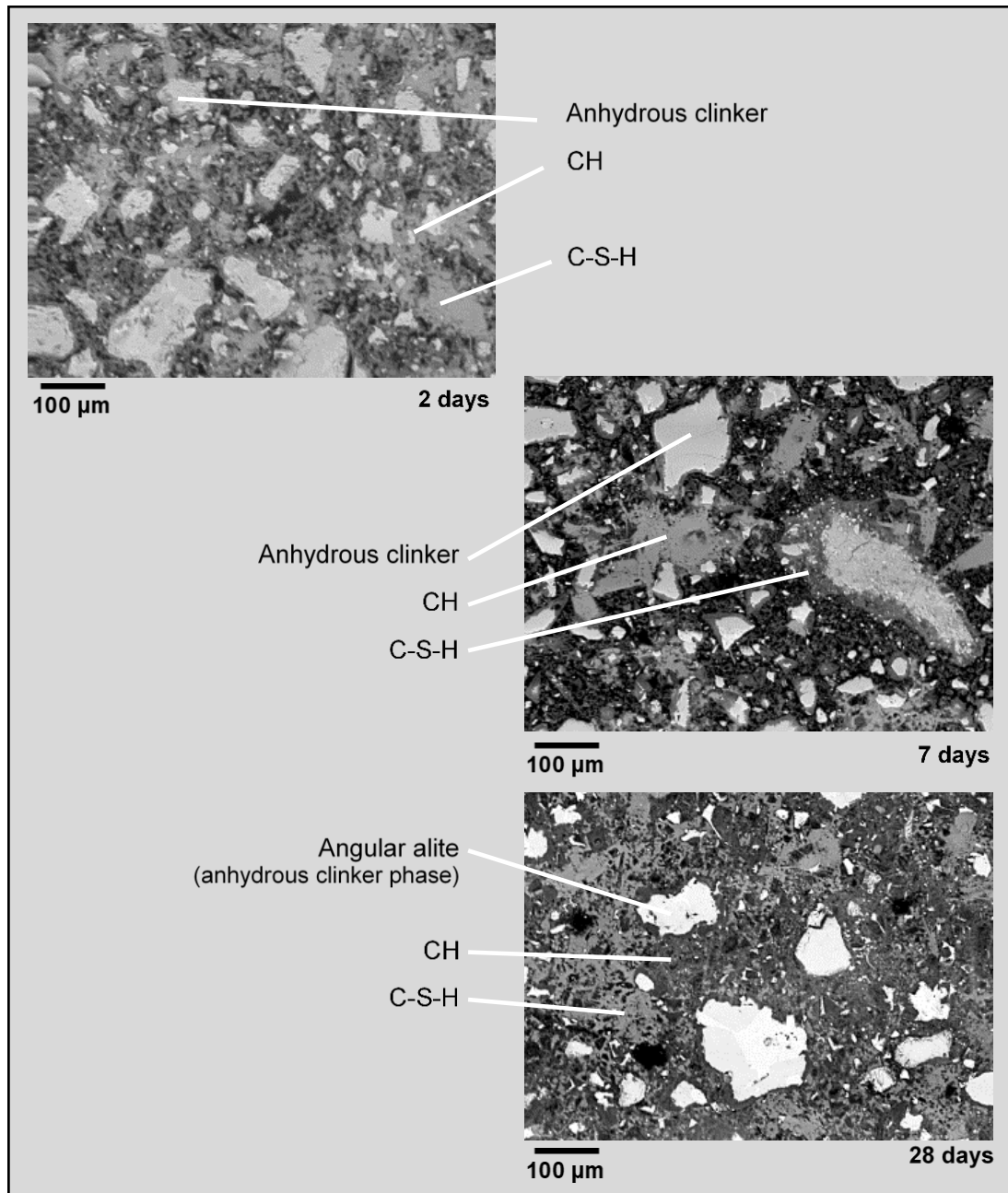


Figure 57 SEM image of Cmt55% hydrated for 2, 7 and 28 days

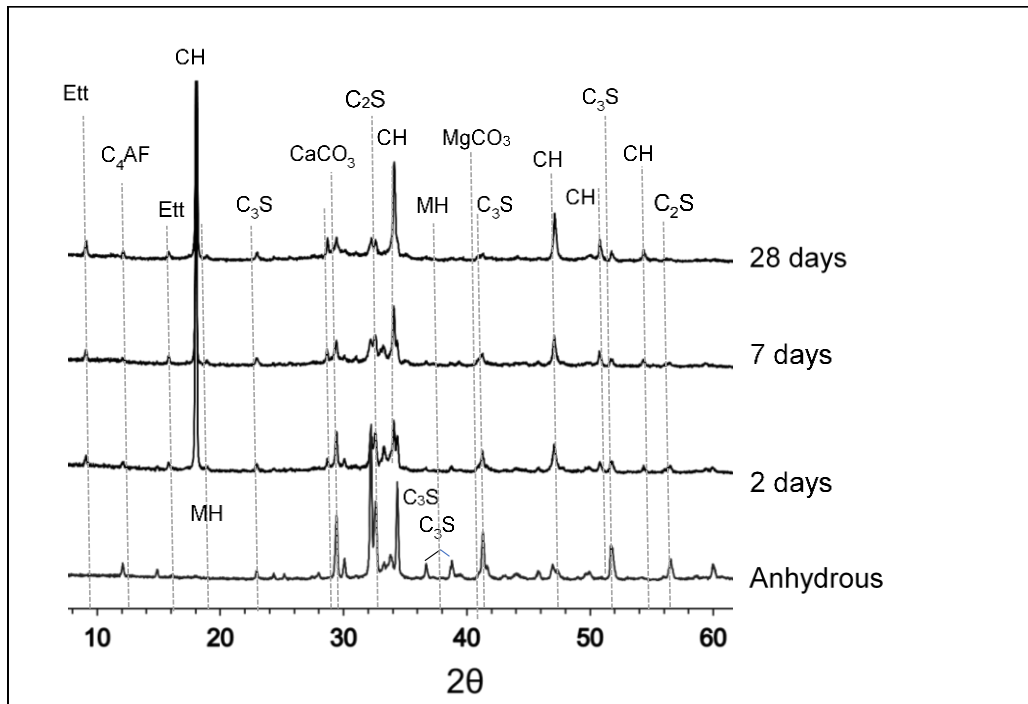


Figure 58 XRD analysis of anhydrous Cm_{Ind} and up to 28 days.

W/C ratio 0.45

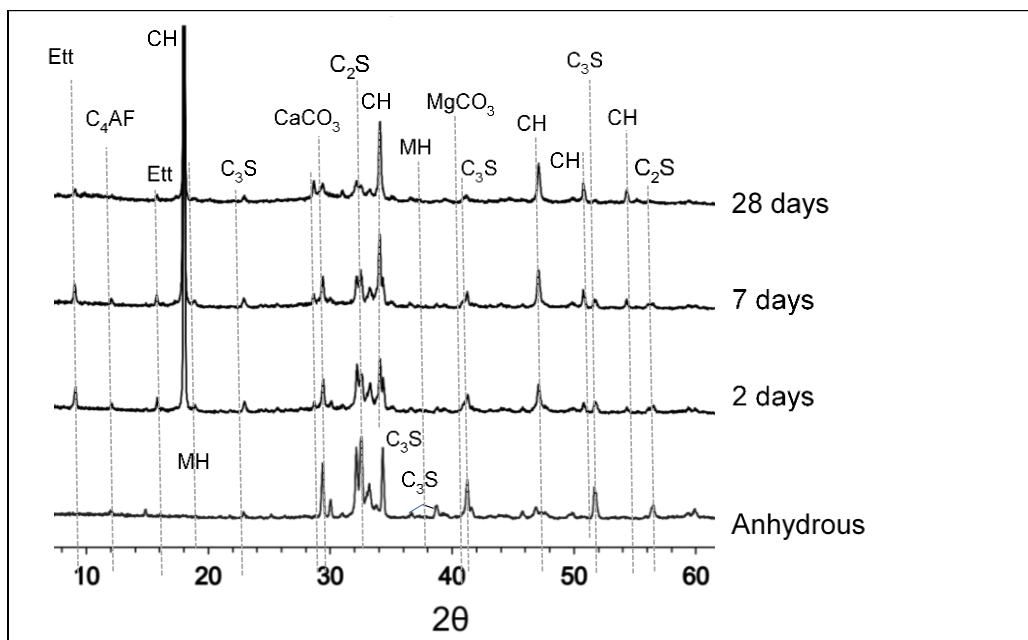


Figure 59 SEM and XRD analysis of anhydrous $Cm_{Ref.}$ and up to 28 days.

W/C ratio 0.45

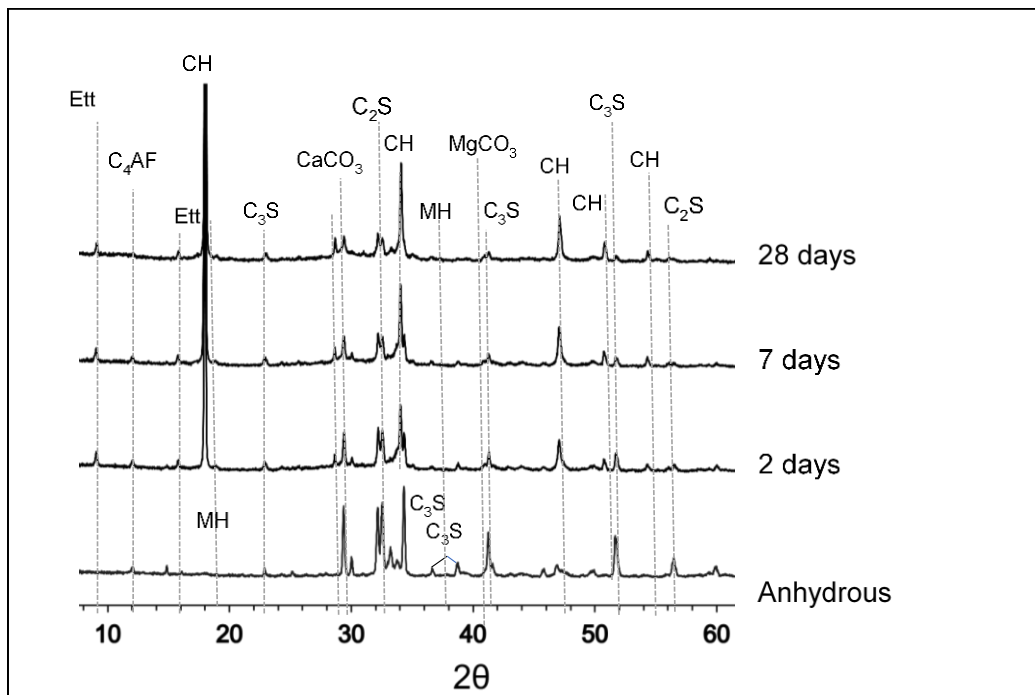


Figure 60 SEM and XRD analysis of anhydrous Cm-12% and up to 28 days.

W/C ratio 0.45

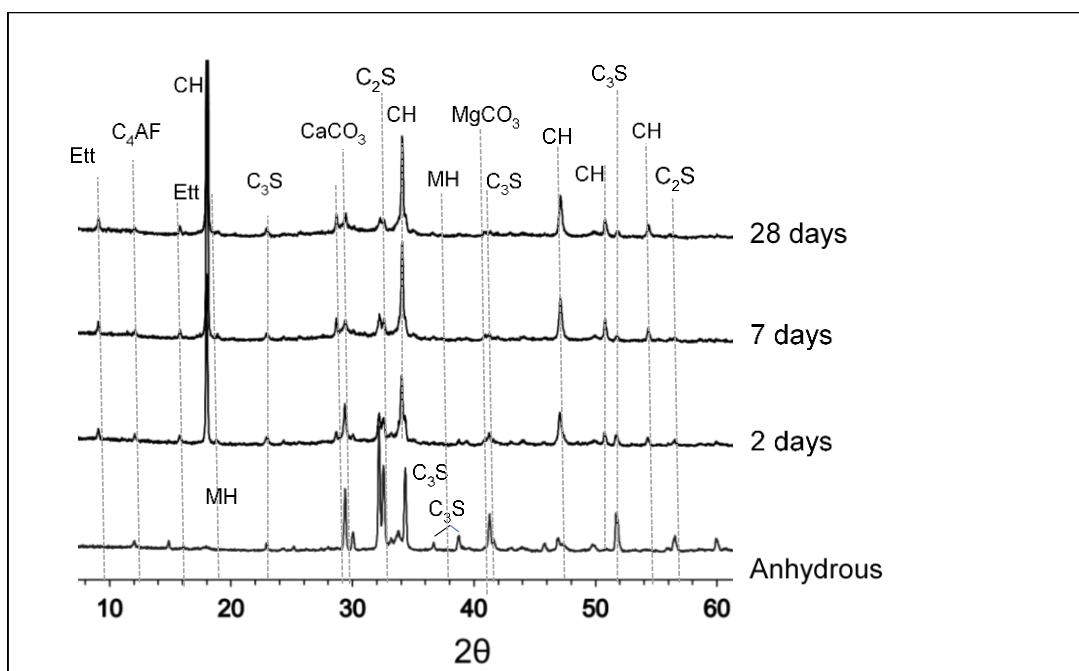


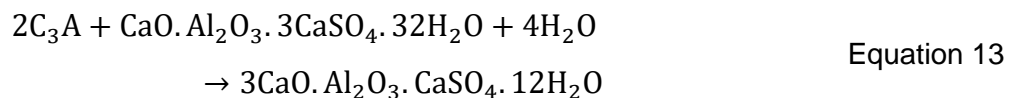
Figure 61 SEM and XRD analysis of anhydrous Cm-55% and up to 28 days.

W/C ratio 0.45

Figures 63 and 64 further highlight depletion of the clinker phases during hydration and formation of new crystalline hydrate phases. In all samples AFm phases were not detected. The XRD patterns for all hydrated cement samples showed similar behaviour. Ettringite (AFt) and C₄AF were observed with the intensity of reflections from the latter diminishing with time. Between 2 to 28 days the intensity of the main clinker phase reflections decrease with growth in reflections due to hydrates. The amount of AFt formed depends on the ratio of sulphates (added during grinding) and the C₃A content of the clinker. At high ratio of C₃A to CaSO₃.2H₂O, the AFt is unlikely to convert to AFm²⁰⁸. In this investigation, the % of gypsum added during the cement grinding of all samples are fixed at about 6% as mentioned in Table 8 in Section 4.3.4. The XRD results is confirming that AFm is not observed in all ages of cement hydration. The rate of reaction between calcium sulfate and C₃A depends on the C₃A polymorph and concentration (C₃A cubic, orthorhombic or monoclinic modification). However, all polymorphs undergo the same reaction. The initial hydration reaction is that between C₃A and calcium sulfate in the presence of water which releases significant heat according to the reaction below²¹⁰⁻²¹².



After all the calcium sulfate has been consumed, any unreacted C₃A will react with the AFt and be converted to AFm^{210,211}.



As seen from Table 11, the C₃A content calculated according to Bogue formula in clinker samples Ref, 12% and 55% are 7.94, 7.77 and 6.74 % respectively. Connecting the results obtained from XRD of hydrated cement and the C₃A content in clinker which showed no indication of AFm formation in the hydrated cement in all samples, therefore, the C₃A seems to be consumed to produce the AFt only. It is possibly that there is no C₃A left after the formation of AFt and hence no additional heat released after the first hydration reaction completed. This is could be an explanation for the similarity of the heat rate shown for the all samples.

The hydration reaction of C₃S is associated with formation of calcium hydroxide (CH) which precipitates in the form of portlandite and is dispersed within the hardened

paste²¹³. The XRD patterns for the hydrated cement (Figure 63) clearly indicates the formation of CH in all samples, with growing intensity as the time passes.

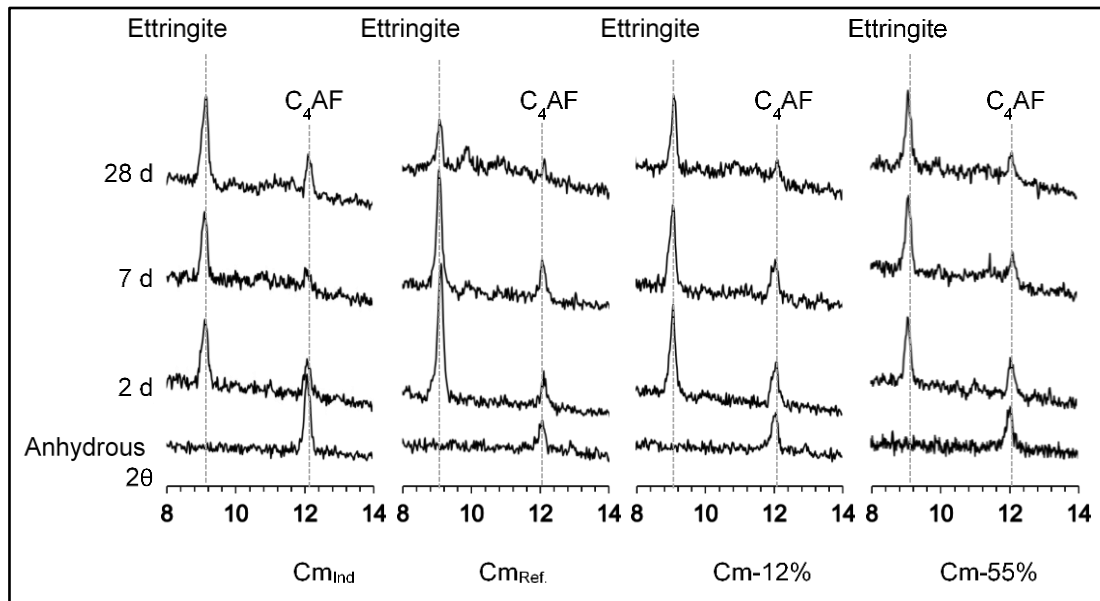


Figure 62 XRD Patterns from 8 to 14° 2θ showing ettringite formation and the C₄AF peak.

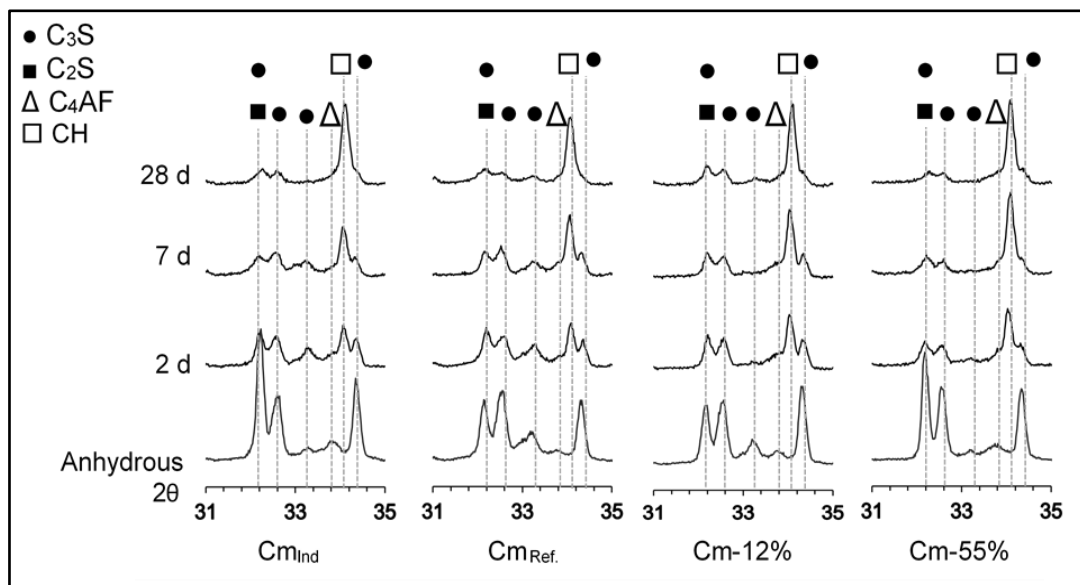


Figure 63 XRD Patterns from 31 to 35° 2θ.

7.3 Thermal Analysis (STA)

Figure 64 shows the DTG of hydrated cement for 28 days. The results obtained show two dehydroxylation reactions at around 465 °C. Brucite ($Mg(OH)_2$) and portlandite ($Ca(OH)_2$) decomposes to oxide and water at about 420 and 460 °C respectively¹¹⁵. The decomposition temperature seen in all hydrated cement samples could be

recognised to decomposition of portlandite. However, the small shoulder adjacent to the portlandite peak at 460 °C is unlikely to be brucite. The XRD patterns of the cement at all hydrated ages do not show any present of formation of brucite. If this was brucite, then would expect to observe a more prevalent peak with increasing OBM cutting content in the DTA analysis at 420 °C as per the literature¹¹⁵. It is more likely that it is microcrystalline formed during hydration.

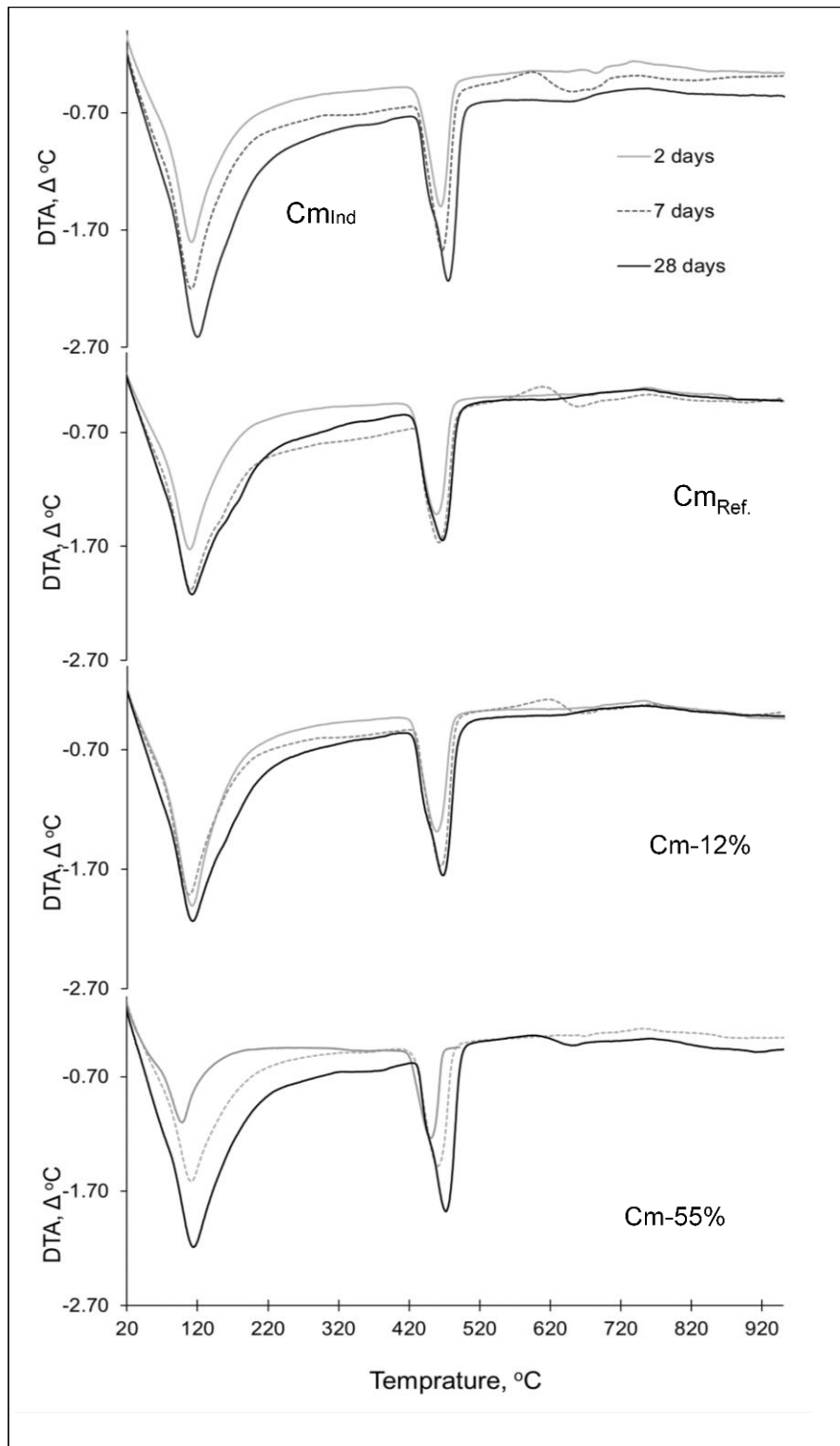


Figure 64 DTA plots from 20 to 950 $^{\circ}\text{C}$ for 2, 7 and 28 day pastes.

7.4 Heat of hydration by ICC

As soon as water comes into contact with cement, hydration starts and heat is released according to the reaction occurring. Different clinker phases release different amount of heat during their hydration^{197,213}. The most heat evolved is upon hydration of C_3S .

Cement goes through five stages during the hydration, as shown in in Figure 65. There is an initial reaction lasting a few minutes (0-15 minutes) in which the calcium ions dissolve in water. This is followed by an induction period lasting from 15 minutes to 4 hours where the overall rate of hydration slows down there is minimal heat released. There then follows the acceleration period (4-8 hours) where the main exothermic peak occurs as a result of alite hydration and formation of calcium silicate hydrate (C-S-H) and portlandite (CH). Finally, there is a deceleration period (8-24 hours) where hydration continues, but slowly.

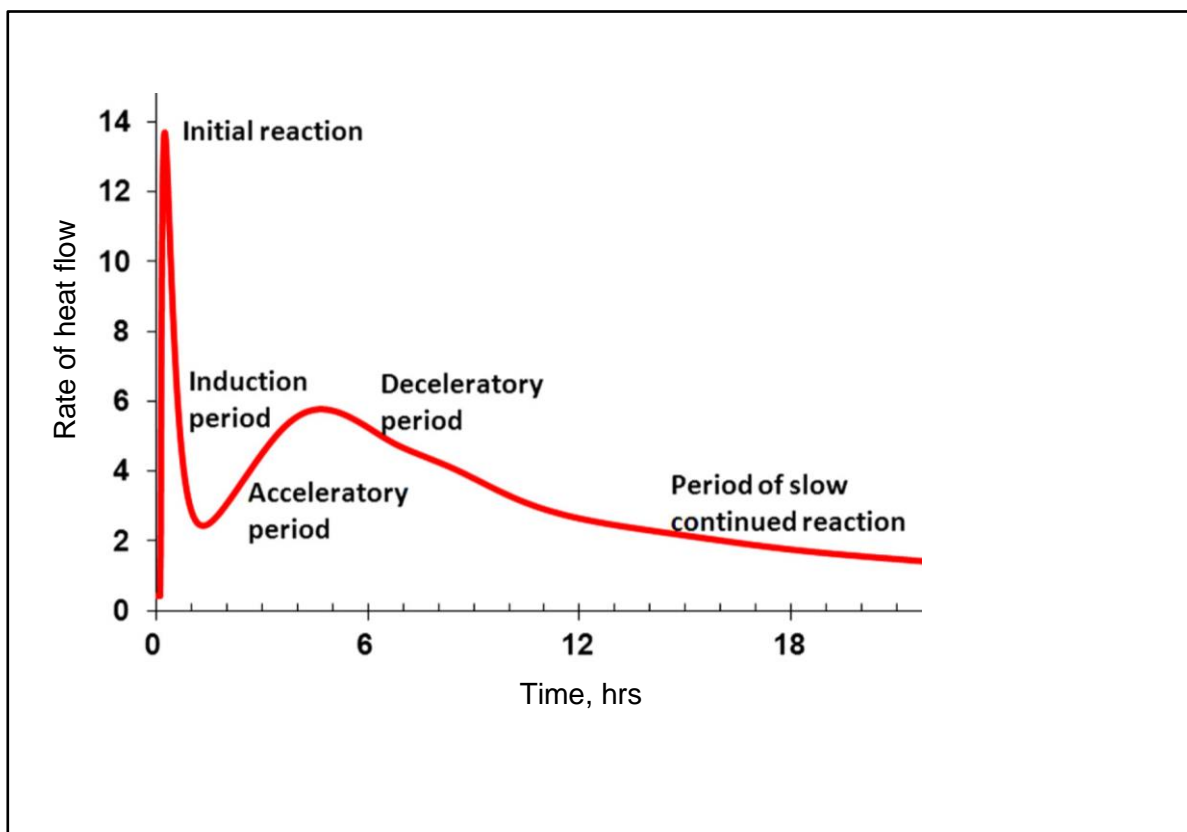


Figure 65 An example of different stages of cement hydration based on heat evolution.

Isothermal calorimetry was conducted to determine the hydration kinetics. Figure 66 and Table 17 show the heat evolution over 21 days for each sample. There was generally no significant difference in the time to onset of the acceleration period (Figure 66). All the results showed one main peak, associated with alite hydration to form calcium silicate hydrate (C-S-H) and portlandite (CH). The highest peak is for the cement containing 55% OBM cutting; appearing after 11.02 hours. The second highest peak is for Cm-12%; after 11.63 hours. Followed by Cm_{Ref.} and Cm_{Ind.} at 11.88 and 12.12 hours respectively. Then, the heat rate slowed down gradually and reached very low values within few days.

It has been reported in the literature²¹⁴, but not seen in this investigation, that a shoulder can appear on the tailing edge of the main peak, due to AFt formation. A second shoulder can also appear due to conversion of AFt to AFm²¹³.

In terms of total heat evolution, there were very little difference between the four cement samples. However, during the first 12 hours of hydration there were slight differences in heat evolution, there being a more intense peak, at shorter time with increasing OBM cutting content. Compared to Cm_{Ref.}, relative heat release from samples Cm-12% and Cm-55% were 116% and 129% respectively.

Over the next 24 hours, all samples showed a decrease in heat evolution, in line with the literature²¹⁵ as the hydration reaction entered the deceleration stage. The upper part Figure 66 shows the total heat evolved for the 4 samples investigated. The total heat released was in the range 247 to 256 J/g at 21 days with maximum 3% difference with the industrial sample. There is no much to compare, since all results shows very close values from each other and compering with the reference and industrial cement. It is difficult to draw conclusions from the ICC analysis due to the large convergence of results. And it seems that all the cement samples give very similar results, without any clear differences in the heat released upon hydration. Thus, it may be concluded that the inclusion of OBM cuttings in cement raw meal gives properties very close to the reference cement (Cm_{Ref.}) and industrial cement (Cm_{Ind.}).

Table 17 The main heat results from ICC test.

| Cement paste | Age of hydration peak | | Intensity of hydration peak | | Total heat evolved (after 21 days of hydration) | |
|--------------------|-----------------------|--------------------|-----------------------------|--------------------|---|---------------------|
| | Measured* (hrs) | Relative value (%) | Measured* (mW/g) | Relative value (%) | Measured* (J/g) | Relative values (%) |
| Cm _{Ref.} | 11.88 ±1.47 | 1 | 1.71 ±1.47 | 1 | 256.00 ±1.47 | 1 |
| Cm _{Ind} | 12.12 ±2.03 | 1.02 | 1.67 ±2.03 | 0.98 | 247.41 ±2.03 | 0.97 |
| Cm-12% | 11.63 ±1.30 | 0.98 | 1.98 ±1.30 | 1.16 | 254.33 ±1.30 | 0.99 |
| Cm-55% | 11.02 ±1.40 | 0.93 | 2.2 ±1.40 | 1.29 | 252.66 ±1.40 | 0.99 |

*Measurement of three independent samples, Measurement error is standard division (SD).

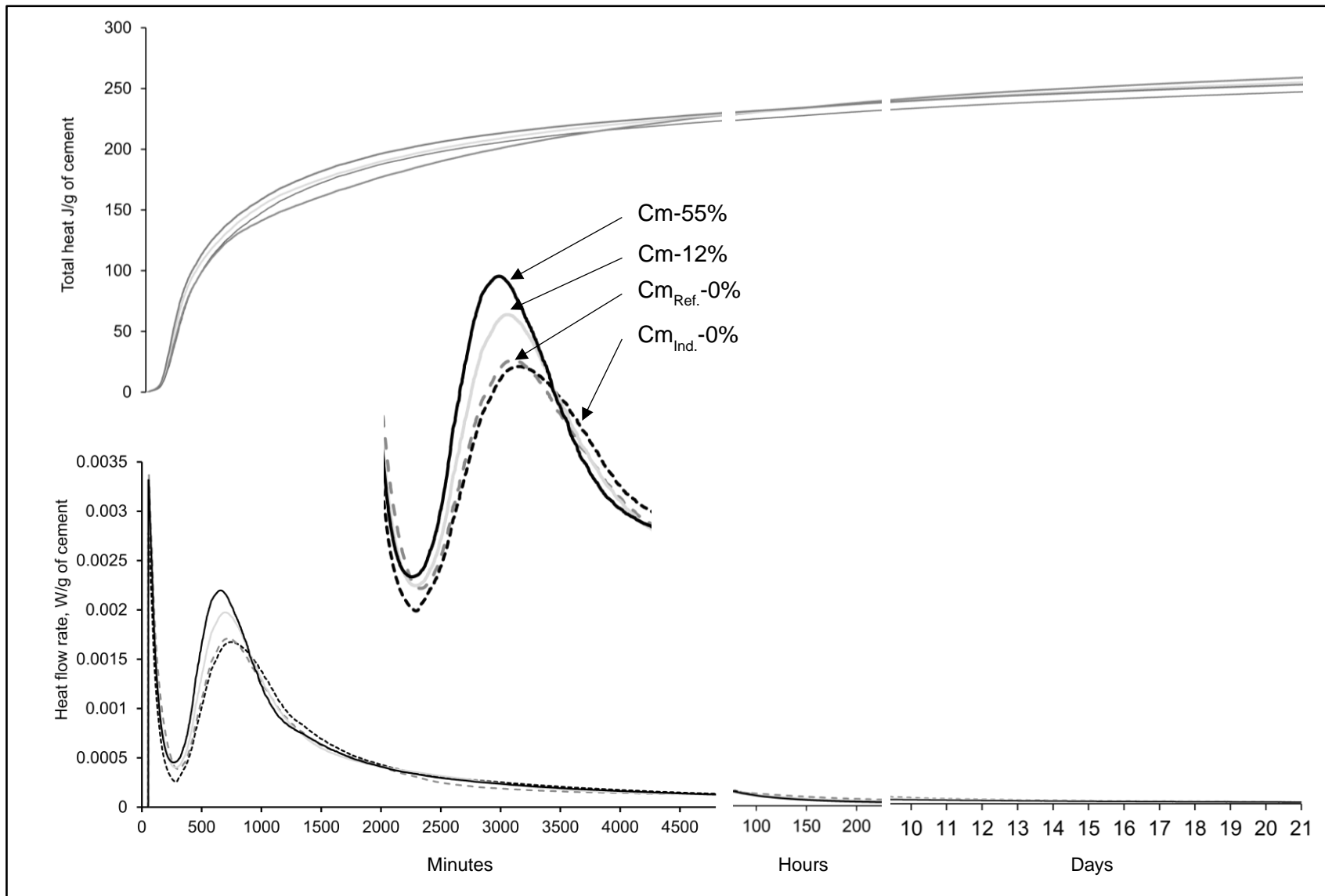


Figure 66 Isothermal Calorimetry results showing rate of heat evolution and total cumulative heat to 21 days

7.5 Degree of hydration (DoH)

Degree of hydration (DoH) can be defined as the fraction of Portland cement that has fully reacted with water²¹⁶. The volume segment of a specified phase is identical to the average surface portion in a 2D microstructure if the number of sections analysed is large enough to be statistically representative²¹⁷. It is therefore possible to apply grey level segmentation based on the histogram of BSE images to quantify features in polished section of cement samples¹¹⁴.

Figure 67 shows the degree of hydration (DoH) calculated by measuring the variation in area of the anhydrous component over time²¹⁸. The standard error (SE) is used to estimate the error in measurement rather than the standard deviation (SD) among the images which are reported in Appendix 10. The SE calculated according to the following equation.

$$SE = \frac{SD}{\sqrt{n}} \quad (n = \text{number of images measured})$$

At all ages up to 28 days, the Cm_{ind} samples exhibited a higher degree of hydration, as seen in Figure 67. Except for at 2 days where hydration was lower than the reference sample. This is expected due to that the industrial cement is prepared under different conditions than the laboratory cement (including better homogenisation, consistence quality, using grinding aids etc). Further, the DoH of Cm-12% and Cm-55% after 2 days curing was found respectively 62.03 and 59.30 % which are lower when compared with the reference sample (66.03%). The Cm-55% showed a marginally lower degree of hydration at all ages than the other samples, while the reference sample showed the highest degree of hydration at all ages. The cement with OBM cutting generally showed slightly lower degrees of hydration than the reference cement. The compressive strength and CH content are demonstrated in Figures 70 and 71. The degree of hydration, based on the compressive strength and CH results, did not improve in cement that prepared using OBM cutting. Although, compressive strength of Cm-12% at 28 days increase when compared with other results, still, all DoH results at 28 days fall within 5% difference range considering the standard errors is less than 1%. Additionally, as demonstrated earlier in section 5.3 that alite content in clinker decreasing as the OBM cuttings content increasing (Figure 26). In parallel, the DoH in hydrated cement is decreasing as the OBM cutting increases. This is likely

have a direct impact of degree of hydration of the prepared cement suggesting that continued clinker phase hydration was minimal as the OBM cutting increases.

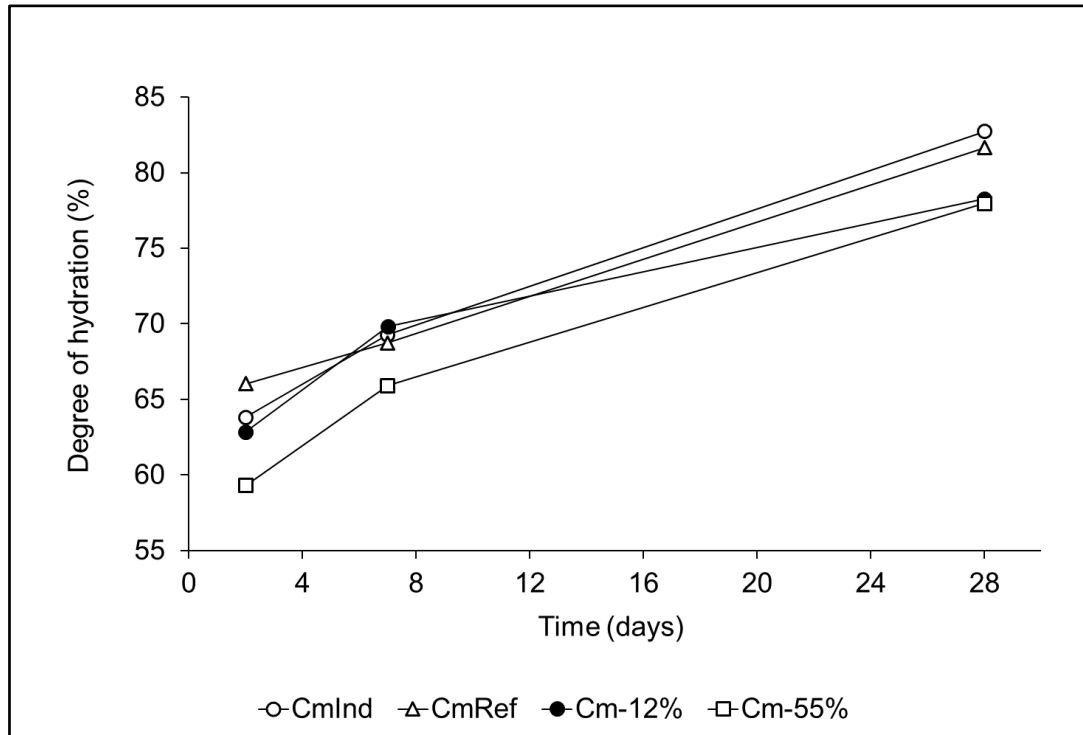


Figure 67 Degree of hydration obtained by SEM BSE vs time

Chapter 8

Impact of using OBM cuttings in cement industries

Chapter 8: Impact of usings OBM cutting in cement industry

8.1 Recycling in non-cement industry

In March 2017, a treatment concept was introduced in Oman that utilized OBM cuttings to a small degree. The OBM cuttings are treated in the Aero Thermal Dissolution Unit³⁶ (ATDU). The treatment recovers the oil from OBM cuttings by heating the OBM cuttings to about 400°C under atmospheric conditions, as illustrated in Figure 68. This treatment creates three main products: oil, water and solid OBM cuttings. The recovered oil is reused in the OBM preparation plant. About 200 Ltr. can be used in the OBM preparation. The ATDU process can recover just under 1 wt% of OBM cuttings as oil. This is because the optimum temperature balance between water evaporation and oil recovery is approximately 400 °C. The water produced from the recycling process is stored in an open lagoon. The majority of solid OBM cuttings, with moisture below 0.01%, is stored in a special landfill without further utilization or treatment. However, this method of treatment using the ATDU does not completely solve the problem. The by-product of the treatment process remains the same; it requires special handling and storing in an engineered storage yard that can protect the ground from any spillage. It is especially harmful to the environment because the material is extremely fine and difficult to handle, as can be seen in Figure 69. It needs a closed handling system to prevent dust emissions. Figure 70 shows the quantities of OBM cuttings treated in the ATDU for a period of two years with the recovered oil quantities. The recovered oil is used again to prepare fresh OBM for drilling operations.

There are some difficulties for treating the OBM cutting using this unit, which include:

- The effort of recycling is too high compared to the output. The recovered oil is only 1% under ideal operating conditions.
- The operating cost is too high compared with the economic value of the output.
- The by-product from this treatment is still considered a hazardous material that must be handled in accordance with the regulations regarding environmental and health conditions.
- The gas emissions caused by heating to a low temperature (400°C), when compared to the burning temperature in a cement kiln, are not enough to break

down all the hydrocarbons to CO₂ and water. The exhaust gases are expected to have higher unburned hydrocarbon contents.

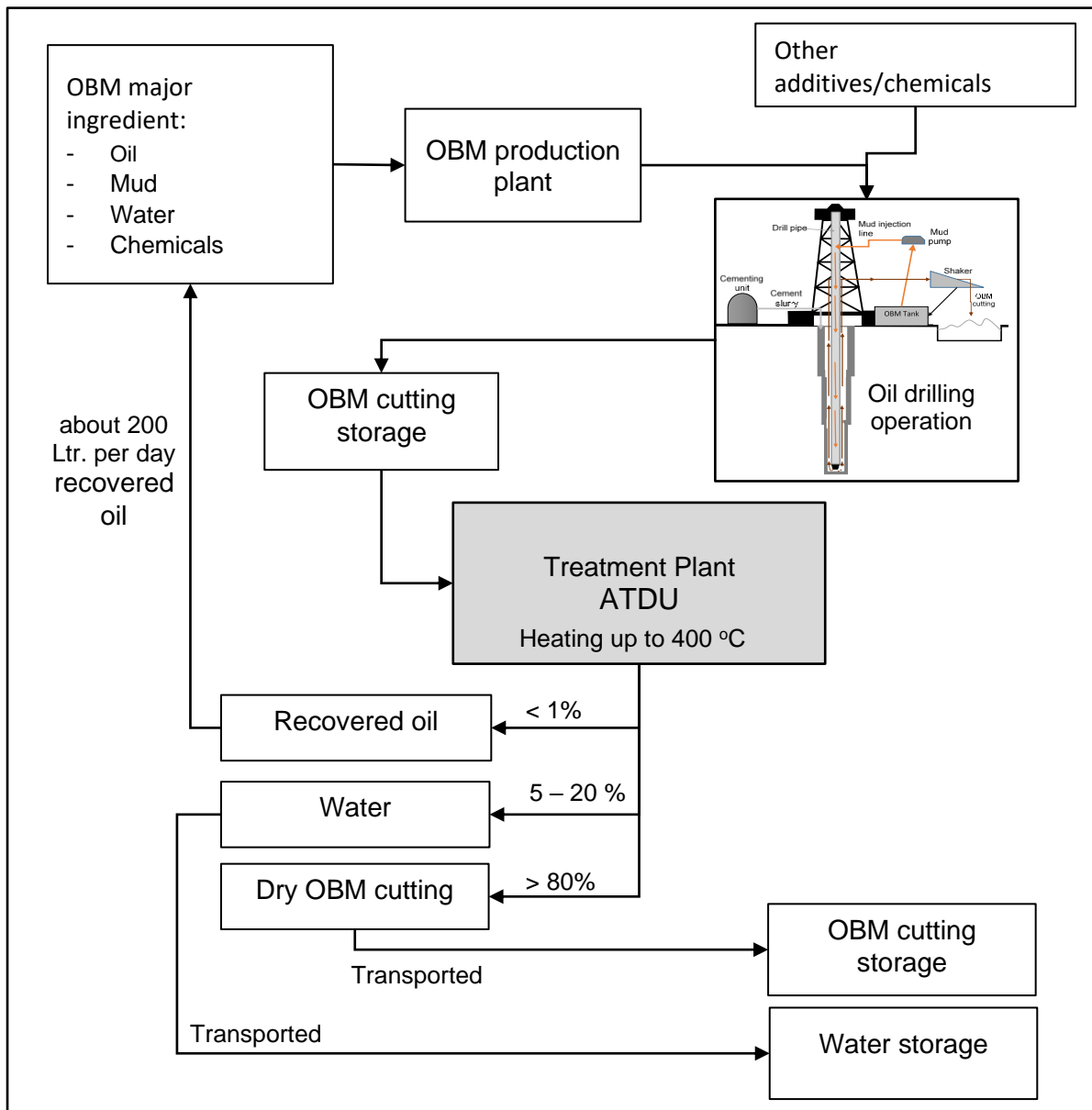


Figure 68 Aero Thermal Dissolution Unit (ATDU) for thermal treatment of OBM cuttings.

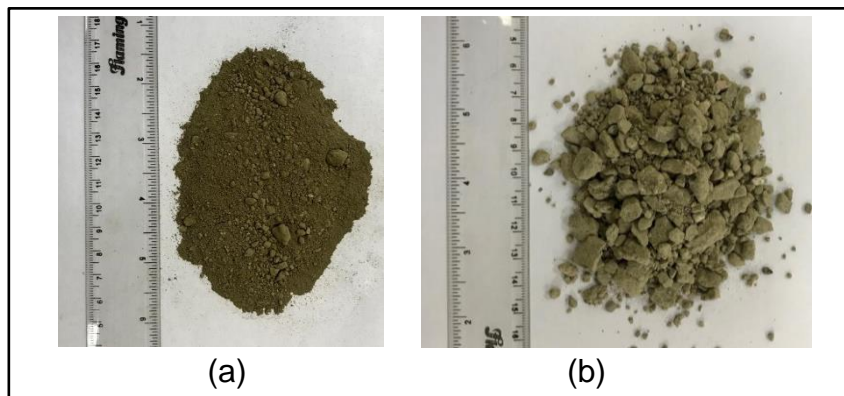


Figure 69 Two types of OBM cuttings collected from storage yard.

(a) Treated OBM cuttings in ATDU, and (b) untreated OBM cuttings

The cost of separating and recycling the oil is summarised in Table 18. In option one, the OBM cutting is treated by the ATDU oil recovery method. In option two, it is used as raw material in cement clinker manufacturing. The third option combines options one and two so that the raw OBM cutting from drilling operations goes directly to the ATDU unit for oil recovery. The output of the OBM cutting from the ATDU is then recycled as raw material through the cement manufacturing process. The cost of option one is about 195 OMR per tonne of OBM cutting to recover 1% of oil for each tonne of treated OBM cutting. This includes the cost of transporting materials from the drilling field to the treatment plant. The recovered oil also has costs of handling, transporting and mixing with fresh oil.

After considering all these costs, when comparing the feasibility of recycling OBM cuttings by the ATDU or utilizing it as raw material in cement manufacturing, the latter is clearly more feasible and requires less effort. However, the OBM cutting produced from the ATDU is attractive for further study as a raw material in cement manufacturing and an additive in cement grinding. The OBM cutting contain clay that comes from the ground during the drilling process; if thermally treated, this clay could be converted to material that has pozzolanic behaviour in cement hydration.

Table 18 Cost calculation for OBM cuttings recycling options*(S. Al-Aghbari, personal communications, May 7th 2019)*

| Item | Option 1 | Option 2 | Options 1+2 |
|--|------------------|---------------------------------------|--|
| | Oil recovery | As raw material in clinker production | 1) Oil recovery 2) As raw material in cement production |
| Capital investment, OMR | 250,000 | 175,000 | 425,000 |
| Operation and Maintenance, OMR/T | 100 | 15 | 85 |
| Transportation OMR/T | 25 | 15 | 20 |
| Storage, OMR/T | 5 | - | - |
| Cost of oil recovered*, OMR/T | -10 | - | -10 |
| Storage of treated OBM cuttings, OMR/T | 75 | - | - |
| Handling & feeding of OBM cuttings | High | Low | Moderate |
| Environmental monitoring | High | High | High |
| Total | 195 OMR/T | 30 OMR/T | 125 OMR/T |

*Each 1 T OBM cuttings give 1% oil which is about 1 Kg oil. The price of 1Kg oil is 10 OMR. Therefore, the saving from oil recovery is 10 OMR for recycling of each tonne of OBM cuttings. The currency 1 OMR is equal to 2.6 USD at the time of calculation.

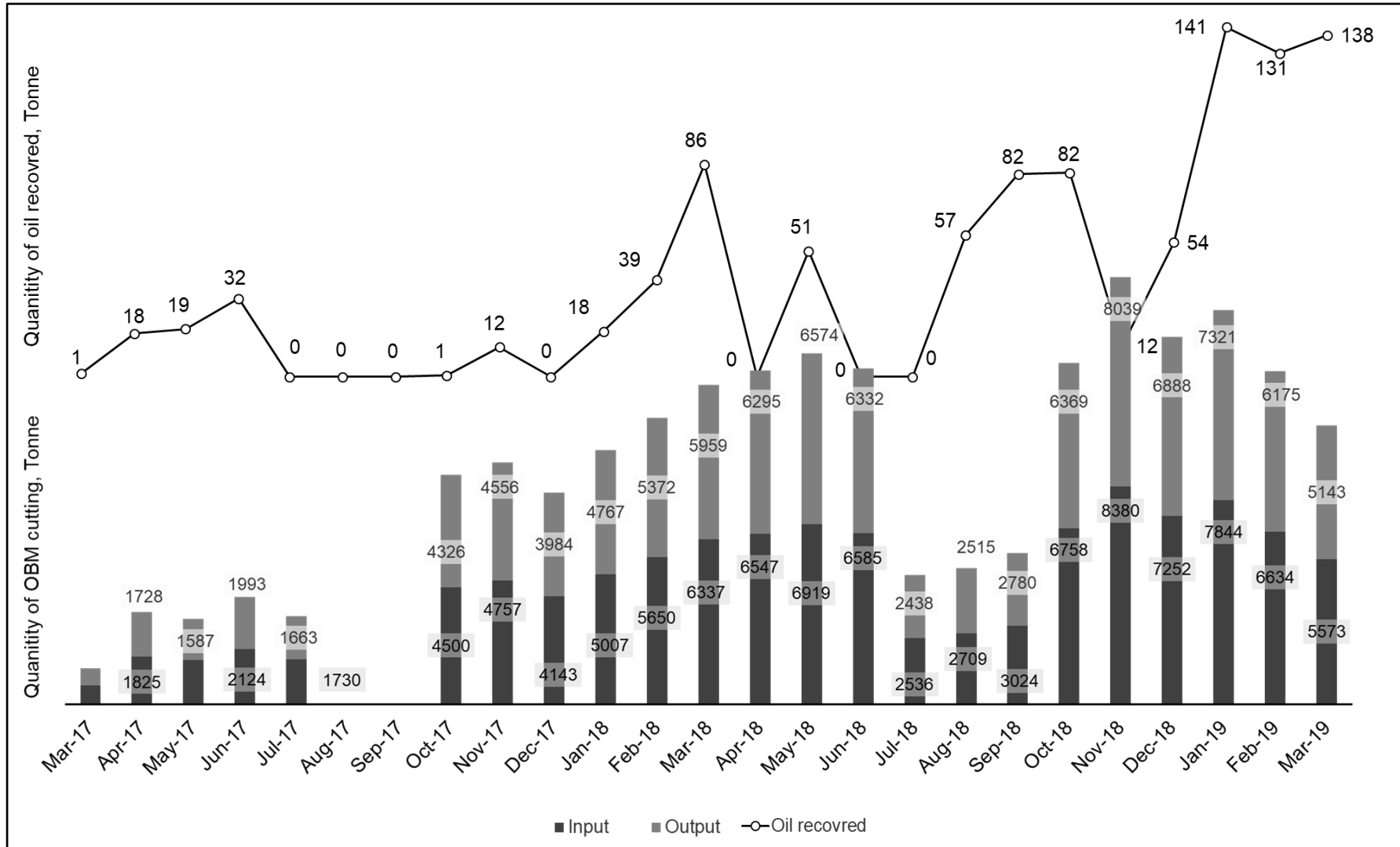


Figure 70 Quantities of treated OBM cuttings using ATDU and oil recovered²⁹

8.2 Oman Cement Company case

The Oman Cement Company produces 2.6 million tonnes of cement annually. It requires about 2.47 million tonnes of clinker (5% additives + 95% clinker). About 4.1 million tonnes of raw materials required annually for clinker consumption. Furthermore, an extension of this factory to a new location²¹⁹ in Oman will require even more raw materials. The present factory has three production kilns line. kiln 1 and 2 is producing 2,700 and 2,000 tonne per day clinker respectively. Kiln 3 is producing 4,000 tonne per day equivalent to 1.2 million tonne annually (considering 300 days operation annually). The annual requirement of raw materials for kiln line 3 is about 2 million tonne. The volume of OBM cuttings expected to be produced by 2020 (as shown in Table 19) is double the present production rate which is sufficient to be 100 % consumed by cement industry in Oman if 12% of OBM cutting is used to replace raw materials.

Table 19 The estimated OBM cutting production and the rate of growth

| Year | Production, x1000 T | Rate growing, x1000 TPY | % growing |
|---------|------------------------|----------------------------|-----------|
| 2013 | 60 | 10 | 17% |
| 2014 | 67 | 7.5 | 11% |
| 2015 | 75 | 7.5 | 10% |
| 2016 | 95 | 20 | 21% |
| 2017 | 115 | 20 | 17% |
| 2018* | 147 | 32.5 | 22% |
| 2019* | 172 | 25 | 14% |
| 2020* | 201 | 29 | 14% |
| Average | 109.33 | 18.94 | 15.75 |

*Estimated quantities

Three important aspects of handling OBM cuttings must be considered when deciding whether to use them in cement manufacture. First, they must be transported from the generation site at the oil well field to the cement factory. Although internationally and, according to their OBM Safety Data Sheet, OBM cuttings are not regulated as a dangerous good. However, in Oman, the Ministry of Environment and Climate Affairs does classify them as a dangerous material. Hence, all aspects of managing OBM cuttings must be performed in accordance with the procedures required for dangerous substances. To ensure OBM cuttings are transported safely and avoid spilling them on the ground during transportation, the truck must (1) have an open top and a

container that is sealed without any gaps to avoid leaching and (2) carry no more than 30 tonnes of OBM cuttings at any given time. Handling the cuttings after they arrive at the cement factory is also regulated to avoid environmental problems, such as soil and water pollution. Once the truck arrives at the cement plant, the OBM cuttings are unloaded onto a concreted area adjacent to the raw material feeding point.

There are several suggestions regarding feeding point of OBM cuttings in cement plant. First, OBM cuttings should be mixed with limestone before they are sent to the crusher (mixed with limestone and then combined with other raw materials, such as quartzo-phillite, iron ore, and kaolin) as shown Figure 71. After being mixed, ground, and homogenised, the OBM cuttings become raw meal that is (1) introduced to the heating system at the pre-heater tower from the top and (2) calcined at about 850 °C at the stage before entering the kiln. As the raw meal is falling by gravity into the pre-heater tower, a flow of hot gases is directed against the flow of the material. These gases are directed to the baghouse for filtration and to remove dust, and then they are released as exhaust from the chimney Figure 72. The gases are mainly CO₂ produced during the calcination process and fuel burning. At the top of the pre-heater tower, hydrocarbons from the OBM cuttings are initially exposed to temperatures in the range of 280–350 °C. However, this temperature range is not hot enough for the complete combustion of the hydrocarbons, which may lead to an increase in the amount of unburned compounds, such as hydrocarbons, NO_x, and SO_x, released into the atmosphere²²⁰. However, the concentration of unburned compounds depends on the kiln system's many operational conditions and the chemistry of the raw materials.

The second suggestion (introducing OBM cutting at the calciner) is an extension of the first and has several advantages and disadvantages. For example, a higher percentage of OBM cuttings could be utilised because the hydrocarbons can undergo complete combustion at higher temperatures in the calciner. The release of unburned compounds is expected to be reduced because the exhaust gases take a longer path⁷⁹. However, this step requires a special conveyor system and feeding system that can control the amount of OBM cuttings introduced to the calciner integrated with the quality control system. This option is expected to limit the amount of OBM cuttings that can be utilised. In addition, technical consideration to be taken during the kiln operation. Possible variations in several parameters during the feeding of OBM cutting through the calciner include moisture content, flame shape changing and calciner rise

in carbon monoxide²²¹. The arrangement for feeding through the calciner is illustrated in Figure 73.

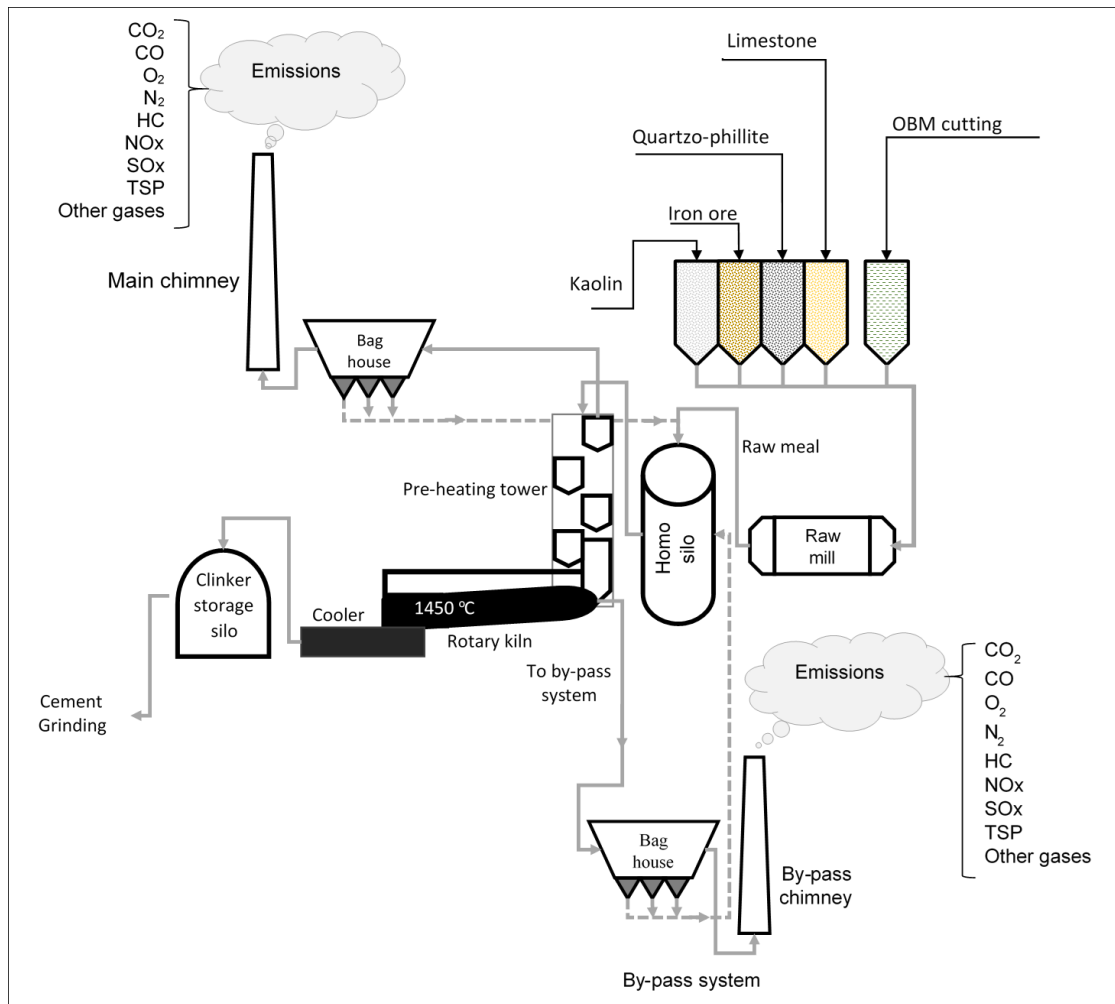


Figure 71 Main source of emissions from the cement kiln system.

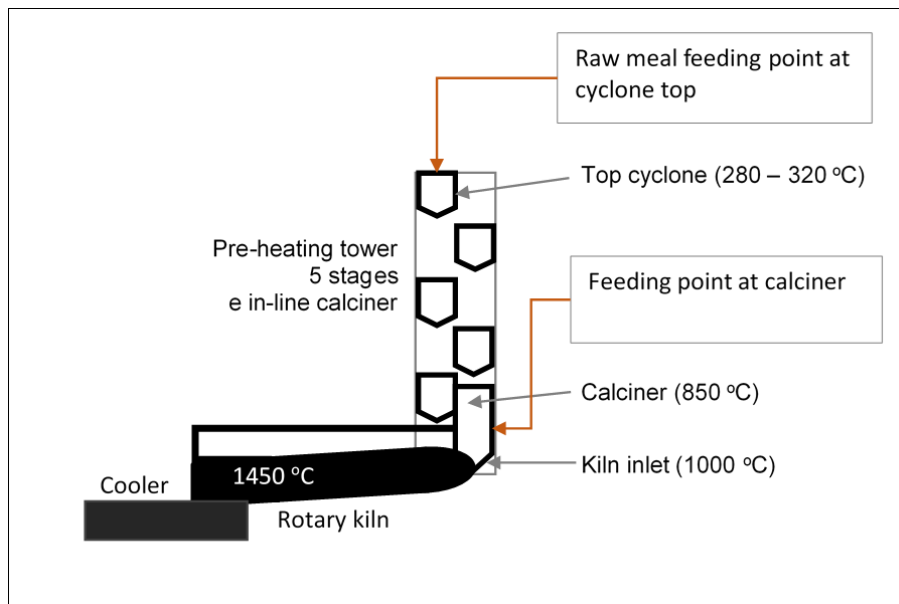


Figure 72 Proposed feeding points of OBM cutting.

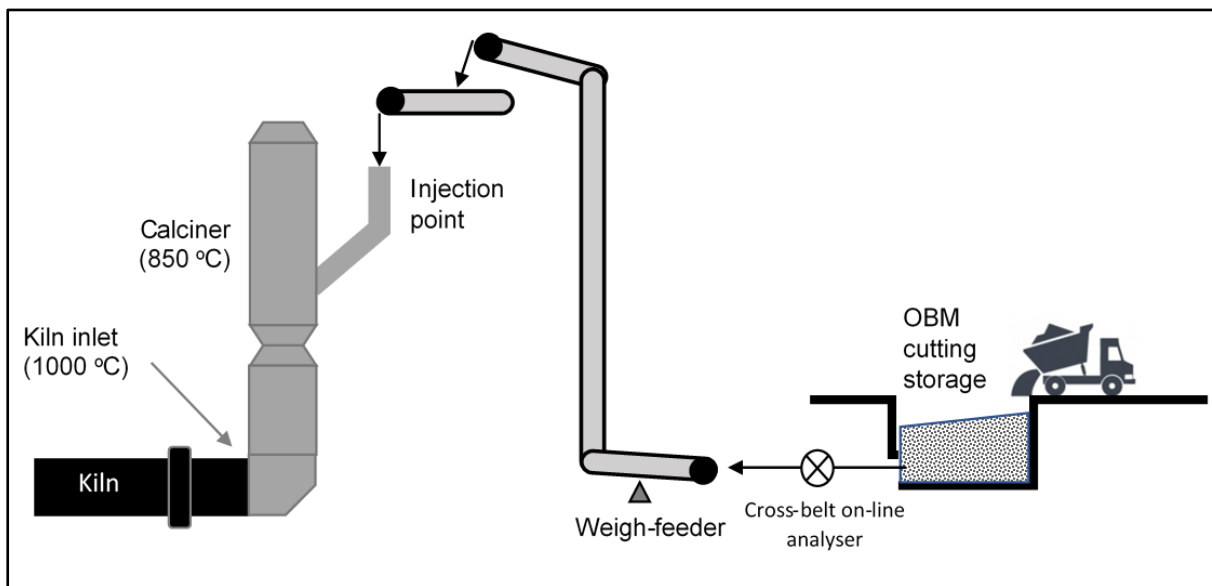


Figure 73 Arrangement for feeding OBM cutting at the calciner.

(after Mouayed M. ²²²)

8.3 Impact of introducing OBM cutting to Oman Cement Company as additional raw material

The Oman Cement Company plant is located very close to high-quality limestone containing 90–95% pure CaCO_3 with sufficient reserves to produce cement clinker for at least 100 years. Furthermore, the plant is adjacent to two additional raw materials,

iron ore and quartzo-phillite (QPh). However, QPh has two limitations. First, it has a high free silica content, which makes it difficult to grind²²³ and so increases the cost. Second, the reserve of QPh is very small and insufficient for future production needs, which will require the company to search for an alternative substitute sources. In addition, while its purity can be considered a positive, the limestone in Oman Cement Company quarry is deficient in alumina (Al_2O_3 content in limestone 0.62 %wt. ± 0.19 , [Appendix 15B]), requiring the company to use an expensive alumina source material as a corrective raw material, such as bauxite or kaolin. Bauxite does not occur naturally in Oman, so is imported. However, kaolin is available in limited quantities, but the reserves are located far from the plant. The cost of kaolin (mining and transportation) is ten times the cost of limestone, which makes the raw material costly^{10,97}.

Introducing alternative material to the Oman Cement Company plant, such as OBM cuttings, may provide material that supports the raw material currently being used. The chemical composition and characteristics of OBM cuttings are an advantage and could replace QPh. The Rm-55% sample, which contains 55% OBM cuttings, would be ideal for cement manufacturing. It has zero QPh and minimum kaolin consumption (0.50% kaolin). The reference sample of the raw meal contains 4.70% kaolin, which means OBM cuttings have almost 9-times less kaolin. The industrial raw meal sample contains about 5.65% kaolin. Furthermore, the iron ore % needed in the raw mix to prepare the Rm-55% also dropped to 1.50% (Table 7)

Table 7. This approach should be viewed favourably by the cement plant as it would save the company operational and raw material costs. The cement prepared from raw material that contains the highest percentage of OBM cuttings (i.e., 55%) meets the clinker manufacturing requirements. Furthermore, the calcination temperature required to decompose CaCO_3 decreases as the OBM cuttings are added and, thus, reduces fuel consumption. In fact, 60% of fuel consumption in the clinkerisation process occurs during calcination²²⁴. Thus, less fuel would be needed, which would have a direct impact on decreasing the plant's CO_2 emissions^{225,226} and lowering the production cost. However, looking considering the quantity of OBM cutting produced from the oil field, seeing the oil operation growth in coming years, the amount of OBM cutting is not sufficient to sustain cement production using OBM cutting at 55% level. Consequently, 12% could be a better choice.

Chapter 9

Summary discussion

Chapter 9 Summary discussion

9.1 Introduction

OBM cuttings are wastes from the oil drilling process and are polluted with oil, making them a potentially hazardous waste that should not be released into the environment. OBM cuttings have numerous characteristics that could be utilised in the cement industry. The cuttings all contain oxides which are essential in cement manufacture. Utilization of cuttings in cement manufacture will provide an environmentally friendly waste management solution for this potentially hazardous waste.

The objective of this study was to create background knowledge concerning the effect of using OBM cuttings as raw material in cement manufacture. This study provides momentum for the oil and cement sectors to seize a recycling opportunity and maximise the utilisation of resources and by-products, such as OBM cuttings.

Clinker was prepared in a laboratory with different OBM cutting contents. The resultant clinker was tested by XRD, XRF, SEM-EDX, and for free lime. The clinkers were ground with gypsum using a tube ball mill to produce cement. The cement was tested according to appropriate standards (i.e., mechanical, physical, and chemical testing) and, in addition, the hydration behaviour was investigated by (ICC) and (STA).

9.2 OBM cutting

XRD analysis of the OBM cuttings found that the OBM contains mainly calcite (CaCO_3), dolomite ($\text{CaMg}(\text{CO}_3)_2$), quartz (SiO_2), iron oxide (Fe_2O_3) and barite (BaSO_3).

In addition, the analyses showed that the OBM cuttings are a heterogeneous mixed material composed of a few major types: gravel, limestone, clay and shale. The gravel and limestone are cuttings from the oil drilling process that contaminate the recirculated material and become part of the OBM cutting. Limestone (calcite) and clay are added during the preparation of the OBM. Shale is of low CaO content (below 40%) and high SiO_2 content (above 20%). The alumina content in OBM cuttings probably arises from the clay used in OBM preparation. Clay is a major source of aluminium in the form of aluminosilicates.

Analysis also showed the presence of barium in the OBM cuttings as barite (barium sulphate, BaSO_4). The major source of barite is the preparation of the OBM used during the oil well drilling process. OBM cuttings likewise contain heavy and trace metals from several sources in very low concentrations. These are mainly from the use of additives or from the cutting and the crude oil. The OBM cuttings obtained in this study have metal contents that fall below the limits specified by Petroleum Development Oman (PDO).

9.3 The effect of OBM cutting on the clinkerization process

The main phases in all the investigated clinkers were alite (C_3S), belite (C_2S), tricalcium aluminate (C_3A) and ferrite (C_4AF). There were no noticeable changes in the alite or belite polymorph with changes in OBM cutting content. However, the levels of alite and belite formed were dependent on the OBM cutting content. This result was not predicted by the Bogue calculations, but the Rietveld refinement data showed a gradually decreasing alite content and corresponding increasing belite content with increasing OBM cutting content.

Thermal analyses of various raw meal samples showed that the calcination temperature (CaCO_3 decomposition temperature) decreased with increasing OBM cutting content. Calcite decomposition occurred at 817 °C when no OBM was present, falling consistently with increasing OBM cutting content until the OBM cutting alone (Rm100%) showed decomposition at 763 °C.

Analyses of petrographic thin sections of the limestone used here shows calcite crystals of a depositional texture, with no regular shape and unevenly distributed without common direction. The grains are coarse (>3mm) and compact with no void space between calcite crystals, appearing flat and with some fractures. This limestone can be classified as crystalline limestone according to the Dunham classification¹⁵⁸.

The OBM cuttings, meanwhile, show different petrography, with the calcite being mud-supported with loosely packed grains and high porosity. The clay grains are mostly present as developed clusters and immersed in oil. Lath-shaped plagioclase grains with sharp grain margins are also present. The calcite show round sub-millimetre grains, which are highly brittle and fragile in nature. XRD analyses of OBM cuttings show the presence of dolomite. Therefore, the OBM cuttings' classification can be considered be a mix between two or three types of limestone, falling between

mudstone and Wake stone. However, the classification is certainly different from the limestone used in this research.

Literature showed that limestone decomposition starts with the rapid dissociation of dolomite in the first few min, followed by calcite decomposition. Dolomite dissociation occurs in a single step without a calcite intermediate phase. This suggests that the presence of dolomite reduces the calcination activation energy. It is proposed that limestone dissociation starts with dolomite decomposition, resulting in the formation of grain cracks due to the $\text{CaMg}(\text{CO}_3)_2$ structure, growing the surface area, allowing CO_2 diffusion.

The lower decomposition temperature in OBM cuttings may also be related to the calcite texture therein, which differs from the calcite in limestone as explained above. Finally, OBM cuttings are more porous than limestone, allowing more surface area for heat transfer. As seen petrographically, the calcite grains float in the mud, with larger spaces between grains than in the limestone.

The calcite grain size also has an effect on both the rate of decomposition and the temperature at which decomposition occurs. Coarser grains show higher decomposition temperatures and lower rates of decomposition.

The burnability of raw meal was investigated. The results show that the free lime content for raw meal obtained from industrial ($\text{Rm}_{\text{Ind.}}$) and the one prepared in lab ($\text{Rm}_{\text{Ref.}}$) mixes fell with increasing temperature. However, the free lime content of Rm_{Ind} was always greater than that of $\text{Rm}_{\text{Ref.}}$, with the difference between the two decreasing with increasing temperature, until the difference was minimal at 1400 °C and above. The higher free lime content for Rm_{Ind} could be due to its higher LSF, i.e. 92.53 compared to 90.50 for $\text{Rm}_{\text{Ref.}}$. Thus, there is more CaO to be consumed during clinkering. This is supported by the convergence of the two data sets with increasing temperature. Both mixes showing similar burnability behaviour validates the use of the reference raw meal in comparisons with raw meal prepared using OBM cutting.

The burnability results for Rm_{Ref} plus raw meal prepared using 12%, 55% and 100% OBM cuttings showed that, despite the falling free lime contents with increasing temperature, there was an increase in free lime with increasing OBM cutting content, suggesting harder burnability. However, this did not apply to the sample prepared from 100% OBM cutting. This sample showed very easy burning behaviour. The free lime

dropped significantly, even at 1300 °C (0.2% free lime), then showing only 0.02% free lime content when heating at 1500 °C. However, when burned at 1200 °C, the 100% OBM cutting showed belite formation and a very low free lime content. Higher temperatures still led to no alite formation due to there being no CaO remaining. Instead, belite grains were within a high melt content, a result of the high concentration of Al₂O₃ and Fe₂O₃ % in the mix. The absence of alite can easily be understood in terms of the LSF, which at 48.45 was considerably lower than for all of the other samples.

In $R_{m_{Ref}}$, the belite and liquid phase formation temperature was 1284 and 1331 °C respectively, but these fell upon incorporation of OBM cutting. SEM-EDX and ICP analysis both showed an increase in barium content with increasing OBM cutting content. Furthermore, SEM-EDX analysis revealed the distribution of barium through the clinker phases, with the highest concentration found in the liquid phase.

The effect of barium on phase composition is related to the free lime content. An increased free lime content indicates reduced burnability and incomplete formation of the main clinker phases. This is possibly due to alite formation being destabilized. The addition of OBM cutting decreased burnability and the free lime contents increased. With the OBM cutting containing 0.85 wt% BaO, the barium content of the clinker increases with increasing OBM cutting content. BaO has a negative influence on alite formation, thus increasing the free lime content. This is in line with many studies^{175,176,177,168,148} showing that the free lime content increases with barium content, and that barium is mainly concentrated in the melting phase.

9.4 The effect of OBM cutting on the cement properties and hydration

Cement hydration was studied by a number of techniques. The mechanical strength was determined and compared with the standard specification implemented in Oman (OS7/2001). Also, the physical testing such as setting time, Blaine, soundness and density were measured. Using XRD complemented by SEM-EDX analyses of polished cross-sections, the major hydrate phases were studied. SEM was also used to understand if there were any significant changes in the microstructure.

The chemical composition limits in OS are similar to those in BS/EN standard except regarding MgO, insoluble residue (IR), and C₃A content. In addition, OS specifies the

range of cement LSF and AM factors. The cement produced using the OBM cutting meets the standard requirement and fulfils the chemical and physical/mechanical limits.

The soundness of the prepared cement increased as OBM cutting content increased. Higher expansion could be due to several reasons, such as i) high free lime content in clinker (above 2%) or ii) high MgO content in cement (above 3%). The free lime contents in all samples were kept below 2%. The significant contribution for the expansion may be attributed to the presence of a high concentration of MgO (periclase) in cement prepared with higher OBM cutting contents in the raw meal.

Hence, higher soundness in the cement sample of 55 % OBM cutting is more likely due to the higher content of MgO coming from OBM cutting. The SEM-EDX analysis also confirms the presence of MgO in cements prepared with 30% and above OBM cutting. Setting time results show no significant change between the samples with OBM cutting and the reference sample.

Compressive strength results increased with hydration for 2, 7 and 28 days. At two days, the two reference samples (C_{mInd} and C_{mRef}) showed slightly lower strengths than the samples prepared with OBM cutting (12% and 55%). By 7 days, the strengths of all samples increased and the OBM-containing samples remained slightly stronger than the reference samples. At 28 days, $C_{mt-12\%}$ was the strongest, with no significant difference between others. With alite being the principal phase responsible for later-age strength, given the minimal difference in alite contents between the samples, the similarity in performance is not surprising. It is possible that the slight variations in Blaine fineness could explain the slight differences in strength. Fineness plays a dominant role in compressive strength development, with higher fineness leading to higher strength due to cement grains having more surface area exposed during hydration.

There was no significant effect on the crystal phases formed upon hydration, despite the greater potential of magnesite ($MgCO_3$) formation. In all investigated samples AFm (ettringite) was present at 2 days hydration, while no AFm formation was observed in any samples. The formation of AFt is highly dependent on the C_3A content in cement. With high C_3A contents, the monocarboaluminate appears at early age of hydration, often within 7 days of hydration²⁰⁹.

The optical microscopy analysis showed an increase in C_3A content as the OBM cutting increased. The C_3A content in $Ck_{Ref.}$, Ck_{12} and Ck_{55} are 12, 16 and 17% respectively. However, AFm phases were not detected. The XRD patterns for all hydrated cement samples showed similar behaviour. Ettringite (AFt) and C_4AF were observed with the intensity of reflections from the latter diminishing with time. Between 2 to 28 days the intensity of the main clinker phase reflections decreased with growth of reflections due to hydrates. The amount of AFt formed depends on the ratio of sulphates (added during grinding) and the C_3A content of the clinker. At high ratio of C_3A to $CaSO_3 \cdot 2H_2O$, the AFt is unlikely to convert to AFm. In this investigation, the % of gypsum added during the cement grinding was fixed at about 6% for all samples.

The C_3A content calculated according to Bogue formula in clinker samples Ref, 12% and 55% are 7.94, 7.77 and 6.74 % respectively, with no change in polymorph (which is known to affect the rate of hydration). Therefore, the absence of AFm can be explained by the increasing sulphate to aluminate ratio in the cement. Furthermore, the absence of the AFt \rightarrow AFm conversion means that no additional heat is released after the first hydration reaction is completed. This is could be an explanation for the similarity of the heat rate shown for the all samples.

The hydration reaction of C_3S is associated with formation of calcium hydroxide (CH) which precipitates in the form of portlandite and is dispersed within the hardened paste. The XRD patterns for the hydrated cement clearly indicates the formation of CH in all samples, with growing intensity as the time passes.

Isothermal calorimetry (ICC) was conducted to determine the hydration kinetics. There was generally no significant difference in the time to onset of the acceleration period. All the results showed one main peak, associated with alite hydration to form calcium silicate hydrate (C-S-H) and portlandite (CH). The highest peak is for the cement containing 55% OBM cutting; appearing after 11.02 hours. The second highest peak is for $Cm_{12\%}$; after 11.63 hours. Followed by $Cm_{Ref.}$ and $Cm_{Ind.}$ at 11.88 and 12.12 hours respectively. Then, the heat rate slowed down gradually and reached very low values within few days.

The total heat released was in the range 247 to 256 J/g at 21 days with maximum 3% difference with the industrial sample. This confirms the similarity in behaviour of the various cements.

At 7 and 28 days, the $C_{m_{ind}}$ samples exhibited a higher degree of hydration (DoH), but at 2 days hydration was lower than the reference sample. This is likely due to variation in cement preparation, e.g. the use of industrial grinding with grinding aids. Additionally, the DoH of Cm-12% and Cm-55% after 2 days curing were found respectively 62.03 and 59.30 % which are lower when compared with the reference sample (66.03%). The Cm-55% showed a marginally lower degree of hydration at all ages than the other samples, while the reference sample showed the highest degree of hydration at all ages.

9.5 Impact of using OBM cutting in cement industries

Three important aspects of handling OBM cuttings must be considered when deciding whether to use them in cement manufacture.

- i- They must be transported from the generation site at the oil well field to the cement factory. Although internationally and, according to their OBM Safety Data Sheet, OBM cuttings are not regulated as a dangerous good. However, in Oman, the Ministry of Environment and Climate Affairs does classify them as a dangerous material. Hence, all aspects of managing OBM cuttings must be performed in accordance with the procedures required for dangerous substances.
- ii- The truck must (1) have an open top and a container that is sealed without any gaps to avoid leaching and (2) carry no more than 30 tonnes of OBM cuttings at any given time.
- iii- Once the truck arrives at the cement plant, the OBM cuttings are unloaded onto a concreted area adjacent to the raw material feeding point.

There are several suggestions regarding feeding point of OBM cuttings in cement plant as following:

- OBM cuttings should be mixed with limestone before they are sent to the crusher. After being mixed, ground, and homogenised, the OBM cuttings become raw meal that is (1) introduced to the heating system at the pre-heater tower from the top and (2) calcined at about 850 °C at the stage before entering the kiln.

- The second suggestion (introducing OBM cutting at the calciner) is an extension of the first and has several advantages and disadvantages. For example, a higher percentage of OBM cuttings could be utilised because the hydrocarbons can undergo complete combustion at higher temperatures in the calciner. The release of unburned compounds is expected to be reduced because the exhaust gases take a longer path. This option is expected to limit the amount of OBM cuttings that can be utilised. In addition, technical consideration to be taken during the kiln operation. Possible variations in several parameters during the feeding of OBM cutting through the calciner include moisture content, flame shape changing and calciner rise in carbon monoxide.

Chapter 10

Conclusions and further work

Chapter 10: Conclusions and further work

10.1 Conclusions

The hydration behaviour of the cement prepared with and without OBM cutting has been studied by many techniques such as ICC, STA and mechanical properties. Using XRD complemented with SEM-EDX analyses of polished sections, the major hydrate phases were studied. The SEM and optical microscopy of the clinker was also used to understand if there are any significant changes to the microstructure and main phases, which may influence hydration. The degree of hydration was obtained and the main hydration products such as C-S-H and CH were identified.

After heating and burning the raw meal of different OBM cutting ratios, and Portland cement clinker obtained, the clinker phases formed in all samples having the required composition of main clinker phases that essential to complete the hydration process stages in like to normal cement. To obtained comparable results, the cement clinker ground at similar fixed condition, physical parameters and gypsum quality and quantity. This allow to understand if OBM cutting ratio has impact on the cement behaviour hydration. The technique adopted in this study for the investigation, is to understand whether OBM cutting has any substantial impact that could interrupt manufacturing of cement using OBM cutting as an additional raw material. The results obtained show that the hydration behaviour as normal with no significant change observed and no distinguished change comparing to the reference sample and industrial cement. The progress of hydration of cement prepared for the ones with OBM cutting and comparing to the reference and industrial cement are following similar hydration behaviour.

Clinker prepared using OBM waste had very similar properties to clinker prepared from the limestone normally used in cement production. These results demonstrate that OBM cutting could be recycled in the manufacture of Portland cement clinker. This could present an opportunity for re-use of OBM cutting waste and solve an environmental problem. This will also reduce the cost of cement production. The main result in this study are as follows:

- The addition of OBM cutting lowers the calcination temperature. This is because the calcite in OBM cutting has a smaller grain size than that in the limestone.
- Furthermore, the OBM cutting contained some dolomite ($\text{CaMg}(\text{CO}_3)_2$). This increases the rate of carbonate dissociation and so also contributed to the lowering of the calcination temperature.
- However, the addition of OBM cutting to the raw meal led to a higher free lime content in the resultant clinker. There are many reasons for this, but the role of trace elements, especially barium, in destabilizing alite has been demonstrated here.
- While it would likely have no commercial potential, clinker could be prepared by just heating OBM cutting at 1200 °C, without any addition. The XRD and SEM-EDX analysis of the resultant clinker showed formation of belite with a very low free lime content and no alite formation.
- There are several benefits that could be gained from the successful recycling of OBM cuttings in cement manufacture. The OBM cuttings provide a source of fuel. They also reduce the consumption of natural resources. In oil drilling operations, the reuse of OBM cuttings in cement production provides an environmentally-friendly waste management solution for large quantities of OBM cuttings, reducing landfill by effective recycling of waste, without the need for any pre-treatment.
- The inclusion of ca. 12% OBM cuttings in raw meal for cement manufacture has no significant effect on clinker composition. Thus, this provides a cost-effective, environmentally-friendly route for the management of OBM cuttings derived from the oil industry.
- Introducing alternative material to the Oman Cement Company plant, such as OBM cuttings, may provide material that supports the raw material currently being used.

10.2 Further work

The results of this thesis can help to improve the quality control of the cement production using OBM cutting as an additional raw material. The lower burnability behaviour of the raw meal that contain OBM cutting could be further explored to

produce clinker with less fuel consumption. However, the impurities present in OBM cutting could be additional studied to explore the method and ways for preparing the raw meal that fit to be used in cement manufacturing. A pilot investigation at cement kiln plant is essential to study the actual characteristic of the clinker produced using OBM cuttings and likewise to measure the main stack gaseous emissions, i.e. carbon monoxide (CO), sulphur oxides (SO_x), nitrogen oxides (NO_x), hydrocarbons (H/C), hydrogen sulphide (H₂S), volatile organic compounds (VOCs), particulate matter (PMs) and substances of environmental concern (e.g. Hg, Cd, Pb, etc)

The pilot investigation could extend to test the produced clinker and cement. Similarly, it is worth comparing the differences between the clinker and cement prepared in the laboratory with that produced from a real-kiln. This would highlight potential differences between the different scales of production, for example in the duration of the clinkering process.

Furthermore, it would be worth studying the potential of using OBM cuttings for other purposes in the cement industry such as to replace additives (e.g. pozzolana and fly ash). Also, to study thermal treatment of OBM cuttings and observe the effect on its properties.

References

1. U.S. Geological Survey, Mineral Commodity Summaries, January 2018 , <https://minerals.usgs.gov/minerals/pubs/commodity/cement/mcs-2018-cemen.pdf>.
2. *Fitch Solutions MBI, on-Line Database, Http://fitchsolutions.Com*.
3. Portland Cement Association. World Cement Consumption. *World Cem.* 2013.
4. Deloitte. *GCC of Construction 2014 in Construction Sector Overview.*; 2014.
5. Cement G. Global Research Sector - Cement. *Glob Invest House.* 2013;March.
6. National Centre for Statistics and Information, Oman, website: www.ncsi.gov.om.
7. Abdul-Wahab SA, Al-Rawas GA, Ali S, Al-Dhamri H. Impact of the addition of oil-based mud on carbon dioxide emissions in a cement plant. *J Clean Prod.* 2016;112:4214-4225. doi:10.1016/j.jclepro.2015.06.062
8. Gao T, Shen L, Shen M, Liu L, Chen F, Gao L. Evolution and projection of CO₂emissions for China's cement industry from 1980 to 2020. *Renew Sustain Energy Rev.* 2017;74(December 2016):522-537. doi:10.1016/j.rser.2017.02.006
9. Imbabi MS, Carrigan C, McKenna S. Trends and developments in green cement and concrete technology. *Int J Sustain Built Environ.* 2012;1(2):194-216. doi:10.1016/j.ijbsbe.2013.05.001
10. Oman Cement Company SAOG. Production Department. Oman. www.occ.om. Published 2018. Accessed November 1, 2018.
11. Bites N. Oman Cement : Natural Gas Price increase. 2014:1-2.
12. Caenn R, Chillingar G V. Drilling fluids: State of the art. *J Pet Sci Eng.* 1996;14(3-4):221-230. doi:10.1016/0920-4105(95)00051-8
13. Al-Ansary MS, Al-Tabbaa A. Stabilisation/solidification of synthetic petroleum drill cuttings. *J Hazard Mater.* 2007;141(2):410-421. doi:10.1016/j.jhazmat.2006.05.079
14. Leonard SA, Stegemann JA. Stabilization/solidification of petroleum drill cuttings: Leaching studies. *J Hazard Mater.* 2010;174(1-3):484-491. doi:10.1016/j.jhazmat.2009.09.078
15. Davies JM, Addy JM, Blackman RA, et al. Environmental effects of the use of oil-based drilling muds in the North Sea. *Mar Pollut Bull.* 1984;15(10):363-370. doi:10.1016/0025-326X(84)90169-3
16. Almudhhi SM. Environmental impact of disposal of oil-based mud waste in Kuwait. *Pet Sci Technol.* 2016;34(1):91-96. doi:10.1080/10916466.2015.1122630
17. Robinson JP, Kingman SW, Snape CE, et al. Remediation of oil-contaminated drill cuttings using continuous microwave heating. *Chem Eng J.* 2009;152(2-3):458-463. doi:10.1016/j.cej.2009.05.008
18. Xie SX, Jiang GC, Chen M, et al. Harmless treatment technology of waste oil-based drilling fluids. *Pet Sci Technol.* 2014;32(9):1043-1049. doi:10.1080/10916466.2011.638691
19. Henry LA, Harries D, Kingston P, Roberts JM. Historic scale and persistence of drill cuttings impacts on North Sea benthos. *Mar Environ Res.* 2017;129:219-228. doi:10.1016/j.marenvres.2017.05.008
20. Ghazi M, Quaranta G, Duplay J, et al. Life-Cycle Impact Assessment of oil drilling mud system in Algerian arid area. *Resour Conserv Recycl.* 2011;55(12):1222-1231. doi:10.1016/j.resconrec.2011.05.016
21. Ministry of Environment & Claimt afferias. MD 18-93 Regulations for the Management of Hazardous Waste. 1993.
22. Cripps SJ. *Disposal of Oil-Based Cuttings.*; 1998.
23. Strachan MF. Studies on the impact of a water-based drilling mud weighting agent (Barite) on some Benthic invertebrates. 2010:13-17. [file:///C:/Users/em0899/Desktop/hilal2017/Journals 2018/OBM/studies on the impact of a water-based drilling mud in North Sea.pdf](file:///C:/Users/em0899/Desktop/hilal2017/Journals%202018/OBM/studies%20on%20the%20impact%20of%20a%20water-based%20drilling%20mud%20in%20North%20Sea.pdf).
24. Fakoya MF, Ahmed RM. A generalized model for apparent viscosity of oil-based muds. *J Pet Sci Eng.* 2018;165(December 2017):777-785. doi:10.1016/j.petrol.2018.03.029

25. Agwu OE, Okon AN, Udoh FD. A Comparative Study of Diesel Oil and Soybean Oil as Oil-Based Drilling Mud. *J Pet Eng*. 2015. doi:10.1155/2015/828451
26. Abduo MI, Dahab AS, Abuseda H, AbdulAziz AM, Elhossieny MS. Comparative study of using Water-Based mud containing Multiwall Carbon Nanotubes versus Oil-Based mud in HPHT fields. *Egypt J Pet*. 2016;25(4):459-464. doi:10.1016/j.ejpe.2015.10.008
27. Lechtenberg D, Diller H. Alternative Fuels and Raw Materials (AFR) review "oil mud drillings." In: *Alternative Fuels and Raw Materials Handbook for the Cement and Lime Industry, Volume 2*. Dusseldorf: MVW Lechtenberg & Partner; 2012:303-320.
28. Industriail and Hazardous Waste Survey Summery Report. Oman: Oman Environmental Service Holding Company S.A.O.C (be'ah), 2018.
29. Petroleum Development Oman. Department of Chemistry. <https://www.pdo.om>. Published 2019. Accessed February 1, 2019.
30. Taha R, Al-Rawas A, Al-Jabri K, Al-Harthy A, Hassan H, Al-Oraimi S. An overview of waste materials recycling in the Sultanate of Oman. *Resour Conserv Recycl*. 2004;41(4):293-306. doi:10.1016/j.resconrec.2003.10.005
31. Zacks Investment Research: BP Commences Natural Gas Production in Oman's Khazzan Field. *Newstex Financ Account Resour*. 2017.
32. Oman Supreme Council for Planning. The National Program for Enhancing Economic Diversification: TANFEEDH Handbook. *Tnafaeth*. 2017;(July):71. <http://www.tanfeedh.gov.om/en/handbook.php>.
33. Eldridge RB. Oil Contaminant Removal from Drill Cuttings by Supercritical Extraction. *Induserial Eng Chem Res*. 1996;5885(95):1901-1905.
34. Khanpour R, Sheikhi-kouhsar MR, Esmaeilzadeh F. Removal of contaminants from polluted drilling mud using supercritical carbon dioxide extraction. *J Supercrit Fluids*. 2014;88:1-7. doi:10.1016/j.supflu.2014.01.004
35. Mcdonald JA, Portier RJ. Feasibility studies on in-situ biological treatment of drilling muds at an abandoned site in Sicily. 2003;716(May 2002):709-716. doi:10.1002/jctb.847
36. Young GA, Growcock FB, Talbot KJ, Lees J, Allis B, Worrell B. Elements of Thermally Treating Oil-Base Mud Cuttings. In: *SPE/IADC Drilling Conference*. Amsterdam; 1991:365-374.
37. Erickson P, Fowler B, Thomas D. *Oil-Based Drilling Muds: Off Structure Monitoring, Beaufort Sea.*; 1988. https://books.google.com.sa/books/about/Oil_based_Drilling_Muds.html?id=gPwaAQAAIAAJ&pgis=1.
38. Breuer E, Stevenson AG, Howe JA, Carroll J, Shimmield GB. Drill cutting accumulations in the Northern and Central North Sea: A review of environmental interactions and chemical fate. *Mar Pollut Bull*. 2004;48(1-2):12-25. doi:10.1016/j.marpolbul.2003.08.009
39. Khanpour R, Sheikhi-Kouhsar MR, Esmaeilzadeh F, Dariush Mowla. Removal of contaminants from polluted drilling mud using supercritical carbon dioxide extraction. *J Supercrit Fluids*. 2014;88:1-7. doi:doi.org/10.1016/j.supflu.2014.01.004
40. Hou B, Chen M, Liu M, Xiong Q. Safe disposal technology of waste oil-based drilling fluids. *J Japan Pet Inst*. 2013;56(4):221-229. doi:10.1627/jpi.56.221
41. Qin X, Lu H, Li Y, et al. Preparation and Evaluation of a Profile Control Agent Base on Waste Drilling Fluid. *J Chem*. 2017;(1). doi:<https://doi.org/10.1002/ep.10568>
42. International Council on Clean Transportation. China V - gasoline and disel fuel quality standards. 2014. http://www.theicct.org/sites/default/files/publications/ICCTupdate_ChinaVfuelquality_jan2014.pdf.
43. Amani M, Al-Jubouri M, Shadravan A. Comparative Study of Using Oil-Based Mud Versus Water-Based Mud in HPHT Fields. *Adv Pet Explor Dev*. 2012. doi:10.3968/j.aped.1925543820120402.987
44. Abbe OE, Grimes SM, Fowler GD, Boccaccini AR. Novel sintered glass-ceramics from vitrified

- oil well drill cuttings. *J Mater Sci.* 2009;44(16):4296-4302. doi:10.1007/s10853-009-3637-y
45. Oreshkin D V., Chebotaev AN, Perfilov VA. Disposal of drilling sludge in the production of building materials. *Procedia Eng.* 2015;111:607-611. doi:10.1016/j.proeng.2015.07.053
 46. Nahmad D, Lepe A, Environmental E, Group RAYI, Rasheed R. Treatment of Contaminated Synthetic Based Muds (SBM) Drilling Waste in Block 47 Oman. In: *Abu Dhabi International Petroleum Exhibition and Conference.* Abu Dhabi; 2014:1-15.
 47. Gogan R, Operating KP, Mendalieva DK, Kunasheva ZK. Usage of Oil Based Carbonate Mud Drilling Cuttings Post Thermo-treatment as Secondary Raw Mineral Materials. In: *SPE Annual Caspian Technical Conference and Exhibition.* Astana; 2014:1-6.
 48. Edwan Kardena QH. Petroleum Oil and Gas Industry Waste Treatment; Common Practice in Indonesia. *J Pet Environ Biotechnol.* 2015;06(05). doi:10.4172/2157-7463.1000241
 49. Mostavi E, Asadi S, Ugochukwu E. Feasibility Study of the Potential Use of Drill Cuttings in Concrete. *Procedia Eng.* 2015;118(2):1015-1023. doi:10.1016/j.proeng.2015.08.543
 50. Shon CS, Estakhri CK, Lee D, Zhang D. Evaluating feasibility of modified drilling waste materials in flexible base course construction. *Constr Build Mater.* 2016;116:79-86. doi:10.1016/j.conbuildmat.2016.04.100
 51. Piazza, D., Pelegriani, K., Dra RNB. Recyclability of polypropylene (PP) and polyethylene (PE) waste from the Hawaii coastline. *Int J Waste Resour.* 2017;7(5211). doi:doi.org/10.4172/2252-5211-c1-006
 52. Aeslina AK, Ali B. Petroleum sludge treatment and reuse for cement production as setting retarder. *IOP Conf Ser Mater Sci Eng.* 2017;203(1). doi:10.1088/1757-899X/203/1/012010
 53. Shon CS, Estakhri CK. In-situ and laboratory investigation of modified drilling waste materials applied on base-course construction. *Int J Pavement Res Technol.* 2018;11(3):225-235. doi:10.1016/j.ijprt.2017.11.001
 54. Ayati B, Molineux C, Newport D, Cheeseman C. Manufacture and performance of lightweight aggregate from waste drill cuttings. *J Clean Prod.* 2019;208:252-260. doi:10.1016/j.jclepro.2018.10.134
 55. U.S. Energy Information Administration. *Www.Eia.Gov* [Accessed on 1 Feb. 2019].
 56. British Petroleum. *Statistical Review of World Energy 2018.*; 2018.
 57. Al Naamani, M.: Al Sharafi M. Drilling optimization benchmark set for deep HP/HT wells in Oman. *E&P Mag.* 2013;(1 August 2013).
 58. Al Sharafi M, Al Naamani M, Al Shidhani I, Thani YA, Hariri N. Drilling optimization in deep tight gas field. In: *SPE/IADC Drilling Conference and Exhibition 2013.* Amsterdam; 2013.
 59. Al Salmi A, Al Haji Y, Al-Hamhami S, Sabhi I, Al Fadhli A. New technique to sidetrack across hard formation in north Oman. In: *17th Middle East Oil and Gas Show and Conference 2011.* Manama; 2011.
 60. Sanchez F, Turki M, Nabhani Y, Cruz M, Houqani S. Casing while Drilling (CwD); A new approach drilling FIQA formation in the Sultanate of Oman. A success story. In: *14th Abu Dhabi International Petroleum Exhibition and Conference 2010, ADIPEC 2010.* ; 2010.
 61. Khalil M, Rumhi H, Randrianavony M, Cig K, Mullins OC, Godefroy S. Downhole fluid analysis integrating insitu density and viscosity measurements - Field test from an Oman sandstone formation. In: *14th Abu Dhabi International Petroleum Exhibition and Conference 2010, ADIPEC 2010.* Abu Dhabi; 2014:231-244.
 62. Bernardo G, Marroccoli M, Nobili M, Telesca A, Valenti GL. The use of oil well-derived drilling waste and electric arc furnace slag as alternative raw materials in clinker production. *Resour Conserv Recycl.* 2007;52:95-102. doi:10.1016/j.resconrec.2007.02.004
 63. Scire JS, Escoffier-Czaja C, Phadnis MJ. Application of MM5 and CALPUFF to a complex terrain environment in eastern Iceland. In: *The 11th Harmonization within Atmospheric Dispersion Modeling for Regulatory Purposes, Cambridge, United Kingdom, July 2-5.* Cambridge; 2007.
 64. Scire JS, Robe FR, Strimaitis D. A. User's guide for the CALMET meteorological model (Version 5). 2000.

-
65. Lee H-D, Yoo J-W, Kang M-K, Kang J-S, Jung J-H, Oh K-J. Evaluation of concentrations and source contribution of PM10 and SO2 emitted from industrial complexes in Ulsan, Korea: Interfacing of the WRF-CALPUFF modeling tools. *Atmos Pollut Res.* 2014;5:664-676. doi:10.5094/APR.2014.076
 66. Oman Environmental Services Holding Company (Be'ah). Transformation of waste management in Oman. In: *ISWA Energy Recovery WG Meeting, 25th May 2016, West Palm Beach, Florida. Be'ah; Oman.* ; 2016.
 67. Oil & Gas Journal. Worldwide Look at Reserves and Production. 2017.
 68. Central Bank of Oman. *Annual Report 2017.* Muscat; 2017.
 69. Hatmi Y Al, Tan CS, Badi A Al, Charabi Y. Assessment of the consciousness levels on renewable energy resources in the Sultanate of Oman. *Renew Sustain Energy Rev.* 2014;40:1081-1089. doi:10.1016/j.rser.2014.08.012
 70. Abdul-wahab SA, Charabi Y, Al-rawas GA, Al-maamari R. Greenhouse gas (GHG) emissions in the Sultanate of Oman. 2016;17(4):338-354. doi:10.1002/ghg
 71. Al-Dhamri H, Black L. Use of Oil-Based Mud Cutting waste in Cement Clinker Manufacturing. In: *34th Cement and Concrete Science Conference, 14-17 September 2014, University of Sheffield.* Sheffield; 2014.
 72. Oman Petroleum Development. *Environmental Assessment of Nimr Asset - 2002 Review and Update Petroleum Development Oman.* Muscat; 2002. doi:10.1111/jonm.12011
 73. Al Dhamri HS, Abdul-wahab SA, Velis C, Black L. Oil-based mud cutting as an additional raw material in clinker production. *J Hazard Mater.* 2020;384(121022). doi:org/10.1016/j.jhazmat.2019.121022
 74. Al Dhamri HS, Abdul-wahab SA, Velis C, Black L, G OCCSAO. Oil-based mud cutting as an additional raw material in clinker production. *J Hazard Mater.* 2020;384(121022):1-17. doi:10.1016/j.jhazmat.2019.121022
 75. Chatterjee TK. Clinker grinding and cement making. In: *Cement Production Technology.* 1st ed. Taylor & Francis; 2018:175-212.
 76. Cretaceous TV. Raw materials. In: *Portland Cement.* London: Thomas Telford; 1999:15-29.
 77. Philip A. Alsop. *Cement Plant Operation Handbook.* 3rd Editio. UK: David Hargreaves, Tradeship Publication; 2001. file:///C:/Users/em0899/OneDrive - Oman Cement Company SAOG/Desktop/Officials/cement studies/Books/3. Cement Manufacturing/Cement Plant Operation Hand Book-Phillip/Cement Plant Operation Handbook.pdf.
 78. Alsop PA. *The Cement Plant Operations Handbook.* 3rd Ed. UK: International Cement Review; 2001.
 79. Walter H. Duda. *Cement-Data-Book: International Process Engineering in the Cement Industry.* Wiesbaden: Bauverlag GmbH; 1975.
 80. Basheer PAM, Barbhuiya S. Different types of cement used in concrete. In: *ICE Manual of Construction Materials.* ; 2009:61-68. doi:10.1680/mocm.35973.0061
 81. Galbenis CT, Tsimas S. Use of construction and demolition wastes as raw materials in cement clinker production. *China Particuology.* 2006;4(2):83-85. doi:10.1016/S1672-2515(07)60241-3
 82. Schoon J, De Buysser K, Van Driessche I, De Belie N. Fines extracted from recycled concrete as alternative raw material for Portland cement clinker production. *Cem Concr Compos.* 2015;58:70-80. doi:10.1016/j.cemconcomp.2015.01.003
 83. Aranda Usón A, López-Sabirón AM, Ferreira G, Llera Sastresa E. Uses of alternative fuels and raw materials in the cement industry as sustainable waste management options. *Renew Sustain Energy Rev.* 2013;23:242-260. doi:10.1016/j.rser.2013.02.024
 84. Schepper M De, Buysser K De, Driessche I Van, Belie N De. *The Regeneration of Cement out of Completely Recyclable Concrete: Clinker Production Evaluation.* Vol 38.; 2013. doi:10.1561/22000000016
 85. Shahriar A. Investigation on Rheology of Oil Well Cement Slurries. 2011;(April). <http://ir.lib.uwo.ca/etd>.

86. de Paula JN, Calixto JM, Ladeira LO, et al. Mechanical and rheological behavior of oil-well cement slurries produced with clinker containing carbon nanotubes. *J Pet Sci Eng.* 2014;122:274-279. doi:10.1016/j.petrol.2014.07.020
87. Kuzielová E, Žemlička M, Másilko J, Palou MT. Pore structure development of blended G-oil well cement submitted to hydrothermal curing conditions. *Geothermics.* 2017;68:86-93. doi:10.1016/j.geothermics.2017.03.001
88. Arbelaez C. THE PRODUCTION OF API CLASS H OILWELL CEMENT. file:///C:/Users/em0899/AppData/Local/Mendeley Ltd./Mendeley Desktop/Downloaded/Arbelaez - Unknown - THE PRODUCTION OF API CLASS H OILWELL CEMENT.pdf.
89. American Petroleum Institute. Specification 10A, Specification for Cements and Materials for Well Cementing. 2010.
90. Jackson PJ. Portland Cement: Classification and Manufacture. In: *Lea's Chemistry of Cement and Concrete*. Fourth Edi. Elsevier Ltd.; 2003:25-94. doi:10.1016/B978-075066256-7/50014-X
91. Chatterjee AK. Chemico-Mineralogical Characteristics of Raw Materials. In: GHOSH SNBT-A in CT, ed. *Advances in Cement Technology*. 1st Editio. Pergamon Press; 1983:39-68. doi:https://doi.org/10.1016/B978-0-08-028670-9.50008-9
92. Chatterjee TK. Pyroprocessing and clinker cooling. In: *Cement Production Technology*. 1st ed. Taylor & Francis; 2018:141-173.
93. Bensted J. Special Cements. In: *Lea's Chemistry of Cement and Concrete*. Fourth Edi. Elsevier Ltd.; 2003:783-840. doi:10.1016/B978-075066256-7/50026-6
94. Adamson K, Birch G, Gao E, et al. High-Pressure, High-Temperature Well Construction. *Schlumberger Oilf Rev.* 1998;Summer 199:36-49. http://www.slb.com/resources/publications/industry_articles/oilfield_review/1998/or1998sum03_hpht_wellconstruction.aspx%5Cnhttps://www.slb.com/~media/Files/resources/oilfield_review/ors98/sum98/pgs_36_49.pdf.
95. Al-dhamri HS. Use of kaolin and spent catalyst (Spent Alumina & RFCC from refinery) to substitute Bauxite in the preparation of Portland cement clinker, Sultan Qaboos University, PhD thesis. 2010.
96. AL-Dhamri H, Melghit K, Taha R, Ram G. Utilization of by-product from petroleum refinery in Portland clinker and cement manufacturing. In: *13th International Congress on the Chemistry of Cement.* ; 2011:1-7.
97. Al-Dhamri H, Melghit K. Use of alumina spent catalyst and RFCC wastes from petroleum refinery to substitute bauxite in the preparation of Portland clinker. *J Hazard Mater.* 2010;179(1-3):852-859. doi:10.1016/j.jhazmat.2010.03.083
98. Al-Dhamri HS. Towards Sustainable Production. *World Cem.* February 2012:35-39.
99. Hewlett P. *Lea's Chemistry of Cement and Concrete*. Vol 58.; 2004. doi:10.1016/B978-0-7506-6256-7.50031-X
100. Stutzman P, Heckert A, Tebbe A, Leigh S. Uncertainty in Bogue-calculated phase composition of hydraulic cements. *Cem Concr Res.* 2014;61-62:40-48. doi:10.1016/j.cemconres.2014.03.007
101. Alemayehu F, Omprakash Sahu. Minimization of variation in clinker quality. *Adv Mater.* 2013;2(2):23-28. doi:10.11648/j.am.20130202.12
102. Taylor H. The chemistry of portland cement. *Cem Chem.* 1997:55-87. doi:10.1016/0016-0032(48)90024-6
103. Taylor HFW. Portland cement and its major constituent phases. *Cem Chem.* 1997:1-28.
104. Both D, The S. High-temperature chemistry.
105. Directorate General of Standards & Metrology. *Omani Standard (OS 7/2001)*. Muscat, Oman; 2001.
106. ASTM. ASTM C 150-99a Type I.
107. Kurt E. Peray. *Cement Manufacture Handbook*. New York: Chemical Publishing Co.; 1979.

- file:///C:/Users/em0899/OneDrive - Oman Cement Company
SAOG/Desktop/Officials/cement studies/Books/3. Cement Manufacturing/Cement
Manufacturing Hand Book-Kurt E. Peray/Cement Manufacture Handbook(Kurt E. Peray).pdf.
108. Scrivener K, Snellings R, Lothenbach B. Sample Preparation. In: *A Practical Guide to Microstructural Analysis of Cementitious Materials*. Taylor & Francis; :1-35. doi:10.1007/978-3-540-71951-9_4
 109. *European Standard, EN 196-2, Methods of Testing Cement-Part 2: Chemical Analysis of Cement, Determination of Loss on Ignition.*; 2005.
 110. Chatterjee TK. Burnability and Clinkerization of Cement Raw Mixes. In: GHOSH SNBT-A in CT, ed. Pergamon; 1983:69-113. doi:https://doi.org/10.1016/B978-0-08-028670-9.50009-0
 111. European Standard. *EN 451-1, Methods for Portland Cement Testing, Methods of Testing Fly Ash-Part:1 Determination of Free Calcium Oxide Content.*; 2005.
 112. ASTM International. Extraction of Free Lime in Portland Cement and Clinker by Ethylene Glycol. In: *Rapid Methods for Chemical Analysis of Hydraulic Cement.* ; 1988. doi:10.1520/STP34297S
 113. Delimi R. Determination of Free Lime in Industrial Products. 1991:593-600.
 114. Scrivener K, Bazzoni A, Mota B, John E. Rossen. Electron Microscopy. In: *A Practical Guide to Microstructural Analysis of Cementitious Materials*. Taylor & Francis; 2015:351-417. doi:10.1021/ac60237a015
 115. Lothenbach B, Durdzinski P, Klaartje De Weerd. Thermogravimetric Analysis. In: *A Practical Guide to Microstructural Analysis of Cementitious Materials*. Taylor & Francis; 2015. doi:10.1038/1731011b0
 116. T. K. Chatterjee. Burnability and clinkerization of cement raw-mixes. In: *Cement and Concrete Science and Technology*. New Delhi: ABI Books Pvt. Ltd. India; 1991:10-57.
 117. Galimberti M, Marinoni N, Della Porta G, Marchi M, Dapiaggi M. Effects of limestone petrography and calcite microstructure on OPC clinker raw meals burnability. *Mineral Petrol.* 2017;111(5):793-806. doi:10.1007/s00710-016-0485-8
 118. Al-Maqbali A, Feroz S, Ram G, Hilal Al-Dhamri. Feasibility Study on Spent Pot Lining (SPL) as Raw Material in Cement Manufacture Process. *Int J Environ Chem.* 2016;2(2):18-26.
 119. H. Donald. *Microscopical Examination and Interpretation of Portland Cement and Clinker*. 2nd Editio. (Natalie C. Holz, ed.). Portland Cement Association; 1999.
 120. C1356-07. Standard Test Method for Quantitative Determination of Phases in Portland Cement Clinker by Microscopical Point-Count Procedure. *Annu B ASTM Stand ASTM Int West Conshohocken, PA.* 2007;07(Reapproved 2012):1-6. doi:10.1520/C1356-07.2
 121. Robert E. Carver. *Procedures in Sedimentary Petrology*. California: Wiley-Interscience; 1971.
 122. ASTM. *Petrography of Cementitious Materials: Petrographic Methods for Analysis of Cement Clinker and Concrete Microstructure*. USA; 1994. doi:10.1520/STP1215-EB
 123. ASTM. *C188-16 Standard Test Method for Density of Cement.*; 2016.
 124. European Standard. *EN 196-6, Methods of Testing Cement-Part 6: Determination of Fineness.*; 2005.
 125. European Standard. *EN 196-3, Methods of Testing Cement-Part 3: Determination of Setting Time and Soundness.*; 2005.
 126. European Standard. *EN 196-1, Methods of Testing Cement-Part 1: Determination of Strength.*; 2005.
 127. Wadsö L, Winnefeld F, Riding K, Sandberg P. Calorimetry. In: *A Practical Guide to Microstructural Analysis of Cementitious Materials*. Taylor & Francis; 2015:37-74.
 128. Ayers R. C., Sauer T. C., Anderson R. W. The generic mud concept for NPDES permitting of offshore drilling discharges. *J Pet Technol.* 1985;37:475-480.
 129. Bennett RB. New drilling fluid technology-mineral oil mud. *J Pet Technol.* 1984:975-981.
 130. Yousef K, AlQallaf Y, Fouzy HA. Oil based mud drill cutting (OBM) treatment and management at KOC. *Int J waste Resour Resour.* 2017;7(3):5211. doi:10.4172/2252-5211-C1-006

131. J.E. F, H.L. C. Second generation synthetic fluids in the North Sea: are they better? In: *IAD/SPE Drilling Conference*. New Orleans; 1996.
132. Candler J., Hebert R., A.J. L. Effectiveness of a 10 day ASTM amphipod sediment test to screen drilling mud base fluids for benthic. In: *SPE/EPA Exploration and Production Environmental Conference*. Dallas TX: Society of Petroleum Engineers; 1997.
133. Caenn R, Darley HCH, Gray GR. Drilling and Drilling Fluids Waste Management. In: *Composition and Properties of Drilling and Completion Fluids*. ; 2011:617-654. doi:10.1016/B978-0-12-383858-2.00012-3
134. Caenn R, Darley† HCH, Gray† GR. Drilling Fluid Components. In: *Composition and Properties of Drilling and Completion Fluids*. ; 2017:537-595. doi:10.1016/B978-0-12-804751-4.00013-4
135. Fluids C. Evaluating Drilling Fluid Performance. In: *Composition and Properties of Drilling and Completion Fluids*. 7th ed. Joe Hayton; 2017.
136. Darley HCH, Gray GR. Clay Mineralogy and the Colloid Chemistry of Drilling Fluids. In: *Composition and Properties of Drilling and Completion Fluids*. 7th ed. ; 1988:140-183. doi:10.1016/B978-0-08-050241-0.50008-4
137. Grim Ralph E. *Clay Mineralogy*. 2nd ed. New York, London: McGraw-Hill; 1968.
138. American Petroleum Institute. *API Specification 13A*. Washington D.C.; 1979. www.api.org.
139. Cheatham Jr. JB. Wellbore Stability. In: ; 1984. doi:10.2118/13340-PA
140. Abdou MI, Ahmed HE, Fadel AM. Impact of barite and ilmenite mixture on enhancing the drilling mud weight. *Egypt J Pet*. 2018;27(4):955-967. doi:10.1016/j.ejpe.2018.02.004
141. *Drilling Fluids Manual*. USA; 1998.
142. Peray KE. Chapter4: Chemical and physical properties of materials used in cement manufacturing. In: *Cement Manufacture Handbook*. New York: Chemical Publishing Co. Inc.; 1979. file:///C:/Users/em0899/OneDrive - Oman Cement Company SAOG/Desktop/Officials/cement studies/Books/3. Cement Manufacturing/Cement Manufacturing Hand Book-Kurt E. Peray/Cement Manufacture Handbook(Kurt E. Peray).pdf.
143. MOhamed Al-Bagoury. Chris Steel March. In: *IADC/SPE Drilling Conference and Exhibition*. San Diego, California, USA; 2012:6-8.
144. PDO. *Health, Safety and Environment Guideline - Environmental Assessment GU 195*. Muscat; 2002.
145. PDO. *SP-1009 & SP-1010: Specification for Waste Management*. Muscat; 1995.
146. Deng R, Huang D, Wan J, Xue W, Wen X. Recent advances of biochar materials for typical potentially toxic elements management in aquatic environments : A review. *J Clean Prod*. 2020;255:119523. doi:10.1016/j.jclepro.2019.119523
147. American Petroleum Institute. API E5 Environmental guidance document: waste amangement in exploration and production operations. 1997.
148. Bhatti JI. *Role of Minor Elements in Cement Manufacture and Use.*; 1995.
149. C. David Lawrence. The Constitution and Specification of Portland Cement. In: *Lea's Chemistry of Cement and Concret (4th Edition)*. Fourth Edi. Elsevier Ltd.; 1998:131-193. doi:10.1016/B978-0-7506-6256-7.50016-3
150. Soltan AMM, Kahl WA, Hazem MM, Wendschuh M, Fischer RX. Thermal microstructural changes of grain-supported limestones. *Mineral Petrol*. 2011;103(1-4):9-17. doi:10.1007/s00710-011-0151-0
151. Soltan AM, Kahl W-A, Wendschuh M, Hazem M. Microstructure and reactivity of calcined mud supported limestones. *Miner Process Extr Metall*. 2012;121(1):5-11. doi:10.1179/1743285511Y.0000000024
152. Allegretta I, Pinto D, Eramo G. Effects of grain size on the reactivity of limestone temper in a kaolinitic clay. *Appl Clay Sci*. 2016;126:223-234. doi:10.1016/j.clay.2016.03.020
153. Hills AWD. The mechanism of the thermal decomposition of calcium carbonate. *Chem Eng Sci*. 1968;23(4):297-320. doi:10.1016/0009-2509(68)87002-2
154. Lin S, Kiga T, Wang Y, Nakayama K. Energy analysis of CaCO₃ calcination with CO₂ capture.

- Energy Procedia*. 2011;4:356-361. doi:10.1016/j.egypro.2011.01.062
155. Criado JM, Ortega A. A study of the influence of particle size on the thermal decomposition of CaCO₃ by means of constant rate thermal analysis. *Thermochim Acta*. 1992;195:163-167. doi:10.1016/0040-6031(92)80059-6
 156. Beruto DT, Botter R, Cabella R, Lagazzo A. A consecutive decomposition-sintering dilatometer method to study the effect of limestone impurities on lime microstructure and its water reactivity. *J Eur Ceram Soc*. 2010;30(6):1277-1286. doi:10.1016/j.jeurceramsoc.2009.12.012
 157. Marinoni N, Bernasconi A, Della Porta G, Marchi M, Pavese A. The role of petrography on the thermal decomposition and burnability of limestones used in industrial cement clinker. *Mineral Petrol*. 2015;109(6):719-731. doi:10.1007/s00710-015-0398-y
 158. Dunham RJ. Classification of carbonate rocks according to depositional texture. In: *Classification of Carbonate Rocks*. Am. Assoc. Pet. Geol. Mem.; 1962:108–121.
 159. Embry AF, Klovan JE. A Late Devonian reef tract on northeastern Banks Island, NWT. *Bull Can Pet Geol*. 1971;19(4):730-781. doi:10.5072/PRISM/22817
 160. Lokier SW, Al Junaibi M. The petrographic description of carbonate facies: are we all speaking the same language? *Sedimentology*. 2016;63(7):1843-1885. doi:10.1111/sed.12293
 161. Wright VP. A revised classification of limestones. *Sediment Geol*. 1992;76(3-4):177-185. doi:10.1016/0037-0738(92)90082-3
 162. Scholle PA, Ulmer-Scholle DS. *A Color Guide to the Petrography of Carbonate Rocks: Grains, Textures, Porosity, Diagenesis*. AAPG Memoir; 2003.
 163. Marinoni N, Allevi S, Marchi M, Dapiaggi M. A kinetic study of thermal decomposition of limestone using in situ high temperature X-ray powder diffraction. *J Am Ceram Soc*. 2012;95(8):2491-2498. doi:10.1111/j.1551-2916.2012.05207.x
 164. Escardino A, García-Ten J, Feliu C, Moreno A. Calcium carbonate thermal decomposition in white-body wall tile during firing. I. Kinetic study. *J Eur Ceram Soc*. 2010;30(10):1989-2001. doi:10.1016/j.jeurceramsoc.2010.04.014
 165. Fredrik P. Glasser. The Burning of Portland Cement. In: Hewlett PC, ed. *Lea's Chemistry of Cement and Concrete*. Fourth Edi. Butterworth Heinemann; 1998:195-240. doi:10.1016/B978-0-7506-6256-7.50017-5
 166. Kakali G, Kolovos K, Tsivilis S. Incorporation of minor elements in clinker: their effect on the reactivity of the raw mix and the microstructure of clinker. In: *11th International Congress on the Chemistry of Cement*. Durban, South Africa; 2003:2885-2897.
 167. Kurdowski W. Influence of Minor Components on Hydraulic Activity of Portland Cement Clinker. In: *Congress of Chemistry of Cement*. Moscow; 1974:1-4.
 168. Kolovos K, Tsivilis S, Kakali G. The effect of foreign ions on the reactivity of the CaO-SiO₂-Al₂O₃-Fe₂O₃ system II : Cations. 2001;32:463-469.
 169. De Noirfontaine MN, Tusseau-nenez S, Signes-frehel M, Gasecki G, Girod-labianca C. Effect of Phosphorus Impurity on Tricalcium Silicate T 1 : From Synthesis to Structural Characterization. *J Am Ceram Soc*. 2009;2344:1-8. doi:10.1111/j.1551-2916.2009.03092.x
 170. Stephan D, Mallmann R, Knöfel D, Härdtl R. High intakes of Cr, Ni, and Zn in clinker Part I. Influence on burning process and formation of phases. *Cem Concr Res*. 1999;29(12):1949-1957. doi:10.1016/S0008-8846(99)00195-7
 171. Stephan D, Mallmann R, Knöfel D, Härdtl R. High intakes of Cr, Ni, and Zn in clinker Part II. Influence on the hydration properties. *Cem Concr Res*. 1999;29(12):1959-1967. doi:10.1016/S0008-8846(99)00198-2
 172. Stephan D, Maleki H, Knöfel D, Eber B, Härdtl R. Influence of Cr, Ni, and Zn on the properties of pure clinker phases Part I. C3S. *Cem Concr Res*. 1999;29(4):545-552. doi:10.1016/S0008-8846(99)00009-5
 173. Stephan D, Maleki H, Knöfel D, Eber B, Härdtl R. Influence of Cr, Ni, and Zn on the properties of pure clinker phases Part II. C 3 A and C 4 AF. *Cem Concr Res*. 1999;29:651-657. doi:10.1007/s11595-013-0724-3

-
174. Kolovos K, Tsivilis S, Kakali G. SEM examination of clinkers containing foreign elements. *Cem Concr Compos.* 2005;27(2):163-170. doi:10.1016/j.cemconcomp.2004.02.003
175. Zezulová A, Staněk T, Opravil T. Influence of barium oxide additions on Portland clinker. *Ceram - Silikaty.* 2017;61(1):20-25. doi:10.13168/cs.2016.0055
176. Guo X, Wang S, Lu L, Wang H. Influence of barium oxide on the composition and performance of alite-rich Portland cement. *Adv Cem Res.* 2012;24(3):139-144. doi:10.1680/adcr.10.00033
177. Katyal NK, Ahluwalia SC, Parkash R. Effect of barium on the formation of tricalcium silicate. *Cem Concr Res.* 1999;29(11):1857-1862. doi:10.1016/S0008-8846(99)00172-6
178. Kakali G, Kolovos K, Tsivilis S. Incorporation of minor elements in clinker: their effect on the reactivity of the raw mix and the microstructure of clinker. In: *11th International Congress on the Chemistry of Cement.* Durban, South Africa; 2003:2885-2897.
179. Cohn J. Reactions in solid state. *Cem Rev.* 1948;42:527.
180. Li X, Shen X, Tang M, Li X. Stability of tricalcium silicate and other primary phases in portland cement clinker. *Ind Eng Chem Res.* 2014;53(5):1954-1964. doi:10.1021/ie4034076
181. Ma S, Snellings R, Li X, Shen X, Scrivener KL. Alite-ye'elimité cement: Synthesis and mineralogical analysis. *Cem Concr Res.* 2013;45(1):15-20. doi:10.1016/j.cemconres.2012.10.020
182. Zhang J, Gong C, Wang S, Lu L, Cheng X. Effect of strontium oxide on the formation mechanism of dicalcium silicate with barium oxide and sulfur trioxide. *Adv Cem Res.* 2015;27(7):381-387. doi:10.1680/adcr.14.00021
183. Li X, Xu W, Wang S, Tang M, Shen X. Effect of SO₃ and MgO on Portland cement clinker: Formation of clinker phases and alite polymorphism. *Constr Build Mater.* 2014;58:182-192. doi:10.1016/j.conbuildmat.2014.02.029
184. Christensen NH, F.L. Smidth and Co. Burnability of cement raw mixes at 1400°C II the effect of the fineness. *Cem Concr Res.* 1979;9(3):285-294. doi:10.1016/0008-8846(79)90120-0
185. Wieslaw Kurdowski. Portland Cement Clinker. In: *Cement and Concrete Chemistry.* Poland: Springer; 2014:21-123.
186. Dunstetter F, De Noirfontaine MN, Courtial M. Polymorphism of tricalcium silicate, the major compound of Portland cement clinker: 1. Structural data: Review and unified analysis. *Cem Concr Res.* 2006;36(1):39-53. doi:10.1016/j.cemconres.2004.12.003
187. De Noirfontaine MN, Courtial M, Noirfontaine M De, Dunstetter F, Gasecki G, Signes-Frehel M. Tricalcium silicate Ca₃SiO₅ superstructure analysis: a route towards the structure of the M1 polymorph. *Zeitschrift für Krist.* 2012;227(2):102-112. doi:10.1524/zkri.2011.1425
188. Nicoleau L, Nonat A, Perrey D. The di- and tricalcium silicate dissolutions. *Cem Concr Res.* 2013;47:14-30. doi:10.1016/j.cemconres.2013.01.017
189. Kakali G. Use of secondary mineralizing raw materials in cement production . A case study of a wolframite – stibnite ore. 2005;27:155-161. doi:10.1016/j.cemconcomp.2004.02.037
190. Zapata A, Bosch P. Low temperature preparation of belitic cement clinker. *J Eur Ceram Soc.* 2009;29(10):1879-1885. doi:10.1016/j.jeurceramsoc.2008.11.004
191. BS:EN:413-1:2011. BSI Standards Publication Masonry cement Part 1 : Composition , specifications and conformity criteria. *BSI Stand Publ.* 2011;(November).
192. ASTM International. C 150/ C150M - Standard Specification for Portland Cement. *Annu B ASTM Stand.* 2017;i:1-8. doi:10.1520/C0150
193. Yan M, Deng M, Wang C, Chen Z. Effect of Particle Size of Periclase on the Periclase Hydration and Expansion of Low-Heat Portland Cement Pastes. *Adv Mater Sci Eng.* 2018;2018:1-8. doi:10.1155/2018/1307185
194. Zhang R, Bassim N, Panesar DK. Characterization of Mg components in reactive MgO - Portland cement blends during hydration and carbonation. *J CO₂ Util.* 2018;27(July):518-527. doi:10.1016/j.jcou.2018.08.025
195. Mikhailova O, Yakovlev G, Maeva I, Senkov S. Effect of dolomite limestone powder on the compressive strength of concrete. *Procedia Eng.* 2013;57:775-780.

- doi:10.1016/j.proeng.2013.04.098
196. Ruan S, Unluer C. Comparative life cycle assessment of reactive MgO and Portland cement production. *J Clean Prod.* 2016;137(x):258-273. doi:10.1016/j.jclepro.2016.07.071
 197. Chatterjee TK. Composition and properties of Portland cements. In: *Cement Production Technology*. 1st ed. Taylor & Francis; 2018:213-250.
 198. Taylor H. Properties of Portland clinker and cement. *Cem Chem.* 1997;89-112. doi:10.1680/cc.25929.0004
 199. Midgley H. The minor elements in alite (tricalcium silicate) and belite (dicalcium silicate) from some Portland cement clinkers. In: *5th International Symposium on the Chemistry of Cement*. Tokyo; 1968:226-233.
 200. Dreisler I, Knofel D. Effect of magnesium oxide on the properties of cement. *Zement-Kalk-Gips.* 1982;35:537-550.
 201. GR G, Bayles J. How the cooling process affects the distribution and particle size of periclase crystals. In: *3rd International Conference on Cement Microscopy*. Houston; 1981:89-98.
 202. Nikiforov Y, Zosoulia R. Crystallization of periclase and soundness of cements. In: *The 7th International Congress on the Chemistry of Cement*. Paris; 1980:Theme I, II:1-34-36.
 203. Shondeep L, Sarkar. Effect of blaine fineness reversal on strength and hydration of cement. *Cem Concr Res.* 1990;20:398-406.
 204. Brown P. Hydration of cementitious materials. In: *ICE Manual of Construction Materials.* ; 2009:69-75. doi:10.1680/mocm.35973.0069
 205. Zajac M, Bremseth SK, Whitehead M, Ben Haha M. Effect of $\text{CaMg}(\text{CO}_3)_2$ on hydrate assemblages and mechanical properties of hydrated cement pastes at 40 °c and 60 °c. *Cem Concr Res.* 2014;65:21-29. doi:10.1016/j.cemconres.2014.07.002
 206. Whittaker MJ. The Impact of Slag Composition on the Microstructure of Composite Slag Cements Exposed to Sulfate Attack. *Civ Eng.* 2014;PhD(November). <http://etheses.whiterose.ac.uk/id/eprint/9307>.
 207. Black L, Breen C, Yarwood J, Deng CS, Phipps J, Maitland G. Hydration of tricalcium aluminate (C3A) in the presence and absence of gypsum - Studied by Raman spectroscopy and X-ray diffraction. *J Mater Chem.* 2006;16(13):1263-1272. doi:10.1039/b509904h
 208. Merlini M, Artioli G, Cerulli T, Cella F, Bravo A. Tricalcium aluminate hydration in additivated systems. A crystallographic study by SR-XRPD. *Cem Concr Res.* 2008;38(4):477-486. doi:10.1016/j.cemconres.2007.11.011
 209. Chowanec O. Limestone Addition in Cement. 2012. doi:10.5075/epfl-thesis-5335
 210. Collepari M, Baldini G, Pauri M CM. Tricalcium aluminate hydration in the presence of lime, gypsum or sodium sulphate. *Cem Concr Res.* 1978;8:571-580.
 211. Kuzel HJ PHC. Hydration of C3S in the presence of $\text{Ca}(\text{OH})_2$, $\text{CaSO}_4 \cdot 2\text{H}_2\text{O}$ and CaCO_3 . *Cem Concr Res.* 1991;21:885-895.
 212. Grandet J OJ. Effect of Selected Compounds on Cement Hydration. In: *Proceedings of the 7th International Congress on the Chemistry of Cement*. Paris; 1980:vol. 3: VI1-63.
 213. Odler I. Hydration, Setting and Hardening of Portland Cement. In: *Lea's Chemistry of Cement and Concrete*. Fourth Edi. Elsevier Ltd.; 2003:241-297. doi:10.1016/B978-075066256-7/50018-7
 214. Taylor H. Hydrated aluminate, ferrite and sulfate phases. *Cem Chem.* 1997;2:157-186. doi:10.1680/cc.25929.0006
 215. Lagier F, Kurtis KE. Influence of Portland cement composition on early age reactions with metakaolin. *Cem Concr Res.* 2007;37(10):1411-1417. doi:10.1016/j.cemconres.2007.07.002
 216. Fagerlund G. *Chemically Bound Water as Measure of Degree of Hydration: Method and Potential Errors*. (Report TV. Division of Building Materials, LTH, Lund University.; 2009.
 217. Chayes F. The Theory of Thin-Section Analysis. *J Geol.* 1954;62(1):92-101.
 218. Whittaker M. Relationship between early stage microstructure and long term durability of slag-containing cements. In: Muller HS, Haist M, Acosta F, eds. *The 9th Fib International PhD*

-
- Symposium in Civil Engineering*. Karlsruhe, Germany: Scientific Publishing; 2012:487-492.
219. Oman cement: Setting up of new company. News Bites - Construction. Aug 16 2016. Available from: <http://0-search.proquest.com.wam.leeds.ac.uk/docview/1811542044?accountid=14664>., Bites N. No Title.2016.
220. Ghosh SN, Kamal Kumar. *Modernisation & Technology Upgradation in Cement Plants*. 1st ed. New Delhi: Akademia Books International; 1999.
221. Mouayed Makhlof. *Unlocking Value: Alternative Fuels For Egypt's Cement Industry.*; 2016. <http://alinement.net/home/142?Itemid=35>.
222. Mouayed Makhlof. *Unlocking Value: Alternative Fuels For Egypt's Cement Industry.*; 2016.
223. Locher FW. Cement clinker. In: *Cement-Principles of Production and Use*. 1st ed. Dusseldorf: Verlag Bau+Technik GmbH; 2006:32-88.
224. Telschow S. Clinker Burning Kinetics and Mechanism. 2012. https://orbit.dtu.dk/files/51216918/PhD_thesis_Samira_Telschow..PDF.
225. Abdul-Wahab S, Al-Rawas G, Ali S, Fadlallah S, Al-Dhamri H. Atmospheric dispersion modeling of CO₂ emissions from a cement plant's sources. *Clean Technol Environ Policy*. 2017;19(6):1621-1638. doi:10.1007/s10098-017-1352-y
226. Abdul-Wahab SA, Al-Rawas GA, Ali S, Al-Dhamri H. Assessment of greenhouse CO₂ emissions associated with the cement manufacturing process. *Environ Forensics*. 2016;17(4):338-354. doi:10.1080/15275922.2016.1177752

Appendices

Appendix 1

Percentage mixing of the raw materials for preparation of raw meal

| Raw meal | Limestone | Quartzo-phillite | Kaolin | Iron | OBM cuttings | Total |
|------------------------|-----------|------------------|--------|------|--------------|--------|
| Rm _{Ref.} -0% | 80.90 | 11.35 | 5.65 | 2.10 | - | 100.00 |
| Rm½% | 80.00 | 12.70 | 4.70 | 2.10 | 0.50 | 100.00 |
| Rm1% | 80.00 | 12.70 | 4.20 | 2.10 | 1.00 | 100.00 |
| Rm2% | 80.00 | 12.10 | 3.80 | 2.10 | 2.00 | 100.00 |
| Rm3% | 79.10 | 10.15 | 5.65 | 2.10 | 3.00 | 100.00 |
| Rm5% | 77.25 | 10.00 | 5.65 | 2.10 | 5.00 | 100.00 |
| Rm7% | 76.60 | 10.00 | 4.00 | 2.40 | 7.00 | 100.00 |
| Rm10% | 74.40 | 9.80 | 3.70 | 2.10 | 10.00 | 100.00 |
| Rm12% | 72.60 | 8.60 | 4.70 | 2.10 | 12.00 | 100.00 |
| Rm15% | 70.40 | 8.50 | 4.00 | 2.10 | 15.00 | 100.00 |
| Rm20% | 67.00 | 6.25 | 4.65 | 2.10 | 20.00 | 100.00 |
| Rm30% | 60.00 | 4.50 | 3.40 | 2.10 | 30.00 | 100.00 |
| Rm55% | 43.00 | 0.00 | 0.50 | 1.50 | 55.00 | 100.00 |
| Rm100% | - | - | - | - | 100.00 | 100.00 |

Appendix 2

The clinker prepared chemical analysis and calculated mineral composition

| | CK _{ind} | CK _{Ref.} | CK _{1/2} | CK ₁ | CK ₂ | CK ₃ | CK ₅ | CK ₇ | CK ₁₀ | CK ₁₂ | CK ₁₅ | CK ₂₀ | CK ₃₀ | CK ₅₅ | CK ₁₀₀ |
|--|-------------------|--------------------|-------------------|-----------------|-----------------|-----------------|-----------------|-----------------|------------------|------------------|------------------|------------------|------------------|------------------|-------------------|
| OBM cuttings % | 0 | 0 | 0.5 | 1 | 2 | 3 | 5 | 7 | 10 | 12 | 15 | 20 | 30 | 55 | 100 |
| SiO ₂ | 23.50 | 24.49 | 24.67 | 24.49 | 23.81 | 23.50 | 23.50 | 22.90 | 23.27 | 23.03 | 23.33 | 22.46 | 22.43 | 22.24 | 34.49 |
| Al ₂ O ₃ | 5.82 | 5.51 | 5.55 | 5.32 | 5.82 | 5.82 | 5.82 | 5.30 | 5.27 | 5.76 | 5.59 | 5.95 | 5.74 | 5.21 | 7.82 |
| Fe ₂ O ₃ | 4.71 | 4.77 | 4.79 | 4.77 | 4.71 | 4.71 | 4.71 | 5.01 | 4.71 | 4.74 | 4.77 | 4.75 | 4.78 | 4.19 | 3.88 |
| CaO | 71.08 | 70.40 | 70.66 | 70.91 | 71.08 | 71.08 | 71.08 | 70.86 | 70.51 | 69.93 | 69.57 | 69.07 | 68.07 | 66.01 | 52.55 |
| MgO | 0.62 | 0.65 | 0.67 | 0.68 | 0.62 | 0.62 | 0.62 | 0.84 | 0.92 | 0.97 | 1.06 | 1.18 | 1.48 | 2.20 | 3.66 |
| K ₂ O | 1.31 | 1.30 | 1.31 | 1.31 | 1.31 | 1.31 | 1.31 | 1.28 | 1.27 | 1.25 | 1.23 | 1.21 | 1.15 | 1.03 | 0.68 |
| Na ₂ O | 0.14 | 0.14 | 0.15 | 0.15 | 0.14 | 0.14 | 0.14 | 0.23 | 0.27 | 0.30 | 0.34 | 0.41 | 0.54 | 0.86 | 1.47 |
| LOI | 57.52 | 56.75 | 57.02 | 57.18 | 57.52 | 57.52 | 57.52 | 57.99 | 57.98 | 57.98 | 57.94 | 58.35 | 58.61 | 59.54 | 53.96 |
| LSF | 93.71 | 89.92 | 89.63 | 90.82 | 92.66 | 93.71 | 93.71 | 96.11 | 94.58 | 93.89 | 92.62 | 94.46 | 93.50 | 92.65 | 48.45 |
| SM | 2.23 | 2.38 | 2.39 | 2.43 | 2.26 | 2.23 | 2.23 | 2.22 | 2.33 | 2.19 | 2.25 | 2.10 | 2.13 | 2.36 | 2.95 |
| AM | 1.23 | 1.15 | 1.16 | 1.12 | 1.23 | 1.23 | 1.23 | 1.06 | 1.12 | 1.22 | 1.17 | 1.25 | 1.20 | 1.24 | 2.02 |
| Calculated mineral composition using Bogue equations | | | | | | | | | | | | | | | |
| C ₃ S | 64.56 | 56.23 | 55.65 | 59.47 | 62.21 | 64.56 | 64.56 | 70.77 | 66.87 | 62.84 | 60.02 | 61.73 | 58.47 | 53.92 | 0.00 |
| C ₂ S | 18.67 | 27.80 | 28.73 | 25.36 | 21.32 | 18.67 | 18.67 | 12.26 | 16.27 | 18.62 | 21.60 | 17.83 | 20.21 | 23.08 | <36.63 |
| C ₃ A | 7.44 | 6.53 | 6.60 | 6.04 | 7.44 | 7.44 | 7.44 | 5.56 | 5.99 | 7.25 | 6.74 | 7.74 | 7.12 | 6.72 | 14.16 |
| C ₄ AF | 14.34 | 14.52 | 14.58 | 14.51 | 14.34 | 14.34 | 14.34 | 15.24 | 14.35 | 14.41 | 14.50 | 14.44 | 14.56 | 12.76 | 11.80 |
| LP | 29.61 | 28.85 | 29.03 | 28.33 | 29.61 | 29.61 | 29.61 | 28.99 | 28.37 | 29.93 | 29.60 | 30.79 | 30.62 | 28.69 | 37.41 |

Appendix 3

Free lime content in % (wt./wt.) repeated test of the prepared clinker samples

| | analysis 1 | analysis 2 | analysis 3 | analysis 4 | analysis 5 | analysis 6 | Average |
|--------------------|------------|------------|------------|------------|------------|------------|------------|
| Ck _{ind.} | 0.78 | 0.70 | 0.64 | 0.89 | 0.76 | 0.77 | 0.76 ±0.08 |
| Ck _{Ref.} | 0.31 | 0.71 | 0.64 | 0.28 | 0.22 | 0.54 | 0.45 ±0.21 |
| Ck -12% | 1.10 | 1.20 | 1.01 | 1.05 | 0.76 | 1.30 | 1.07 ±0.18 |
| Ck -55% | 1.33 | 1.29 | 1.47 | 1.96 | 1.75 | 1.41 | 1.54 ±0.26 |

Appendix 4

Burnability test for Raw mix prepared with OBM cuttings

| °C* | RM _{ind} -0% | | | | RM _{Ref} -0% | | | | RM12% | | | |
|-------------|-----------------------|----------|---------|-------|-----------------------|----------|---------|-------|----------|----------|---------|-------|
| | Record-1 | Record-2 | Average | | Record-1 | Record-2 | Average | | Record-1 | Record-2 | Average | |
| 1300 | 11.5 | 12.26 | 11.88 | ±0.54 | 7.95 | 9.13 | 8.54 | ±0.83 | 8.00 | 9.54 | 8.77 | ±1.09 |
| 1350 | 2.77 | 3.25 | 3.01 | ±0.34 | 2.04 | 1.86 | 1.95 | ±0.13 | 3.80 | 3.9 | 3.85 | ±0.07 |
| 1400 | 1.43 | 0.87 | 1.15 | ±0.40 | 1.03 | 0.95 | 0.99 | ±0.06 | 2.33 | 2.59 | 2.46 | ±0.18 |
| 1450 | 0.88 | 0.38 | 0.63 | ±0.35 | 0.60 | 0.40 | 0.50 | ±0.14 | 2.45 | 2.35 | 2.40 | ±0.07 |
| 1500 | 0.25 | 0.13 | 0.19 | ±0.08 | 0.17 | 0.17 | 0.17 | ±0.00 | 1.01 | 1.07 | 1.04 | ±0.04 |

*heating the raw meal for 45 minutes

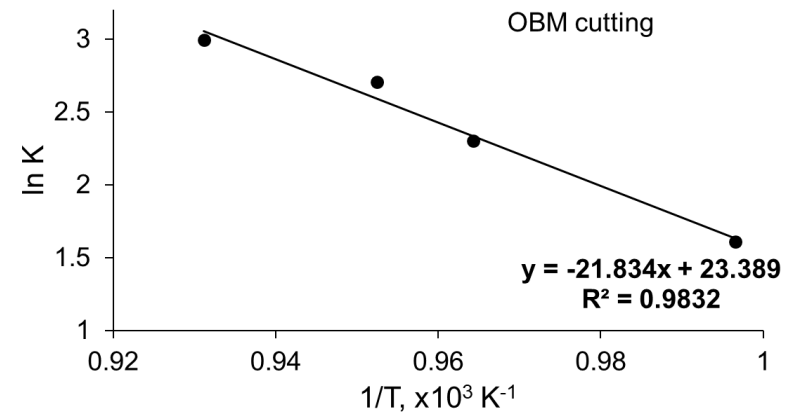
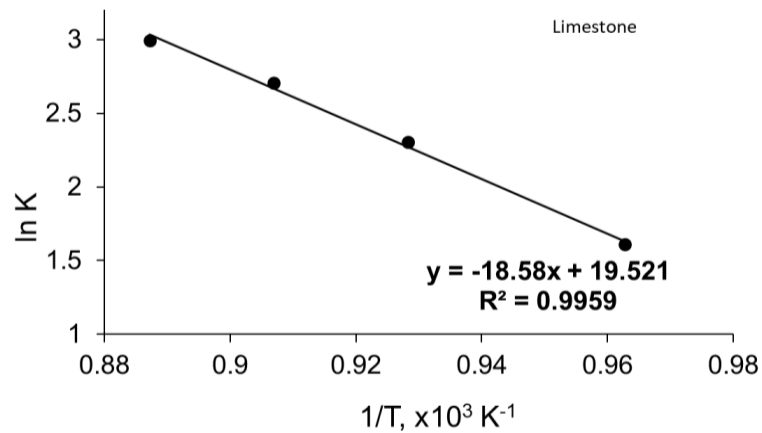
| °C* | RM55% | | | | RM100% | | | |
|-------------|----------|----------|---------|-------|----------|----------|---------|-------|
| | Record-1 | Record-2 | Average | | Record-1 | Record-2 | Average | |
| 1300 | 9.75 | 9.29 | 9.52 | ±0.33 | 0.19 | 0.20 | 0.20 | ±0.01 |
| 1350 | 7.06 | 6.04 | 6.55 | ±0.72 | 0.14 | 0.11 | 0.13 | ±0.02 |
| 1400 | 5.10 | 5.24 | 5.17 | ±0.10 | 0.05 | 0.06 | 0.06 | ±0.01 |
| 1450 | 3.57 | 2.87 | 3.22 | ±0.49 | 0.03 | 0.03 | 0.03 | ±0.00 |
| 1500 | 2.32 | 2.86 | 2.59 | ±0.38 | 0.02 | 0.02 | 0.02 | ±0.00 |

*heating the raw meal for 45 minutes

Appendix 5

Calculations of activation energy of decomposition of limestone and OBM cuttings

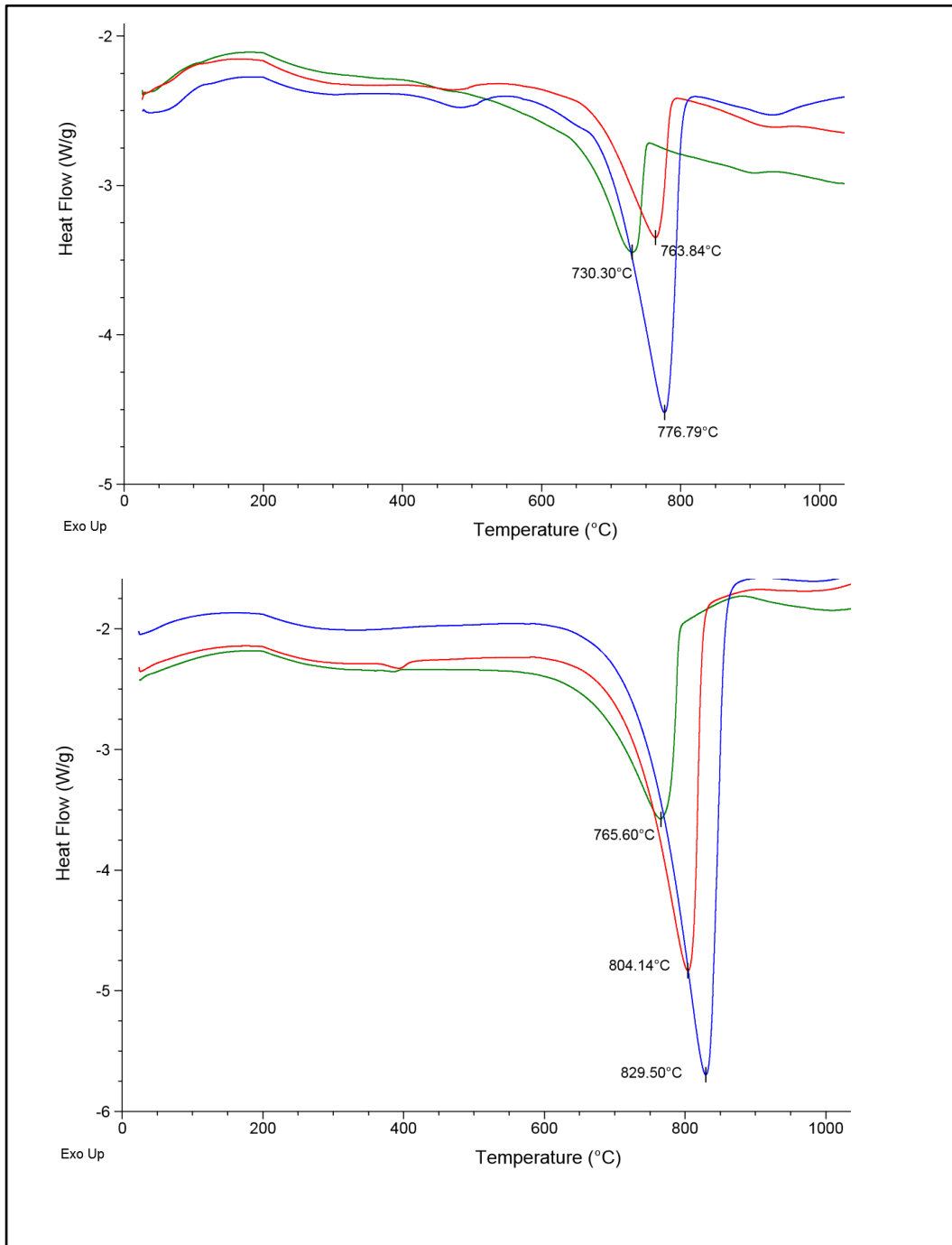
| Temperature (°C/min) | Temperature (K/min) | Temperature (°C) | Temperature (K) | 1/Temperature (K) | 1/Temperature $\times 10^3$ | ln K in °C |
|----------------------|---------------------|------------------|-----------------|-------------------|-----------------------------|------------|
| <u>Limestone</u> | | | | | | |
| 5 | 278.15 | 765.60 | 1038.75 | 0.000962696 | 0.962695548 | 1.609 |
| 10 | 283.15 | 804.14 | 1077.29 | 0.000928255 | 0.928255159 | 2.303 |
| 15 | 288.15 | 829.50 | 1102.65 | 0.000906906 | 0.906906090 | 2.708 |
| 20 | 293.15 | 853.96 | 1127.11 | 0.000887225 | 0.887224849 | 2.996 |
| <u>OBM cuttings</u> | | | | | | |
| 5 | 278.15 | 730.30 | 1003.45 | 0.000996562 | 0.996561862 | 1.609 |
| 10 | 283.15 | 763.84 | 1036.99 | 0.000964329 | 0.964329454 | 2.303 |
| 15 | 288.15 | 776.79 | 1049.94 | 0.000952435 | 0.952435377 | 2.708 |
| 20 | 293.15 | 800.75 | 1273.15 | 0.003660992 | 3.660992129 | 2.996 |



Appendix 6

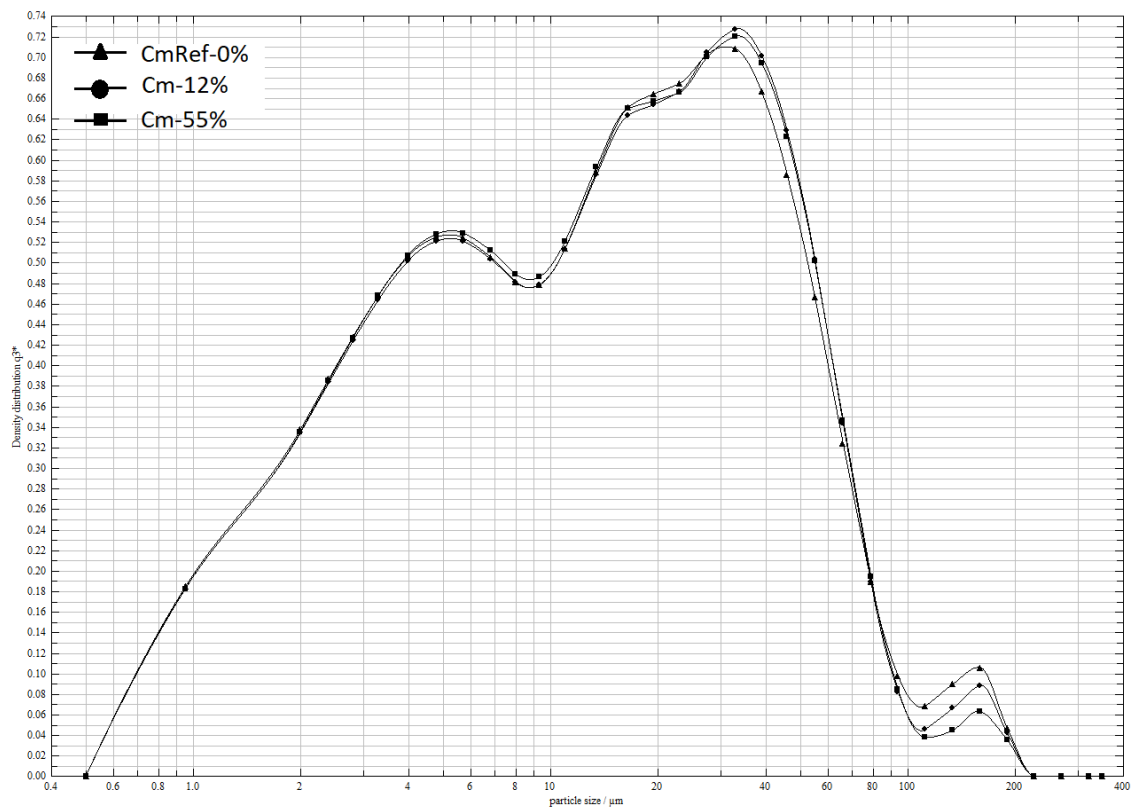
TGA of OBM cuttings and limestone in four different heating rates (5, 10, 15 and 20 °C/mint.)

Top graph: OMB cuttings and below graph: limestone



Appendix 7

Particle size distribution for the cement samples



More particle sizes in the range 100 – 200 μm in the order $Cm_{Ref.} > Cm-12\% > Cm-55\%$.

Appendix 8**Cement density measurement**

Standard test method for density of Cement: ASTM C188-16

| Cm_{ind.} | | | | |
|--------------------------|-----------|-----------|-----------|--------------|
| Test No. | Vi | Vf | Vd | D |
| 1 | 0.300 | 20.700 | 20.400 | 3.137 |
| 2 | 0.400 | 20.900 | 20.500 | 3.122 |
| 3 | 0.800 | 21.200 | 20.400 | 3.137 |
| 4 | 0.000 | 20.400 | 20.400 | 3.137 |
| Average | | | | 3.133 |

| Cm_{Ref.} (zero OBM cutting) | | | | |
|---|-----------|-----------|-----------|--------------|
| Test No. | Vi | Vf | Vd | D |
| 1 | 0.800 | 21.200 | 20.400 | 3.137 |
| 2 | 0.000 | 20.400 | 20.400 | 3.137 |
| 3 | 0.600 | 21.000 | 20.400 | 3.137 |
| 4 | 0.300 | 20.800 | 20.500 | 3.122 |
| Average | | | | 3.133 |

| Cm₁₂ | | | | |
|------------------------|-----------|-----------|-----------|--------------|
| Test No. | Vi | Vf | Vd | D |
| 1 | 0.300 | 20.800 | 20.500 | 3.122 |
| 2 | 0.400 | 20.900 | 20.500 | 3.122 |
| 3 | 0.900 | 21.400 | 20.500 | 3.122 |
| 4 | 0.300 | 20.900 | 20.600 | 3.107 |
| Ave | | | | 3.118 |

| Cm₅₅ | | | | |
|------------------------|-----------|-----------|-----------|--------------|
| Test No. | Vi | Vf | Vd | D |
| 1 | 0.400 | 21.000 | 20.600 | 3.107 |
| 2 | 0.200 | 20.800 | 20.600 | 3.107 |
| 3 | 0.400 | 21.000 | 20.600 | 3.107 |
| 4 | 0.200 | 20.700 | 20.500 | 3.122 |
| Average | | | | 3.111 |

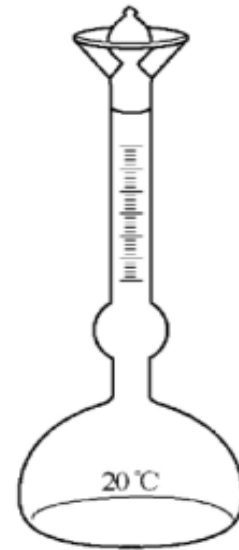
Sample weight = 64 grams

Vi Initial volume in mL

Vf Final volume in mL

Vd (Vf-Vi), Volume displacement in mL

$$D = \frac{\text{Weight of sample in grams}}{Vd}$$



Le Chatelier flask

Density, g/mlCm_{ind.}-0% 3.133 ±0.008Cm_{Ref.}-0% 3.133 ±0.008Cm₁₂% 3.118 ±0.008Cm₅₅% 3.111 ±0.008

Appendix 9

Cement Blaine test measurement

| | | Blaine Fineness, m ² /Kg | | | | | | | |
|------------------------|-------------|-------------------------------------|---------------|---------------|---------------|---------------|---------------|---------|-------|
| | | Analysis 1 | Analysis 2 | Analysis 3 | Analysis 4 | Analysis 5 | Analysis 6 | Average | |
| Cm _{ind.} -0% | Industrial | 319 | 319 | 318 | 320 | 319 | 317 | 319 | ±1.03 |
| Cm _{Ref.} -0% | Zero OBM | 326 | 325 | 323 | 324 | 322 | 327 | 325 | ±1.87 |
| Cm12% | 12 % OBM | 327 | 328 | 329 | 329 | 329 | 329 | 329 | ±0.84 |
| Cm55% | 55 % OBM | 324 | 324 | 324 | 323 | 325 | 325 | 324 | ±0.75 |

Appendix 10

Compressive strength measurement for the cement sample obtained from cement industry Cm_{Ind}

Table 10A For 2 days strength

| | Analysis 1 | Analysis 2 | Analysis 3 | Analysis 4 | Analysis 5 | Analysis 6 | Average | |
|--|------------|------------|------------|------------|------------|------------|---------|-------|
| Machine reading, N | 32.00 | 31.00 | 30.00 | 32.00 | 32.00 | 31.00 | 31.50 | ±0.71 |
| Compressive strength*, N/mm ² | 20.00 | 19.38 | 18.75 | 20.00 | 20.00 | 19.38 | 19.69 | ±0.44 |

Table 10B For 7 days strength

| | Analysis 1 | Analysis 2 | Analysis 3 | Analysis 4 | Analysis 5 | Analysis 6 | Average | |
|--|------------|------------|------------|------------|------------|------------|---------|-------|
| Machine reading, N | 56 | 57 | 54 | 54 | 51 | 50 | 50.50 | ±0.71 |
| Compressive strength*, N/mm ² | 35.00 | 35.63 | 33.75 | 33.75 | 31.88 | 31.25 | 31.56 | ±0.44 |

Table 10C For 28 days strength

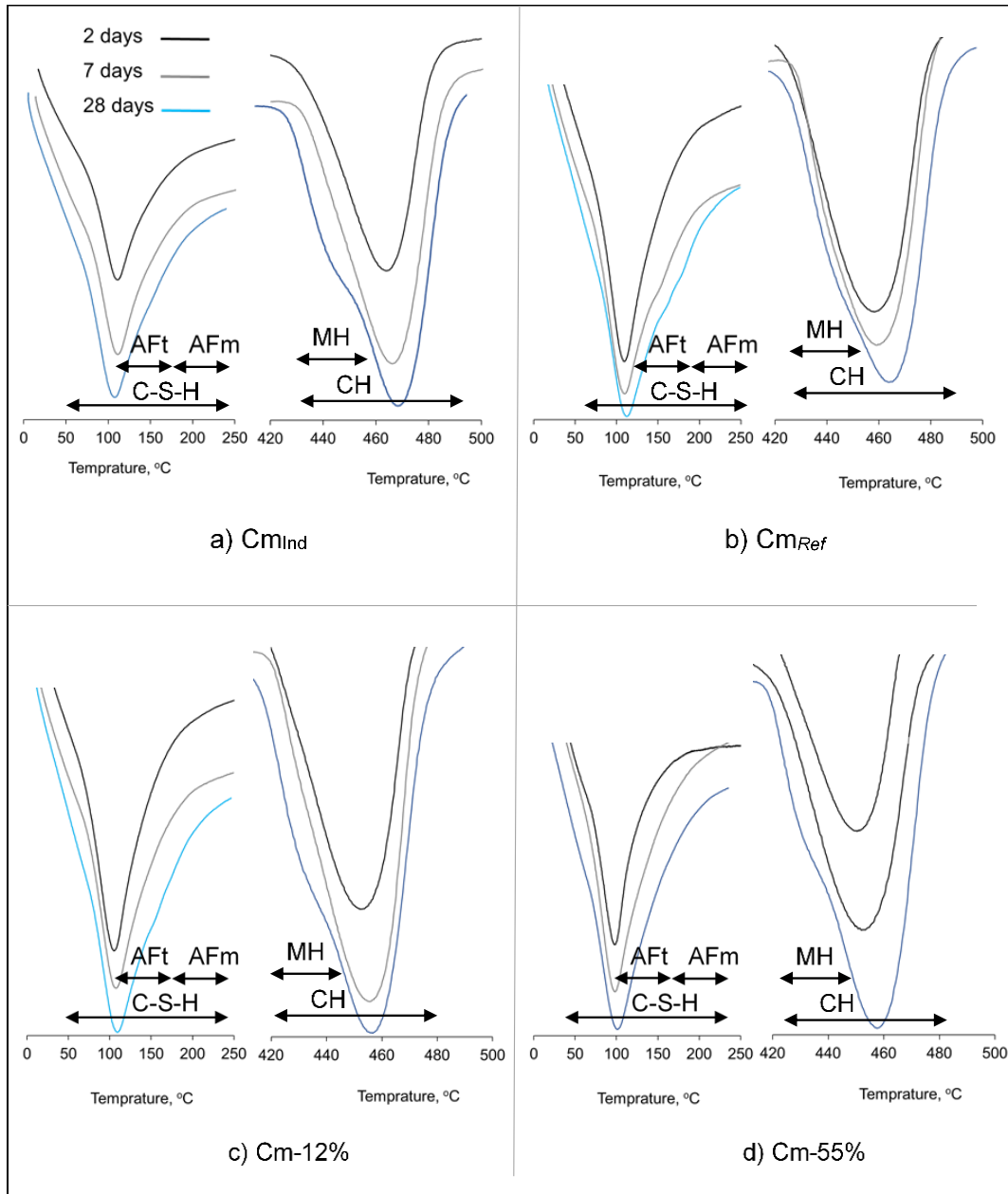
| | Analysis 1 | Analysis 2 | Analysis 3 | Analysis 4 | Analysis 5 | Analysis 6 | Average | |
|--|------------|------------|------------|------------|------------|------------|---------|-------|
| Machine reading, N | 75 | 74 | 75 | 76 | 76 | 75 | 75.67 | ±0.58 |
| Compressive strength*, N/mm ² | 46.88 | 46.25 | 46.88 | 47.50 | 47.50 | 46.88 | 47.29 | ±0.36 |

* Compressive strength calculated as per the equation below:

$$\text{Compressive strength} = \frac{\text{maximum load applied to the cube (N)}}{\text{cube surface area (1.6mm}^2\text{)}}$$

Appendix 11

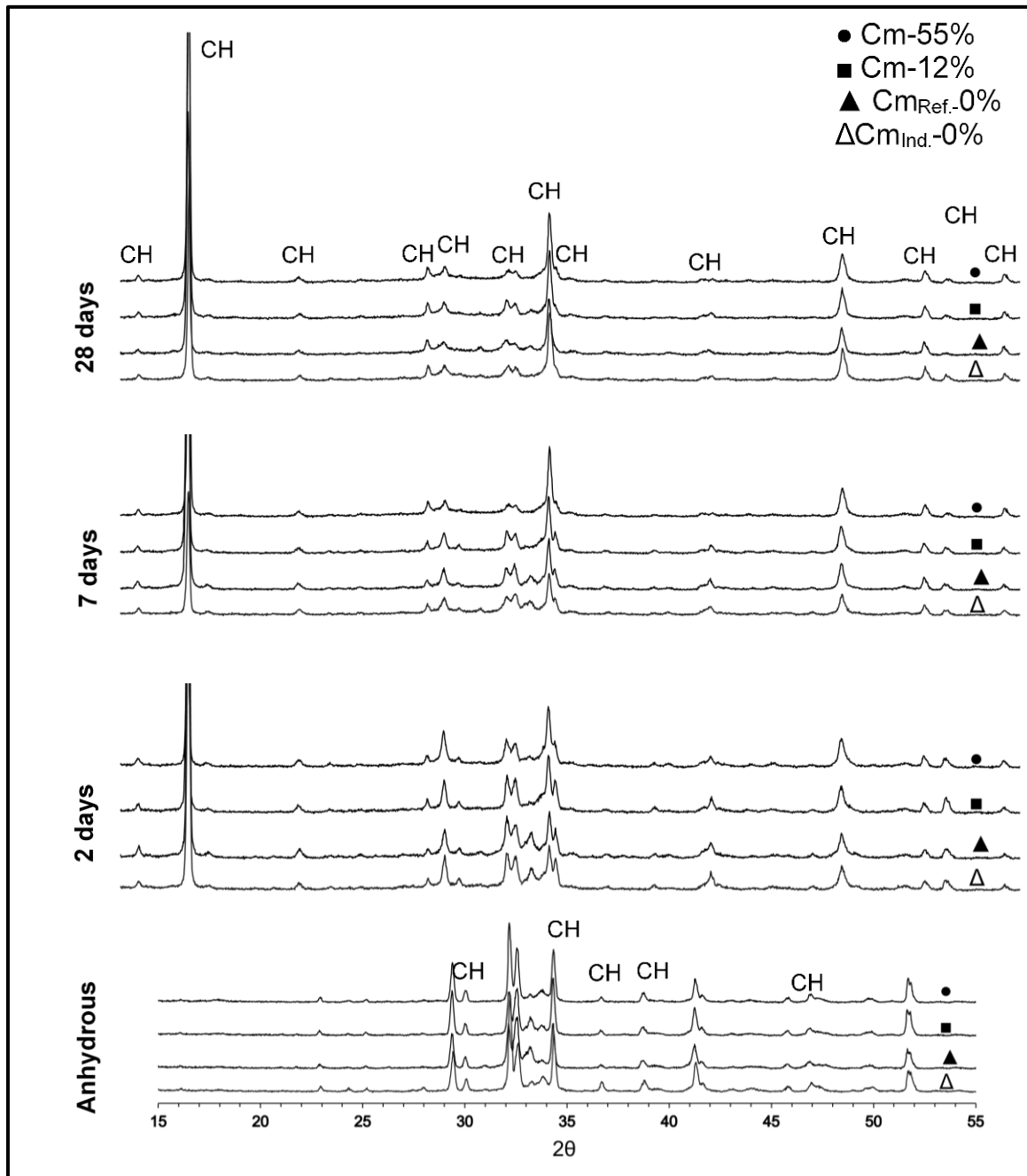
STA analysis of hydrated cement



Appendix 12

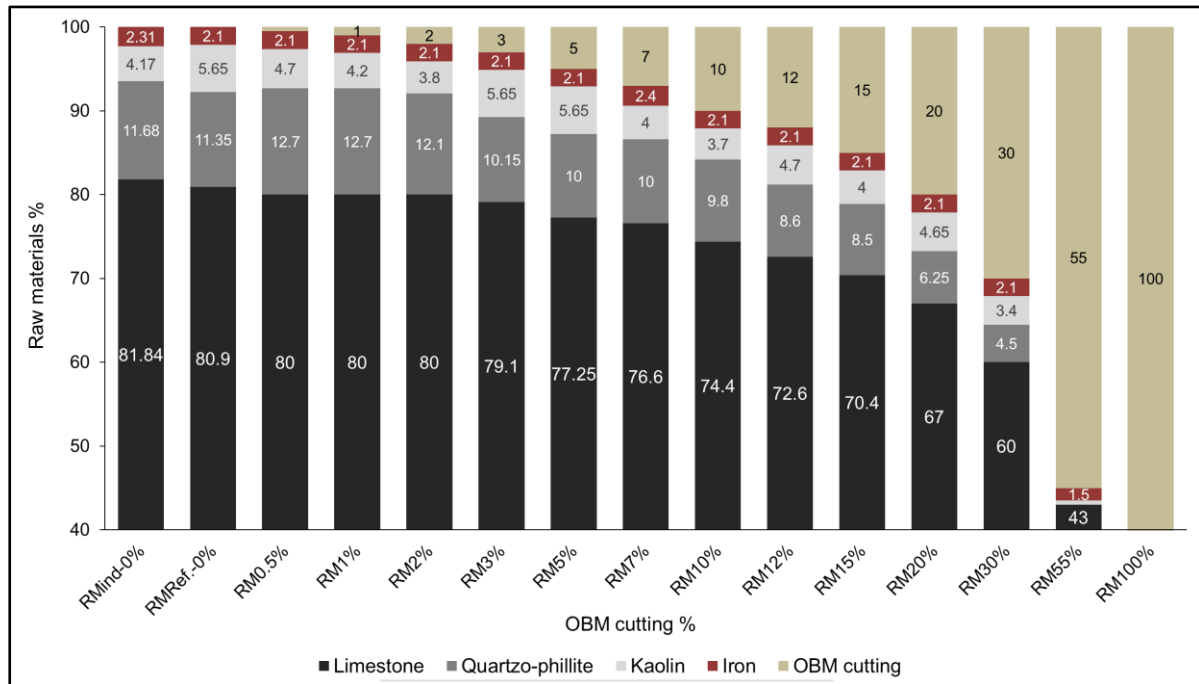
XRD analysis of hydrated cement samples for 2, 7 and 28 days.

(Water ratio 0.45)



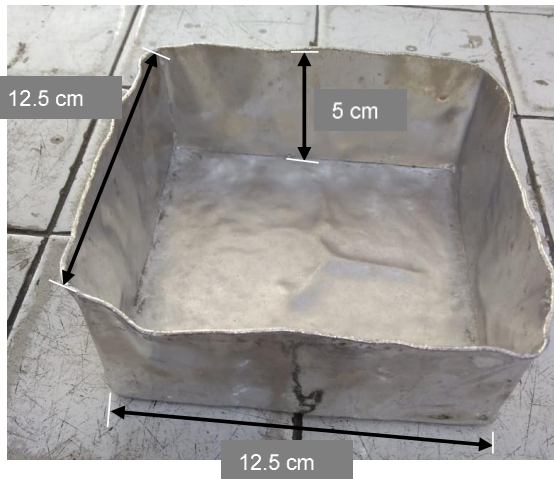
Appendix 13

Raw mix design of the prepared raw meal



Appendix 14A

Clinker preparation in lab

**Platinum container:**

- Dimensions: 12.5 cm x 12.5 cm x 5 cm.
- Thickness: 3 mm.
- Capacity: approximately 1250 gram of raw meal.



Appendix 14B**Clinker preparation in lab**

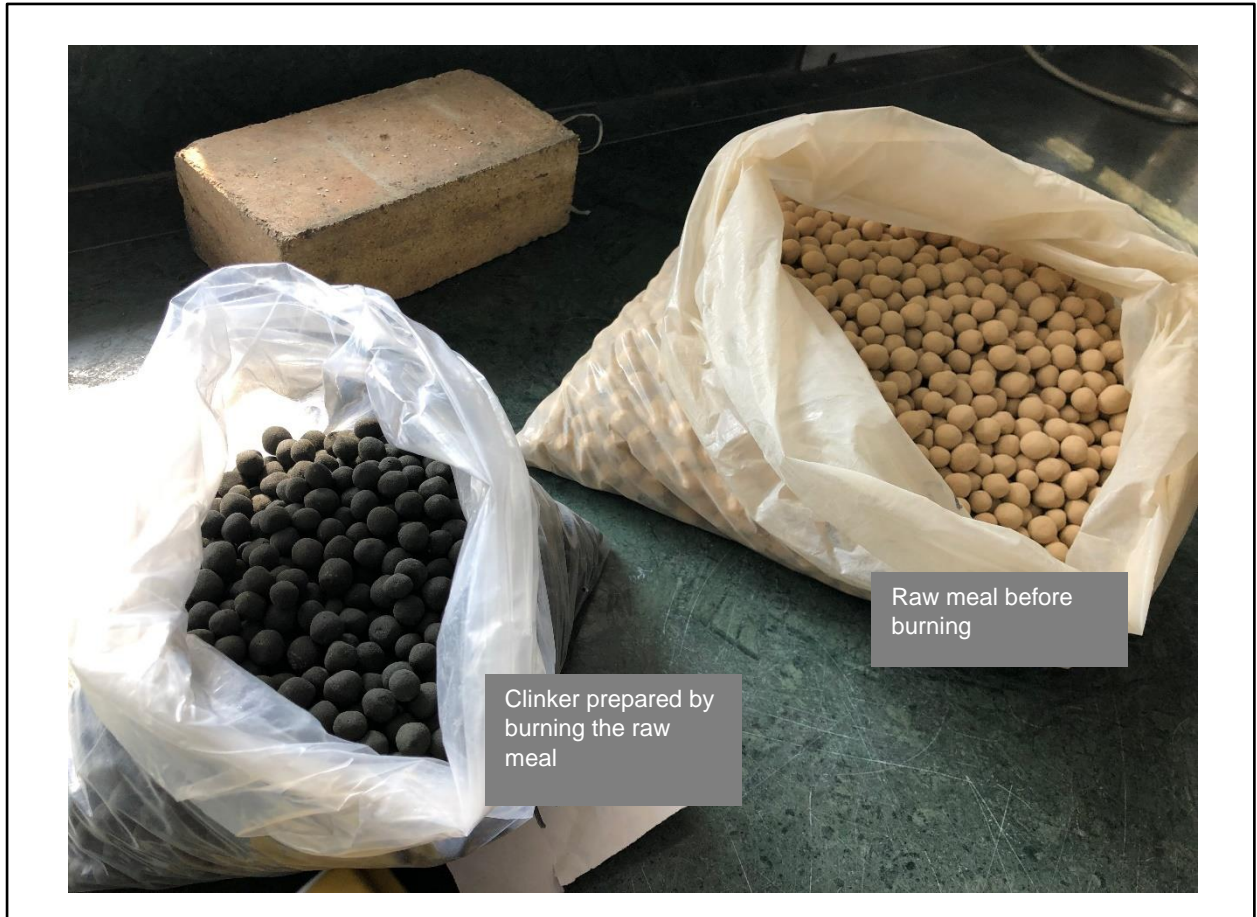
The prepared clinker after burning in the furnace and placed in a tray for cooling under ambient lab temperature.

Safety procurement: Must ware:

- safety google that suitable for watching material at 1450 °C.
- Heat resistance long sleeve gloves.
- Safety shoes.

Appendix 14C

Clinker preparation in lab (continuo)



Appendix 15

Chemical analysis of raw materials

Appendix 15A: Chemical analysis of Quartzo-phillite %wt./wt, (repeated 13 independent samples)

| | Analysis 1 | Analysis 2 | Analysis 3 | Analysis 4 | Analysis 5 | Analysis 6 | Analysis 7 | Analysis 8 | Analysis 9 | Analysis 10 | Analysis 11 | Analysis 12 | Analysis 13 | Average | |
|--------------------------------|------------|------------|------------|------------|------------|------------|------------|------------|------------|-------------|-------------|-------------|-------------|---------|-------|
| SiO ₂ | 81.97 | 74.50 | 68.64 | 71.68 | 81.23 | 69.66 | 82.01 | 74.08 | 71.27 | 74.43 | 75.83 | 71.63 | 68.30 | 74.25 | ±4.84 |
| Al ₂ O ₃ | 3.09 | 5.88 | 6.71 | 6.42 | 4.86 | 6.57 | 4.97 | 5.61 | 6.14 | 5.87 | 4.90 | 5.01 | 5.39 | 5.49 | ±0.97 |
| Fe ₂ O ₃ | 2.62 | 5.79 | 6.65 | 6.28 | 4.48 | 6.92 | 4.61 | 5.41 | 5.93 | 5.55 | 5.12 | 5.93 | 6.56 | 5.53 | ±1.15 |
| CaO | 5.47 | 4.37 | 5.12 | 4.55 | 2.69 | 4.73 | 3.28 | 4.52 | 4.24 | 4.00 | 2.23 | 3.20 | 3.78 | 4.01 | ±0.95 |
| MgO | 3.99 | 3.26 | 3.42 | 3.37 | 2.66 | 3.50 | 2.37 | 3.12 | 3.62 | 3.22 | 6.43 | 6.73 | 7.55 | 4.09 | ±1.67 |
| SO ₃ | 0.02 | 0.02 | 0.05 | 0.02 | 0.02 | 0.03 | 0.02 | 0.02 | 0.03 | 0.04 | 0.02 | 0.03 | 0.02 | 0.03 | ±0.01 |
| Na ₂ O | 0.87 | 1.33 | 1.54 | 1.53 | 1.07 | 1.57 | 1.20 | 1.25 | 1.29 | 1.20 | 1.03 | 0.98 | 1.07 | 1.22 | ±0.22 |
| K ₂ O | 0.18 | 0.70 | 0.75 | 0.76 | 0.71 | 0.62 | 0.59 | 0.71 | 0.76 | 0.76 | 0.80 | 0.77 | 0.75 | 0.68 | ±0.16 |
| Mn ₂ O ₃ | 0.43 | 0.18 | 0.15 | 0.15 | 0.17 | 0.15 | 0.23 | 0.18 | 0.22 | 0.16 | 0.16 | 0.18 | 0.17 | 0.19 | ±0.08 |
| TiO ₂ | 0.27 | 0.56 | 0.64 | 0.61 | 0.40 | 0.65 | 0.45 | 0.53 | 0.57 | 0.54 | 0.42 | 0.50 | 0.55 | 0.51 | ±0.11 |
| LOI @950 | 1.104 | 3.419 | 6.344 | 4.624 | 1.716 | 5.623 | 0.273 | 4.565 | 5.946 | 4.239 | 3.059 | 5.052 | 5.866 | 3.99 | ±1.96 |

Appendix 15B: Chemical analysis of limestone %wt./wt, (repeated 10 independent samples)

| | Analysis 1 | Analysis 2 | Analysis 3 | Analysis 4 | Analysis 5 | Analysis 6 | Analysis 7 | Analysis 8 | Analysis 9 | Analysis 10 | Average | |
|--------------------------------|------------|------------|------------|------------|------------|------------|------------|------------|------------|-------------|---------|-------|
| SiO ₂ | 5.18 | 6.28 | 3.25 | 4.71 | 8.57 | 5.41 | 6.89 | 8.59 | 4.91 | 5.56 | 5.94 | ±1.69 |
| Al ₂ O ₃ | 0.48 | 0.99 | 0.58 | 0.65 | 0.89 | 0.38 | 0.57 | 0.45 | 0.54 | 0.64 | 0.62 | ±0.19 |
| Fe ₂ O ₃ | 0.51 | 0.86 | 0.64 | 0.50 | 0.66 | 0.32 | 0.31 | 0.30 | 0.49 | 0.47 | 0.51 | ±0.18 |
| CaO | 50.97 | 50.10 | 52.05 | 51.55 | 49.05 | 50.70 | 50.84 | 49.97 | 51.92 | 51.47 | 50.86 | ±0.95 |
| MgO | 0.46 | 0.63 | 0.45 | 0.42 | 0.50 | 0.37 | 0.32 | 0.38 | 0.48 | 0.80 | 0.48 | ±0.14 |
| SO ₃ | 0.10 | 0.39 | 0.13 | 0.07 | 0.13 | 0.08 | 0.08 | 0.08 | 0.11 | 0.09 | 0.13 | ±0.10 |
| Na ₂ O | 0.04 | 0.05 | 0.04 | 0.03 | 0.04 | 0.04 | 0.04 | 0.05 | 0.05 | 0.08 | 0.05 | ±0.01 |
| K ₂ O | 0.03 | 0.13 | 0.09 | 0.10 | 0.11 | 0.03 | 0.03 | 0.04 | 0.04 | 0.08 | 0.07 | ±0.04 |
| Mn ₂ O ₃ | 0.02 | 0.02 | 0.02 | 0.02 | 0.02 | 0.02 | 0.02 | 0.02 | 0.02 | 0.02 | 0.02 | ±0.00 |
| TiO ₂ | 0.03 | 0.06 | 0.03 | 0.04 | 0.07 | 0.03 | 0.04 | 0.03 | 0.04 | 0.04 | 0.04 | ±0.01 |
| LOI@950 °C | 42.18 | 40.48 | 42.72 | 41.9 | 39.96 | 42.61 | 40.86 | 40.09 | 41.4 | 40.75 | 41.295 | ±1.02 |

Appendix 15C: Chemical analysis of OBM cutting %wt./wt, (repeated 20 independent samples)

| | Analysis 1 | Analysis 2 | Analysis 3 | Analysis 4 | Analysis 5 | Analysis 6 | Analysis 7 | Analysis 8 | Analysis 9 | Analysis 10 | Analysis 11 | Analysis 12 | Analysis 13 | Analysis 14 | Analysis 15 | Analysis 16 |
|--------------------------------|------------|------------|------------|------------|------------|------------|------------|------------|------------|-------------|-------------|-------------|-------------|-------------|-------------|-------------|
| SiO ₂ | 9.75 | 15.71 | 1.2 | 42.85 | 21.46 | 12.56 | 18.99 | 25.74 | 57.42 | 54.84 | 10.91 | 11.12 | 10.84 | 12.16 | 11.94 | 11.62 |
| Al ₂ O ₃ | 2.45 | 4.58 | 0.57 | 3.17 | 7.65 | 4.56 | 6.25 | 8.83 | 4.02 | 4.27 | 2.59 | 2.51 | 2.52 | 2.59 | 2.65 | 2.6 |
| Fe ₂ O ₃ | 1.42 | 1.8 | 0.72 | 1.13 | 1.45 | 1.02 | 1.69 | 3.55 | 1.52 | 1.67 | 1.62 | 1.71 | 1.68 | 1.65 | 1.91 | 1.81 |
| CaO | 38.74 | 34 | 47.18 | 25.23 | 35.56 | 41.56 | 32.35 | 25.19 | 7.19 | 7.08 | 39.11 | 37.92 | 39.14 | 38.81 | 39.05 | 38.92 |
| MgO | 3.45 | 4.4 | 1.89 | 1.42 | 1.99 | 1.25 | 3.25 | 2.19 | 1.01 | 1.37 | 3.81 | 3.65 | 3.55 | 3.45 | 3.62 | 3.69 |
| SO ₃ | 2.19 | 1.34 | 2.17 | 0.45 | 0.86 | 2.15 | 1.85 | 2.32 | 0.18 | 0.24 | 2.42 | 2.52 | 2.66 | 2.41 | 2.25 | 2.32 |
| Na ₂ O | 0.86 | 0.82 | 0.98 | 0.89 | 0.78 | 0.87 | 0.9 | 0.88 | 2.3 | 1.22 | 0.81 | 0.77 | 0.69 | 0.65 | 0.74 | 0.78 |
| K ₂ O | 0.72 | 0.7 | 0.26 | 0.24 | 0.42 | 0.46 | 0.39 | 0.53 | 0.93 | 0.91 | 0.76 | 0.74 | 0.55 | 0.65 | 0.59 | 0.59 |
| LOI@950 °C | 39.48 | 36.4 | 44.15 | 23.5 | 28.85 | 34.56 | 33.29 | 30.03 | 22.06 | 22.91 | 37.24 | 37.92 | 37.65 | 36.76 | 36.51 | 36.75 |
| H ₂ O | 4.35 | 1.78 | 15.6 | 9.35 | 4.99 | 6.25 | 5.55 | 5.24 | 0.90 | 1.04 | 7.40 | 7.12 | 9.80 | 6.50 | 5.20 | 6.80 |

| | Analysis 17 | Analysis 18 | Analysis 19 | Analysis 20 | Average | |
|--------------------------------|-------------|-------------|-------------|-------------|---------|--------|
| SiO ₂ | 12.49 | 12.35 | 13.01 | 13.12 | 19.00 | ±15.11 |
| Al ₂ O ₃ | 2.65 | 2.55 | 2.71 | 3.42 | 3.66 | ±1.96 |
| Fe ₂ O ₃ | 1.79 | 1.82 | 1.95 | 1.47 | 1.67 | ±0.54 |
| CaO | 38.61 | 38.95 | 39.42 | 37.12 | 34.06 | ±10.47 |
| MgO | 3.58 | 3.66 | 3.78 | 3.77 | 2.94 | ±1.07 |
| SO ₃ | 2.58 | 2.65 | 2.56 | 2.21 | 1.92 | ±0.83 |
| Na ₂ O | 0.7 | 0.68 | 0.87 | 0.68 | 0.89 | ±0.36 |
| K ₂ O | 0.65 | 0.6 | 0.78 | 0.69 | 0.61 | ±0.19 |
| LOI@950 °C | 36.01 | 35.95 | 34.29 | 37.04 | 34.07 | ±5.78 |
| H ₂ O | 5.20 | 5.10 | 6.12 | 4.98 | 5.96 | ±3.23 |

Appendix 15D: Chemical analysis of iron ore %wt./wt, (repeated 11 independent samples)

| | Analysis 1 | Analysis 2 | Analysis 3 | Analysis 4 | Analysis 5 | Analysis 6 | Analysis 7 | Analysis 8 | Analysis 9 | Analysis 10 | Analysis 11 | Average | |
|--------------------------------|------------|------------|------------|------------|------------|------------|------------|------------|------------|-------------|-------------|---------|-------|
| SiO ₂ | 25.91 | 28.44 | 19.54 | 17.46 | 12.24 | 15.89 | 10.21 | 19.43 | 13.23 | 24.39 | 11.61 | 18.03 | ±6.16 |
| Al ₂ O ₃ | 7.10 | 7.57 | 8.60 | 6.93 | 6.57 | 5.64 | 6.75 | 6.24 | 6.54 | 6.81 | 5.96 | 6.79 | ±0.80 |
| Fe ₂ O ₃ | 47.33 | 43.44 | 50.82 | 51.76 | 54.24 | 51.21 | 57.14 | 53.97 | 59.29 | 47.44 | 53.35 | 51.82 | ±4.56 |
| CaO | 2.14 | 1.78 | 1.72 | 1.96 | 1.82 | 2.32 | 1.55 | 1.24 | 1.01 | 2.73 | 1.81 | 1.83 | ±0.48 |
| MgO | 2.75 | 2.59 | 1.91 | 2.15 | 1.47 | 1.53 | 1.26 | 2.05 | 1.32 | 2.29 | 1.39 | 1.88 | ±0.53 |
| SO ₃ | 0.11 | 0.09 | 0.08 | 0.1 | 0.08 | 0.18 | 0.12 | 0.07 | 0.08 | 0.27 | 0.13 | 0.12 | ±0.06 |
| Na ₂ O | 0.42 | 0.44 | 0.38 | 0.36 | 0.34 | 0.34 | 0.32 | 0.37 | 0.31 | 0.44 | 0.32 | 0.37 | ±0.05 |
| K ₂ O | 0.25 | 0.27 | 0.31 | 0.26 | 0.19 | 0.15 | 0.09 | 0.17 | 0.11 | 0.32 | 0.14 | 0.21 | ±0.08 |
| Mn ₂ O ₃ | 0.15 | 0.15 | 0.15 | 0.15 | 0.15 | 0.15 | 0.15 | 0.15 | 0.15 | 0.15 | 0.15 | 0.15 | ±0.00 |
| TiO ₂ | 0.15 | 0.16 | 0.17 | 0.15 | 0.15 | 0.12 | 0.17 | 0.13 | 0.13 | 0.15 | 0.14 | 0.15 | ±0.02 |
| LOI@950 °C | 13.69 | 15.07 | 16.72 | 18.72 | 22.75 | 22.47 | 22.24 | 16.18 | 17.83 | 15.01 | 25.00 | 18.66 | ±3.84 |

Appendix 15E: Chemical analysis of kaolin %wt./wt, (repeated 13 independent samples)

| | Analysis 1 | Analysis 2 | Analysis 3 | Analysis 4 | Analysis 5 | Analysis 6 | Analysis 7 | Analysis 8 | Analysis 9 | Analysis 10 | Analysis 11 | Analysis 12 | Analysis 13 | Average | |
|--------------------------------|------------|------------|------------|------------|------------|------------|------------|------------|------------|-------------|-------------|-------------|-------------|---------|-------|
| SiO ₂ | 42.10 | 40.77 | 42.66 | 41.355 | 42.138 | 42.439 | 42.728 | 42.332 | 41.805 | 42.501 | 42.997 | 42.684 | 42.541 | 42.24 | ±0.61 |
| Al ₂ O ₃ | 33.81 | 32.60 | 32.11 | 33.078 | 33.53 | 32.788 | 34.074 | 33.671 | 33.05 | 32.275 | 32.491 | 33.256 | 32.19 | 33.00 | ±0.65 |
| Fe ₂ O ₃ | 8.35 | 6.95 | 6.186 | 8.598 | 8.016 | 6.755 | 6.453 | 8.011 | 8.267 | 5.789 | 8.39 | 7.71 | 9.51 | 7.61 | ±1.09 |
| CaO | 1.06 | 3.64 | 3.102 | 2.202 | 0.756 | 2.213 | 1.507 | 0.743 | 1.302 | 2.507 | 1.271 | 1.568 | 0.614 | 1.73 | ±0.94 |
| MgO | 0.43 | 0.39 | 0.643 | 0.45 | 0.532 | 0.469 | 0.6 | 0.488 | 0.44 | 0.777 | 0.555 | 0.432 | 0.443 | 0.51 | ±0.11 |
| SO ₃ | 0.06 | 0.06 | 0.15 | 0.075 | 0.083 | 0.117 | 0.173 | 0.126 | 0.11 | 0.207 | 0.078 | 0.051 | 0.032 | 0.10 | ±0.05 |
| Na ₂ O | 0.33 | 0.32 | 0.363 | 0.383 | 0.397 | 0.324 | 0.362 | 0.369 | 0.371 | 0.355 | 0.351 | 0.329 | 0.328 | 0.35 | ±0.02 |
| K ₂ O | 0.18 | 0.17 | 0.217 | 0.187 | 0.182 | 0.186 | 0.203 | 0.185 | 0.186 | 0.195 | 0.193 | 0.19 | 0.192 | 0.19 | ±0.01 |
| LOI | 13.50 | 14.92 | 14.415 | 13.523 | 14.217 | 14.567 | 13.756 | 13.929 | 14.321 | 15.249 | 13.532 | 13.638 | 14.007 | 14.12 | ±0.56 |

Appendix 16

Agreement between Oman Cement Company and OBM cuttings generator company in Oman



Agreement has been sign between Petroleum Development Oman, PDO (OBM cuttings generator) and Oman Cement Company, OCC (OBM cuttings disposer) for conducting a plant pilot trail after considering the results and endorsement obtained in this thesis study.

(Source: <https://www.omandaily.om/?p=708518>)

Phototgraph:

Front left : Musalam Al-Mandhry – Production Chemistry Manager, PDO

Front right: Hilal Al Dhamri – General Manager Manufacturing, OCC

Back from left: Said Al Adwai, Nasser Al-Alwai, Dr. Sultan Al-Shethani, Salim Al-Hajri, Shwket Bahat, Nasser Al Amri.

Appendix 17

Photos for the visit to oil drilling field (Qaran Al-Alam, Oman)



Oil drilling field visit and collection of information about the OBM cuttings at each generation step.

Appendix 18

Published papers, conferences papers and posters

Hilal S. Al Dhamri, Sabah A. Abdul-Wahab, Costas Velis, Leon Black, *Oil-based mud cutting as an additional raw material in clinker production*, *Journal of Hazardous Materials*, Volume 384, 2020, 121022, doi.org/10.1016/j.jhazmat.2019.121022.

Journal of Hazardous Materials 384 (2020) 121022

Contents lists available at [ScienceDirect](https://www.sciencedirect.com)

Journal of Hazardous Materials

journal homepage: www.elsevier.com/locate/jhazmat



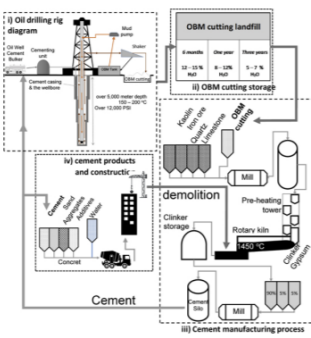

Oil-based mud cutting as an additional raw material in clinker production

Hilal S. Al Dhamri^{a,b,c,*}, Sabah A. Abdul-Wahab^b, Costas Velis^c, Leon Black^c

^a Oman Cement Company S.A.O.G, Muscat, Oman
^b Department of Mechanical and Industrial Engineering, Sultan Qaboos University, Muscat, Oman
^c School of Civil Engineering, University of Leeds, United Kingdom



GRAPHICAL ABSTRACT



ARTICLE INFO

Editor: Deyi Hou

Keywords:
Hazardous waste
Oil-based mud cutting
OBM
Cement
Clinker
Oil well drilling
Alternative raw materials

ABSTRACT

Oil-Based Mud (OBM) cutting is a hazardous by-product generated during oil-well drilling. Its chemical composition suggests that it might be suitable as a raw material in cement manufacturing. It is rich in calcium oxide, silica, and aluminium oxide, which are the major oxides in raw materials for cement manufacturing. In this research, OBM cutting is used as a constituent of the raw meal for cement clinker production. Raw meal mixtures were prepared by mixing different ratios of raw materials increasing OBM content. The impact of the addition of OBM cutting on the resulting clinker has been investigated. The results demonstrate that OBM cutting could be recycled in the manufacturing of Portland cement clinker. Clinker prepared using OBM cutting had very similar properties to that prepared from limestone. This result could represent an opportunity for solving an environmental problem.

The addition of OBM cutting lowers the calcination temperature, and increases the rate of carbonate dissociation. However, it also leads to a higher free lime in clinker, which is a result of the presence of trace elements, such as barium. Overall, its use as a raw material in cement production could provide a cost-effective, environment-friendly route for the management of OBM cutting.

Sabah A. Abdul-Wahab, Hilal Al-Dhamri, Ganesh Ram, Leon Black, *The use of oil-based mud cuttings as an alternative raw material to produce high sulfate-resistant oil well cement*, *Journal of Cleaner Production*, 2020, 122207, doi.org/10.1016/j.jclepro.2020.122207.

Journal of Cleaner Production 269 (2020) 122207



ELSEVIER

Contents lists available at [ScienceDirect](#)

Journal of Cleaner Production

journal homepage: www.elsevier.com/locate/jclepro



The use of oil-based mud cuttings as an alternative raw material to produce high sulfate-resistant oil well cement

Sabah A. Abdul-Wahab ^{a,*}, Hilal Al-Dhamri ^{a,b,c}, Ganesh Ram ^b, Leon Black ^c

^a Department of Mechanical and Industrial Engineering, Sultan Qaboos University, Muscat, Oman
^b Oman Cement Company S.A.O.G, Muscat, Oman
^c School of Civil Engineering, University of Leeds, United Kingdom



ARTICLE INFO

Article history:
 Received 24 December 2019
 Received in revised form 19 March 2020
 Accepted 11 May 2020
 Available online 25 May 2020

Handling Editor: Baoshan Huang

Keywords:
 Thermal analysis
 Mineralizers
 Burnability
 Decarbonation
 Rosin-rammler distribution
 Phase formation

ABSTRACT

Oil-based mud (OBM) is used during the oil well drilling processes to cool drilling pits and remove the cuttings. As a result of these processes, the oil-based mud (OBM) cuttings are produced. The composition of the OBM cuttings depends on the geological conditions of the boreholes and the OBM used during the drilling operation. In this study, the OBM cuttings were used as an alternative material to produce a special cement known as oil-well cement (OWC). Raw meal mixtures were prepared with various percentages of OBM cuttings (5, 11, 13, 15, 18, and 20%). Then they were sintered up to a temperature of 1450 °C, and the resulting cement clinker was ground to produce highly sulfate resistant OWC. The burnability of the raw meal was studied to explore the effect of OBM cuttings on raw meal behavior during the clinkerization process. The results of the study indicated a decrease in the decarbonation temperature and an increase in the rate of clinkerization as the OBM cuttings increased. The produced cement was tested per American Petroleum Institute's testing procedure for OWC. Also, the cement hydration for 2, 7 and 28 days was carried out to study the behavior of the produced OWC.

© 2020 Elsevier Ltd. All rights reserved.

1. Introduction

Amongst the world's major industries, the petroleum and gas industry plays a vital role in fulfilling global energy demand, with oil and gas providing, respectively, for 31% and 23% of the total global energy supply in 2018 (The International Energy Agency, 2019). The Sultanate of Oman contributed around 1% of the world's total oil production for 2018, producing on average 978,000 barrels per day with a growth of 0.8% from 2017 (BP Statistical Review of World Energy, 2019). The production of oil and gas results in the co-production of waste materials, some of which are environmentally hazardous. The predominant waste is drill cuttings, comprising soil cuttings mixed with oil-based drilling fluids, generally referred to as oil-based (OBM) cuttings (Siddique et al., 2017). These OBM cuttings are considered potentially hazardous for the surrounding environment due to the presence of hydrocarbons and their chemical composition (Davies et al., 1984). The inorganic chemical composition of these OBM cuttings is

predominantly defined by the geology around the well (Abdul-Wahab et al., 2016) while the cuttings may also contain 6–17 wt% of diesel oil, which adheres to the cuttings (Dow et al., 1990). Discharge-related pollutants, like hydrocarbons and heavy metals within the cuttings, may have both acute and chronic toxicological effects through post-sedimentary migration of contaminants within the sediment or leakage into the areas surrounding the drilling site (Allers et al., 2013). Waste cuttings can also spread by air, although this type of dissemination is greatly influenced by the cuttings' particle size, which can range from 2 to 275 μm (Al-Dhamri et al., 2019a).

In Oman, most oil exploration sites are on top of limestone deposits (Al-Dhamri et al., 2019b). The OBM cuttings from Oman's PDO sites located at Qarn-Alam and Fahud contain calcium carbonate, which is the main raw material for cement production. So, along with the calorific content of the oil and drilling fluids, this calcium-rich waste material could be utilized as a raw material in cement production. Furthermore, as the cement manufacturing process involves a high-temperature pyro-process, the addition of hazardous industrial wastes like OBM cuttings is a viable and safe way to dispose of such material (Van Oss and Padovani, 2002). This study focuses on the utilization of these

* Corresponding author.
 E-mail address: sabah1@sq.edu.om (S.A. Abdul-Wahab).

<https://doi.org/10.1016/j.jclepro.2020.122207>
 0959-6526/© 2020 Elsevier Ltd. All rights reserved.

Hilal Al-Dhamri, Sabah A. Abdul-Wahab, Ganesh Ram, Abdulaziz Al-Moqbali, Leon Black
“Microstructure of Clinker prepared using different ratio of OBM cutting as raw material”
Proceedings of the 15th International Congress of the Chemistry of Cement, Prague September
2019.



15th International Congress on the Chemistry of Cement
Prague, Czech Republic, September 16–20, 2019

Microstructure of Clinker prepared using different ratio of OBM cutting as raw material

Hilal Al Dhamri^{1,a}, Sabah Abdul-Wahab^{2,b}, Ganesh Ram^{3,c}, Abdulaziz Al-Moqbali^{3,d},
Leon Black^{1,e}

¹Civil Engineering, University of Leeds, Leeds, United Kingdom

²Sultan Qaboos Univeristy, Muscat, Oman

³Oman Cement Company, Muscat, Oman

^acnhsad@leeds.ac.uk

^bsabah1@squ.edu.om

^cganeshram@omacement.com

^dabdulazizalmoqbali@omacement.com

^el.black@leeds.ac.uk

ABSTRACT

Oil-Based Mud (OBM) cutting is a waste that generated by the oil drilling companies during the crude oil drilling. Furthermore, OBM cutting is classified as a hazardous waste because it contains industrial lubricant oil, heavy metals and some organic compounds. In Oman, the options for the treatment of OBM cutting waste are very limited, and they are often simply stored in special storage specification which is enforced by the environmental authority in Oman. The mineralogical composition of OBM cutting, plus the presence of organic residues from the crude oil make it a possible material to be used as additives in cement clinker production. The chemical compounds such as calcium, silica and alumina contents are of the basic raw material composition in cement manufacturing. Also some trace elements could be of useful in enhancing the reaction of clinkerization.

In this research, OBM cutting has been used as a raw materials in the preparation of the cement clinker. It is calcined at 650 oC and burned gradually up to a temperature of 1450 oC in a laboratory furnace to produce Portland cement clinker. Clinker samples were then prepared by using different levels of OBM cutting waste (from zero to 55% weight by weight). XRD has been used to examine the mineralogy, while SEM-EDX has been used to determine the trace elements from the OBM present in clinker phases. Furthermore, the raw meal was characterized using differential thermal analysis to study the effect of present of OBM minerals in clinker chemistry.

Hilal Al-Dhamri, Leon Black, Sabah A. Abdul-Wahab, "Oil-Based Mud Cutting as an Additional Raw Materials in Clinker Production: The Impact on Phase Composition", Proceedings of the 14th International Congress of the Chemistry of Cement, Beijing 2015.

14th International Congress on the Chemistry of Cement, Beijing, China, October 13–16, 2015

Oil-Based Mud Cutting as an Additional Raw Material in Clinker Production: The Impact on Phase Composition

Hilal Al-Dhamri^{1,2*}, Leon Black², Sabah A. Abdul-Wahab³

¹Oman Cement Company S.A.O.G, Muscat, Sultanate of Oman

²School of Civil Engineering, University of Leeds, UK

³Department of Mechanical and Industrial Engineering, Sultan Qaboos University, Sultanate of Oman

Abstract

Oil-Based Mud (OBM) cutting waste, generated by the petroleum and drilling companies during the process of crude oil drilling, is a common waste generated across many of the Arabian Gulf countries. Currently the options for the treatment of OBM cutting waste are very limited, and they are often simply stored in a lined pit, awaiting further treatment. In addition, OBM cutting is classified as a hazardous waste, and therefore the Government of Oman is keen to find a suitable waste management solution for this industrial waste. However, the mineralogical composition of OBM cutting, plus the presence of organic residues from the crude oil make it a possible candidate to be used during cement clinker production.

In this study, OBM cutting has been added, as received, to the raw meal of a cement plant. It is calcined at 650 °C and burned gradually up to a temperature of 1450 °C in a laboratory furnace to produce Portland cement clinker. Eleven clinker samples were then prepared by using different levels of OBM cutting waste (zero: reference sample, 1.0, 2.0, 3.0, 5.0, 7.0, 15.0 and 30.0 %). The potential for incorporation in clinker has then been assessed by a range of techniques. Powder X-ray Diffraction (XRD) has been used to examine the mineralogy, while Scanning Electron Microscopy (SEM) has been used to examine the clinker microstructure to determine the fractionation of trace elements from the OBM in each clinker phase. The free lime in the prepared samples was found to fall within a range of 2.0% to 2.88 %. The XRD pattern showed some slight differences in the phases formed in the clinker as the OBM content increased. However, the main clinker phases were found to be formed in all clinker samples. The initial results concluded that OBM cutting waste may be successfully used during the production of Portland cement clinker. Subsequent work is recommended to examine the hydration behavior of each phase within the clinker to further examine the effects of OBM addition.

H. Saif Al-Dhamri and Leon Black "Use of Oil-Based Mud Cutting Waste in Cement Clinker Manufacturing" In: Bernal, SA and Provis, JL, (eds.) 34th Cement and Concrete Science Conference, 14-17 Sep 2014, Sheffield, UK., pp. 427-430, 2014.

34th Cement and Concrete Science Conference
14-17 September 2014
University of Sheffield

Paper Number 212

Use of Oil-Based Mud Cutting waste in Cement Clinker Manufacturing

Hilal Saif Al-Dhamri^{1,2}, Leon Black²

hilalsr@omancement.com, l.black@leeds.ac.uk

¹ Oman Cement Company SAOG, Muscat, Oman

² Institute for Resilient Infrastructure, School of Civil Engineering, University of Leeds, Leeds, LS2 9JT

ABSTRACT

Oil-Based Mud (OBM) cutting waste is generated during the process of oil well drilling. The drilled rocks are removed from deep within the drilled well and pumped to the surface. The portion removed, known as "Cutting", is a mixture of rocks, mud, water and oil. Most drilling companies store this waste in open yards with no specific treatment solution. The environmental regulations in Oman specify that storage should involve isolation, to prevent penetration of the contamination to surface and underground water. This has made the OBM waste an environmental problem, with an associated cost for oil companies. OBM chemical analysis shows an interesting composition that may be used in cement manufacture. It has high calcium, silicon and aluminum contents, which are the major oxides in cement manufacture. Also the oil contents are useful for reducing the fuel used during the calcining and clinkerization process. In this research, the OBM waste has been analysed and used as a constituent of the raw meal for cement clinker production. The impact of OBM addition on the resultant clinker has also been investigated.

1. INTRODUCTION

Oil-Based Mud cutting, OBM, is a waste generated during the process of drilling an oil well. The drilled rocks are removed from deep within the drilled well and pumped to the surface in circulation. The portion removed, known as "Cutting", is a mixture of rocks, mud, water and oil. Most drilling companies store this waste in open yards with no specific treatment solution [1]. The environmental regulations in Oman specify that the storage should involve isolation to prevent penetration of the contamination to underground water. This has made the OBM waste an environmental problem with an associated cost for oil field companies in Oman. There is about 150,000 tons of OBM stored in specially constructed yards, with costly monitoring programs [2].

Valorisation of this waste material offers financial as well as environmental benefits. OBM chemical analysis shows a composition which may be applicable for use in the manufacture of cement. The mineral components are rich in calcium, silica and alumina; which are the major oxides used in cement manufacture. Also the oil contents are useful for reducing the fuel used during the calcining and clinkerization processes.

There are three stages to the storage of OBM waste produced from the oil drilling operation, based on the oil and water content. During the initial stage, immediately after extraction from the ground, the material is fluid and has a high moisture content. These wastes are transported direct to the storage yard (Fig. 1).



Figure 1. The storage facility of OBM cutting waste. The figure shows OBM three days after extraction during the oil drilling operation. The high oil content of the OBM is clearly evident.



Oil-Based Mud Cutting as an Additional Raw Material in Clinker Production: The Impact on Phase Composition

Hilal Al-Dhamri^{1,2*}, Leon Black², Sabah A. Abdul-Wahab³

¹Oman Cement Company S.A.O.G, Muscat, Sultanate of Oman

²School of Civil Engineering, University of Leeds, UK

³Department of Mechanical and Industrial Engineering, Sultan Qaboos University, Sultanate of Oman

Introduction

Oil-Based Mud (OBM) cutting waste, generated by the petroleum and drilling companies during the process of crude oil drilling, is a common waste generated across many of the Arabian Gulf countries. Currently the options for the treatment of OBM cutting waste are very limited, and they are often simply stored in a lined pit, awaiting further treatment. In addition, OBM cutting is classified as a hazardous waste, and therefore the Government of Oman is keen to find a suitable waste management solution for this industrial waste. However, the mineralogical composition of OBM cutting, plus the presence of organic residues from the crude oil make it a possible candidate to be used during cement clinker production.

In this study, OBM cutting has been added, as received, to the raw meal of a cement plant. It is calcined at 650 °C and burned gradually up to a temperature of 1450 °C in a laboratory furnace to produce Portland cement clinker. Eleven clinker samples were then prepared by using different levels of OBM cutting waste (zero: reference sample, 1.0, 2.0, 3.0, 5.0, 7.0, 15.0 and 30.0 %). The potential for incorporation in clinker has then been assessed by a range of techniques. Powder X-ray Diffraction (XRD) has been used to examine the mineralogy, while Scanning Electron Microscopy (SEM) has been used to examine the clinker microstructure to determine the fractionation of trace elements from the OBM in each clinker phase. The free lime in the prepared samples was found to fall within a range of 2.0% to 2.88 %. The XRD pattern showed some slight differences in the phases formed in the clinker as the OBM content increased. However, the main clinker phases were found to be formed in all clinker samples. The initial results concluded that OBM cutting waste may be successfully used during the production of Portland cement clinker. Subsequent work is recommended to examine the hydration behavior of each phase within the clinker to further examine the effects of OBM addition.

Results

In all samples, the results obtained, although the free lime contained is affected by the OBM added, are still showing major clinker phases as C₂S, C₃S, C₃A and C₄AF as indicated in figure 1. In all clinker samples, the free lime was detected in relatively high concentrations which are shown in Table 2. Specifically, the free lime concentration in reference sample and sample number 6 (OBM 7%) is the highest. In fact, it is expected that the clinker prepared at the laboratory is higher in free lime compared with the clinker prepared in rotary kiln. The clinker prepared in the laboratory is stationary, unlike the rotational movement in rotary kiln.

Figure 1 is showing the microstructure micrograph for the prepared clinker samples analyzed using Scanning Electron Microscope (SEM). The belite crystals appeared round shape with sizes range from 24.9 μm to 31.7 μm (Figure 1). It can be observed that the size of belite crystals relatively bigger than alite crystals in samples 2, 5 and 7 (Figure 1: b, e and j). The alite phase in clinker sample 4 is showing angular alite shape with relatively high concentration of liquid phase compared to the other samples. Furthermore, Figure 1e shows the belite crystals in higher concentrations compared with other samples, specifically to clinker samples 3 and 4 (Figure 1c and 1d). Those two samples 3 and 4 are the least free lime content of 1.26 and 2.26 % respectively. Thus suggesting that all uncombined CaO are consumed during the clinkerization reaction to form the alite which may attributed to the easy burning and optimized raw meal chemistry in these two samples. However, there are variation in the free lime content between the clinker samples, especially the reference sample 1 and sample 6 are the highest.

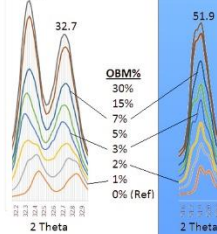


Figure 3: The XRD patterns in the range 32-33 and 51-52 2theta

According to Taylor, alite phase modification type is could be obtained by the XRD spectra intensities at the range between 51 to 52.5 °2θ. The monoclinic polymorph M₂ is indicated by observing two similar intensities in this range. However, higher intensity of the first peak indicates the presence of the monoclinic polymorph M₁ as shown in figure 3a. Thus, the XRD patterns of samples 2,3,4,5 and 6 are indicating that those samples have a combination of both polymorph M₁ and M₂. Where, on the other hand sample 1, 7 and 8 are properly monoclinic Alite M₁.

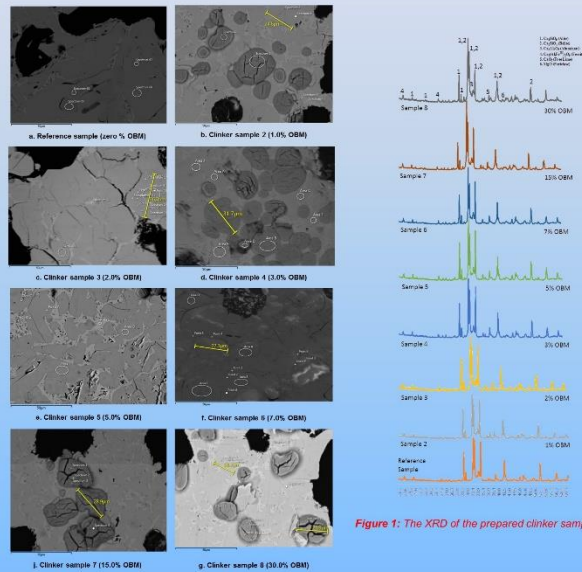


Figure 1: The XRD of the prepared clinker samples

Figure 2: The SEM micrographs of the clinker samples

Table 1: The Chemical analysis of the raw meals used to prepare the Clinker samples

| Chemical Analysis | 1 Ref | Raw meals samples prepared with different OBM % | | | | | | | |
|--------------------------------|-------|---|-------|-------|-------|-------|-------|-------|-------|
| | | 2 | 3 | 4 | 5 | 6 | 7 | 8 | |
| Oxides | | | | | | | | | |
| OBM % | 0.0 | 1.0 | 2.0 | 3.0 | 5.0 | 7.0 | 15.0 | 30.0 | |
| SiO ₂ | 25.9 | 15.06 | 13.66 | 13.7 | 13.82 | 13.88 | 14.02 | 14.17 | 14.76 |
| Al ₂ O ₃ | 4.74 | 3.01 | 3.01 | 3.03 | 3.04 | 3.08 | 3.10 | 3.13 | 3.27 |
| Fe ₂ O ₃ | 2.55 | 2.71 | 2.71 | 2.71 | 2.70 | 2.75 | 2.69 | 2.68 | 2.60 |
| CaO | 31.05 | 43.58 | 43.35 | 43.24 | 43.12 | 43.21 | 42.76 | 42.95 | 41.63 |
| MgO | 2.22 | 0.86 | 0.85 | 0.87 | 0.89 | 0.93 | 0.93 | 0.95 | 1.05 |
| SO ₃ | 1.81 | 0.12 | 0.12 | 0.14 | 0.15 | 0.17 | 0.20 | 0.24 | 0.37 |
| Na ₂ O | 0.89 | 0.06 | 0.06 | 0.09 | 0.10 | 0.10 | 0.12 | 0.14 | 0.20 |
| K ₂ O | 0.41 | 0.24 | 0.24 | 0.24 | 0.24 | 0.25 | 0.25 | 0.25 | 0.27 |
| LOI @ 950 °C | 32.7 | 30.21 | 30.21 | 30.14 | 30.08 | 30.01 | 30.88 | 30.75 | 30.25 |

Figure 2: Free Lime concentrations of the prepared clinker

| Sample No. | 1 | 2 | 3 | 4 | 5 | 6 | 7 | 8 |
|----------------|------|------|------|------|------|------|------|------|
| % of OBM added | 0.00 | 1.00 | 2.00 | 3.00 | 5.00 | 7.00 | 15.0 | 30.0 |
| Free Lime % | 2.87 | 2.35 | 1.26 | 2.26 | 2.66 | 2.90 | 2.57 | 2.05 |
| AM | 1.11 | 1.10 | 1.13 | 1.13 | 1.15 | 1.17 | 1.23 | 1.36 |

Conclusions

- The clinker produced using the OBM did not reveal significant differences in term of clinker phases formation.
- The free lime decreases with increasing the % of OBM up to 2%OBM addition. However, the free lime increases in the range 3 – 7 % OBM followed decrease free lime concentration at higher % of OBM.
- The Belite size is in the range of 24.9 μm to 31.7 μm.
- The addition of OBM % is likely to control the alite polymorph type.

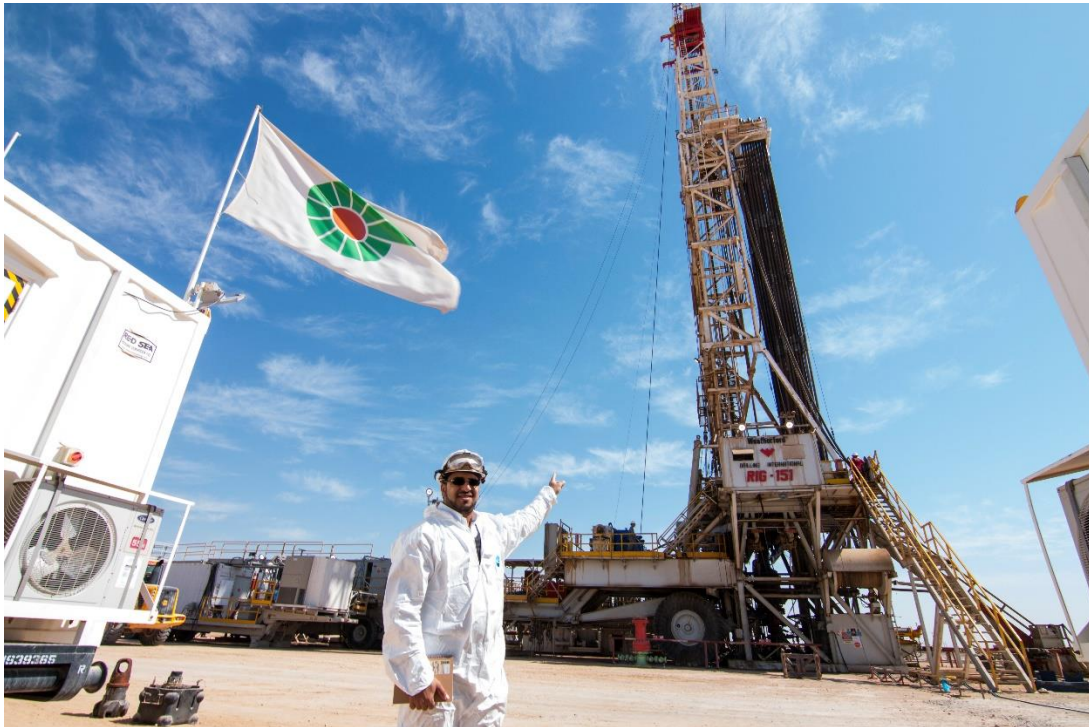


UNIVERSITY OF LEEDS



Appendix 19

Photos during the PhD study at University of Leeds



Oil drilling field during collecting OBM cuttings in Oman

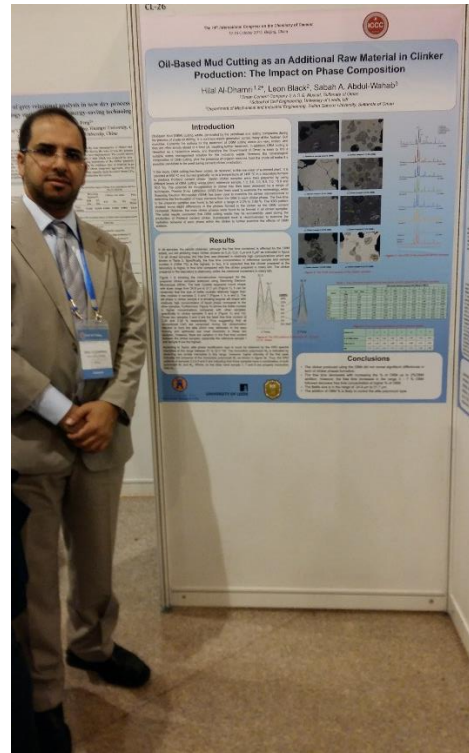


Competing for Adam Neville Prize for the best national PhD in the field of cement and concrete. 30 Oct 2019

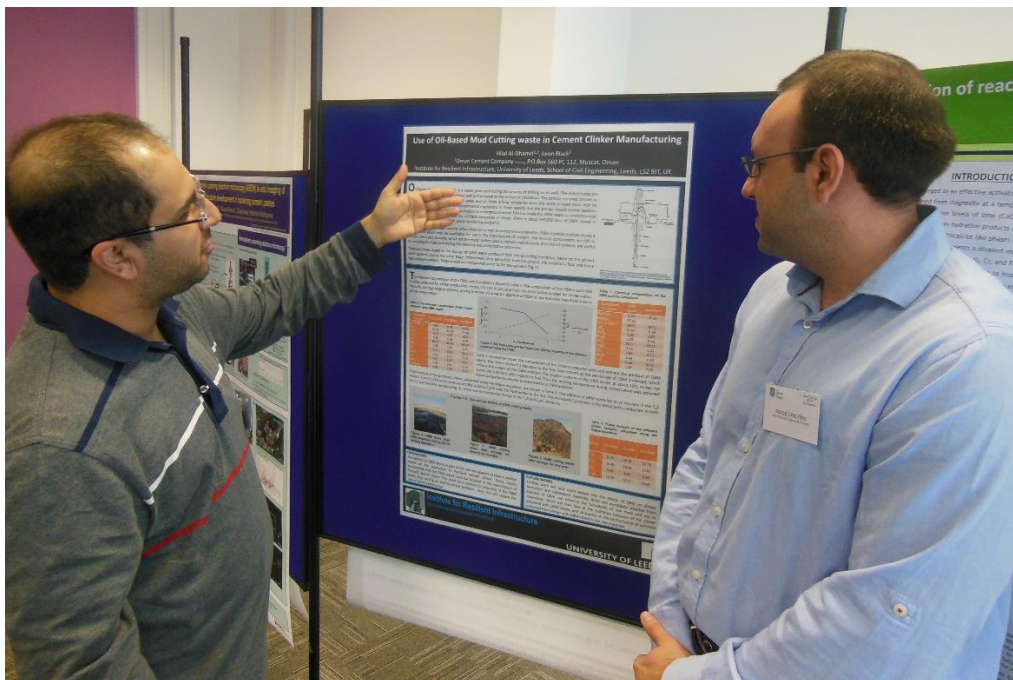
Source: <https://eps.leeds.ac.uk/faculty-engineering-physical-sciences/news/article/5597/the-adam-neville-prize-awarded-for-best-phd-in-cement-and-concrete>



Proceedings of the 15th International Congress of the Chemistry of Cement, Prague September 2019.



Proceedings of the 14th International Congress of the Chemistry of Cement, Beijing 2015.



34th Cement and Concrete Science Conference, 14-17 Sep 2014, Sheffield, UK.



With Professor Fredrik Glasser at University of Sheffield during the 34th Cement & Concrete Science Conference.



With Prof. Leon Black, my PhD supervisor. Picture during the Congress of the Chemistry of Cement, Prague September 2019.

